TOPOGRAPHIC AND BASE-LEVEL CONTROL ON BACK-BARRIER LAGOON

EVOLUTION: WEST GALVESTON BAY, TEXAS

A Thesis

by

PAUL HAZEN LAVERTY

Submitted to the Office of Graduate and Professional Studies of
Texas A&M University
in partial fulfillment of the requirements for the degree of

MASTER OF SCIENCE

Chair of Committee,	Timothy Dellapenna
Committee Members,	Robert Reece
	Peter van Hengstum
Head of Department,	Deborah Thomas

December 2014

Major Subject: Oceanography

ABSTRACT

Estuaries are economically and ecologically significant regions that are highly sensitive to external forcing from sea-level rise, storm events, and anthropogenic change. West Galveston Bay (West Bay) is a back-barrier lagoon system located immediately landward of Galveston Island, Texas, and it represents a sub-system of the larger Galveston estuary complex in the Northern Gulf of Mexico (NGOM). Previous studies have documented the evolution of many large estuaries along the NGOM in response to Holocene sea-level rise. However, the prehistory of smaller estuaries like West Bay remain largely overlooked and poorly understood. The primary purpose of this study is to complete a paleoenvironmental reconstruction of West Bay in Texas using geophysical and sedimentological approaches. A total of 30 core samples and more than 160 km of CHIRP seismic data were collected from West Bay and neighboring Chocolate Bay, within which several unique lithofacies and seismic facies were identified. As with other regional studies, the Pleistocene unconformity presents as an impedance change in the seismic profiles, and is most likely the Beaumont Formation. Multiple incised channels were observed on the Pleistocene Unconformity that are most likely seaward extensions of the tributaries that flow into Chocolate Bay, and formed the basal surface of the accommodation available for Holocene infill.

Radiocarbon dating of salient lithologic and seismic transitions in a few key cores revealed that several flooding events related to Holocene sea-level rise caused the landward back-stepping and geographic reorganization of depositional environments within West Bay. The first flooding event occurred at ~7,600 Cal. yr. BP caused both

ii

fluvial-dominated sedimentation to cease and initiation of estuarine conditions. The next flooding event occurred at ~6,800 Cal. yr. BP tripled the spatially inundated area and created ideal brackish conditions for oyster reef proliferation. This was short lived, however, as reduced salinity and increased turbidity from the paleo-Brazos River that was flowing into the area between ~6,100 and ~4,400 Cal. yr. BP ceased oyster reef production. The final flooding event occurred at ~4,400 Cal. yr. BP, which possibly established the connection between Galveston Bay and West Bay. At this time, an ephemeral tidal inlet formed within the incised channels, and then migrated west until stabilizing in the paleo-Brazos River incised valley as the modern day San Luis Pass.

This study reveals how the antecedent topography and sea-level rise controlled the environmental changes within West Bay throughout the Holocene. It also provides insight into how a small coastal system responds to varying rates of sea-level rise. Additionally, it may be useful as a baseline for West Bay for predicting future flooding associated with accelerating rates of sea-level rise.

DEDICATION

       This manuscript is dedicated to my wife, Nicki Starks Laverty. The best part of my life began the day I met you. Thank you for encouraging me to pursue my passion in geoscience and supporting me throughout this research. If any credit is given to me for this work, then it must also be given to you.

ACKNOWLEDGEMENTS

TABLE OF CONTENTS

LIST OF FIGURES

LIST OF TABLES

1. INTRODUCTION

Estuaries are ecologically, economically and socially important because they provide habitat for critical fisheries (Frey and Basan 1978, Day et al. 2007), they buffer the terrestrial impact of catastrophic storms and tsunamis on coastal human populations and infrastructure, (Danielsen et al. 2005, Day et al. 2007, Loder 2008), and critical navigable waterways for global port and harbor facilities. According to the most recent United Nations data, more than 40% of the global human population resides within the 4% of total landmass that constitutes the world's coast, and more than 60% of the global gross national product is generated within 100 km of the coastline (UNEP 2006). Recent studies suggest that the rate of eustatic sea-level rise is accelerating (Kemp et al. 2009), which will impart significant physical changes to global coastlines such as inundation and accelerated erosion (Haer et al. 2013, Wallace and Anderson 2013). Additionally, due to the local geomorphology, coastal slope, relative tide range, and subsidence rates, many estuaries on the Northern Gulf of Mexico (NGOM) are among the most vulnerable to the effects of sea-level rise (Thieler and Hammar-Klose 2000). Understanding how these systems respond to sea-level rise is therefore essential in sustaining the ecological health and economic viability of the global coast.

Estuaries in the NGOM frequently develop in drowned incised river valley systems during eustatic transgressions, and several studies have used the stratigraphy preserved within these incised valleys to document the Holocene paleo-environmental change in response to sea-level rise (e.g. Anderson et al. 2014, Rodriguez et al. 2004, Simms et al. 2006, Rodriguez, Anderson, and Simms 2005, Anderson 2007, Thomas and

Anderson 1994, Anderson and Rodriguez 2008). Incised-valley systems, consisting of an incised-valley and its associated sedimentary fill, are an economically and scientifically critical component of the stratigraphic record (Boyd, Dalrymple, and Zaitlin 1994). A significant number of discovered hydrocarbon reservoirs are located within incised-valley systems (Howard and Whitaker 1990, Zaitlin and Shultz 1990), including some of the largest hydrocarbon reservoirs (Peijs-van Hilten, Good, and Zaitlin 1998), and shallow biogenic gas (Lin et al. 2004, Garcia-Gil, Vilas, and Garcia-Garcia 2002). For the purposes of understanding sequence stratigraphy, the erosional surface that constitutes the base of an incised-valley system is essential in identifying sequence boundaries (Weimer 1984, Posamentier and Vail 1988). Additionally, incised-valleys provide accommodation space for sedimentary infill that can preserve the sedimentary record throughout the erosional process of ravinement, and often provide the only complete record of marine transgression (Van Wagoner et al. 1990).

Many studies detail the Quaternary evolution of large coastal systems that reside in the drowned incised-valleys of significant rivers (e.g. Allen and Posamentier 1993, Zhang et al. 2014, Foyle and Oertel 1997, Ta et al. 2001, Anderson et al. 2014). Given their economic and social significance, considerable research attention has been devoted to reconstructing the Holocene paleo-environmental histories of estuaries located along the Texas and Louisiana Gulf Coasts, which are extensively reviewed by Anderson and Rodriguez (2008). Each study identified episodic flooding events attributed to a variety of mechanisms, including antecedent topography, Relative Sea-Level Rise (RSLR), and sedimentary budget changes. These flooding events resulted in a radical geographical

redistribution of depositional environments within each respective estuary. Certain flooding events were unique to the estuary of focus, attributed to the unique antecedent topography, while others showed strong correlations across the NGOM.

While the paleo-environmental histories of large estuaries located in the NGOM have received much attention, small coastal systems that develop within the peripheral incised channels of large incised valleys (e.g. Rodriguez et al. 2008) are largely overlooked. The purpose of this study will be to (1) reconstruct the paleoenvironmental history of a transgressed small coastal system, and (2) document its response to accelerating rates of sea-level rise, while operating under the hypothesis that the antecedent topography and RSLR controlled the environmental transitions that occurred in West Bay throughout the Holocene.

2. BACKGROUND: ESTUARIES AND INCISED VALLEYS

There are over 40 different recognized and applied definitions of an estuary (Perillo 1995). From a physical oceanographic point of view, an estuary can be defined as a salinity gradient that occurs when freshwater from land-derived drainage mixes with ocean water (Pritchard 1967). From a sedimentology perspective, an estuary is the seaward portion of a drowned valley, where fluvial and marine sediments are mixed, and sedimentary depositional environments are controlled by unique processes such as river currents, tidal currents, and wave action (Dalrymple, Zaitlin, and Boyd 1992). Estuaries can be further divided into wave- and tide-dominated systems, depending on the dominant local hydrodynamics (Dalrymple, Zaitlin, and Boyd 1992). Most definitions use a two end-member system, where a fluvial source provides the landward end-member, and a marine source provides the seaward end-member. The varying energies and salinities that occur between these two end-members produce unique depositional realms that may be identified by their biogenic and physical sedimentary characteristics (Lankford and Rogers 1969).

The landward boundary of an estuary is often a river mouth, where coarse grained sediment and river currents often produce deltaic geomorphologies (Syvitski and Farrow 1983). In wave-dominated estuaries, there is a reduction of energy moving seaward into the central-basin, where finer sediments such as silts and clays are deposited (Thorbjarnarson et al. 1985). A wave-dominated central-basin may be configured in one of several geomorphologies, such as an open bay, or a semi-enclosed bay or lagoon separated from the marine environment by a spit or barrier island (Oertel

4

1985). These spits and barrier islands often form as a result of several high-energy processes such as wave-action and tidal-currents, and are subsequently comprised of coarser-grained sediments such as sands and gravels (Swift 1975). Storm events such as hurricanes produce tidal surges that inundate and breach barriers, transporting shoreface sediments to the otherwise quiescent lagoon (Davis, Knowles, and Bland 1989, Donnelly et al. 2004). These inundation events often produce characteristically lobate washover fans on the back side of the barrier (Davis Jr, Andronaco, and Gibeaut 1989, Israel, Ethridge, and Estes 1987), and can create tidal inlets that connect the bay or lagoon to the ocean (Mallinson et al. 2011, Oertel 1985). While tidal inlets can close as the barrier recovers after the storm, occasionally the inlet will stabilize and facilitate continuing tidal exchange between the ocean and bay (Hayes and FitzGerald 2013).

Drowned-valleys are inundated incised-valleys that initially form through the process of incision, which is erosion at the base of a fluvial system (Schumm 1994). Base-level drop, tectonic uplift, changes in climate, or a combination of these factors may contribute to the incision of an incised valley, with the primary requirement being that the transport capacity of a fluvial system exceeds its sedimentary load (Dalrymple 2006). The locations favoring incised valley formation include low-lying topography such as previously incised valleys not buried during the depositional phase and deltaic lobes exposed by sea-level fall (Dalrymple 2006).

A transition from incision to deposition often accompanies the inundation of an incised valley by sea-level rise (Dalrymple 2006), but the depositional processes governing the filling of an incised valley are highly variable. Overfilled incised valleys

contain only fluvial sediments from rivers with relatively high sediment loads (e.g. Simms et al. 2006, Garrison Jr and van den Bergh 2006). Studies of the stratigraphy within underfilled incised valleys are more common, however, and they predominantly contain a fluvial-estuarine-marine facies succession that reflects the changes in depositional environments in response to sea-level rise (e.g. Thomas and Anderson 1994, Simms et al. 2010, Zhang et al. 2014, Nichol, Boyd, and Penland 1996, Allen and Posamentier 1993). Several depositional models have been developed to explain the complex mechanisms responsible for the diversity of incised valley fills (Tessier 2012, Boyd, Dalrymple, and Zaitlin 2006, Zaitlin 1994, Dalrymple, Zaitlin, and Boyd 1992).

During a marine transgression, the depositional environments of an estuary may back-step landward in response to sea-level rise (e.g. Rodriguez, Simms, and Anderson 2010). Accommodation space provided by an incised-valley may preserve evidence of the depositional environments that occurred within a specific area throughout a marine transgression (Van Wagoner et al. 1990). These deposits will be expressed in a vertical sedimentary sequence, with the deepest sedimentary layer in the sequence assumed to be the oldest (Friedman, Sanders, and Kopaska-Merkel 1992). A detailed investigation of this sedimentary sequence can potentially reveal the timing and locations of paleo-environmental changes.

3. STUDY AREA

3.1 Regional and Geological Setting

The Galveston estuary complex on the NGOM (Fig. 1) is the 7th largest estuary in the United States (McKinney et al. 1989), and is home to one of the busiest international ports and largest petrochemical complexes in the world (Port of Houston Authority of Harris County 2012). West Bay is the back-barrier lagoon of Galveston Island, and is a sub-system of the Galveston estuary complex (Fig. 1). The lagoon is divided into two tidal systems by a relatively thin, transverse oyster reef known as Carancahua Reef. The primary focus of this study is the western half of West Bay that constitutes the distal flood tidal delta of San Luis Pass (Fig. 1), which is one of the few Texas tidal inlets not subject to direct anthropogenic modification (Anderson 2007, Israel, Ethridge, and Estes 1987). The study area is wave-dominated, microtidal (Morton and McGowen 1980) and exhibits an average water depth of ~2 m. It is connected along its northern border to Chocolate Bay, which is a shallow (1-2 m), sandy bay with several living oyster reefs (Fig. 1). An artificially dredged channel runs though the center of Chocolate Bay, leading to a large petrochemical complex that houses the second largest hydrocarbon cracker in the United States (INEOS 2014).

Four tributaries flow into Chocolate Bay (Wharton, Mustang, Chocolate, and Halls Bayous; Fig. 1), and are subsidiary incised channel features that form a peripheral drainage network on the edge of either the Brazos or Trinity/Sabine River incised valleys as mapped in Taha and Anderson (2008) and Anderson et al. (1996). It is presumed that this subsidiary drainage network was once connected with either the Trinity or Brazos
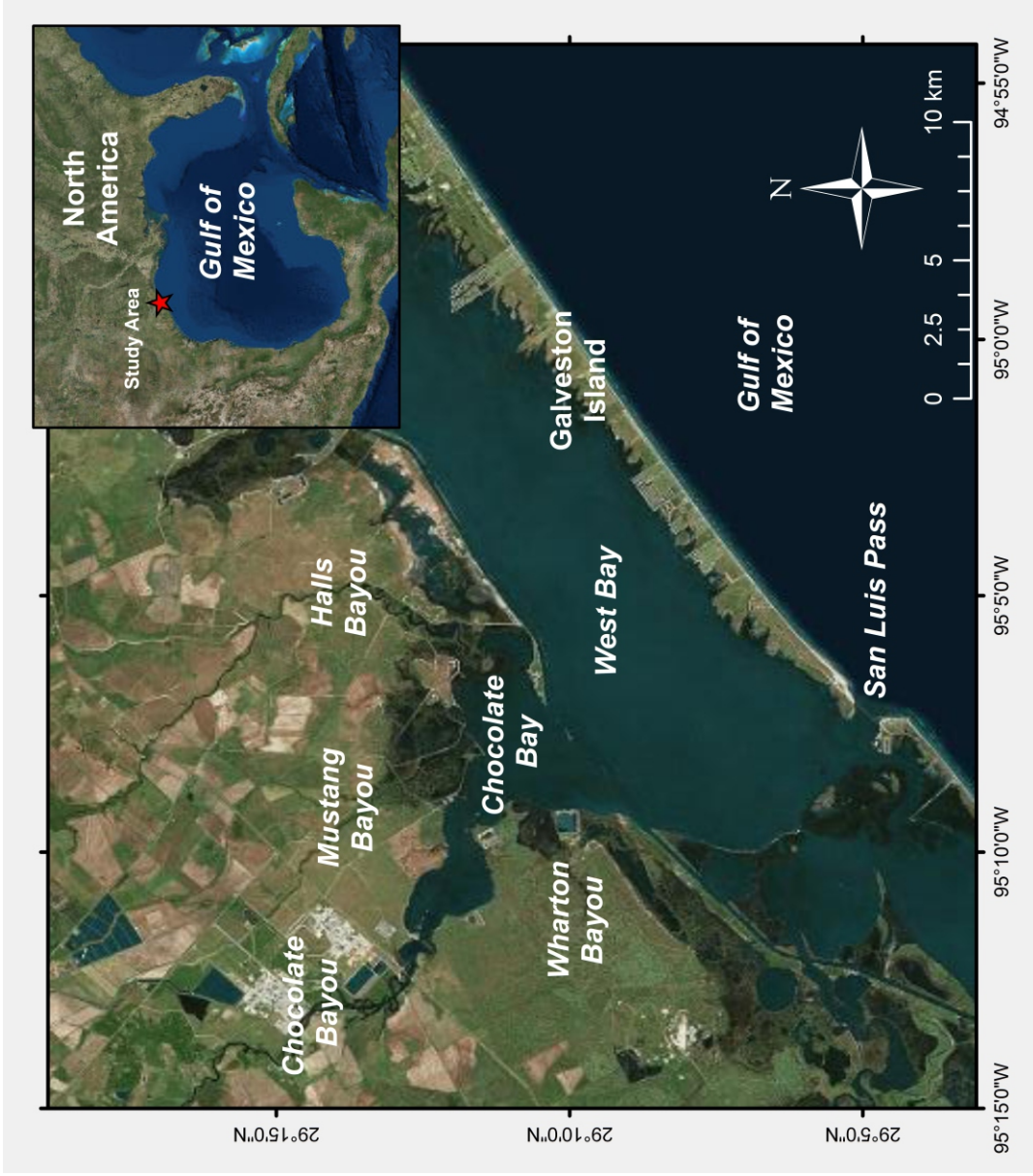
Figure 1: Regional Setting.

incised valleys, but evidence for this connectivity, likely just seaward of the current shoreline, was most likely eroded during Holocene ravinement. Published data specifically detailing the formation of these tributaries and Chocolate Bay is not available.

The formation of Galveston Island ~5 kya (Bernard et al. 1970) established West Bay as the RSLR decelerated from an average of 2.0 mm/yr to 0.6 mm/yr (Milliken, Anderson, and Rodriguez 2008a). Galveston Island was originally a rapidly prograding barrier island (Bernard, Major Jr, and Parrott 1959) as ravinement processes reworked sediment from offshore sand banks into characteristic ridge and swale topography of the barrier island (Morton 1994, Rodriguez et al. 2004). The greatest progradation occurred in the prominent direction of longshore drift, however, significant seaward and minor landward progradation is also observable in the sedimentary record (Otvos 1970). At ~2000 Cal yrs BP, island progradation ceased and island erosion began when these offshore sediment supplies were exhausted (Siringan and Anderson 1994). Galveston Island is currently considered to be inundating in place due to a rapidly increasing RSLR and accelerated erosion from storms (Wallace, Anderson, and Fernández 2010).

3.2 Hydrology and Climate

The four tributaries that flow into Chocolate Bay provide the proximal source of fluvial input for the study area with a combined drainage area of ~1000 km^2. A stream gauge located on Chocolate Bayou near Alvin, Texas reports an average annual discharge rate of 3.2 m^3/s between the years of 1960 and 2013 with a high of 9.6 m^3/s and a low of 0.5 m^3/s (USGS 2014). No hydrological data is available for the three remaining tributaries.

The study area is located in a humid climate (Thornthwaite 1948) and characterized by consistent storminess (Morton 1994). Approximately 47 cold fronts cross the Texas coast annually (Henry 1979), and historical records indicate that the study area lies in one of the most hurricane-strike prone areas of the Texas Gulf Coast (Simpson and Riehl 1981). Coastal wave heights in the study area remain below 1 m in height 77% of the year (Hall 1976), however, wave heights can exceed 7 m during tropical cyclones (Wallace, Anderson, and Fernández 2010). Winds are predominately from the southeast, producing shoreward-refracting waves responsible for the prevailing westerly longshore currents (Bernard, Major Jr, and Parrott 1959).

3.3 Subsidence and Relative Sea-Level Rise

Long-term subsidence rates for the Texas Coast throughout the last interglacial are estimated at ~0.01 mm/yr (Paine 1993). Local subsidence rates can vary widely due to the compressibility of the underlying strata (Morton, Bernier, and Barras 2006). Over the past century, localized subsidence has increased to rates as high as ~14 mm/yr

largely due to sub-surface anthropogenic fluid withdrawal (Galloway, Jones, and

Ingebritsen 1999, Gabrysch 1976, Morton, Bernier, and Barras 2006).

The RSLR within the NGOM has decelerated throughout the Holocene from ~9

mm/yr to ~0.6 mm/yr (Törnqvist et al. 2004, Milliken, Anderson, and Rodriguez 2008a).

Over the last ~50 years, the RSLR for the Galveston area has accelerated to ~6.24 mm/yr

(Kolker, Allison, and Hameed 2011), which is similar to the accepted RSLR that

occurred in the region from 8000 to 6000 Cal yrs BP (Milliken, Anderson, and

Rodriguez 2008a). Therefore, environmental changes observed within the early

Holocene depositional history of the study area may provide a valuable analogue to

future accelerating RLSR trends.

4. METHODS

4.1 Geophysical Survey

Over 160 km of seismic sub-bottom data was collected (Fig. 2) using an Edgetech® 216 Full Spectrum Sub-bottom CHIRP seismic sonar towfish operating on frequencies between 2 and 16 kHz. This was accomplished aboard the R/V Big Daddy, a 10 m custom-fabricated aluminum barge owned by Texas A&M University at Galveston. In West Bay, survey lines were arranged in a configuration that optimized coverage area and survey efficiency. Survey lines were plotted closer together over a small sub-feature within the southeast portion of the study area to obtain greater detail. Due to the numerous hazards to navigation within Chocolate Bay, the survey was largely improvised in-situ, and coverage was determined based on navigability. Data from these seismic surveys was processed and interpreted using Chesapeake® SonarWiz software. Gain values for each individual section were adjusted to enhance acoustic reflectors. Depth calculations were calculated using two-way travel time and an assumed seismic velocity of 1500 m/s. This velocity was selected based on the relatively shallow depths of the studied strata and velocities applied in similar studies (Simms et al. 2010, Anderson et al. 2004). Maps, interpolated surfaces, surface difference calculations, and 3-dimensional models were generated using Fledermaus® and ESRI® software suites.
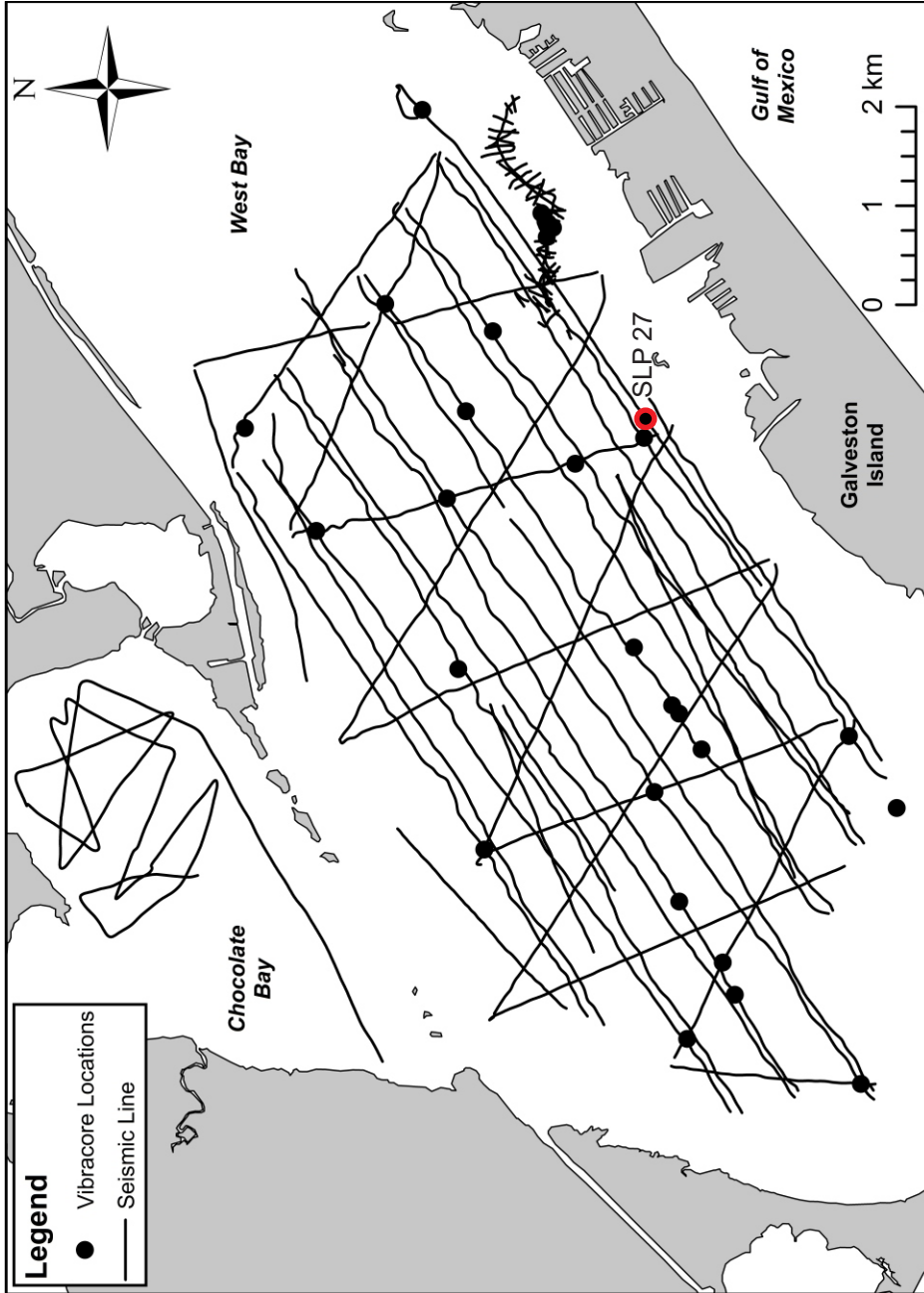
Figure 2: Sampling Locations. Map of seismic survey and core locations. The location of core SLP 27 is circled in red. This core is detailed in a later figure.

4.2 Sedimentary Analysis

A total of 30 sediment cores (Fig. 2), ranging in length from 1-11 m, were collected using a mechanical vibra-core rig deployed off the bow of the R/V Big Daddy. The cores are 7.62 cm (3 in) in diameter, and have a maximum depth of 12 m (limited by the length of the core barrel). Cores were stored upright and refrigerated until analyzed. Cores were then sectioned lengthwise, photographed, and visual descriptions of the lithology were recorded. One-half of each core was archived for future reference. Cores were sub-sampled for every lithological unit, as determined by visual analysis, in sections ranging from 1-5 cm thick depending on the unit for the length of the core. Downcore particle size distributions were measured using a Malvern Mastersizer 2000® laser particle diffractometer. A representative aliquot of each sample was extracted and placed in a 100 mL glass jar. Deionized water and 10 mL of a 5.5-g/L sodium hexametaphosphate solution was added to the jar to disaggregate the sample. The sample slurry was then stirred for ~10 minutes to assist in disaggregation. The slurry was deposited into the Malvern Mastersizer 2000® until a pre-determined level of obscuration was reached. At this point the instrument conducted three measurements and averaged the three results. The instrument determined percent composition of sand (calibrated to a range of 63-2000 μm), silt (4-63 μm) and clay (0.1-4 μm), along with the volume-weighted mean grain size (D 3,4) and standard deviation (1σ) for each respective sample.

4.3 Geochronology

Chronological constraint for the cores were obtained through traditional accelerated mass spectrometry radiocarbon techniques on carbonate and terrestrial material (Purser, Liebert, and Russo 1980) at the National Ocean Sciences Accelerator Mass Spectrometry (NOSAMS) Facility at Woods Hole Oceanographic Institution. Material dated included articulated bivalves to reduce taphonomic problems associated with post-mortem transport of the shell material, bulk benthic foraminifera (primarily *Ammonia* and *Elphidium spp.*), and terrestrial plant fragments. Before analysis, each sample was wet sieved though a 63 μm sieve and sonicated in a bath of 5.5 g/L sodium hexametaphosphate to remove adhering authigenic carbonate and clay particles. Foraminifera specimens were concentrated by wet-sieving sediment samples over a 63 μm sieve and picked dry from remaining sediment residues using stereomicroscopy. The conventional ^{14}C age reported by NOSAMS was then calibrated to calendar years before present (Cal yrs BP) using either the Intcal13 or Marine13 calibration curve (Reimer et al. 2013) in the software Calib 7.02. No reservoir effect specific to West Bay was included when calibrating the results from marine material (e.g., benthic foraminifera, bivalves).

5. RESULTS AND INTERPRETATIONS

5.1 Establishing the Sequence Boundary

The focus of this study was intended to be an investigation of the Holocene evolution of West Bay. Therefore, it was critical to first establish the sequence boundary marking the transition from Pleistocene to Holocene sediments. After establishing this sequence boundary, a more detailed investigation of the lithological and seismic facies located stratigraphically above this boundary was conducted.

Within the seismic data, truncated, sub-parallel, high-amplitude reflectors underlying downlapping high amplitude reflectors are observed in relatively deep features that meander through the study area (Fig. 3). Reflectors with similar geometry and configuration are also observed in several incised valleys along the Texas Gulf Coast, and were interpreted as an erosional surface representing the local Pleistocene Unconformity (Simms et al. 2010, Simms et al. 2006, Anderson et al. 2008). Based on the erosional appearance of this surface, combined with the similarity of its presentation to previous regional studies, this surface is interpreted to also represent a sequence boundary in West Bay that represents the local Pleistocene Unconformity (PU).

A sedimentary contact was observed between dry, indurated clay of varying colors, and moist, unconsolidated sediment of varying colors and textures (Fig. 3). The depth of this sedimentary contact correlated strongly to the depth of a stark change from low to high impedance within the seismic data (Fig. 3). The dry, indurated clay is interpreted to be the Beaumont Formation (Hayes and Kennedy 1903, Rodriguez, Anderson, and Simms 2005), a Pleistocene paleosol that represents the Holocene-
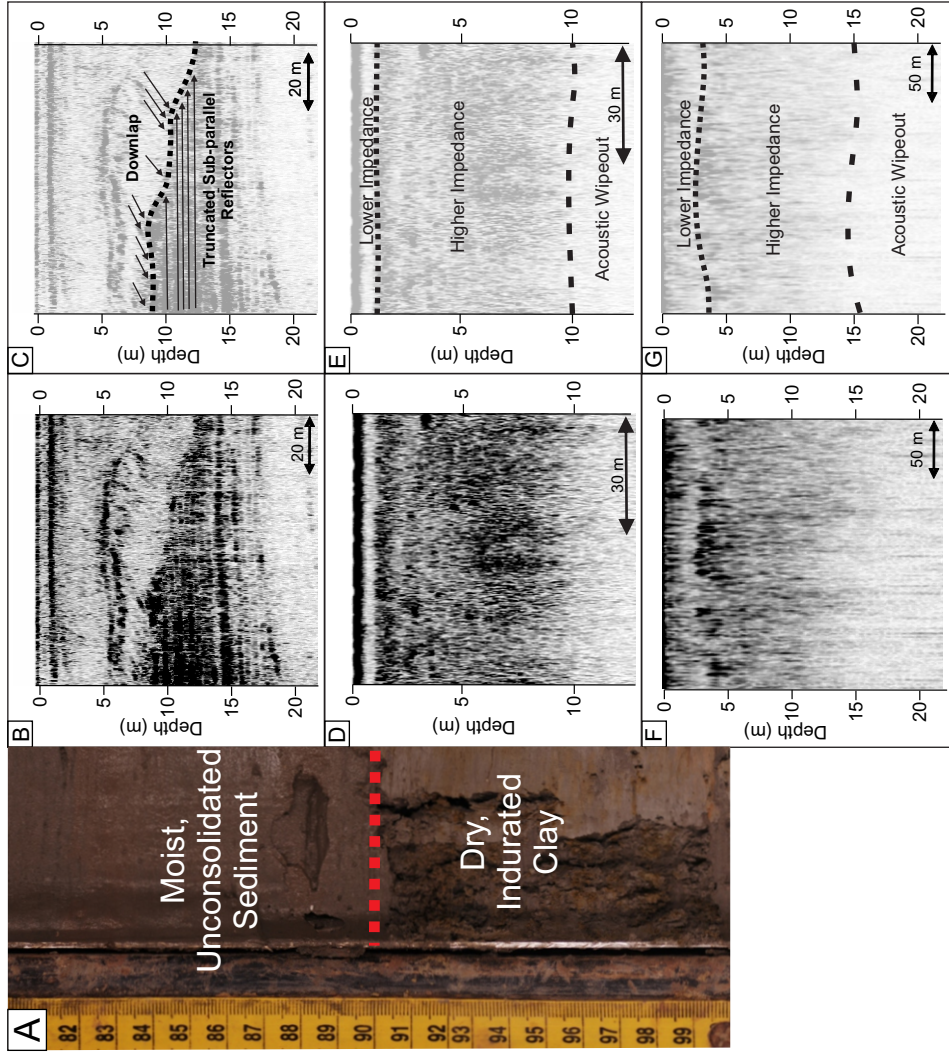
Figure 3: Pleistocene Unconformity (PU).A. Image from Core SLP 11 showing the contact (red dashed line) interpreted as the PU. The dry, indurated clay is interpreted to be the Beaumont Formation (Hayes and Kennedy, 1903; Rodriguez et al., 2995). **B**. Uninterpreted and **C**. interpreted seismic sections showing the PU as it appears within the incised channels. **D**. Uninterpreted and **E**. interpreted seismic sections showing the PU as it appears within West Bay outside the incised channels.The depth of this impedance change correlated to the depth of the depicted sedimentary contact **(A)**. **F**. Uninterpreted and **G**. interpreted seismic sections showing the PU as it appears within Chocolate Bay

17

Pleistocene boundary across the NGOM. The sediment above this contact is interpreted to be Holocene based on the lack of consolidation and relative moisture. The impedance change is interpreted to be a product of density changes related to the different levels of sedimentary consolidation between the Holocene sediment and the Beaumont Formation.

A continuous, stark change from low to high impedance, similar to that identified in West Bay, is observed throughout the seismic data acquired from modern Chocolate Bay (Fig. 3). Interpretations of the PU within Chocolate Bay are not as robust as those within West Bay due to the lack of lithological data. However, based on the strong similarities of the impedance changes seen in seismic data from Chocolate and West Bay, the impedance change is interpreted to be the PU in Chocolate Bay as well.

5.2 Interpolated 3-Dimensional PU Surface

To assist in visualizing the antecedent Pleistocene exposure surface, a three-dimensional surface representing the PU was generated using a kriging interpolation (Fig. 4). Kriging was accomplished using a 30 m cell size. No local subsidence effects were applied when generating this surface, as subsidence data for West Bay is currently unknown. Regional subsidence was also not applied during the initial generation of this surface.

Within the modern boundaries of West Bay, the surface shows two distinct channels of dissimilar relative size. The larger channel extends from northwest to southeast, and is interpreted to be the seaward extension of the Chocolate Bayou incised
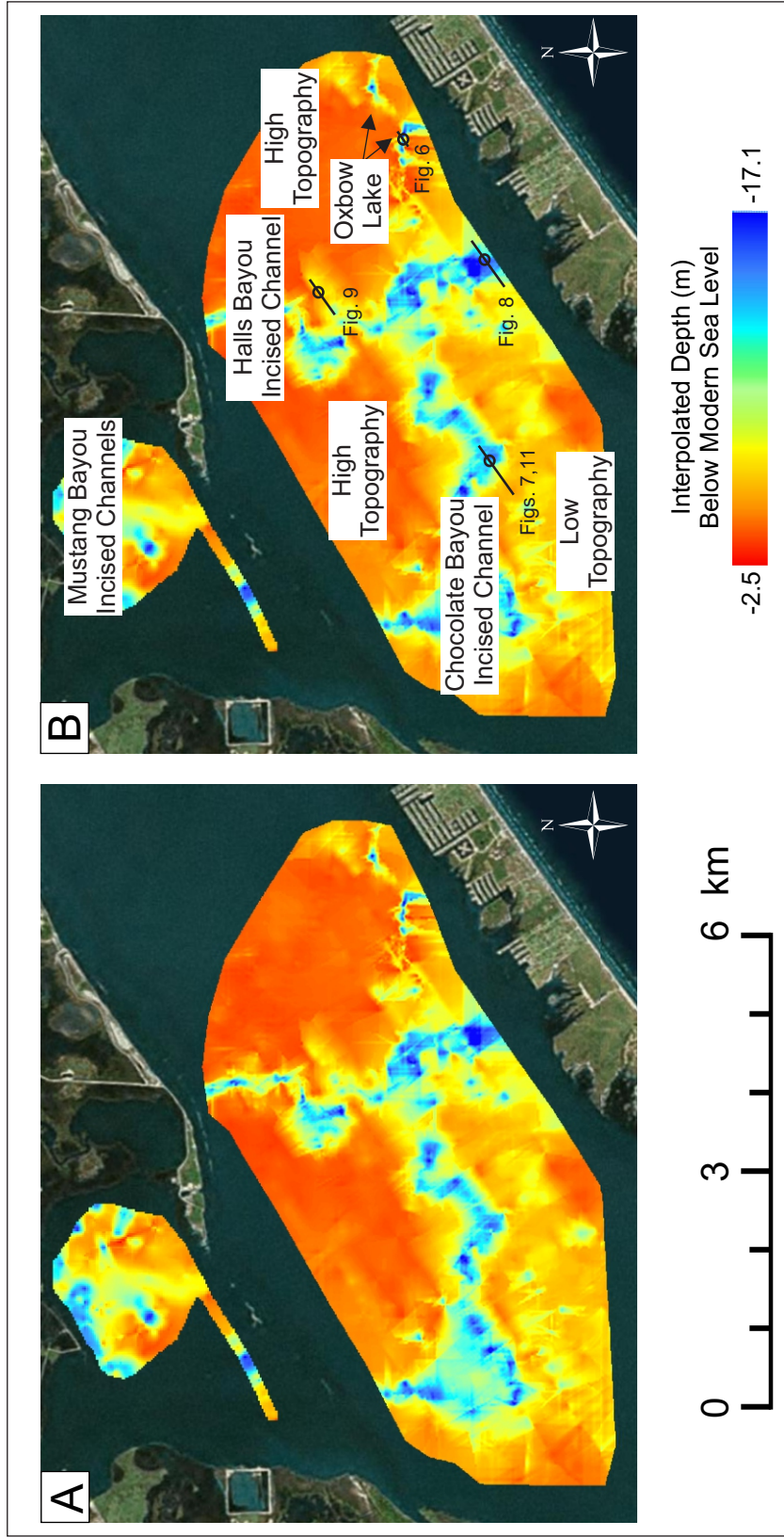
Figure 4: Three-Dimensional Surface of Pleistocene Unconformity. A. Uninterpreted and **B.** interpreted surface of the Pleistocene Unconformity (PU). The PU was interpreted on all available seismic data (Fig. 2) and interpolated between to create a surface. The location of seismic sections shown in later figures are indicated as a black line. The core samples used to correlate the lithology within the seismic sections are displayed as a hollow circle.

channel. The smaller channel shows connectivity with the larger channel in the center of the study area, and extends northeast toward the northern extent of the survey. This smaller channel is interpreted to be the seaward extension of the Halls Bayou incised channel.

Within the modern boundaries of Chocolate Bay, the surface shows a relatively small channel extending from the modern mouth of Mustang Bayou in the direction of the interpreted position of the landward Chocolate Bayou incised channel. There is also highly variable topography throughout Chocolate Bay surrounding the interpreted Mustang Bayou incised channel.

The surface also shows broad areas with dissimilar elevations. The broad areas in the northeast portion of the study area, on either side of the interpreted Halls Bayou incised channel, have an average elevation of −3 m mean sea-level. The broad area in the southwest portion of the study area, seaward of the interpreted Chocolate Bayou incised channel, has an average elevation of −6 m mean sea-level.

5.3 Lithofacies

A lithofacies is a distinctive sedimentary deposit (bed or layer in this context) that forms under certain conditions of sedimentation, reflecting a particular process or environment (Bates and Jackson 1984). Nine unique lithofacies were identified in the cores extracted from West Bay. Brief descriptions of these lithofacies can be found in Table 1. Additional core data may be viewed in Appendix A.

Table 1. Lithofacies

Lithofacies	Brief Description of Sediments	Approximated Sedimentation Rate	Interpreted Environment of Deposition	Mean Grain Size (µm)	Standard Deviation (µm, 1σ)	Correlated Seismic Facies
L1	Brown to gray shelly, muddy sand with layers of densely packed shell hash	0.25-10 mm/yr	Tidal Inlet, Lower Estuary	56.1	96.8	S1
L2	Highly oxidized brown to red-brown clay with layers of *R. Cuneata*	0.7 mm/yr	Paleo-Brazos River Pro Delta	4.8	5.9	S1
L3	Light-gray shelly, clayey silt with interspersed layers of densely packed, articulated bivalves	1 mm/yr	Middle Estuary, Interspersed Oyster Reef	14.3	20.2	S2
L4	Light-gray shelly, muddy sand with burrows	1 mm/yr	Upper Estuary	51.3	72.7	S3
L5	Light-gray highly laminated horiztonal to sub-horizontal layers of mud and muddy sand	0.6 - 10 cm/yr	Oxbow Lake	8.7	13.5	S6
L6	Light-gray mud with sub-horizontal to angular laminations of muddy sand	Undetermined	Distributary Channel	22.5	55.3	S5
L7	Organic-rich mud with lamina of muddy sand and interspersed plant fragments	2 mm/yr	Delta Plain	46.6	136.4	S4
L8	Light-gray clayey sand	6 mm/yr	Mouth Bar	146.6	69.7	S4
L9	Dry indurated clay, ranging from blue-gray to red-brown, with numerous burrows	Undetermined	Beaumont Formation (Paleosol)	28.1	38.4	S7

21

5.3.1 Lithofacies 1 (L1)

Lithofacies 1 (e.g., Fig. 5) consists of heavily-mixed, shelly, muddy sand transitioning in color from brown to gray moving down-core. Interspersed layers of densely packed, black- and red-stained estuarine shell fragments (shell hash) occur in cores taken from within the Chocolate and Halls Bayou incised channels. A representative sample of the matrix sediment of this lithofacies taken from core SLP 27 (interval 0-1 cm) contained ~35% sand, ~25% silt, and ~40% clay, with a mean grain size of ~56.1 μm and a standard deviation of 96.8 μm.

5.3.2 Lithofacies 2 (L2)

Lithofacies 2 (e.g., Fig. 5) consists of highly oxidized brown to red-brown clay. A layer of *R. Cuneata* shells and shell fragments was observed in this lithofacies in core samples taken from the topographical low in the southwest portion of the study area and the Chocolate Bayou incised channel. This shell layer is absent in cores taken from the Halls Bayou incised channel. This layer is absent from cores taken from the topographical highs located on either side of the Halls Bayou incised channel. L2 is heavily mixed with estuarine sediment at the upper and lower contacts. It ranges in thickness from several centimeters to several meters. Two relatively thin (~20 cm) layers of L2 are present in Core OC1B (Fig. 6). A representative sample of this lithofacies taken from core SLP 27 (interval 161-162 cm) contained ~38% silt and ~62% clay, with a mean grain size of ~4.8 μm and a standard deviation of 5.9 μm.

Core SLP 27
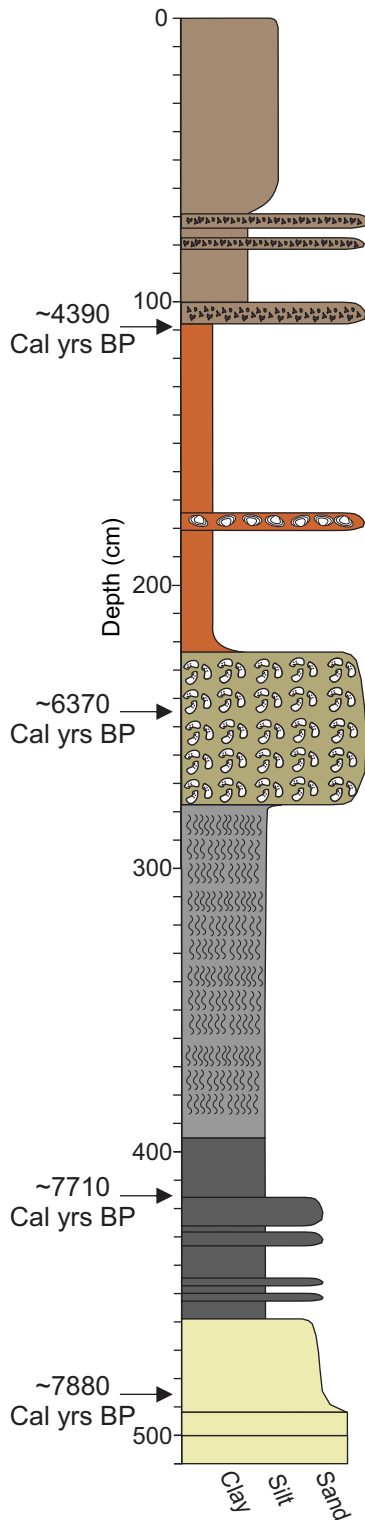
The typical sedimentary succession observed within the incised channels. Locations and ages of radiocarbon dates are depicted. Location for this core can be seen in Figure 2.

~4390
Cal yrs BP

~6370
Cal yrs BP

~7710
Cal yrs BP

~7880
Cal yrs BP

Depth (cm)

0
100
200
300
400
500

Clay   Silt   Sand

Legend

- ▨ Tidal Inlet/Lower Estuary (L1)
- ▨ Paleo-Brazos River Pro Delta (L2)
- ▨ Middle Estuary (L3)
- ▨ Upper Estuary (L4)
- ▨ Delta Plain (L7)
- ▢ Mouth Bar (L8)

- ꝏ Shell Hash
- ꝏ Oyster Reef
- ꝏ *R. Cuneata*
- ⧟ Burrows

Figure 5. Description of Core SLP 27.

5.3.3 Lithofacies 3 (L3)

Lithofacies 3 (e.g., Fig. 5) consists of light gray, clayey silt with fragments of estuarine shell. Densely packed layers of articulated *C. virginica* shells are observed within L3 in core samples taken from the Chocolate and Halls Bayou incised channels. A representative sample of the matrix sediment taken from core SLP 27 (interval 246-247 cm) contained ~4% sand, 53% silt and ~43% clay, with a mean grain size of ~14.3 μm and a standard deviation of 20.2 μm.

5.3.4 Lithofacies (L4)

Lithofacies 4 (e.g., Fig. 5) consists of light gray, shelly, muddy sand. Interspersed layers of small (<1 cm diameter) burrows appear in the upper portions of L4. This lithofacies is predominately structureless. While the color of L4 is similar to L3, lays of articulated oyster shells are not present within L4 in any of the core samples. A representative sample of the L4 sediment taken from core SLP 27 (interval 320-321 cm) contained ~32% sand, ~29% silt and ~39% clay, with a mean grain size of ~51.3 μm and a standard deviation of 72.7 μm.

5.3.5 Lithofacies (L5)

Lithofacies 5 (Fig. 6) is only observed in cores taken from an isolated, relatively deep sub-feature located in the southeast portion of the study area. This lithofacies consists predominantly of light gray, relatively thick mud layers with horizontal to sub-horizontal, thin laminations of muddy sand. One layer of reworked shell material is
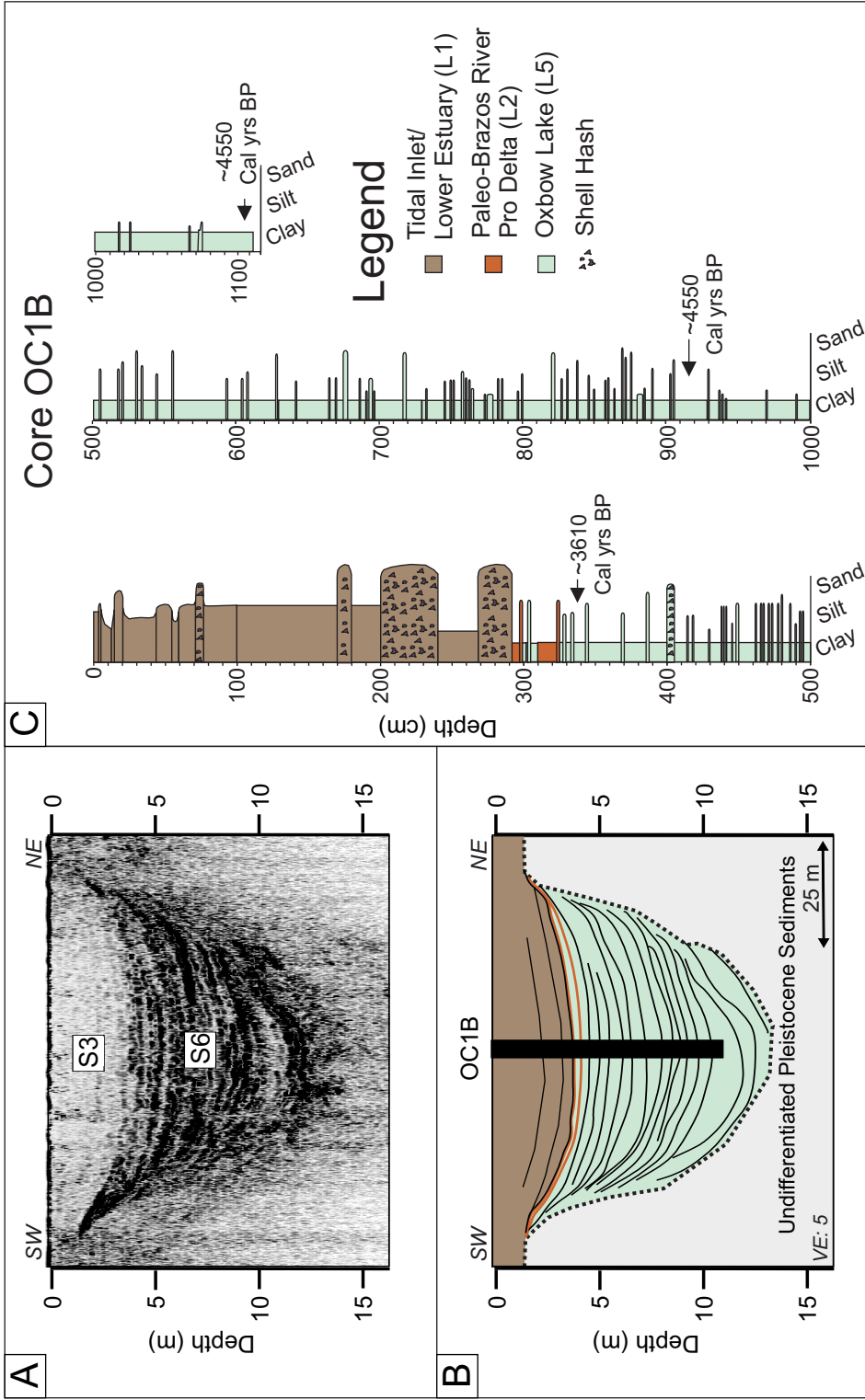
Figure 6: Oxbow Lake Facies. A. Seismic images and **B.** line drawing interpretation showing S6 and other facies of the Oxbow Lake. Seismic Facies 6 and L5 are unique to this feature. VE: Vertical Exaggeration. **C.** Detailed core description of core OC1B showing L5. Radiocarbon results are also depicted. The location for this seismic section and core can viewed in Figure 4.

observed within the uppermost portions of L5. A representative sample of the mud taken

from core OC1B (interval 488-488.5 cm) contained ~1% sand, ~49% silt and ~50% clay,

with a mean grain size of ~8.7 μm and a standard deviation of 13.5 μm. A representative

sample taken from a sand layer within L5 from core OC1B (interval 523.5-524 cm)

contained ~60% sand, ~25% silt and ~15% clay, with a mean grain size of ~104.2 μm

and a standard deviation of 152.3 μm.

5.3.6 Lithofacies 6 (L6)

Lithofacies 6 (Fig. 7) consists predominantly of light gray mud with sub-

horizontal to angular laminations of muddy sand ranging in thickness from 1-3 cm. This

lithofacies only appears in core SLP 21, which was extracted from the Chocolate Bayou

incised channel. A representative sample of the L6 mud taken from core SLP 21

(interval 509-510 cm) contained ~8% sand, ~50% silt and ~42% clay, with a mean grain

size of ~22.5 μm and a standard deviation of 55.3 μm. A representative sample taken

from a sand layer within L6 from core SLP 21 (interval 497-498 cm) contained ~49%

sand, ~27% silt and ~24% clay, with a mean grain size of ~74 μm and a standard

deviation of 76 μm.

5.3.7 Lithofacies 7 (L7)

Lithofacies 7 (e.g., Fig. 5) is observed in cores taken from throughout the Halls

and Chocolate Bayou incised channels. It consists predominantly of organic-rich mud

with layers of muddy sand and contains numerous root structures and plant fragments.

Estuarine shells are not present in this facies. A representative sample of the L7 mud
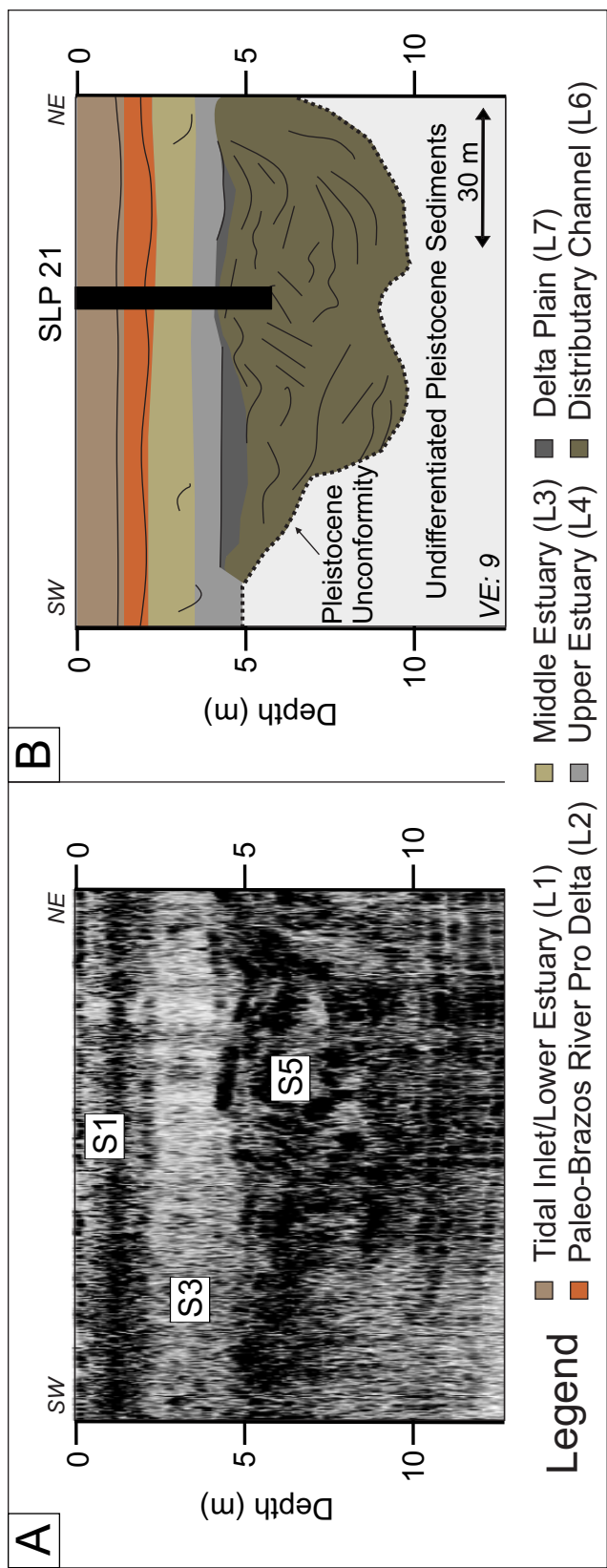
Figure 7: Distributary Channel Facies. A. Seismic images and **B.** line drawing interpretation showing the chaotic fill of a distributary channel and the facies sequence in the Chocolate Bayou incised channel. Location for this seismic section and core can be seen in Figure 4. VE: Vertical Exaggeration.

taken from core SLP 27 (interval 404-405 cm) contained ~13% sand, ~55% silt and ~32% clay, with a mean grain size of~46.6 μm and a standard deviation of 136.4 μm. A representative sample taken from a sand layer within L7 from core SLP 27 (interval 430-431 cm) contained ~50% sand, ~33% silt and ~17% clay, with a mean grain size was ~65.6 μm and a standard deviation of 53.9 μm.

5.3.8 Lithofacies 8 (L8)

Lithofacies 8 (e.g. Fig. 5) consists of light gray, clayey sand. Core samples of this facies are limited due to the required depth of sampling. This facies is only observed in the deepest portion of the Halls and Chocolate Bayou incised channels. A representative sample of L8 from core SLP 27 (interval 506-507 cm) contained ~93% sand, ~0% silt and ~7% clay, with a mean grain size was ~146.6 μm and a standard deviation of 69.7 μm.

5.3.9 Lithofacies 9 (L9)

Lithofacies 9 (e.g., Fig. 3) consists of dry, indurated, clayey silt. It exhibits a mottled coloring pattern, and ranges from blue-gray to red-brown. Samples of L9 contain numerous 2 to 3 cm wide burrows. A representative sample of L9 from core SLP 10 (interval 506-507 cm) contained ~16% sand, ~48% silt and ~36% clay, with a mean grain size was ~28.1 μm and a standard deviation of 38.4 μm.

Table 2. Seismic Facies

Seismic Facies	Brief Description of Attributes	Interpreted Depositional Environment	Example Image
S1	Low- and medium-amplitude reflectors with interspersed high-amplitude reflectors	Tidal Inlet, Lower Estuary	
S2	Relatively thick, chaotic, medium-high-amplitude reflection with discontinuous, sub-parallel, high-amplitude reflectors.	Middle Estuary, Oyster Reef	
S3	Largely acoustically transparent, with isolated medium-amplitude reflectors	Upper Estuary	
S4	High-amplitude, sub-parallel, oblique to sigmoid oblique reflectors	Mouth Bar	
S5	Alternating high- and low-amplitude reflectors exhibiting varying geometry that range from chaotic to sub-parallel and u-shaped	Distributary Channel	
S6	High-amplitude, concordant reflectors that truncate at the Pleistocene Unconformity	Oxbow Lake	
S7	Relatively thick area of high-impedance with interspersed, high-amplitude reflectors	Beaumont Formation/ Undifferentiated	
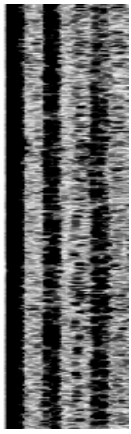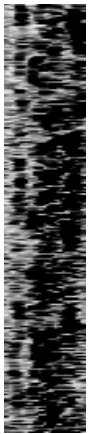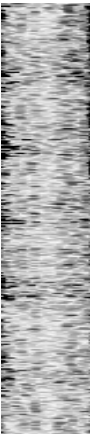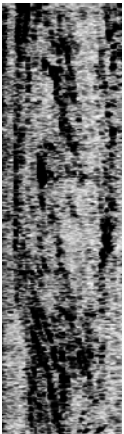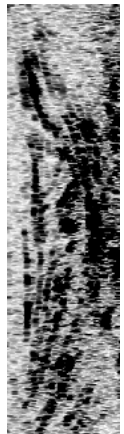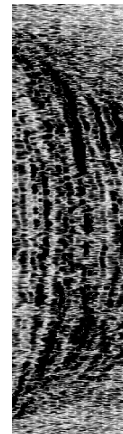
29
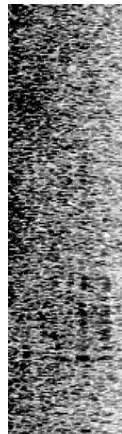
5.4 Geophysical

Seismic facies are separate units distinguishable by unique reflection characteristics, and can used as indicators of depositional environments (Sheriff and Sheriff 1980). Seven unique seismic facies are distinguishable within the study area. Brief descriptions of these facies can be found in Table 2.

5.4.1 Seismic Facies 1 (S1)

Seismic Facies 1 (e.g., Fig. 7) is consistently found in the upper 1-3 meters of the Halls and Chocolate Bayou incised channels. Core samples taken from S1 produced L1 and L2. Seismic Facies 1 is primarily comprised of low- and medium-amplitude reflectors with interspersed high-amplitude reflectors. These high-amplitude reflectors are thin, sub-horizontal, and discontinuous and correlate to the layers of shell hash observed in L1.

5.4.2 Seismic Facies 2 (S2)

Seismic Facies 2 (e.g., Fig. 8) consists of relatively thick, chaotic, medium-high-amplitude reflection with discontinuous, sub-parallel, high-amplitude reflectors. Core samples taken from S2 produced L3 with significant amounts of articulated oyster shells. This seismic facies is only observed in the Halls and Chocolate Bayou incised channels. In multiple seismic sections, it is observed pinching-out at the margins of the incised channels. It is also observed near the sediment-water interface in the seismic data acquired from the modern Chocolate Bay.
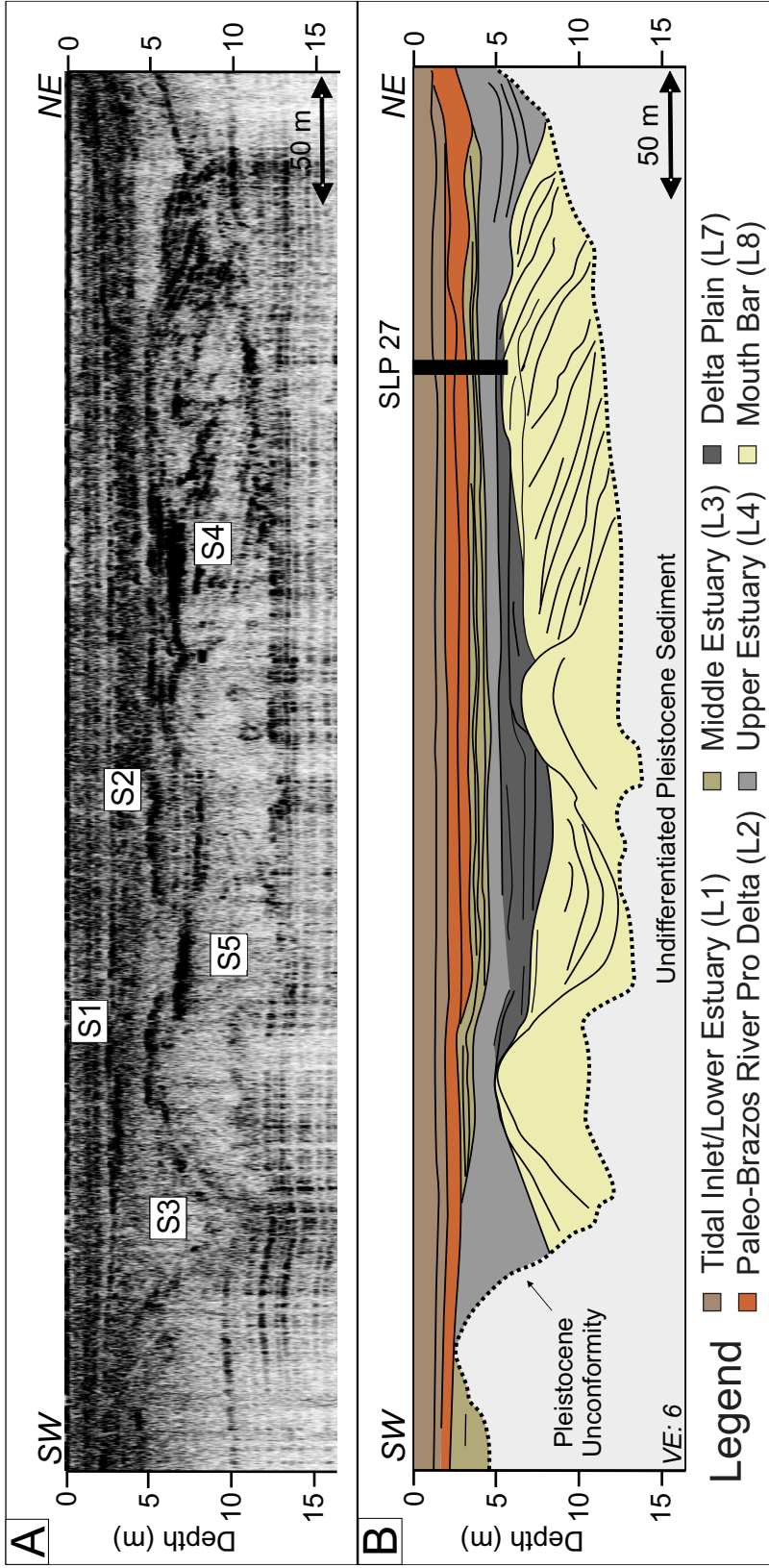
Figure 8: Chocolate Bayou Incised Channel Facies. A. Seismic images and **B.** line drawing interpretation showing the facies sequence in the Chocolate Bayou incised channel. Location for this seismic section and core can be seen in Figure 4. VE: Vertical Exaggeration.

5.4.3 Seismic Facies 3 (S3)

Seismic Facies 3 (e.g., Fig. 8) is observed throughout the seismic data acquired in the modern Chocolate Bay. Within the seismic data acquired in the modern West Bay, it is confined to the Halls and Chocolate Bayou incised channels. Core samples taken from S3 produced L4. Its lower contact exhibits an undulating geometry, while the upper contact is largely parallel to sub-parallel. It is largely acoustically transparent, with isolated medium-amplitude reflectors observed therein. It ranges in thickness from ~1 to ~3 meters.

5.4.4 Seismic Facies 4 (S4)

Seismic Facies 4 (e.g., Fig. 8) only observed directly above the PU within the incised channel. It consists of high-amplitude, sub-parallel, oblique to sigmoid oblique reflectors. The high amplitude reflectors truncate into the interpreted sequence boundary. The geometry of S4 resembles a prograding clinoform. Correlated sedimentary data is sparse due to difficulties encountered when sampling at depth, however available core samples taken from S4 produced L7 and L8.

5.4.5 Seismic Facies 5 (S5)

Seismic Facies 5 (e.g., Fig. 9) is only observed within the Halls and Chocolate Bayou incised channels, proximal to S4. It consists of low-to-high amplitude reflectors exhibiting a u- or v- shaped geometry. These reflectors are concordant or chaotic. The overall dimensions of S5 vary throughout the study area. Correlated sedimentary data is
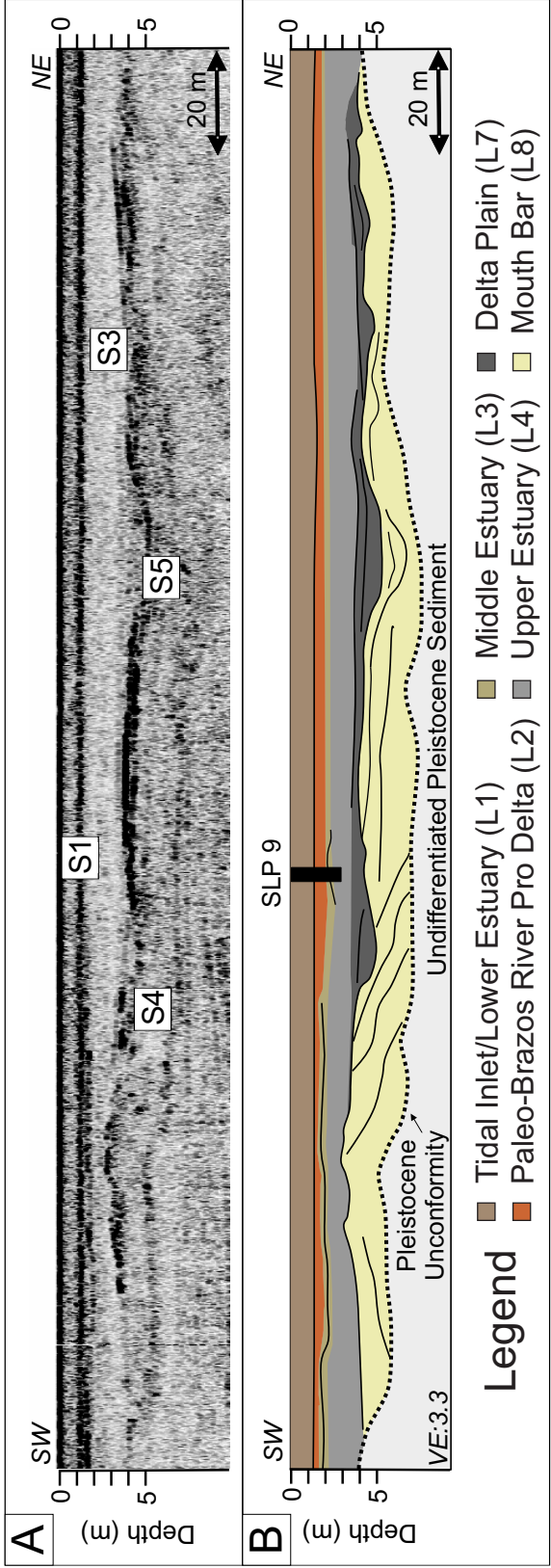
Figure 9: Halls Bayou Incised Channel Facies. A. Seismic images and **B.** line drawing interpretation showing the facies sequence in the Halls Bayou incised channel, bearing strong similarities to those observed in the Chocolate Bayou incised channel (Fig. 8). Location for this seismic section and core can be seen in Figure 4. VE: Vertical Exaggeration.

33

sparse due to difficulties encountered when sampling at depth, however available core samples taken from S5 produced L6.

5.4.6 Seismic Facies 6 (S6)

Seismic Facies 6 (Fig. 6) is only observed in an isolated sub-feature in the southeast portion of the study area. It consists of high-amplitude, concordant reflectors. These reflectors are continuous within the sub-feature, yet truncate at the PU. The geometry of the reflectors consistently follows the geometry of the unconformity at the base of the sequence. Core samples taken from S6 produced L9.

5.4.7 Seismic Facies 7 (S7)

Seismic Facies 7 is observed throughout portions of the seismic data collected in the modern Chocolate and West Bays. It consists of a relatively thick (~10 m) area of relatively high impedance situated beneath an area of low impedance. There are interspersed, high-amplitude reflectors situated at the top of S7 and randomly within S7. L9 was observed in cores taken from the uppermost portions of S7. No core samples penetrated more than 2 m into S7. Below S7, there is a total acoustic wipeout, and no detectable reflection is observed. Because of the lack of data, most of S7 and below is largely undifferentiated.

5.5 Interpreted Depositional Environments

Lithological and seismic data were used in concert to interpret the environments of deposition associated with both the seismic facies and lithofacies observed within the stratigraphy of West Bay. Seismic Facies 7, and the correlated L9, was used only to establish the sequence boundary. While the Beaumont Formation constitutes the uppermost Pleistocene sediments within the West Bay stratigraphy, the sediments below are undifferentiated. Therefore, the depositional environments for these facies remain uninterpreted.

5.5.1 Bayhead Delta (L6, L7, L8, S4, S5)

Multiple lithofacies and seismic facies constitute what is interpreted to be a paleo-bayhead delta deposit in the lowermost portions of the Halls and Chocolate Bayou incised channels. The sigmoidal geometry observed within S4 (Fig. 8) resembles that of a prograding clinoform, and is indicative of the upbuilding and outbuilding processes associated with deltaic growth (Friedman, Sanders, and Kopaska-Merkel 1992). Lithofacies 8 was sampled from the outbuilding, or foreset part of this deltaic feature. The subaqueous foreset portion of a bayhead delta, or mouth bar, is characterized by high sand content, such as that observed in L8 (Bates 1953). Therefore, due to its high sand content and location with the sigmoidal S4, L8 is interpreted to be a mouth bar deposit.

A mouth bar may eventually aggrade to the point of emergence and transition into a delta plain. The delta-plain would represent the upbuilding, or topset of the delta

(Bates 1953). Vegetation and fine-grained sediment, such as those observed in L7, are typically associated with delta plain features (McEwen 1969). Additionally, the horizontal sand layers observed within L7 have may deposit during events such as seasonal floods commonly associated with fluvial systems (Palinkas et al. 2005). Based upon the stratigraphic location of L7 situated directly atop L8, along with its sedimentary content, it is interpreted to be a delta plain.

Distributary channels are also common features to deltas (Edmonds and Slingerland 2007, Olariu and Bhattacharya 2006). The u- and v- shaped geometry observed in S5 (Fig. 8) is similar to features identified as deltaic distributary channels in several previous studies (Anderson et al. 2008, Simms et al. 2010). The sand layers observed within L6 are interpreted to correspond to high-amplitude reflectors observed within the channel fill of S5. The sedimentary patterns and corresponding seismic structure of L6 (Fig.7) and S4 have been seen in previous studies and interpreted to be distributary channels (Hopkins 1985). Due the structure, sedimentary fill, and stratigraphic position proximal to other interpreted deltaic features, L6 and S4 are interpreted to be related to deltaic processes.

5.5.2 Upper Estuary (L4, S3)

Upper estuaries typically develop proximal to the bayhead delta, and can be described as the pro delta (Dalrymple, Zaitlin, and Boyd 1992). Because of their proximity to the delta, they still may receive significant portions of fluvial sand, yet also receive the mud typical of an estuarine central-basin (Friedman, Sanders, and Kopaska-

Merkel 1992). Estuarine shells reworked from seaward geographic regions may also appear in upper estuarine sediments.

Seismic Facies 3 and L4 (Fig. 8) are interpreted to be associated with an upper estuarine environment. While L4 shows a significant increase in estuarine mud with respect to the deltaic deposits, it retains a relatively high percentage of sand. This is attributed to its geographic proximity to the fluvial source during deposition. The burrows observed in L4 indicate a high level of bioturbation. Heavy rates of bioturbation result in homogenous, mixed sediment, which likely explain the absence of salient acoustic reflectors within the seismic data for L4 (Fig. 9). It is possible that the sedimentation rates for L4 were reduced, considering other studies have documented that high rates of burrowing are typically associated with low sedimentations rates (McCall 1982).

5.5.3 Middle Estuary (L3, S2)

The middle portions of estuaries are the most distant from sand sources at the fluvial and marine end members, and are characterized by a relatively low energy environment that promotes fine sediment deposition (Dalrymple, Zaitlin, and Boyd 1992). Additionally, the middle portions of estuaries typically exhibit brackish (mesohaline) water (e.g. 15-17 ppt. Pritchard 1967, Dalrymple, Zaitlin, and Boyd 1992). Previous studies have concluded that oysters proliferate most effectively toward the middle of the estuarine salinity gradient at approximately 15 psu. (Soniat and Brody 1988).

The high amplitude reflectors observed in S2 are interpreted to be a product of the density contrast between the articulated oyster shells and the matrix sediment (Fig. 8). The color and texture of the sediment observed in L3 and L4 are very similar. However, L3 shows a significant reduction in sand content and an increase in estuarine muds. This is attributed to its geographic location in the middle of the central basin and the associated environmental conditions at the time of deposition. The layers of articulated oyster shells are interpreted to be oyster reefs that were living at the time of their burial. The onset of oyster reef growth is attributed to the introduction of middle estuarine conditions.

5.5.4 Paleo-Brazos River Pro Delta (L2, S1)

Several previous studies have observed a layer of highly oxidized and fine-grained red clay within cores taken in areas adjacent to the study area, and this sedimentary signature has been attributed to a deposit from a Paleo-Brazos River Pro Delta. (Rodriguez et al. 2004, Israel, Ethridge, and Estes 1987, Bernard et al. 1970). The color and sedimentary content of L2 correlates strongly to the lithofacies identified in these previous studies, and it is therefore interpreted to part of the same deposit (View Appendix A for color photographs of core samples). Lithofacies 2 was observed in cores taken from S1 (Fig. 8). It is interpreted to be a sub-section of low impedance within S1, containing a prominent medium-to-high amplitude reflector. The low impedance is attributed to density contrast between this sediment and the L1 sediment situated

immediately above L2. The prominent reflector is interpreted to be a product of a separate density contrast between the L2 sediment and the shell layer observed therein.

5.5.5 Lower Estuary (L1, S1)

Sand is often transported into the lower estuary through a variety of processes, thus increasing the sand content of lower estuarine sediment (Dalrymple, Zaitlin, and Boyd 1992). Additionally, layers of shell hash frequently deposit in the lower portions of distributary channels associated with tidal inlets (Moslow and Tye 1985). The layers of shell hash with L1 have been previously identified as relict tidal-inlet deposits (Israel, Ethridge, and Estes 1987, Wallace and Anderson 2013). Based on the relatively high sand content, combined with the layers of shell hash, this lithofacies is interpreted to be associated with a lower estuarine environment. The shell hash layers are also interpreted in S1 as continuous and discontinuous, high amplitude reflectors (Figs. 5, 9). The high-amplitude reflectors are interpreted to be a product of the density gradient between the shell layers and the muddy sand of L1.

5.5.6 Oxbow Lake (L1, L2, L5, S3, S6)

The interpreted geometry of the sub feature located in the southwest portion of the study area (Fig. 4) resembles several modern analogues of oxbow lakes located proximal to the study area (i.e., Freshwater Lake and Square Island Lake in Brazoria County, Texas). Seismic Facies 6 is interpreted to be aggradational based upon the heavily structured appearance that suggests upward growth (Fig. 6). The high amplitude

reflectors are interpreted to be products of a density contrast between the sand layers and mud observed in L5. The heavily laminated sediment and subsequent lack of bioturbation in L5 is interpreted to indicate a rapid infilling. Similar laminated sediment has been observed in oxbow lake features in previous studies (Wolfe et al. 2006). The overall geometry of the sub-feature, along with the sedimentary characteristics of its fill, supports an interpretation of a rapidly-filled oxbow lake. Two relatively thin layers of L2 are also observed within L5. The layers' position within the sediment, separated by a layer of L5, suggests that these L2 layers were deposited episodically and allochthonous. They are thus interpreted to be reworked from other locations proximal to the study area in response to storm events reworking and overwashing sediment from the Paleo-Brazos River Pro Delta deposit located elsewehere into the accommodation space provided by the crescent-shaped oxbow lake feature.

Lithofacies 1 is situated immediately above the uppermost L2 layer within the oxbow lake feature (Fig. 6). Lithofacies 1 is differentiated from L5 based on the structure within the sediment. The onset of L1 is marked by a transition to relatively structureless sediment with an increase in shell content. It is also important to note that this is the thickest layer of L1 observed in the study area.

5.6 ^{14}C Analysis and Geochronology

Results from the ^{14}C analyses can be viewed in Table 3. Samples 1 and 5 within the table are considered reworked due to their inverted age in respect to expected stratigraphic position. The remaining dates were plotted according to their age and depth

Table 3. Radiocarbon Results

Index No.	Lab number / Core	Core depth (cm)	Material dated	Conventional ^{14}C age	d^{13}C (‰)	2s calendar ages in yrs. B$_{1950}$ (probability)	1s calendar ages in yrs. B$_{1950}$ (probability)	Calibrated 1s age (yrs. B$_{1950}$)
1*	OS-110799 OC1B	335	Mollusc	4370 ± 30	-1.08	4410-4609 (1)	4443-4550 (1)	4500 ± 50
2	OS-110798 OC1B	358	Foraminifera	3700 ± 25	-1.89	3537-3702 (1)	3569-3653 (1)	3610 ± 40
3	OS-110800 OC1B	918	Mollusc	4400 ± 25	0.45	4435-4652 (0.991) 4666-4675 (0.009)	4503-4601 (1)	4550 ± 50
4	OS-110932 OC1B	1106	Plant/Wood	4070 ± 25	NM	4441-4484 (0.144) 4510-4628 (0.747) 4638-4641 (0.001) 4762-4790 (0.104) 4791-4797 (0.004)	4520-4580 (0.822) 4452-4462 (0.097) 4770-4780 (0.081)	4550 ± 30
5*	OS-113037 SLP27	26	Foraminifera	4970 ± 25	-2.21	5261-5423 (1)	5271-5335 (0.872) 5338-5349 (0.071) 5374-5384 (0.058)	5300 ± 30
6	OS-112785 SLP 27	107	Foraminifera	4270 ± 20	-1.86	4308-4437 (1)	4365-4416 (1)	4390 ± 25
7	OS-110801 SLP 27	246	Mollusc	5970 ± 30	-0.81	6294-6458 (1)	6328-6416 (1)	6370 ± 40
8	OS-110933 SLP 27	412	Plant/Wood	6880 ± 40	-27.52	7620-7795 (0.998) 7814-7816 (0.002)	7669-7751 (1)	7710 ± 40
9	OS-110934 SLP 27	484	Plant/Wood	7060 ± 45	-14.04	7794-7966 (1)	7851-7909 (0.667) 7912-7966 (0.333)	7880 ± 30

*Sample reworked.

41

within the respective core sample (Fig. 10). The assumption that zero depth aligned with present day was used in constructing both age models. A spline interpolation model was used to describe the radiocarbon results from SLP 27, but simple linear interpolation of the radiocarbon results was completed for the fewer results from OCIB results (Fig. 10). These graphs, or age models, were then used to estimate sediment accumulation rates and salient stratigraphic changes downcore.

The interpreted depth of the L8 lower contact was also used to estimate the sediment accumulation rate of this lithofacies. This estimation of this depth (~12 m) was based on the sequence boundary beneath the location of core SLP 27, as interpreted from seismic data (Fig. 8). Subsidence rates, as provided in Paine (1993), were applied to this estimation (~0.01 mm/yr, calculated as ~ 10 cm). It is then assumed that L8 is the lowermost lithofacies within the sequence, and began depositing at the approximate time sea-level reached this elevation. This date is approximated at 9,000 Cal yrs BP, as indicated by the sea-level height (~14 m below modern sea-level) interpreted from the sea-level curve provided in Milliken, Anderson, and Rodriguez (2008a). For the remaining lithofacies, sediment accumulation rates were extrapolated using the respective thicknesses and dates extrapolated from the age models (Fig. 10). A summary of these estimated accumulation rates can be viewed in Table 1.

5.7 Interpreted Flooding Surfaces

A flooding surface is a surface separating younger from older strata where there is evidence of an abrupt increase in water depth (Van Wagoner 1988). Four flooding
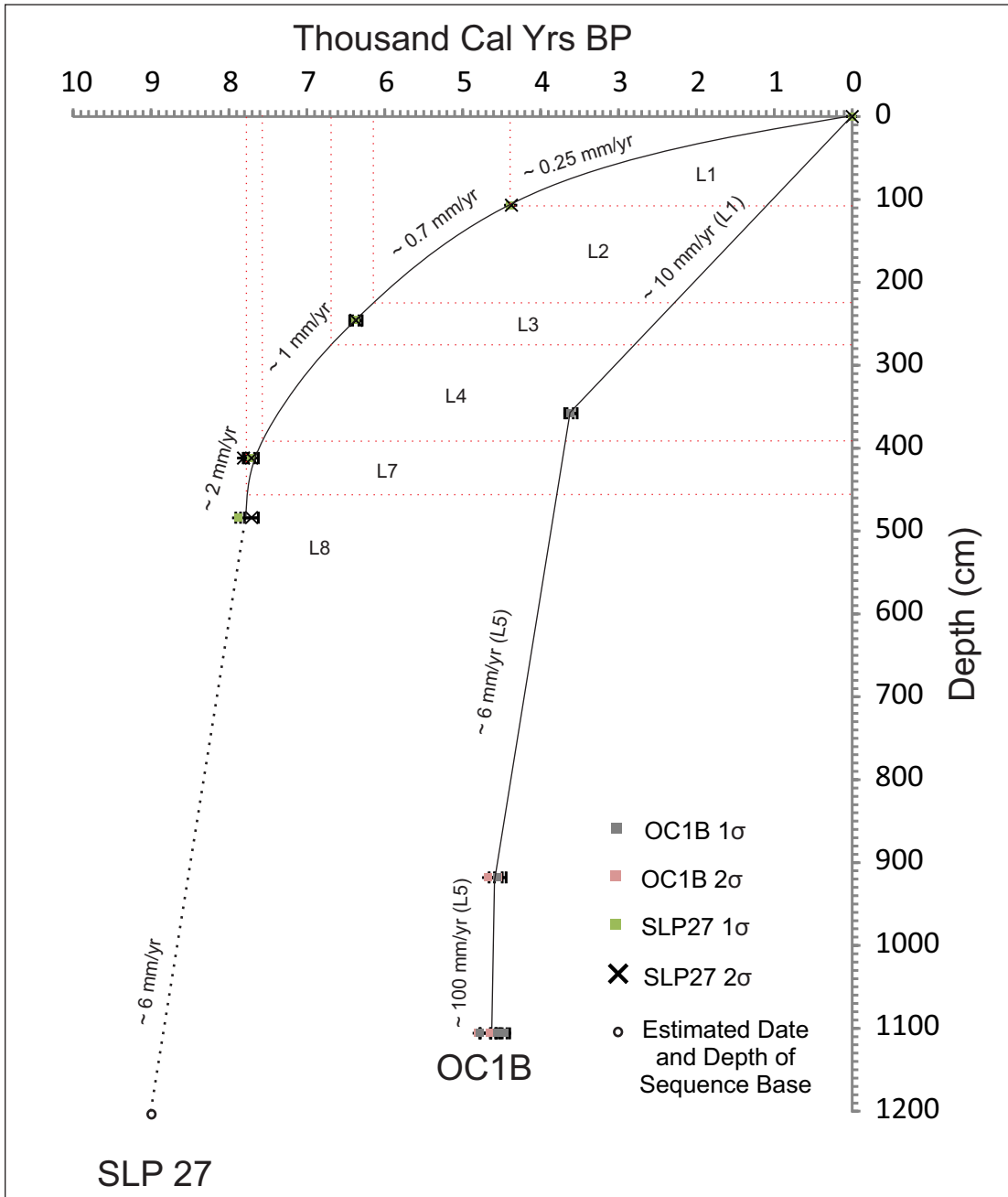
Figure 10: Age Model. Generated using radiocarbon results from cores SLP 27 and OC1B (Table 3). The stratigraphic location of lithofacies boundaries and their respective estimated age are depicted as dotted red lines. Approximated sedimentation rates are depicted in mm/yr. The curved line connecting the radiocarbon results of SLP 27 is a spline interpolation. The estimated sedimentation rate for L8 was determined using the black dotted line. The methods used to construct this age model are explained in greater detail in Section 5.6 of the text.
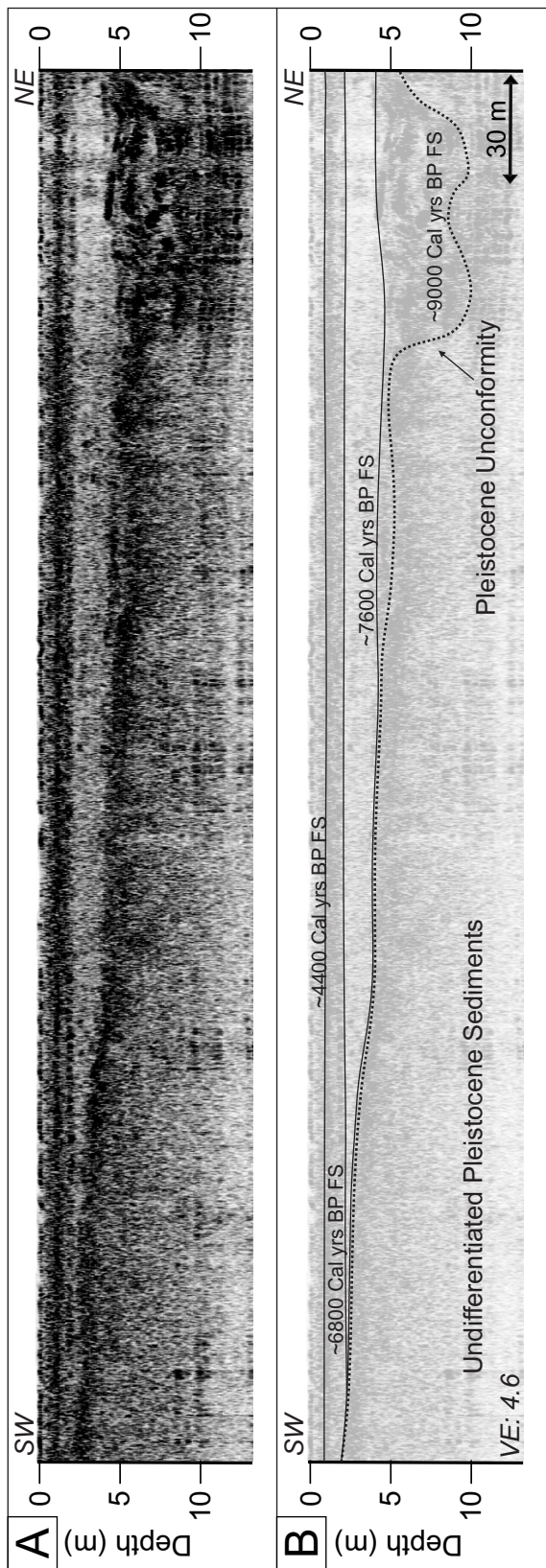
Figure 11: Flooding Surfaces. A. Seismic images and **B.** line drawing interpretation showing the Flooding Surfaces (FS) as they appear in the Chocolate Bayou incised channel and there estimated ages. The ~9,000 Cal. yr. BP FS and Pleistocene Unconformity are depicted as a black dotted line. The location for this seismic section can be seen in Figure 4. VE: Vertical Exaggeration.

surfaces are identified in the stratigraphy of West Bay (Figs. 1 and 2). These flooding

surfaces were interpreted using lithological, seismic, and geochronological data from

this data set, and sea-level data provided in Milliken, Anderson, and Rodriguez (2008a).

Flooding Surface 1 is also identified as the sequence boundary, or PU. This

surface is interpreted to have formed ~9,000 Cal yrs BP as sea-level inundated the

incised channels of the study area (Figs. 11 and 12). This surface is interpreted as the

initial deposition of the paleo bayhead delta.

Flooding Surface 2 (Figs. 11, 12) was formed ~7,600 Cal yrs BP with the

inundation of relatively small channel terraces associated with the incised channels of

the study area. This surface also aligns with the top of the paleo-bayhead delta within the

study area. Throughout much of the study area, this surface marks the transition into

estuarine sedimentation.

Flooding Surface 3 (Figs. 11, 12) was formed ~6,800 Cal yrs BP during the

inundation of the topographical low in the southwest portion of the study area. Within

the topographical low and Chocolate Bayou incised channel, it marks the transition from

upper to middle estuarine sedimentation. Therefore, the transition from upper to middle

estuarine deposition within the Chocolate Bayou incised channel is thought to have been

related to the flooding of the topographical low.

Flooding Surface 4 (Figs. 11, 12) was formed ~4,400 Cal yrs BP with the

inundation of the topographical highs situated on either side of the Halls Bayou incised

channel. This flooding surface is interpreted to align with the lower contact of L1. The
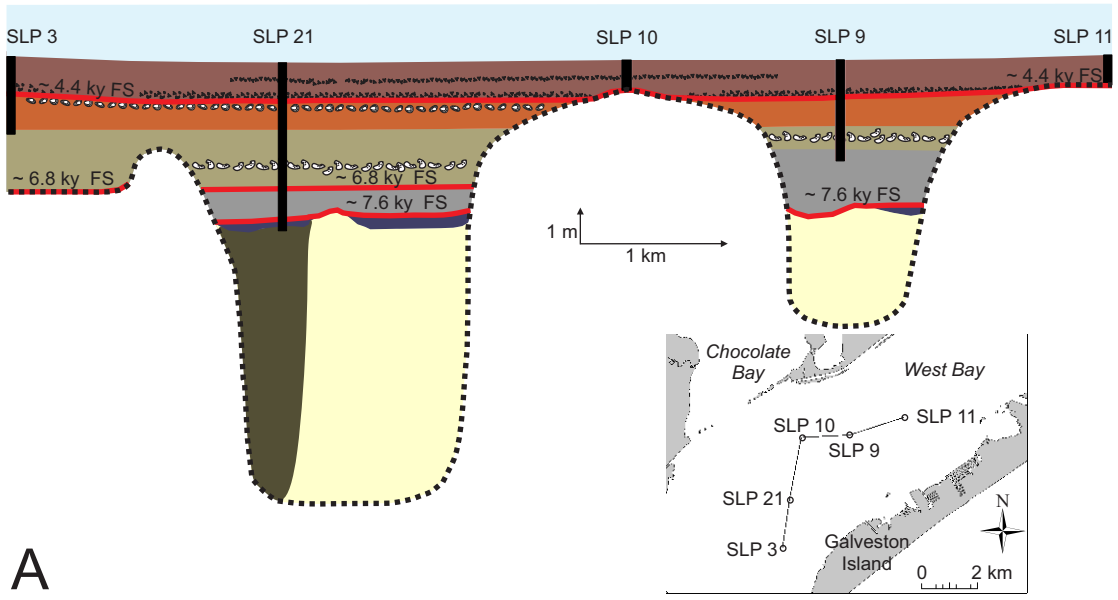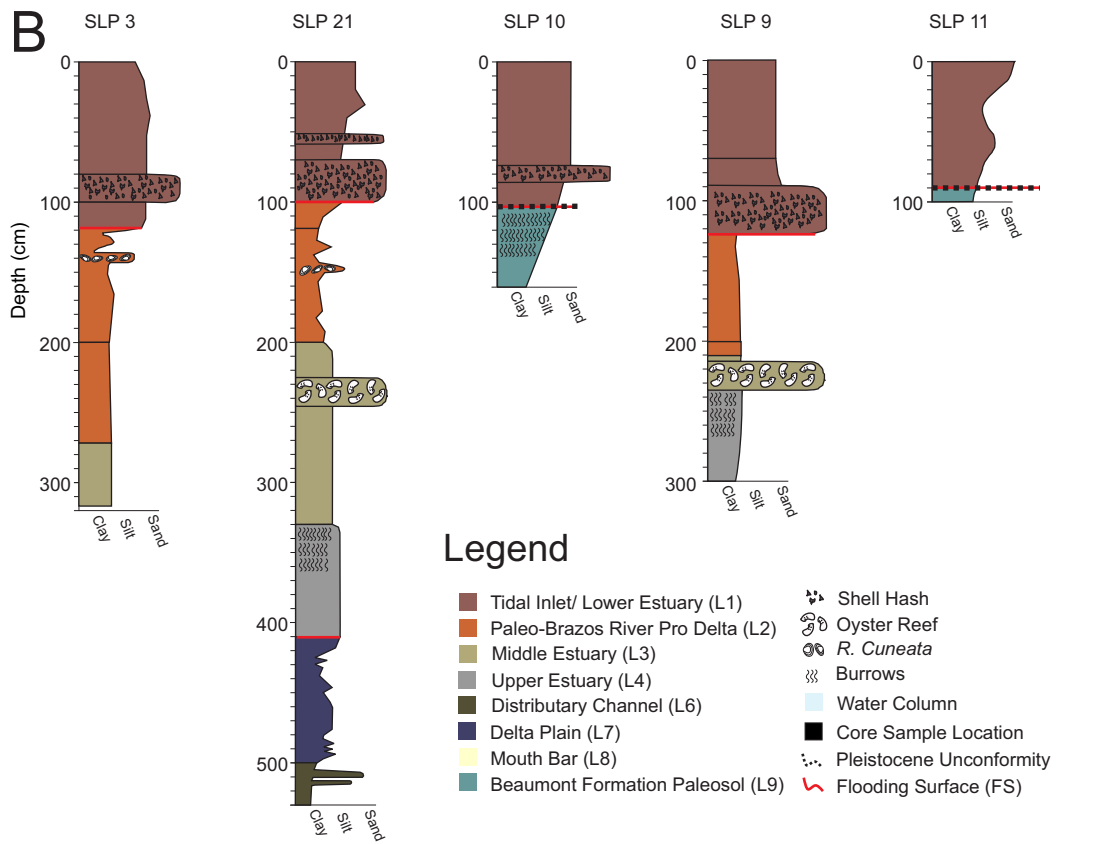
Figure 12: Stratigraphic Cross-Section. A. Idealized illustration combining seismic and core data showing the facies sequence across the study area. **B**. Detailed core descriptions of the individual core samples used in constructing idealized illustration.

46

inception of L1 deposition within West Bay is therefore thought to have been related to the initial flooding of the topographical highs.

5.8 Modeling the Inundation of West Bay

Sea-level is interpreted to have played a fundamental role in the formation and filling of the incised channels observed within West Bay. The sea level curve showing the detailed Holocene RSLR for the NGOM provided in Milliken, et al. (2008) was used extensively in conjunction with the interpolated surface of the PU to establish the timing of channel infilling and flooding events.

For the purpose of visualizing the flooding sequence of West Bay, a series of images were assembled in Fledermaus that model this inundation, based on the interpolated 3-D PU surface and RSLR (Fig. 13). A plain, representing sea level as determined in Milliken, Anderson, and Rodriguez (2008a), was set at a given elevation based on the assessed Cal yrs BP Subsidence was applied uniformly throughout the modeled area, and estimated based on the rates presented in Paine (1993). This model was then used to corroborate the approximate timing of environmental changes observed in the seismic and lithological data.
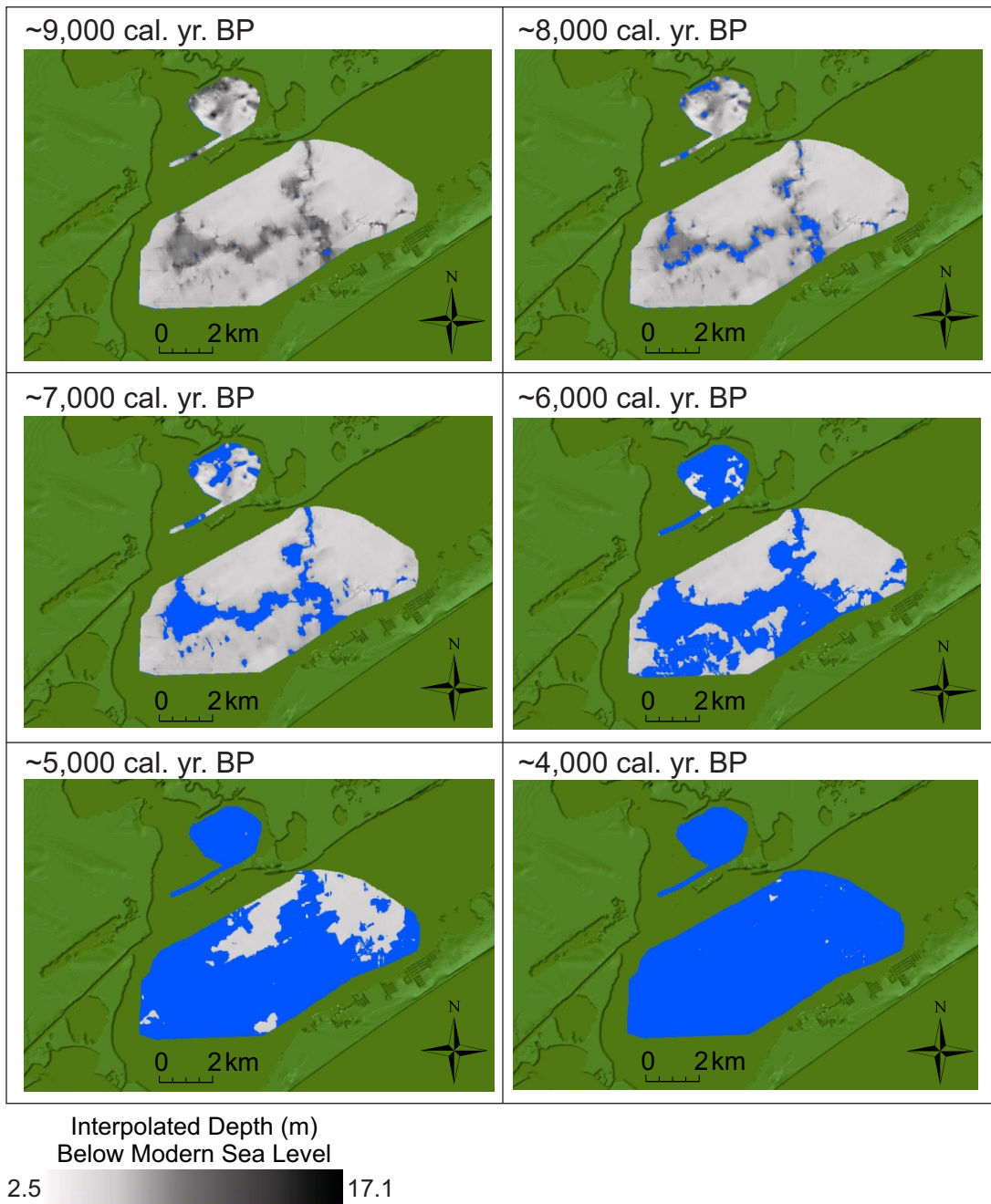
Figure 13: Inundation Model. Screenshots of the model produced in Fledermaus illustrating the inundation of West Bay throughout the Holocene. Blue areas are interpreted to be inundated according to the calibrated time. This model is constrained to the area investigated, and therefore does not predict inundated areas beyond the scope of the seismic survey. The modeled area is depicted in grayscale. The surrounding topography is depicted in green, and included for context only. Sea-level calibrations were completed using data from Milliken, et al. (2008). Subsidence calculations were estimated using rates found in Paine (1993).

6. DISCUSSION

6.1 The Formation of the Chocolate Bayou Incised Channel System

The approximate timing of incision for the incised channels within the study area is assumed to be early Holocene (pre-9000 Cal yrs BP) based on sea level and depth of maximum incision presented in the seismic data. The mechanisms controlling the incision are poorly understood. The Chocolate Bayou incised channel is interpreted as the main trunk based on the size of the channel compared to the smaller Halls and Mustang Bayou incised channels. These smaller channels combined with the main trunk form the Chocolate Bayou Incised Channel System (CBICS). At ~9000 Cal yrs BP, sea level matched the depth of maximum incision at the seaward extent of the CBICS, and it is assumed that at this approximate time sedimentary processes within the channels switched from net-incision to net-deposition.

6.2 Early to Middle Holocene Episodic Flooding in West Bay

In the early stages of channel infilling, the paleo bayhead delta formed within the deepest portions of the Chocolate and Halls Bayou incised channels (Figs. 14, 15). The highest estimated sediment accumulation rate for this deposit (L8, ~6 mm/yr) closely followed RSLR (~5 mm/yr), indicating that the fluvial sediment supply was large enough to cope with a relatively high rate of RSLR. A flooding event occurred at ~7,600 Cal yrs BP, at which time fluvial-dominated deposition abruptly ceased, and the depositional environment transitioned into an estuary. At this point the bayhead delta present in the bottom portion of the CBICS sedimentary fill is assumed to have back-
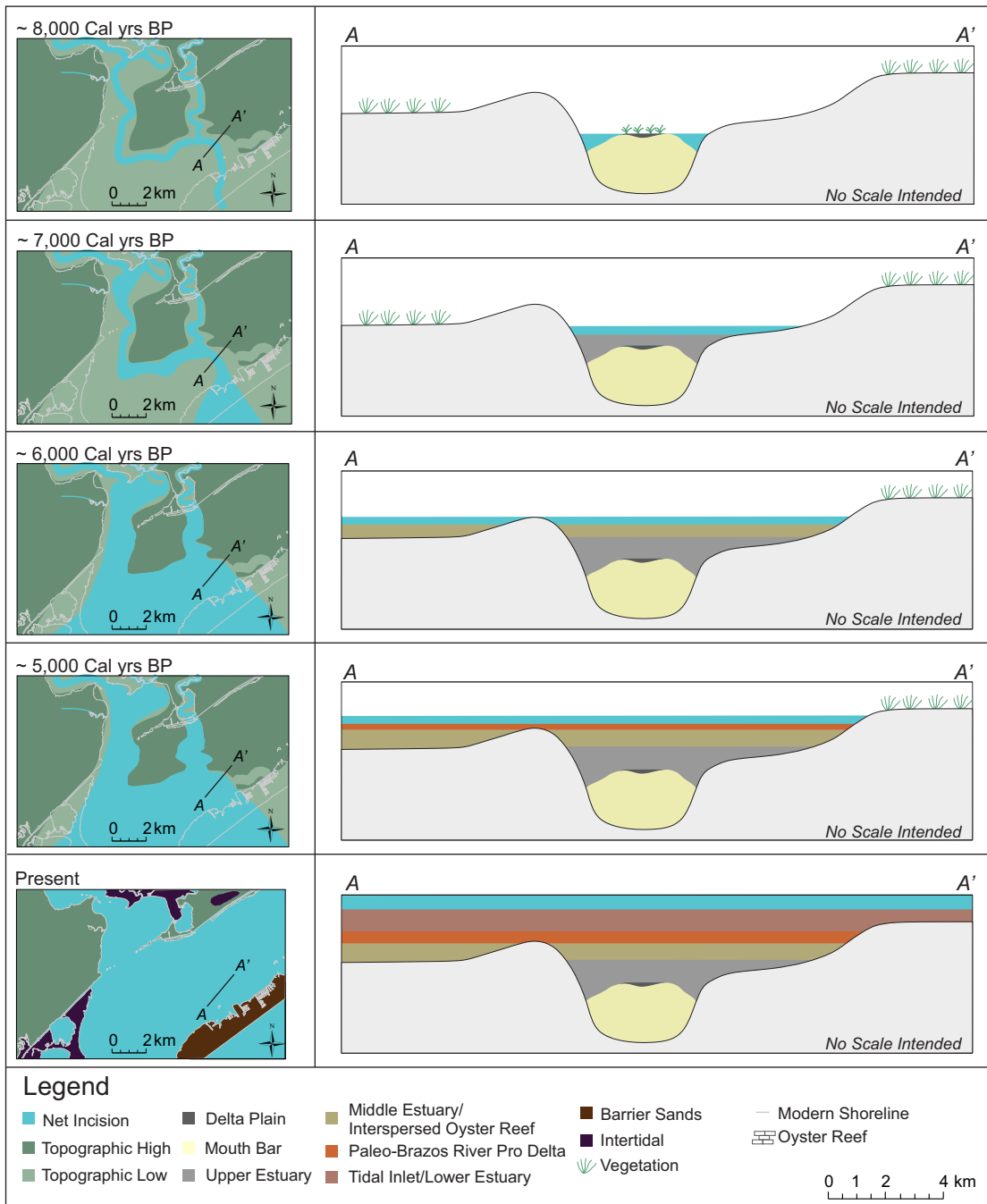
Figure 14: Environmental Changes Reflected in the Stratigraphy of West Bay. The graphic at left in each panel displays the interpreted paleo-geography based on the specific time. The graphic at right in each panel is an idealized illustration showing the changes expressed within the stratigraphy.
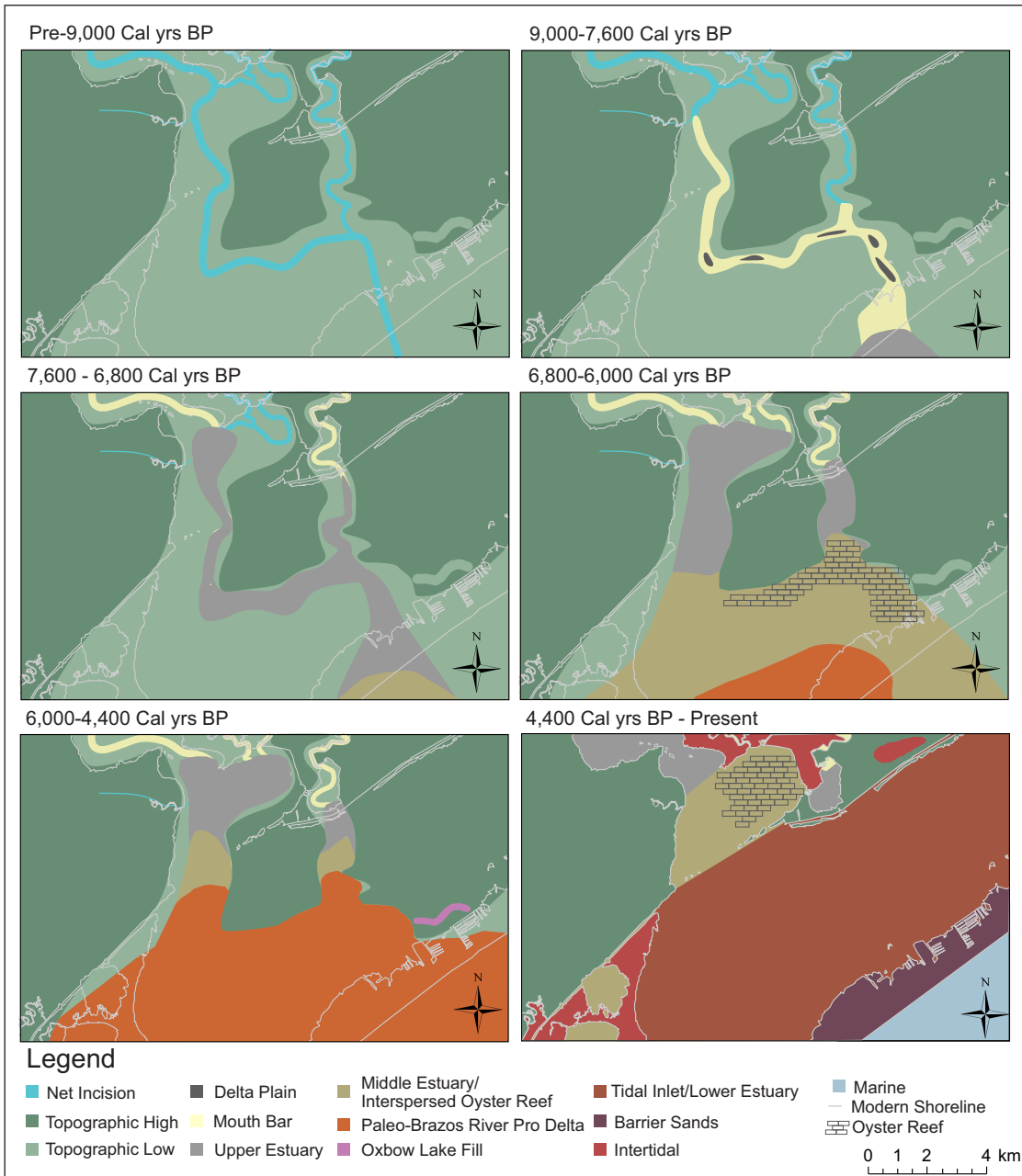
Figure 15: Paleo-Geographic Maps of West Bay. The spatial distribution of depositional environments throughout the Holocene.

stepped to a portion of the CBICS landward of the study area (Fig. 15). Modern

analogues for this feature are either poorly developed or non-existent within the

tributaries associated with the CBICS. The absence of a well-defined bayhead delta

within Chocolate Bayou could be a product of the significant anthropogenic change

caused by the dredging of the Chocolate Bayou navigation channel. However, satellite

imagery predating the navigation channel shows no obvious feature resembling the

bayhead delta present in the seismic and sedimentary data. An alternative hypothesis

might then be a reduction in drainage basin area caused by the landward inundation of

the fluvial system. This would have reduced the erodible area, thus reducing the net-

runoff into Chocolate Bay.

The mechanisms responsible for the initial cessation of fluvial-dominated

sedimentation in the CBICS may be attributed to either (1) an abrupt change in

accommodation volume, (2) a change in the sedimentary budget, or a combination of the

two (Anderson and Rodriguez 2008). The timing of this flooding event in West Bay

closely mimics similar flooding events observed in other estuaries along the NGOM,

including Galveston Bay (Anderson et al. 2008), Sabine Lake (Milliken, Anderson, and

Rodriguez 2008b), the Matagorda and Lavaca estuary complex (Maddox et al. 2008),

and Copano Bay, Texas (Troiani et al. 2011). Evidence is presented in these studies, as

well as Milliken, Anderson, and Rodriguez (2008a), showing a possible episodic rise in

sea level associated with a eustatic event (Bird et al. 2007). This event is attributed to the

rapid deglaciation of the Eastern Nunavut and Southern Quebec regions of the

Laurentide Ice Sheet, which is suspected as contributing to an increase of ~3 mm/yr in

eustatic rates of sea-level rise between 7,600 and 6,800 Cal yrs BP (Carlson et al. 2008).

An alternative interpretation is that the Upper Texas coast has been impacted by Glacial

Isostatic adjustment of the crust in response to loss of the Laurentide Ice Sheet (e.g.,

Milne and Mitrovica, 2008), which may have contributed to some of the observed rapid

flooding in the Study region.

Changes in the sediment supply delivered by the tributaries may have also

contributed to the cessation of fluvial sedimentation. While information concerning the

climate specific to East Texas is scant, significant evidence points to a regional climatic

shift from predominately wet conditions in the early Holocene to drier conditions in the

early-middle Holocene (Toomey III, Blum, and Valastro Jr 1993, Nordt et al. 1994,

Humphrey and Ferring 1994). This shift from a relatively moist to arid climate could

have resulted in a net-reduction in precipitation. Reductions in precipitation have been

shown to reduce erosion and runoff in rivers, and ultimately reduce net-sediment load

carried by a fluvial system (Knox 1983). In Copano Bay, these effects resulted in a

reduced deposition of fluvial sediments during the Holocene (Troiani et al. 2011).

An estuarine sedimentary regime began in the CBICS immediately following the

back-stepping of the bayhead delta during coeval deceleration of sea-level rise from ~ 5

to 2 mm/yr (Figs. 14-15). Fluvial sedimentary input had been greatly reduced, and the

sedimentation rate dropped to ~ 1 mm/yr. The dissimilar sedimentation rates for the

bayhead delta and estuary facies, along with the approximate time of transition, are very

similar to those reported in Galveston Bay (Rodriguez, Anderson, and Simms 2005). An

estuary began to form as RSLR began to outpace sedimentation. At approximately 6,800

Cal yrs BP, low lying areas in the southwest portion of the study area flooded (Figs. 14, 15), marking the beginning of deposition within the southwest portion of the study area (Figs. 14, 15). The geographic area flooded by sea level tripled at this flooding event, creating an open basin that facilitated a more widespread distribution of fluvial sediments and freshwater. Oyster reefs proliferated within the remaining accommodation space of the Chocolate Bayou incised channel in areas proximal to the confluence with the Halls Bayou incised channel (Fig. 15). No evidence of oyster reef deposits was observed in seismic or core data from the topographical lows in the southwest. It is assumed that freshwater provided by the Halls Bayou tributary mixing with the incoming ocean water created ideal brackish conditions for oyster reef development.

6.3 A Brief Return to a Fluvial Environment during the Middle Holocene

Throughout much of the study area, a paleo-Brazos River pro-delta deposit marks a brief hiatus in estuarine sedimentation (Figs. 14, 15). A core sample extracted from a location seaward of this study area for a previous study constrained a ~3 m thick deposit of this facies to between ~4,150 and 7,495 Cal yrs BP (Rodriguez et al. 2004). The facies contains highly oxidized, fine red clay, and is attributed to a paleo-Brazos River tract that flowed through an adjacent fluvial system known as Big Slough and out the modern San Luis Pass (Bartek, Anderson, and Abdulah 1990). Articulated and fragmented *R. Cuneata* shells are consistently found within this facies throughout the southwest portion of the study area. *R. Cuneata* are known to inhabit areas with significant freshwater, and develop poorly in brackish to saline environments (Hopkins

1970). It is therefore thought that the arrival of the paleo-Brazos River temporarily shifted the sedimentary regime in West Bay back to a fluvial environment.

Approximately 12 km off the southwest coast of Galveston Island is a sandy bathymetric high (White et al. 1985) interpreted to be the delta associated with this paleo-Brazos River tract (Bartek, Anderson, and Abdulah 1990). Additional unpublished data collected by the Coastal Geosciences Group at Texas A&M University at Galveston show a significant deposit of this facies immediately seaward of West Galveston Island. This evidence suggests that as the shoreline retreated with RSLR, this delta retreated from its offshore location and became situated in the immediate vicinity of West Bay. The extrapolated time for the initial deposition of this facies at the seaward boundary of the study area is ~ 6,100 Cal yrs BP. This suggests that the paleo-Brazos River pro delta began depositing at the current location of San Luis Pass, and prograded eastward into the study area for ~1400 years, at a rate of ~5 m/yr, until reaching the seaward extent of the CBICS.

The Brazos River drains ~44,788 sq. miles (116,000 km^2) and discharges on average 8,387 ft^3/s (238 m^3/s) of freshwater (USGS 2014). Salinity gradient modification and increased suspended sediment can cause a catastrophic population collapse within estuarine oyster communities (Wells 1961). Sediment accumulation rates (~0.7 mm/yr, Fig. 6) for this facies are thought to have been limited by accommodation space as the delta prograded into the study area following sea level. The fine clay found within this facies is thought to have created a cloud of suspended sediment within the water column that resulted in uninhabitable conditions for oyster communities. Additionally, the

modern Brazos River delivers to the coast 100-200 times more freshwater than the modern Chocolate Bayou fluvial system (USGS 2014). It is therefore thought that this brief influx of freshwater and suspended sediment from the paleo-Brazos River resulted in the death and burial of many or all living oyster reefs in the area. Stream-piracy redirected the Brazos River away from the study area by ~4,000 Cal yrs BP (Rodriguez et al. 2004, Bartek, Anderson, and Abdulah 1990).

6.4 Late Holocene Flooding Event

Galveston Island began prograding westward into the study area ~ 5,000 Cal yrs BP (Bernard et al. 1970). At ~4,400 Cal yrs BP, the topographical highs located in the central and eastern portions of the study area flooded, and the current configuration of West Bay began to take shape (Figs. 14, 15). The extent of flooding within the current boundaries of West Bay east of the study area was not determined in this study. Inundated areas within the range of this data set increased by ~75% during the flooding event at 4,400 Cal yrs BP. If this event established connectivity of West Bay with the larger Galveston Bay and flooded the majority of the area presently occupied by West Bay, then the estimated increase in inundated areas could be as high as 200%.

At the approximate timing of Flooding Surface 4 (Figs. 11,12), an ephemeral tidal inlet existed where the CBICS intersects the modern Galveston Island (Wallace, Anderson, and Fernández 2010). This ephemeral tidal inlet then migrated west until stabilizing in its current configuration within the paleo-Brazos River incised valley (Wallace and Anderson 2013, Bernard et al. 1970). In cores collected from the study

area, L1 is situated directly above the upper contact of the paleo-Brazos River pro-delta

deposit. In cores collected within the seaward-most portion of the CBICS, the upper

contact of the L2 is erosional, whereas this same contact appears gradational in cores

collected from the landward portion of the CBICS. This can be attributed to erosional

processes associated with tidal exchange through the early tidal inlet. The shell hash

layers of L1 are considered to be associated with tidal inlet channels or storm overwash

(Israel, Ethridge, and Estes 1987, Wallace and Anderson 2013). These shell layers

appear throughout the CBICS and southwest terrace, but do not appear in cores collected

from sediment overlying the inundated upland areas. This suggests that the ephemeral

inlet initially developed within the CBICS and most likely did not exist any further east.

The westerly distribution of these shell layers supports the previously assumed direction

of migration for this ephemeral inlet asserted in Wallace and Anderson (2013).

Determining the exact time of the inlet formation using ^{14}C dating techniques is

difficult due to an abundance of reworked material at its lowermost contact, which

biases the radiocarbon results on shells to older ages. The thick layers of reworked shell

hash are indicative of a high energy environment that existed over the relatively broad,

western portion of the study area. The initial deposition of this facies could indicate the

initial connectivity of West Bay with Galveston Bay.

As the inlet migrated west, its overwhelming influence on the sedimentation

within West Bay was reduced, and other processes began to take over. Lithofacies 1 is

heavily mixed and contains significant amounts of sand thought to be sourced from

storm overwash events that have breached the western 7 km of Galveston Island

throughout the past 2,500 years (Gibeaut, Anderson, and Dellapenna 2004), and advection through the migrating tidal inlet and San Luis Pass. The sediment supplied from these processes, and any fluvial sediment entering West Bay from Chocolate Bay, have produced an approximate sediment accumulation rate of ~0.25 mm/yr. This has been outpaced over two-fold by RSLR, and has resulted in the establishment of the back barrier lagoon configuration of West Bay.

6.5 The Significance of the Oxbow Lake

At ~4,550 Cal yrs BP, deposition began within the accommodation space of the crescent-shaped Oxbow Lake. This is attributed to sea level inundating the topography surrounding the lake, and subsequently filling the lake through a combination of background fine-grained sedimentation (silts and clays) and coarse-grained (sand) event sedimentation. Previous work has detailed how overwash events associated with temporary elevations in base level, such as river floods or tidal surges, can result in highly stratified stratigraphy within small coastal basins (van Hengstum et al. 2014, Wolfe et al. 2006, Lane et al. 2011). This occurs as a process of reworking sediment from the surrounding topography and depositing it within the basin. Small coastal basins capable of preserving event sedimentation are significant, as they have proven to be valuable sources of Holocene climate data (Lane et al. 2011, Liu and Fearn 2000, McCloskey and Keller 2009, van Hengstum et al. 2014, Wallace et al. 2014).

The case for the Oxbow Lake being filled with reworked sediments is supported by the appearance of two layers of L2 in the upper reaches of L5. The deposition of L2

(Paleo-Brazos River prodelta) ceased in the study area by ~4,400 Cal yrs BP, but two layers of L2 appear ~800 years younger (later) in the stratigraphy from the Oxbow Lake. Sample 1 in Table 3 is an articulated mollusk extracted from one of the L2 layers observed in the Oxbow Lake. Although articulated, this specimen is considered reworked due to its age (~4,500 Cal yrs BP) in respective to its stratigraphic position. However, the age of this specimen closely correlates to the upper contact of L2, as dated in core SLP 27. It is possible that this mollusk originally lived within L2 sediments, in or proximal to the study area, and was reworked into the Oxbow Lake basin during the same event sedimentation that deposited the layer of L2 in which it was found. Although not explored further in this study, sediments in small flooded coastal lakes such as obseved in West Bay may contain high-resolution records of climate or storm variability for the Upper Texas Coast in the mid- to late Holocene.

Lithofacies 1 is significantly thicker (~300%) in the Oxbow Lake than other parts of the study area. Elsewhere in the study area, L1 was shown to have a sedimentation rate of 0.25 mm/yr. The rate observed in the Oxbow Lake was estimated up to 10 mm/yr. These contrast rates, combined with the relative differences in thickness, suggests that the sedimentation rate of L1 was not merely a product of supply, but perhaps also accommodation space.

7. SUMMARY AND CONCLUSIONS

Using lithological, seismic, and geochronological data, a detailed reconstruction of the Holocene depositional history of West Bay was assimilated. A synthesis of this data reveals that:

1. West Bay began as a drainage network of incised channels located on the periphery of the Brazos River incised valley.

2. The western half of West Bay experienced significant flooding events at ~7,600 Cal yrs BP, ~6,800 Cal yrs BP, and ~4,400 Cal yrs BP. Each of these flooding events resulted in a spatial increase of inundation and a dramatic reorganization of depositional environments.

3. The Paleo-Brazos River flowed into the area ~6,100-4,400 Cal yrs BP, resulting in a significant pro-delta deposit that decimated the oyster populations of West Bay. This environmental change is most likely related to sea-level rise and stream-piracy, as interpreted in this study and previous work.

4. The flooding event occurring at ~7,600 Cal yrs BP may be attributed to a variety of mechanisms, including accommodation increases, climate change, and sedimentary budget changes. Similar flooding events occurring at approximately the same time have been observed in estuaries throughout the NGOM.

5. The flooding events occurring at ~6,800 and ~4,400 Cal yrs BP are unique to West Bay, and were most likely were a product of sea-level rise interacting with the antecedent topography.

While the Holocene flooding histories of large estuaries within the NGOM are well documented, smaller systems such as West Bay are largely overlooked. Several systems analogous to West Bay exist in the NGOM (e.g. Bay St. Louis, MS; Back Bay of Biloxi, MS; East St. Andrew Bay, FL), and along the North American Atlantic Coast (e.g. St. Simons Sound, GA). Each of these estuaries is also the location of coastal communities, economically important fisheries, and/or industrial complexes. Understanding how these systems will respond to accelerated sea-level rise will improve our ability to predict which currently-established areas will be affected by sea-level rise in the near future, and improve our ability to build sustainable coastal infrastructures. This study has provided an effective model for how a small coastal system responds to varying rates of sea-level rise, and the underlying mechanisms that control the changes incurred.

REFERENCES

Allen, G. P., and H. W. Posamentier. 1993. "Sequence stratigraphy and facies model of an incised valley fill: the Gironde estuary, France." *Journal of Sedimentary Research* 63 (3):378-391.

Anderson, J. B. 2007. *The Formation and Future of the Upper Texas Coast*. College Station: Texas A&M Press.

Anderson, J. B., K. C. Abdulah, S. Sarzalejo, F. Siringan, and M. A. Thomas. 1996. "Late Quaternary sedimentation and high-resolution sequence stratigraphy of the east Texas shelf." *Geological Society, London, Special Publications* 117 (1):95-124.

Anderson, J. B., A. Rodriguez, K. C. Abdulah, R. H. Fillon, L. A. Banfield, H. A. McKeown, and J.S. Wellner. 2004. *Late Quaternary Stratigraphic Evolution of the Northern Gulf of Mexico Margin: A Synthesis*. Vol. No. 29, *SEPM (Society for Sedimentary Geology) Special Publication*. Tulsa, Oklahoma.

Anderson, J. B., and A. B. Rodriguez. 2008. *Response of Upper Gulf Coast Estuaries to Holocene Climate Change and Sea-Level Rise*. Vol. 443, *Special Papers*. Boulder, Colorado: Geological Society of America.

Anderson, J. B., A. B. Rodriguez, K. T. Milliken, and M. Taviani. 2008. "The Holocene evolution of the Galveston estuary complex, Texas: evidence for rapid change in estuarine environments." In *Response of Upper Gulf Coast Estuaries to Holocene Climate Change and Sea-Level Rise*, 89-104. Boulder, Colorado: Geological Society of America.

Anderson, J. B., D. J. Wallace, A. R. Simms, A. B. Rodriguez, and K. T. Milliken. 2014. "Variable response of coastal environments of the northwestern Gulf of Mexico to sea-level rise and climate change: Implications for future change." *Marine Geology* 352:348-366.

Bartek, L. R., J. B. Anderson, and K. C. Abdulah. 1990. "The importance of overstepped deltas and interfluvial sedimentation in the transgressive systems tract of high sediment yield depositional systems—Brazos–Colorado deltas, Texas." Sequence Stratigraphy as an Exploration Tool: Concepts and Practices in the Gulf Coast: SEPM, Gulf Coast Section, 11th Annual Research Conference, Program and Abstracts.

Bates, C. C. 1953. "Rational theory of delta formation." *AAPG Bulletin* 37 (9):2119-2162.

Bates, R. L, and J. A. Jackson. 1984. *Dictionary of Geological Terms*. Vol. 584. Garden City, New York: Random House LLC.

Bernard, H. A., C. F. Major Jr, and B. S. Parrott. 1959. "The Galveston barrier island and environs: a model for predicting reservoir occurrence and trend." *Gulf Coast Association of Geological Societies Transactions* 9:221-224.

Bernard, H. A., C. F. Major Jr, B. S. Parrott, and R. J. LeBlanc. 1970. *Recent sediments of southeast Texas-a field guide to the Brazos alluvial and deltaic plains and the Galveston barrier island complex*. Vol. 11, *Guidebooks*. University of Texas at Austin: Bureau of Economic Geology.

Bird, M. I., L. K. Fifield, T. S. Teh, C. H. Chang, N. Shirlaw, and K. Lambeck. 2007. "An inflection in the rate of early mid-Holocene eustatic sea-level rise: A new sea-level curve from Singapore." *Estuarine, Coastal and Shelf Science* 71 (3–4):523-536.

Boyd, R., R. W. Dalrymple, and B. A. Zaitlin. 1994. *Incised-Valley Systems: Origin and Sedimentary Sequences*. Vol. 51, *Special Publication*. Tulsa, Oklahoma: SEPM (Society for Sedimentary Geology).

Boyd, R., R. W. Dalrymple, and B. A. Zaitlin. 2006. "Estuarine and incised-valley facies models." In *Facies Models Revisted*, 171-235. Tulsa, Oklahoma: SEPM (Society for Sedimentary Geology).

Carlson, A. E., A. N. LeGrande, D. W. Oppo, R. E. Came, G. A. Schmidt, F. S. Anslow, J. M. Licciardi, and E. A. Obbink. 2008. "Rapid early Holocene deglaciation of the Laurentide ice sheet." *Nature Geoscience* 1 (9):620-624.

Dalrymple, R. W. 2006. "Incised valleys in time and space: an introduction to the volume and an examination of the controls on valley formation and filling." In *Incised Valleys in Time and Space*, 5-12. Tulsa, Oklahoma: SEPM (Society for Sedimentary Geology).

Dalrymple, R. W., B. A. Zaitlin, and R. Boyd. 1992. "Estuarine facies models: conceptual basis and stratigraphic implications: perspective." *Journal of Sedimentary Research* 62 (6):1130-1146.

Danielsen, F., M. Sørensen, M. Olwig, V. Selvam, F. Parish, N. Burgess, T. Hiraishi, V. Karunagaran, M. Rasmussen, L. Hansen, A. Quarto, and N. Suryadiputra. 2005.

"The Asian tsunami: A protective role for coastal vegetation." *Science* 310 (5748):643. doi: 10.1126/science.1118387.

Davis Jr, R., M. Andronaco, and J. Gibeaut. 1989. "Formation and development of a tidal inlet from a washover fan, west-central Florida coast, U.S.A." *Sedimentary Geology* 65 (1–2):87-94.

Davis, R., S. Knowles, and M. Bland. 1989. "Role of hurricanes in the Holocene stratigraphy of estuaries; examples from the Gulf Coast of Florida." *Journal of Sedimentary Research* 59 (6):1052-1061.

Day, J., D. Boesch, E. Clairain, G. Kemp, S. Laska, W. Mitsch, K. Orth, H. Mashriqui, D. Reed, L. Shabman, C. Simenstad, B. Streever, R. Twilley, C. Watson, J. Wells, and D. Whigham. 2007. "Restoration of the Mississippi Delta: Lessons from Hurricanes Katrina and Rita." *Science* 315 (5819):1679-1684.

Donnelly, J. P., J. Butler, S. Roll, M. Wengren, and T. Webb. 2004. "A backbarrier overwash record of intense storms from Brigantine, New Jersey." *Marine Geology* 210 (1-4):107-121.

Edmonds, D., and R. Slingerland. 2007. "Mechanics of river mouth bar formation: Implications for the morphodynamics of delta distributary networks." *Journal of Geophysical Research* 112 (F2).

Foyle, A., and G. Oertel. 1997. "Transgressive systems tract development and incised-valley fills within a Quaternary estuary-shelf system: Virginia inner shelf, USA." *Marine Geology* 137 (3):227-249.

Frey, R., and P. Basan. 1978. "Coastal salt marshes." In *Coastal Sedimentary Environments*, 101-169. New York: Springer.

Friedman, G., J. Sanders, and D. Kopaska-Merkel. 1992. *Principles of Sedimentary Deposits: Stratigraphy and Sedimentology* New York: Macmillan Publishing Company.

Gabrysch, R. 1976. "Land-surface subsidence in the Houston-Galveston region, Texas." In *Proceedings of the Anaheim Symposium*, 17-24. Anaheim, California: International Association of Hydrological Sciences.

Galloway, D., D. Jones, and S. Ingebritsen. 1999. "Houston-Galveston, Texas." In *Land Subsidence in the United States*, 35-48. Reston, VA: US Geological Survey

Garcia-Gil, S., F. Vilas, and A. Garcia-Garcia. 2002. "Shallow gas features in incised-valley fills (Rıa de Vigo, NW Spain): a case study." *Continental Shelf Research* 22 (16):2303-2315.

Garrison Jr, J., and T. van den Bergh. 2006. "Effects of sedimentation rate, rate of relative rise in sea level, and duration of sea-level cycle on the filling of incised valleys: examples of filled and overfilled incised valleys from the Upper Ferron Sandstone, Last Chance Delta, East-Central Utah." In *Incised Valleys in Time and Space*, 239-280. Tulsa, Oklahoma: SEPM (Society for Sedimentary Geology).

Gibeaut, J., J. Anderson, and T. Dellapenna. 2004. "Living with Geohazards on Galveston Island: A Preliminary Report with Recommendations." University of Texas Accessed July 2. http://www.beg.utexas.edu/coastal/GalvHazIdx.php.

Haer, T., E. Kalnay, M. Kearney, and H. Moll. 2013. "Relative sea-level rise and the conterminous United States: Consequences of potential land inundation in terms of population at risk and GDP loss." *Global Environmental Change* 23 (6):1627-1636.

Hall, G. 1976. "Sediment transport processes in the nearshore waters adjacent to Galveston Island and Bolivar Peninsula." PhD, Texas A&M University.

Hayes, C., and W. Kennedy. 1903. *Oil Fields of the Texas-Louisiana Gulf Coastal Plain*, *USGS Bulletin*. Washington D.C.: Government Printing Office.

Hayes, M., and D. FitzGerald. 2013. "Origin, evolution, and classification of tidal inlets." *Journal of Coastal Research* 69 (SP1):14-33.

Henry, W. 1979. "Some aspects of the fate of cold fronts in the Gulf of Mexico." *Monthly Weather Review* 107 (8):1078-1082.

Hopkins, J. 1985. "Channel-fill deposits formed by aggradation in deeply scoured, superimposed distributaries of the Lower Kootenai Formation (Cretaceous)." *Journal of Sedimentary Research* 55 (1):45-52.

Hopkins, S. 1970. "Studies on brackish water clams of the genus Rangia in Texas." In *Proceedings of the National Shellfisheries Association*, 5-6. Easton, Maryland: Economy Printing Company.

Howard, R., and S. Whitaker. 1990. "Fluvial-estuarine valley fill at the Mississippian-Pennsylvanian unconformity, Main Consolidated field, Illinois." In *Sandstone Petroleum Reservoirs*, 319-341. Springer.

Humphrey, J., and C. Ferring. 1994. "Stable isotopic evidence for latest Pleistocene and Holocene climatic change in north-central Texas." *Quaternary Research* 41 (2):200-213.

INEOS. 2014. "The Word for Chemicals." INEOS Group Limited Accessed September 22. http://www.ineos.com/businesses/ineos-olefins-polymers-usa/sites/.

Israel, A., F. Ethridge, and E. Estes. 1987. "A sedimentologic description of a microtidal, flood-tidal delta, San Luis Pass, Texas." *Journal of Sedimentary Research* 57 (2):288-300.

Kemp, A., B. Horton, S. Culver, D. Corbett, O. van de Plassche, W. Gehrels, B. Douglas, and A. Parnell. 2009. "Timing and magnitude of recent accelerated sea-level rise (North Carolina, United States)." *Geology* 37 (11):1035-1038.

Knox, J. 1983. "Responses of river systems to Holocene climates." *Late Quaternary Environments of the United States* 2:26-41.

Kolker, A., M. Allison, and S. Hameed. 2011. "An evaluation of subsidence rates and sea-level variability in the northern Gulf of Mexico." *Geophysical Research Letters* 38 (21).

Lane, P., J. Donnelly, J. Woodruff, and A. Hawkes. 2011. "A decadally-resolved paleohurricane record archived in the late Holocene sediments of a Florida sinkhole." *Marine Geology* 287 (1-4):14-30.

Lankford, R., and J. Rogers. 1969. *Holocene Geology of the Galveston Bay Area*. Houston, Texas: Houston Geological Society.

Lin, C., L. Gu, G. Li, Y. Zhao, and W. Jiang. 2004. "Geology and formation mechanism of late Quaternary shallow biogenic gas reservoirs in the Hangzhou Bay area, eastern China." *AAPG Bulletin* 88 (5):613-625.

Liu, K., and M. Fearn. 2000. "Reconstruction of prehistoric landfall frequencies of catastrophic hurricanes in northwestern Florida from lake sediment records." *Quaternary Research* 54 (2):238-245.

Loder, N. 2008. "An evaluation of the potential of coastal wetlands for hurricane surge and wave energy reduction." PhD Dissertation, Texas A&M University.

Maddox, J., J. Anderson, K. Milliken, A. Rodriguez, T. Dellapenna, and L. Giosan. 2008. "The Holocene evolution of the Matagorda and Lavaca estuary complex, Texas, USA." In *Response of Upper Gulf Coast Estuaries to Holocene Climate Change and Sea-Level Rise*, 105-119. Geological Society of America.

Mallinson, D., C. Smith, S. Mahan, S. Culver, and K. McDowell. 2011. "Barrier island response to late Holocene climate events, North Carolina, USA." *Quaternary Research* 76 (1):46-57.

McCall, P. 1982. *Animal-Sediment Relations: the Biogenic Alteration of Sediments*. Vol. 2. New York: Springer.

McCloskey, T. , and G. Keller. 2009. "5000 year sedimentary record of hurricane strikes on the central coast of Belize." *Quaternary International* 195 (1–2):53-68.

McEwen, M. 1969. "Sedimentary facies of the modern Trinity delta." In *Holocene Geology of the Galveston Bay Area*, 53-77. Houston, Texas: Houston Geological Society.

McKinney, L., M. Hightower, B. Smith, D. Beckett, and A. Green. 1989. "Management issues: Galveston Bay." In *NOAA Estuary of the Month*, 79-87. Washington D.C.: US Department of Commerce.

Milliken, K., J. Anderson, and A. Rodriguez. 2008a. "A new composite Holocene sea-level curve for the northern Gulf of Mexico." In *Response of Upper Gulf Coast Estuaries to Holocene Climate Change and Sea-Level Change*, 1-11. Boulder, Colorado: The Geological Society of America

Milliken, K., J. Anderson, and A. Rodriguez. 2008b. "Tracking the Holocene evolution of Sabine Lake through the interplay of eustasy, antecedent topography, and sediment supply variations, Texas and Louisiana, USA." In *Response of Upper Gulf Coast Estuaries to Holocene Climate Change and Sea-Level Change*, 65-88. Boulder, Colorado: The Geological Society of America

Morton, R. . 1994. "Texas Barriers." In *Geology of Holocene Barrier Island Systems*, 75-114. New York: Springer.

Morton, R., J. Bernier, and J. Barras. 2006. "Evidence of regional subsidence and associated interior wetland loss induced by hydrocarbon production, Gulf Coast region, USA." *Environmental Geology* 50 (2):261-274.

Morton, R., and J. McGowen. 1980. *Modern depositional environments of the Texas coast*, *Guidebook*. University of Texas at Austin: Bureau of Economic Geology.

Moslow, T., and R. Tye. 1985. "Recognition and characterization of Holocene tidal inlet sequences." *Marine Geology* 63 (1–4):129-151.

Nichol, S., R. Boyd, and S. Penland. 1996. "Sequence stratigraphy of a coastal-plain
   incised valley estuary: Lake Calcasieu, Louisiana." *Journal of Sedimentary
   Research* 66 (4).

Nordt, L., T. Boutton, C. Hallmark, and M. Waters. 1994. "Late Quaternary vegetation
   and climate changes in central Texas based on the isotopic composition of
   organic carbon." *Quaternary Research* 41 (1):109-120.

Oertel, G. 1985. "The barrier island system." *Marine Geology* 63 (1–4):1-18.

Olariu, C., and J. Bhattacharya. 2006. "Terminal distributary channels and delta front
   architecture of river-dominated delta systems." *Journal of Sedimentary Research*
   76 (2):212-233.

Otvos, E. 1970. "Development and migration of barrier islands, northern Gulf of
   Mexico." *Geological Society of America Bulletin* 81 (1):241-246.

Paine, J. 1993. "Subsidence of the Texas coast: inferences from historical and late
   Pleistocene sea levels." *Tectonophysics* 222 (3):445-458.

Palinkas, C., C. Nittrouer, R. Wheatcroft, and L. Langone. 2005. "The use of 7Be to
   identify event and seasonal sedimentation near the Po River delta, Adriatic Sea."
   Marine Geology 222–223 (0):95-112.

Peijs-van Hilten, M., T. Good, and B. Zaitlin. 1998. "Heterogeneity modeling and
   geopseudo upscaling applied to waterflood performance prediction of an incised
   valley reservoir: Countess YY Pool, southern Alberta, Canada." *AAPG bulletin*
   82 (12):2220-2245.

Perillo, G. 1995. "Definitions and Geomorphologic Classifications of Estuaries." In *Developments in Sedimentology*, edited by G. M. E. Perillo, 17-47. Elsevier.

Port of Houston Authority of Harris County, TX. 2012. "Port of Houston." Accessed September 23. www.portofhouston.com/.

Posamentier, H., and P. Vail. 1988. "Eustatic controls on clastic deposition II—sequence and systems tract models." In *Sea-Level Changes - An Integrated Approach*, 125-154. SEPM (Society for Sedimentary Geology).

Pritchard, D. 1967. "What is an estuary: physical viewpoint." *Estuaries* 83:3-5.

Purser, K., R. Liebert, and C. Russo. 1980. "MACS; an accelerator-based radioisotope measuring system." *Radiocarbon* 22 (3):794-806.

Reimer, P., E. Bard, A. Bayliss, J. Beck, P. Blackwell, C. Ramsey, C. Buck, H. Cheng, R. Edwards, and M. Friedrich. 2013. "IntCal13 and Marine13 radiocarbon age calibration curves 0–50,000 years cal BP." *Radiocarbon* 55 (4):1869-1887.

Rodriguez, A., J. Anderson, and A. Simms. 2005. "Terrace inundation as an autocyclic mechanism for parasequence formation: Galveston Estuary, Texas, USA." *Journal of Sedimentary Research* 75 (4):608-620.

Rodriguez, A., J. Anderson, F. Siringan, and M. Taviani. 2004. "Holocene evolution of the east Texas coast and inner continental shelf: along-strike variability in coastal retreat rates." *Journal of Sedimentary Research* 74 (3):405-421.

Rodriguez, A., D. Duran, C. Mattheus, and J. Anderson. 2008. "Sediment accommodation control on estuarine evolution: An example from Weeks Bay, Alabama, USA." *Geological Society of America Special Papers* 443:31-42.

Rodriguez, A., A. Simms, and J. Anderson. 2010. "Bay-head deltas across the northern
    Gulf of Mexico back step in response to the 8.2 ka cooling event." *Quaternary
    Science Reviews* 29 (27):3983-3993.

Schumm, S. 1994. "Origin, evolution and morphology of fluvial valleys." In *Incised-
    Valley Systems: Origin and Sedimentary Sequences*. Tulsa, Oklahoma: SEPM
    (Society for Sedimentary Geology).

Sheriff, R., and M. Sheriff. 1980. *Seismic Stratigraphy*. Boston: International Human
    Resources Development Corporation.

Simms, A., J. Anderson, Z. Taha, and A. Rodriguez. 2006. "Overfilled versus underfilled
    incised valleys: examples from the Quaternary Gulf of Mexico." In *Incised
    Valleys in Time and Space*. Tulsa, Oklahoma: SEPM (Society for Sedimentary
    Geology).

Simms, A., N. Aryal, L. Miller, and Y. Yokoyama. 2010. "The incised valley of Baffin
    Bay, Texas: a tale of two climates." *Sedimentology* 57 (2):642-669.

Simpson, R., and H. Riehl. 1981. *The Hurricane and its Impact*. Baton Rouge, LA:
    Louisiana State University Press.

Siringan, F., and J. Anderson. 1994. "Modern shoreface and inner-shelf storm deposits
    off the east Texas coast, Gulf of Mexico." *Journal of Sedimentary Research* 64
    (2):99-110.

Soniat, T., and M. Brody. 1988. "Field validation of a habitat suitability index model for
    the American oyster." *Estuaries* 11 (2):87-95.

Swift, D. 1975. "Barrier-island genesis: evidence from the central Atlantic shelf, eastern USA." *Sedimentary Geology* 14 (1):1-43.

Syvitski, J., and G. Farrow. 1983. "Structures and processes in bayhead deltas: Knight and Bute Inlet, British Columbia." *Sedimentary geology* 36 (2):217-244.

Ta, T., V. Nguyen, M. Tateishi, I. Kobayashi, and Y. Saito. 2001. "Sedimentary facies, diatom and foraminifer assemblages in a late Pleistocene–Holocene incised-valley sequence from the Mekong River Delta, Bentre Province, Southern Vietnam: the BT2 core." *Journal of Asian Earth Sciences* 20 (1):83-94.

Taha, Z., and J. Anderson. 2008. "The influence of valley aggradation and listric normal faulting on styles of river avulsion: A case study of the Brazos River, Texas, USA." *Geomorphology* 95 (3–4):429-448.

Tessier, B. 2012. "Stratigraphy of tide-dominated estuaries." In *Principles of Tidal Sedimentology*, 109-128. New York: Springer.

Thieler, E., and E. Hammar-Klose. 2000. *National Assessment of Coastal Vulnerability to Sea-level Rise, Preliminary Results for the US Gulf of Mexico Coast*, *Open File Report*. Reston, Virginia: US Geological Survey.

Thomas, M. A., and J. Anderson. 1994. "Sea-level controls on the facies architecture of the Trinity/Sabine incised-valley system, Texas continental shelf." In *Incised-Valley Systems*, 63-82. Tulsa, Oklahoma: SEPM (Society for Sedimentary Geology).

Thorbjarnarson, K., C. Nittrouer, D. J. DeMaster, and R. McKinney. 1985. "Sediment
accumulation in a back-barrier lagoon, Great Sound, New Jersey." *Journal of
Sedimentary Research* 55 (6):856-863.

Thornthwaite, C. 1948. "An approach toward a rational classification of climate."
Geographical Review 38 (1):55-94.

Toomey III, R., M. Blum, and S. Valastro Jr. 1993. "Late Quaternary climates and
environments of the Edwards Plateau, Texas." *Global and Planetary Change* 7
(4):299-320.

Törnqvist, T., J. González, L. Newsom, K. van der Borg, A. de Jong, and C. Kurnik.
2004. "Deciphering Holocene sea-level history on the US Gulf Coast: A high-
resolution record from the Mississippi Delta." *Geological Society of America
Bulletin* 116 (7-8):1026-1039.

Troiani, BT, AR Simms, T Dellapenna, E Piper, and Y Yokoyama. 2011. "The
importance of sea-level and climate change, including changing wind energy, on
the evolution of a coastal estuary: Copano Bay, Texas." *Marine Geology* 280
(1):1-19.

UNEP, UN Environmental Program. 2006. *Marine and Coastal Ecosystems and Human
Well-being: A Synthesis Report Based on the Findings of the Millinnium
Ecosystem Assessment* Nairobi, Kenya: United Nations.

USGS. 2014. "Water Data." Accessed July 9. http://waterdata.usgs.gov/nwis.

van Hengstum, P., J. Donnelly, M. Toomey, N. Albury, P. Lane, and B. Kakuk. 2014. "Heightened hurricane activity on the Little Bahama Bank from 1350 to 1650 AD." *Continental Shelf Research* 86:103-115.

Van Wagoner, J. 1988. "An overview of the fundamentals of sequence stratigraphy and key definitions." In *Sea-Level Changes - An Integrated Approach*. Tulsa, Oklahoma: SEPM (Society for Sedimentary Geology).

Van Wagoner, J., R. Mitchum, K. Campion, and V. Rahmanian. 1990. *Siliciclastic Sequence Stratigraphy in Well Logs, Cores, and Outcrops: Concepts for High-Resolution Correlation of Time and Facies*, *American Association of Petroleum Geologists Methods in Exploration*. Tulsa, Oklahoma: AAPG.

Wallace, D. , and J. Anderson. 2013. "Unprecedented erosion of the upper Texas coast: Response to accelerated sea-level rise and hurricane impacts." *Geological Society of America Bulletin* 125 (5-6):728-740.

Wallace, D. , J. Woodruff, J. Anderson, and J. Donnelly. 2014. "Palaeohurricane reconstructions from sedimentary archives along the Gulf of Mexico, Caribbean Sea and western North Atlantic Ocean margins." *Geological Society, London, Special Publications* 388. doi: 10.1144/sp388.12.

Wallace, D., J. Anderson, and R. Fernández. 2010. "Transgressive ravinement versus depth of closure: A geological perspective from the upper Texas coast." *Journal of Coastal Research* 26 (6):1057-1067.

Weimer, R. 1984. "Relation of unconformities, tectonics, and sea-level changes, Cretaceous of Western Interior, USA." In *Interregional Unconformities and Hydrocarbon Accumulation*, 7-35. Tulsa, Oklahoma: American Association of Petroleum Geologists.

Wells, H. 1961. "The fauna of oyster beds, with special reference to the salinity factor." *Ecological Monographs* 31 (3):239-266.

White, W., T. Calnan, R. Morton, R. Kimble, T. Littleton, J. McGowen, H. Nance, and K. Schmedes. 1985. *Submerged Lands of Texas, Galveston-Houston Area: Sediments, Geochemistry, Benthic Macroinvertebrates, and Associated Wetlands*. University of Texas at Austin: Bureau of Economic Geology.

Wolfe, B., R. Hall, W. Last, T. Edwards, M. English, T. Karst-Riddoch, A. Paterson, and R. Palmini. 2006. "Reconstruction of multi-century flood histories from oxbow lake sediments, Peace-Athabasca Delta, Canada." *Hydrological Processes* 20 (19):4131-4153.

Zaitlin, B. 1994. "The stratigraphic organization of incised-valley systems associated with relative sea-level change." In *Incised-Valley Systems: Origin and Sedimentary Sequences*. Tulsa, Oklahoma: SEPM (Society for Sedimentary Geology).

Zaitlin, B., and B. Shultz. 1990. "Wave-influenced estuarine sand body, Senlac heavy oil pool, Saskatchewan, Canada." In *Sandstone Petroleum Reservoirs*, 363-387. New York: Springer.

Zhang, X., C. Lin, R. W. Dalrymple, S. Gao, and Y. Li. 2014. "Facies architecture and depositional model of a macrotidal incised-valley succession (Qiantang River estuary, eastern China), and differences from other macrotidal systems." *Geological Society of America Bulletin* 126 (3-4):499-522.

APPENDIX A

CORE DESCRIPTIONS

Project: West Bay

Core ID: SLP 1

Section: 0-100 cm

Location (Zone 15 N): 3227324 N, 300402 E
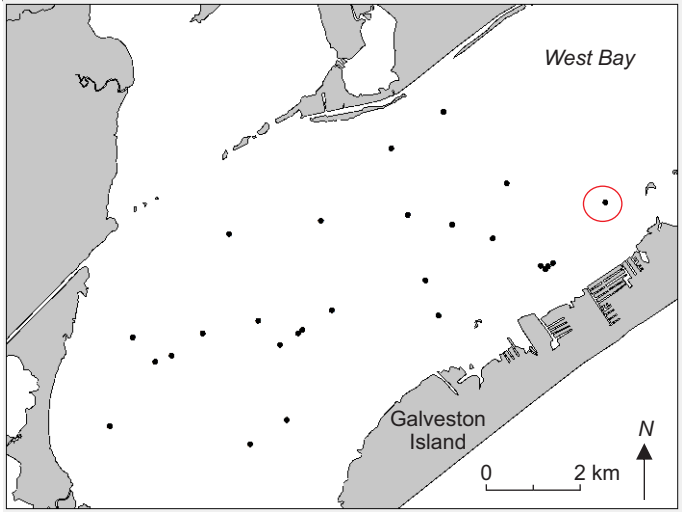
West Bay

Galveston
Island

0   2 km

N

Legend

- Lower Estuary
- Middle Estuary
- Paleo-Brazos River Pro-Delta
- Upper Estuary
- Delta Plain
- Mouth Bar
- Beaumont Formation
- Estuarine Shell
- Burrows

Depth (cm)

0
10
20
30
40
50
60
70
80
90
100

Clay   Silt   Sand

Project: West Bay
Core ID: SLP 1
Section: 100-200 cm
Location (Zone 15 N): 3227324 N, 300402 E

West Bay

Galveston
Island

0   2 km

N

Legend

- Lower Estuary
- Middle Estuary
- Paleo-Brazos River Pro-Delta
- Upper Estuary
- Delta Plain
- Mouth Bar
- Beaumont Formation
- Estuarine Shell
- Burrows

Depth (cm)

Clay Silt Sand
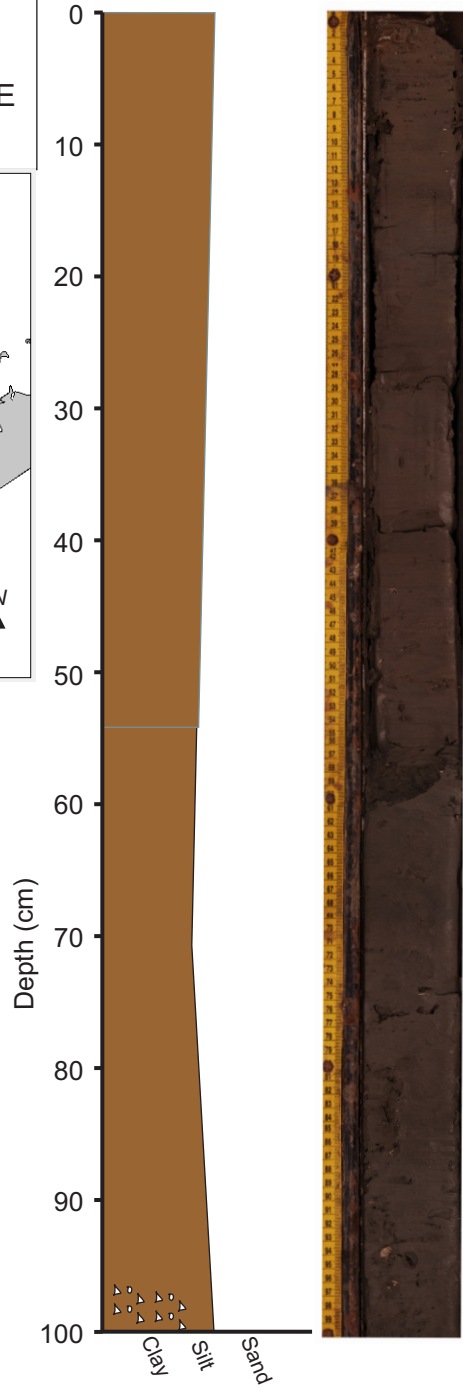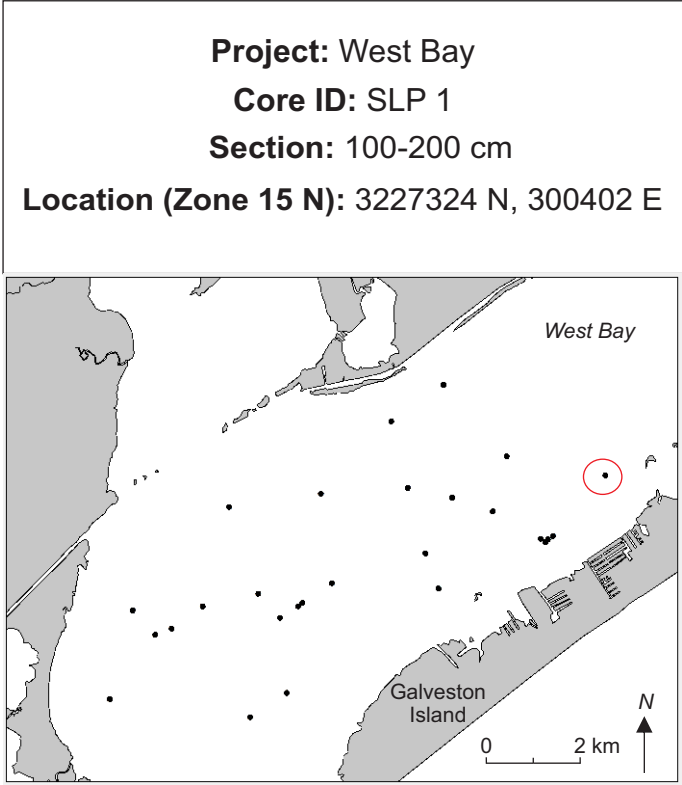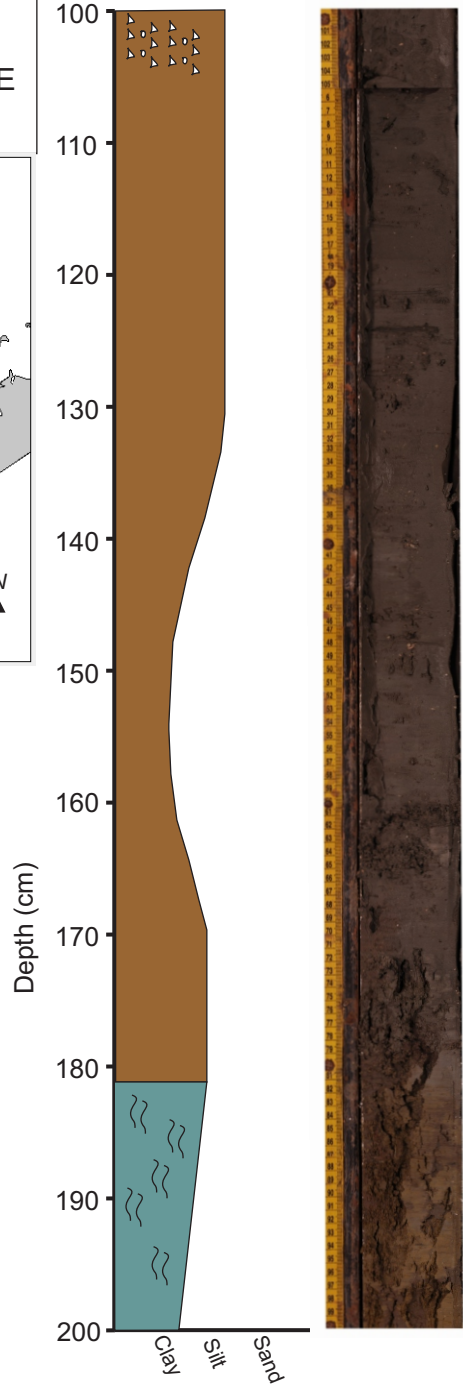
Project: West Bay
Core ID: SLP 2
Section: 0-100 cm
Location (Zone 15 N): 3228395 N, 296151 E
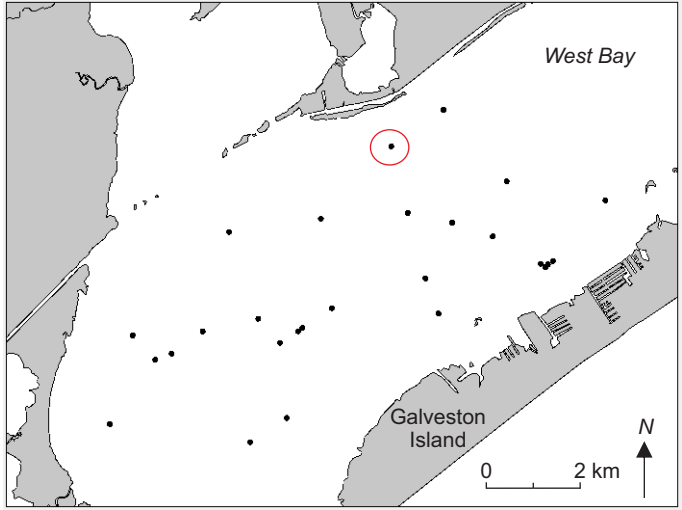
West Bay

Galveston Island

0   2 km

N

Legend

- Lower Estuary
- Middle Estuary
- Paleo-Brazos River Pro-Delta
- Upper Estuary
- Delta Plain
- Mouth Bar
- Beaumont Formation
- Estuarine Shell
- Burrows

Depth (cm)

Clay   Silt   Sand
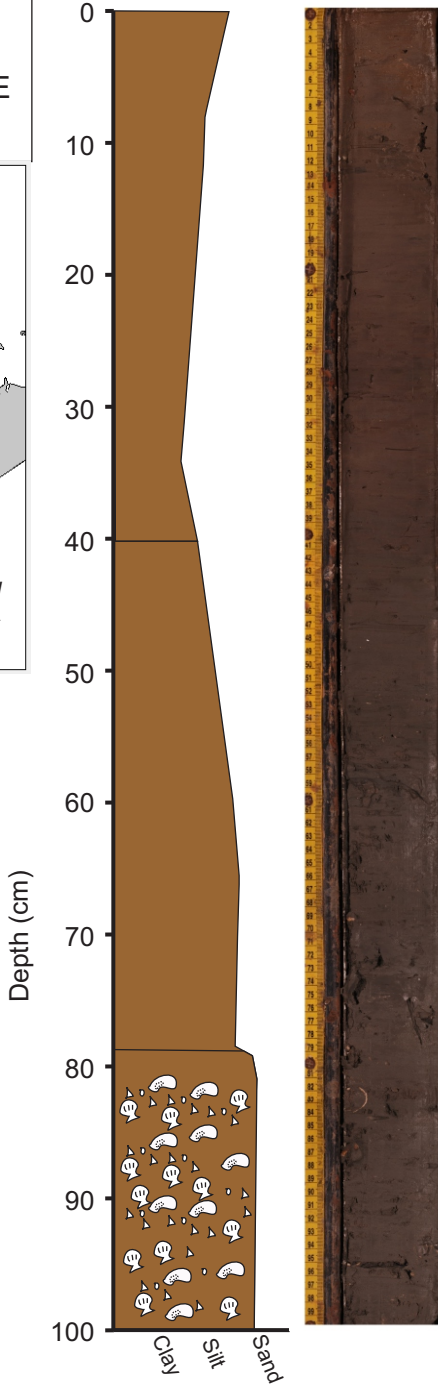
Project: West Bay
Core ID: SLP 2
Section: 100-200 cm
Location (Zone 15 N): 3228395 N, 296151 E
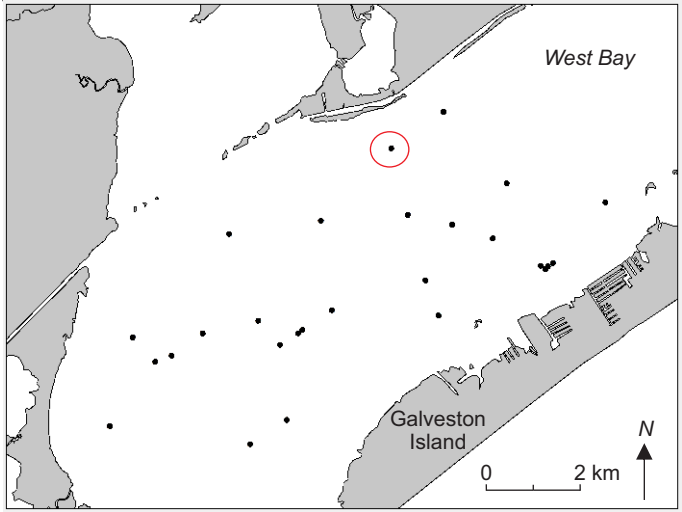
West Bay

Galveston
Island

0   2 km

N

Legend

■ Lower Estuary
■ Middle Estuary
■ Paleo-Brazos River Pro-Delta
■ Upper Estuary
■ Delta Plain
□ Mouth Bar
■ Beaumont Formation
🐚 Estuarine Shell
� Burrows

Depth (cm)

Clay   Silt   Sand
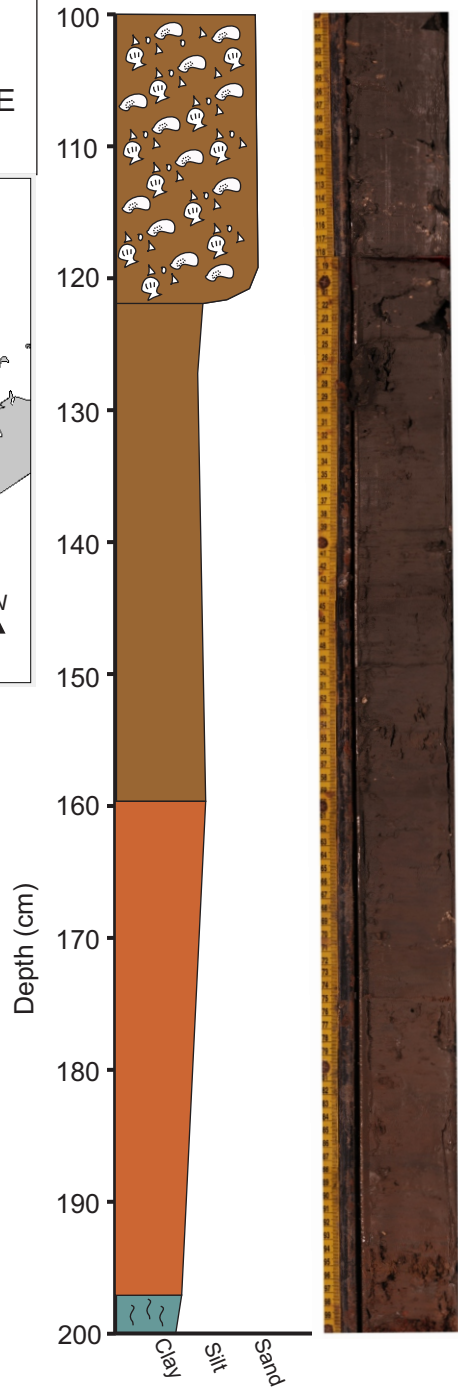
Project: West Bay
Core ID: SLP 3
Section: 0-100 cm
Location (Zone 15 N): 3223012 N, 294078 E
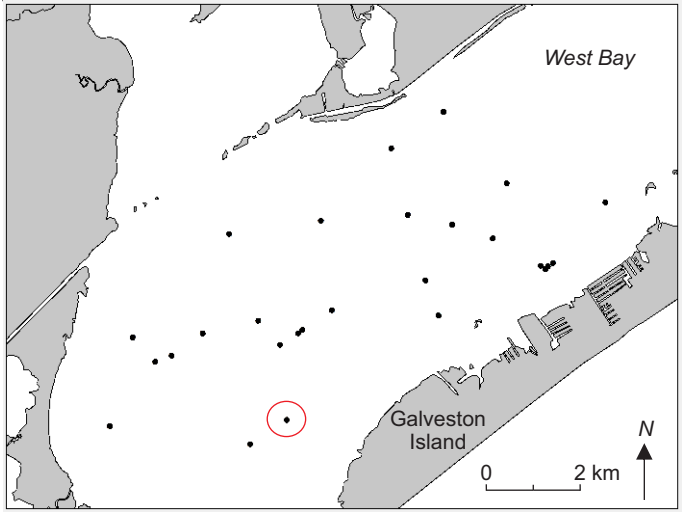
West Bay

Galveston Island

0   2 km

N

Legend

■ Lower Estuary
■ Middle Estuary
■ Paleo-Brazos River Pro-Delta
■ Upper Estuary
■ Delta Plain
□ Mouth Bar
■ Beaumont Formation
🐚 Estuarine Shell
〰 Burrows

Depth (cm)

Clay Silt Sand

Project: West Bay
Core ID: SLP 3
Section: 100-200 cm
Location (Zone 15 N): 3223012 N, 294078 E
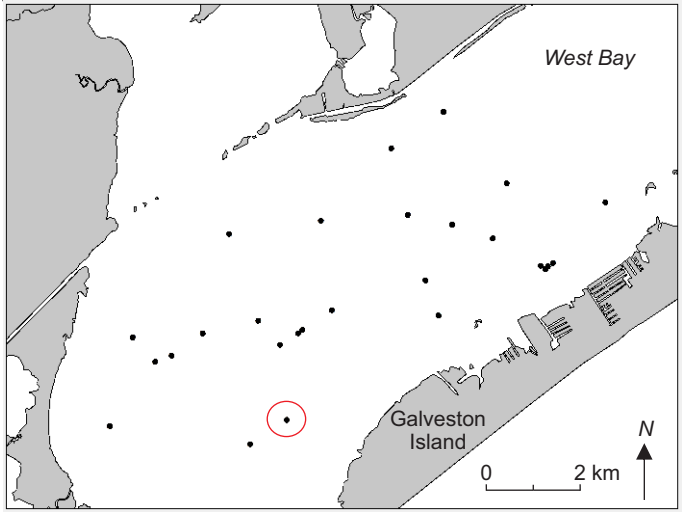
West Bay

Galveston Island

0   2 km

N

Legend

- Lower Estuary
- Middle Estuary
- Paleo-Brazos River Pro-Delta
- Upper Estuary
- Delta Plain
- Mouth Bar
- Beaumont Formation
- Estuarine Shell
- Burrows
- *R. Cuneata*

Depth (cm)

100
110
120
130
140
150
160
170
180
190
200

Clay   Silt   Sand
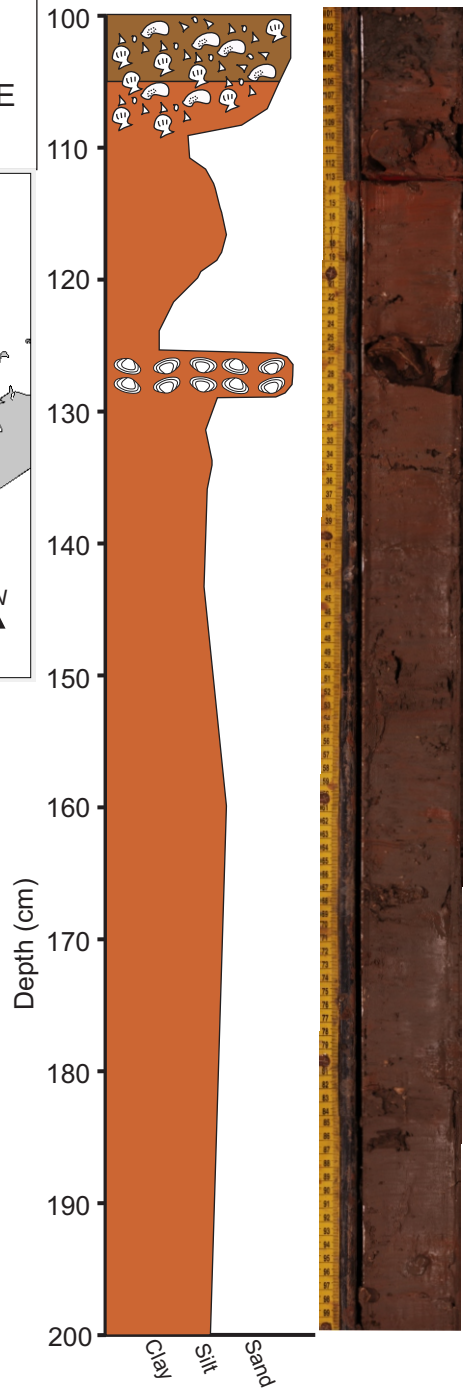
Project: West Bay

Core ID: SLP 3

Section: 200-300 cm
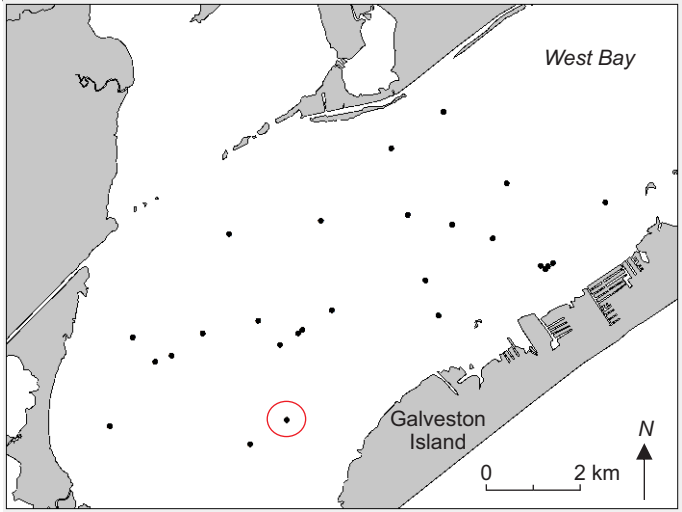
Location (Zone 15 N): 3223012 N, 294078 E

West Bay

Galveston
Island

0   2 km

N

Legend

▪ Lower Estuary
▪ Middle Estuary
▪ Paleo-Brazos River Pro-Delta
▪ Upper Estuary
▪ Delta Plain
▫ Mouth Bar
▪ Beaumont Formation
&° Estuarine Shell
〰 Burrows

Depth (cm)

Clay Silt Sand
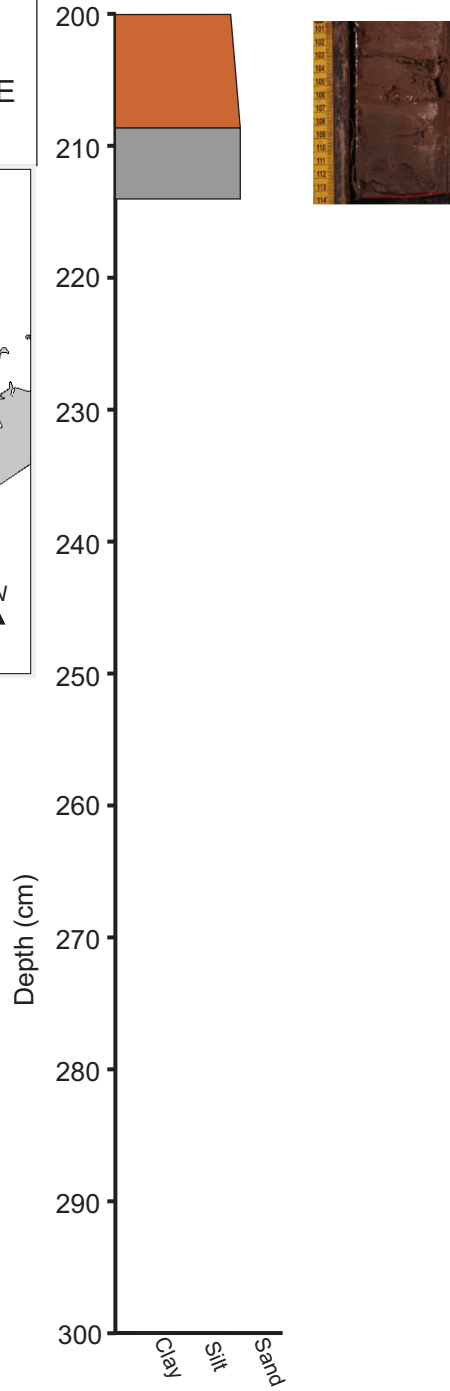
Project: West Bay

Core ID: SLP 4

Section: 0-100 cm

Location (Zone 15 N): 3224647 N, 291020 E
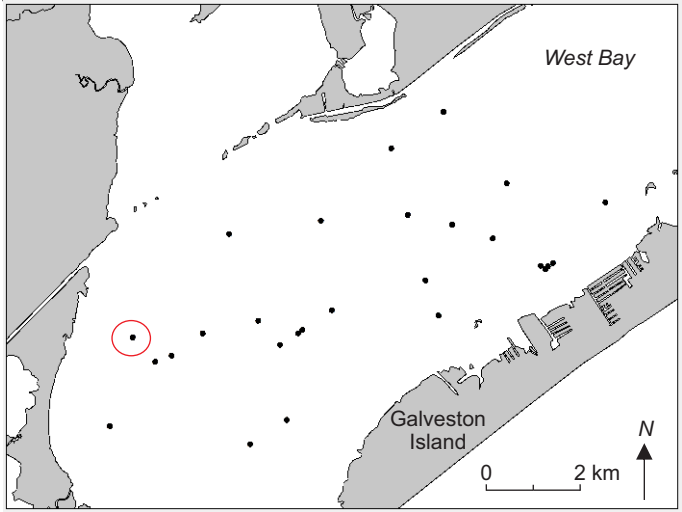
West Bay

Galveston
Island

0   2 km

N

Legend

- Lower Estuary
- Middle Estuary
- Paleo-Brazos River Pro-Delta
- Upper Estuary
- Delta Plain
- Mouth Bar
- Beaumont Formation
- Estuarine Shell
- Burrows

Depth (cm)

Clay   Silt   Sand
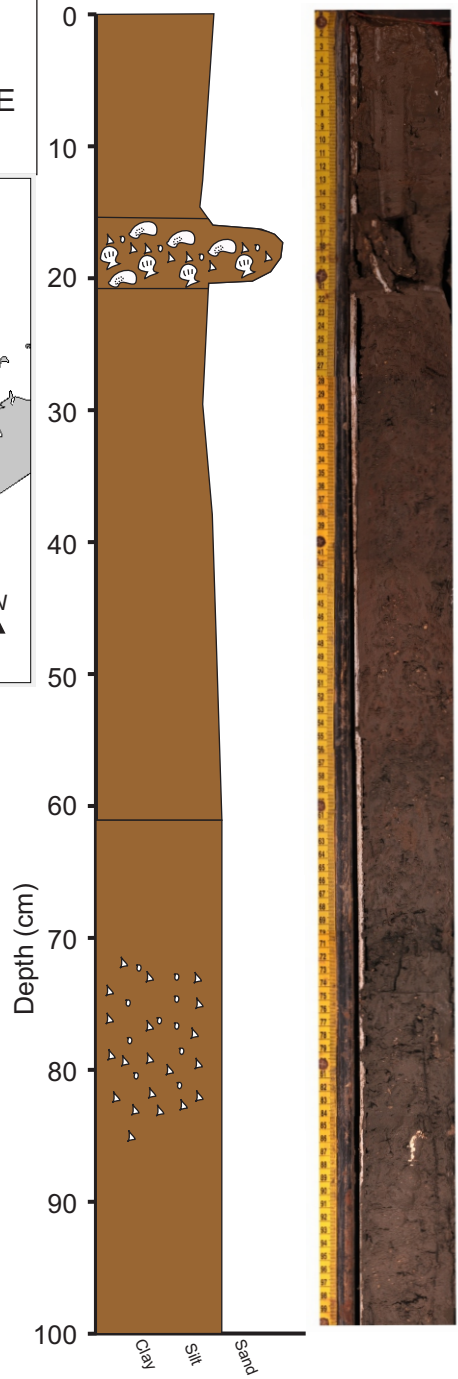
Project: West Bay

Core ID: SLP 4

Section: 200-300 cm
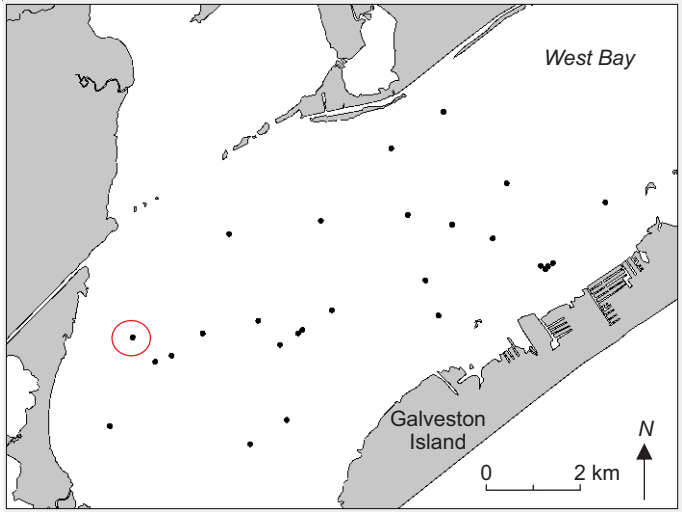
Location (Zone 15 N): 3224647 N, 291020 E

West Bay

Galveston
Island

0   2 km

N

Legend

- Lower Estuary
- Middle Estuary
- Paleo-Brazos River Pro-Delta
- Upper Estuary
- Delta Plain
- Mouth Bar
- Beaumont Formation
- Estuarine Shell
- Burrows

Depth (cm)

Clay   Silt   Sand
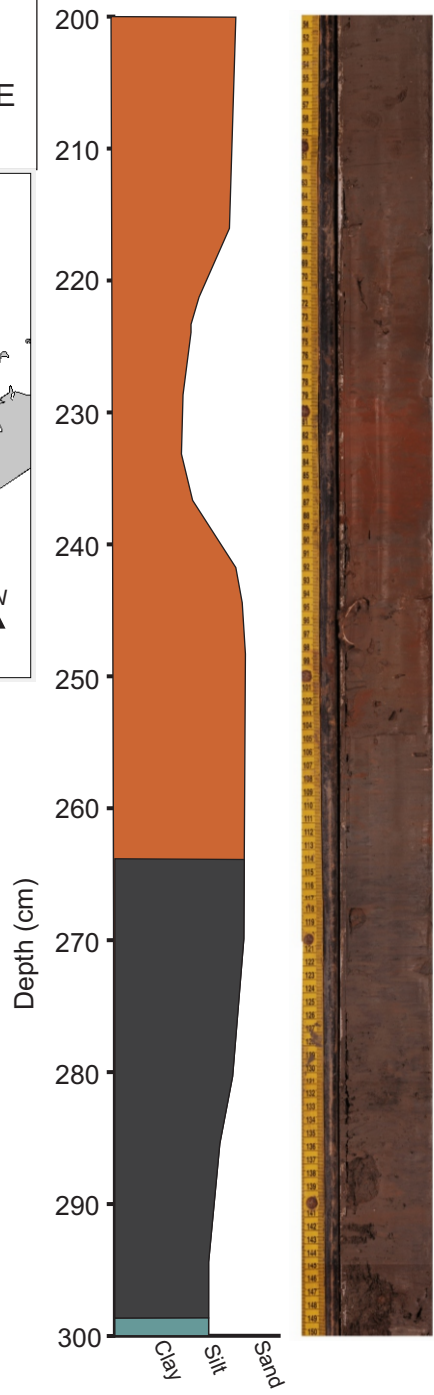
Project: West Bay
Core ID: SLP 5
Section: 0-100 cm
Location (Zone 15 N): 3222891 N, 290566 E
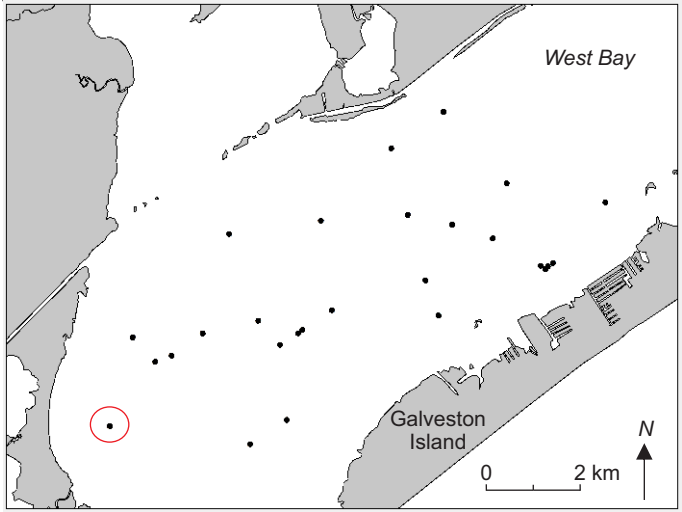
West Bay

Galveston
Island

0   2 km

N

Legend

■ Lower Estuary
■ Middle Estuary
■ Paleo-Brazos River Pro-Delta
■ Upper Estuary
■ Delta Plain
□ Mouth Bar
■ Beaumont Formation
𝔢 Estuarine Shell
〰 Burrows

Depth (cm)

0
10
20
30
40
50
60
70
80
90
100

Clay Silt Sand
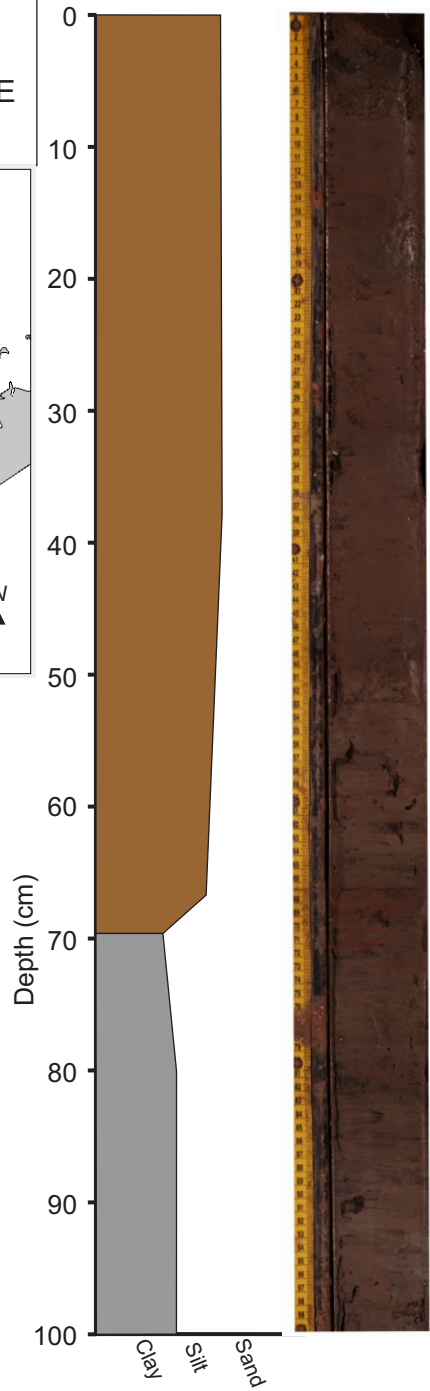
Project: West Bay

Core ID: SLP 5

Section: 100-200 cm
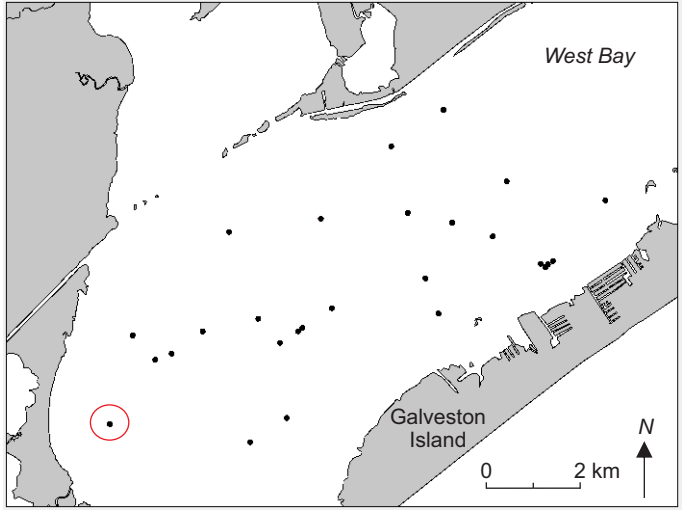
Location (Zone 15 N): 3222891 N, 290566 E

West Bay

Galveston
Island

0   2 km

N

Legend

■ Lower Estuary
■ Middle Estuary
■ Paleo-Brazos River Pro-Delta
■ Upper Estuary
■ Delta Plain
□ Mouth Bar
■ Beaumont Formation
⌇ Estuarine Shell
⟨⟨ Burrows

Depth (cm)

Clay   Silt   Sand
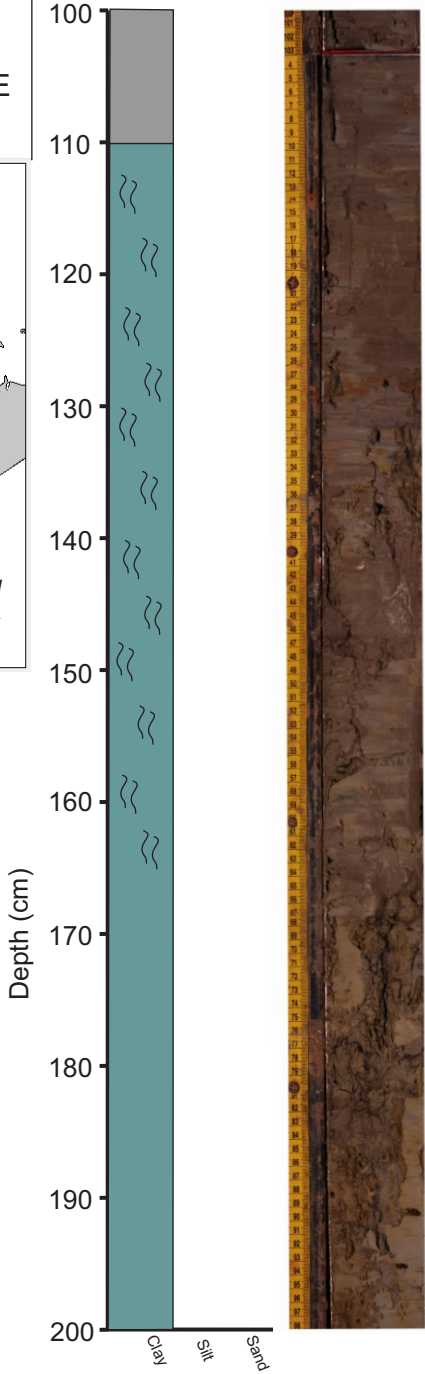
Project: West Bay
Core ID: SLP 6
Section: 0-100 cm
Location (Zone 15 N): 3224978 N, 293513 E
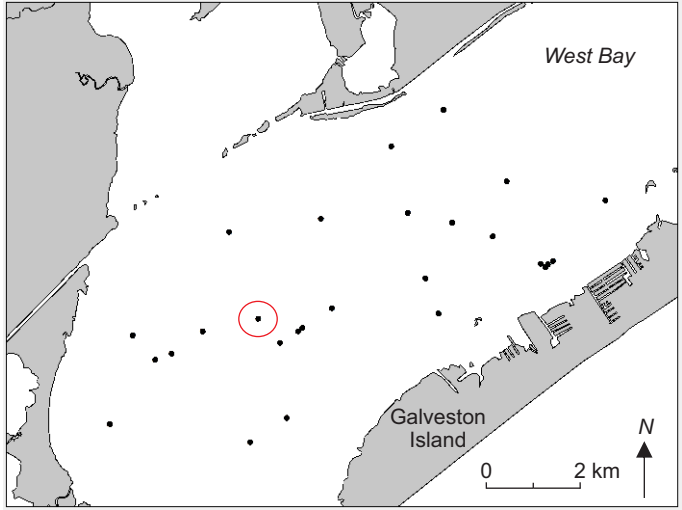
West Bay

Galveston Island

0   2 km

N

Legend

- Lower Estuary
- Middle Estuary
- Paleo-Brazos River Pro-Delta
- Upper Estuary
- Delta Plain
- Mouth Bar
- Beaumont Formation
- Estuarine Shell
- Burrows

Depth (cm)

Clay Silt Sand
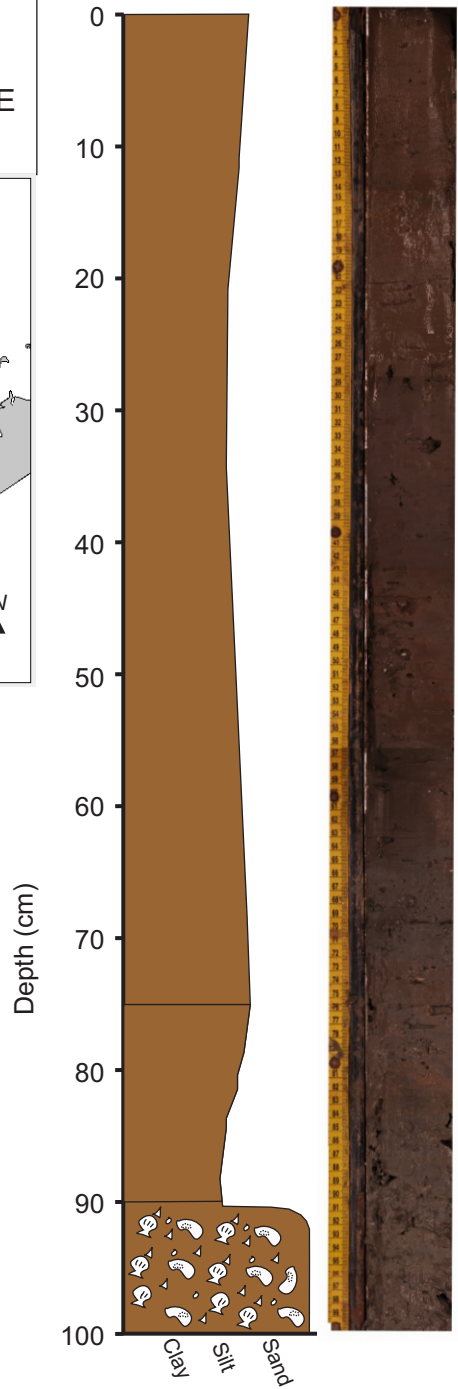
Project: West Bay
Core ID: SLP 6
Section: 100-200 cm
Location (Zone 15 N): 3224978 N, 293513 E
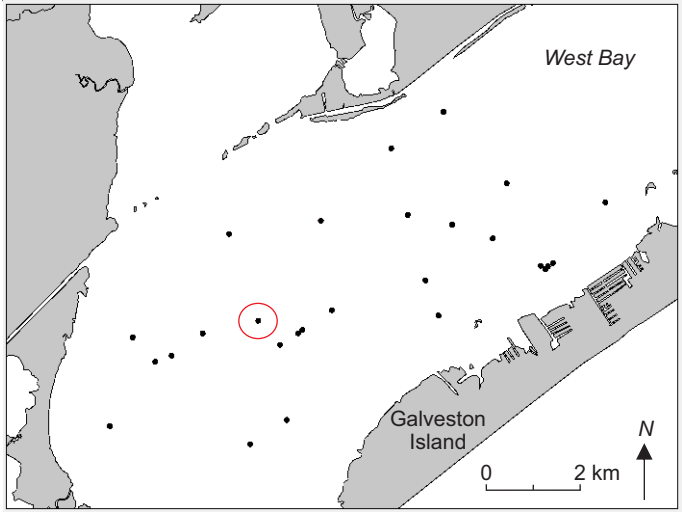
West Bay

Galveston
Island

0   2 km

N

Legend

■ Lower Estuary
■ Middle Estuary
■ Paleo-Brazos River Pro-Delta
■ Upper Estuary
■ Delta Plain
□ Mouth Bar
■ Beaumont Formation
🐚 Estuarine Shell
〰 Burrows
🐚🐚 *R. Cuneata*

Depth (cm)

Clay   Silt   Sand
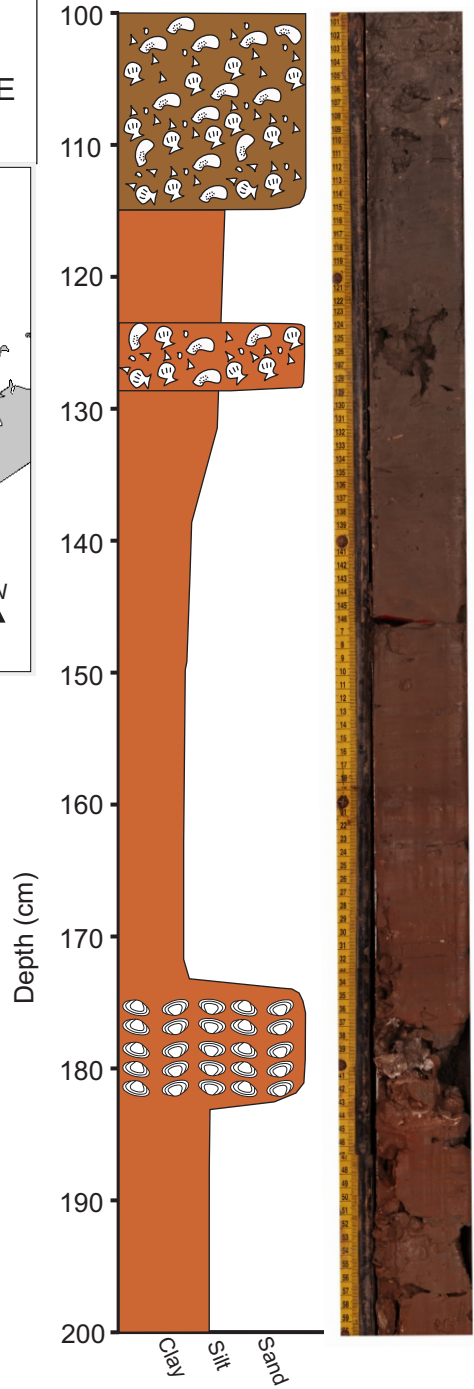
Project: West Bay
Core ID: SLP 6
Section: 200-300 cm
Location (Zone 15 N): 3224978 N, 293513 E
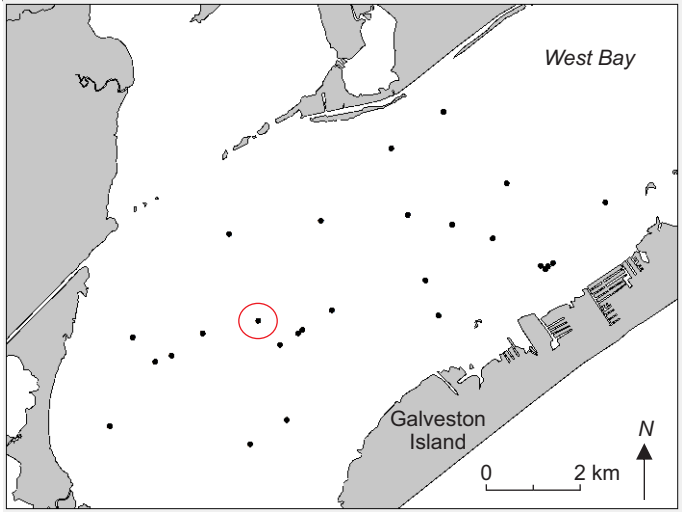
West Bay

Galveston Island

0   2 km

N

Legend

- ■ Lower Estuary
- ■ Middle Estuary
- ■ Paleo-Brazos River Pro-Delta
- ■ Upper Estuary
- ■ Delta Plain
- □ Mouth Bar
- □ Beaumont Formation
- ⌒ Estuarine Shell
- ⌇ Burrows
- ◐◑ *R. Cuneata*

Depth (cm)

Clay Silt Sand
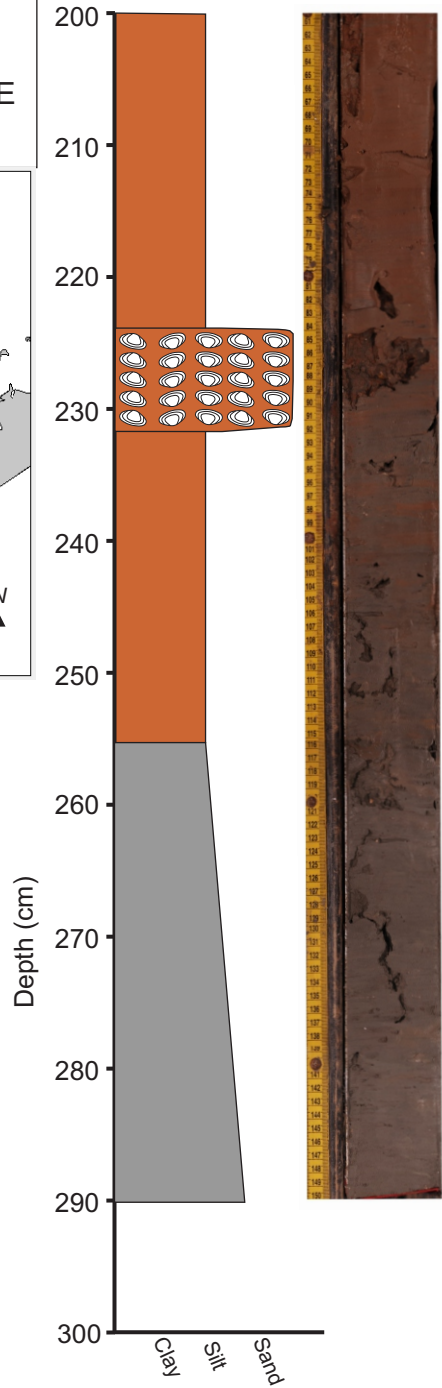
Project: West Bay
Core ID: SLP 7
Section: 0-100 cm
Location (Zone 15 N): 3226697 N, 292933 E
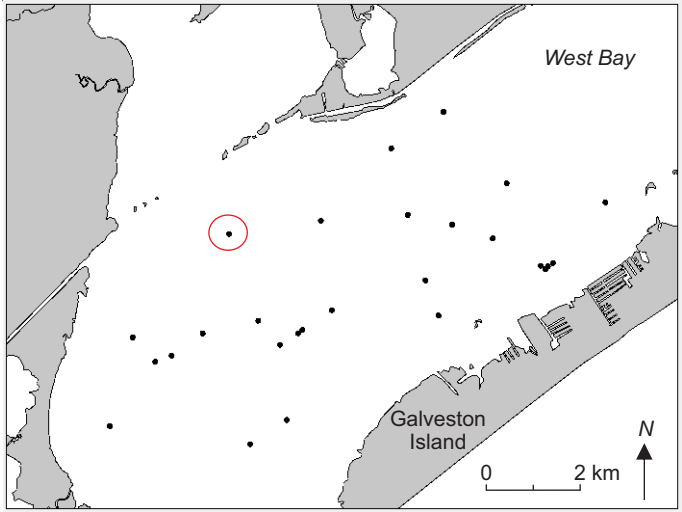
West Bay

Galveston Island

0   2 km

N

Legend

- Lower Estuary
- Middle Estuary
- Paleo-Brazos River Pro-Delta
- Upper Estuary
- Delta Plain
- Mouth Bar
- Beaumont Formation
- Estuarine Shell
- Burrows

Depth (cm)

Clay Silt Sand
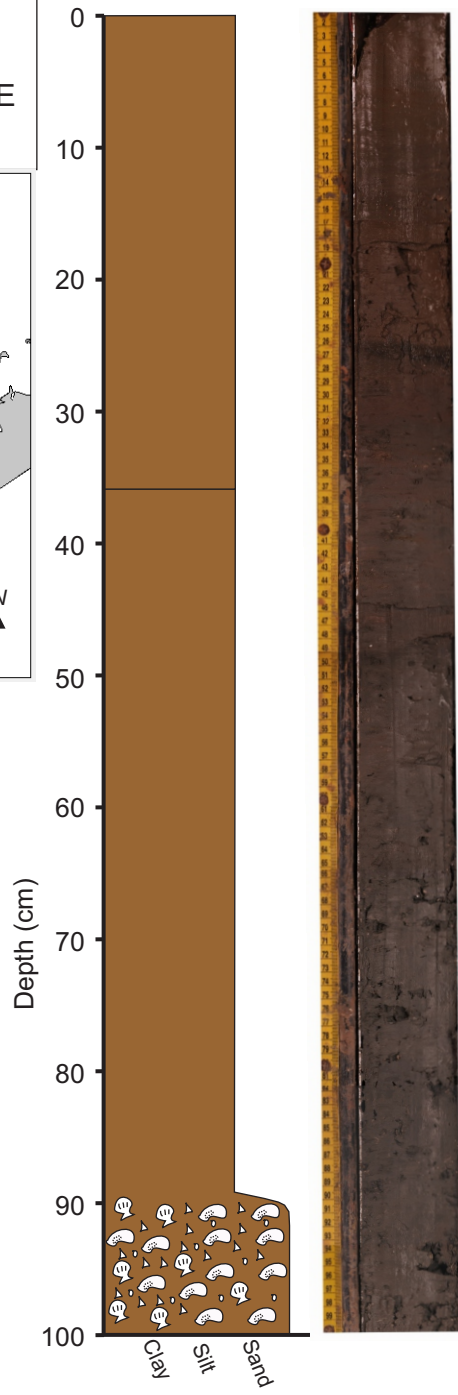
Project: West Bay

Core ID: SLP 7

Section: 100-200 cm
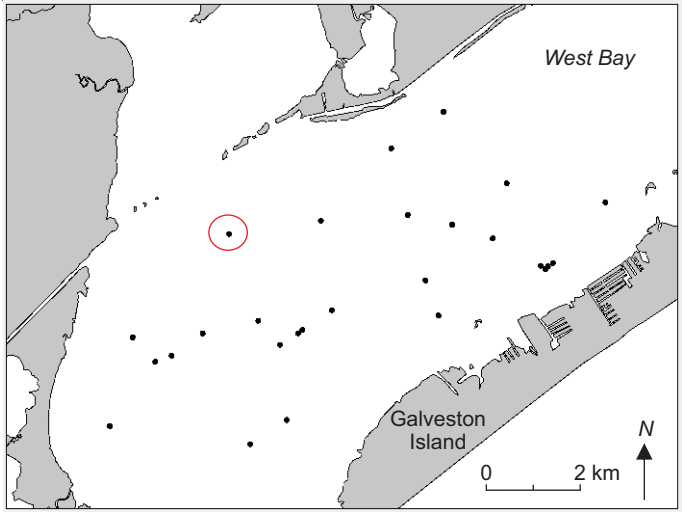
Location (Zone 15 N): 3226697 N, 292933 E

West Bay

Galveston
Island

0   2 km   N

Legend

- Lower Estuary
- Middle Estuary
- Paleo-Brazos River Pro-Delta
- Upper Estuary
- Delta Plain
- Mouth Bar
- Beaumont Formation
- Estuarine Shell
- Burrows

Depth (cm)

Clay   Silt   Sand
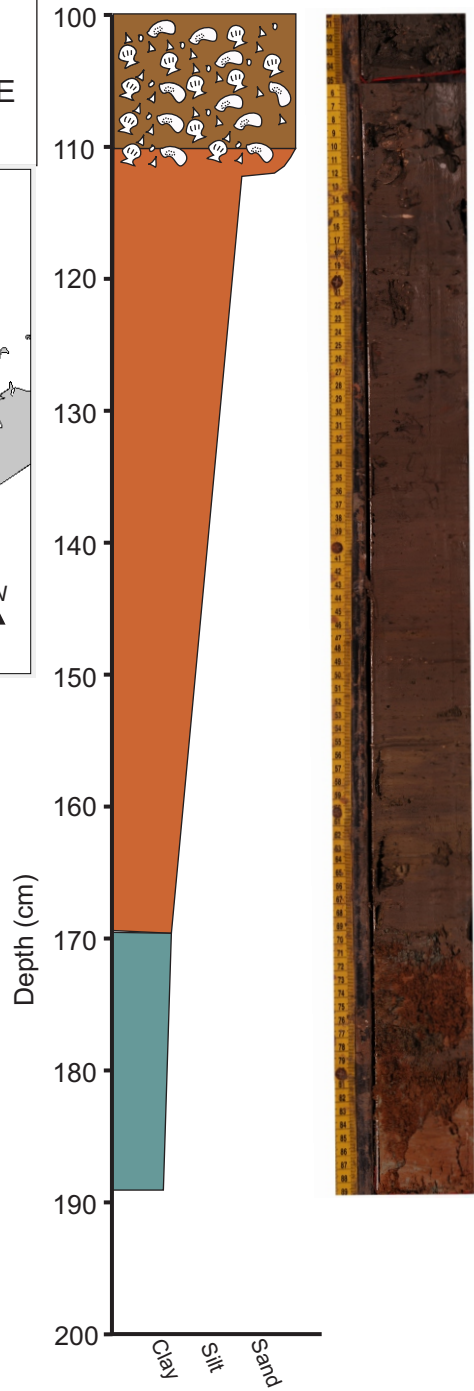
Project: West Bay
Core ID: SLP 8
Section: 100-200 cm
Location (Zone 15 N): 3225083 N, 297090 E
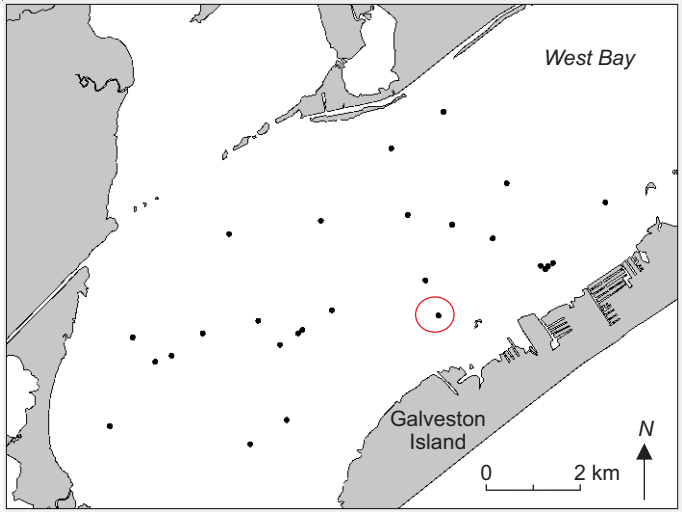
West Bay

Galveston
Island

0   2 km

N

Legend

- Lower Estuary
- Middle Estuary
- Paleo-Brazos River Pro-Delta
- Upper Estuary
- Delta Plain
- Mouth Bar
- Beaumont Formation
- Estuarine Shell
- Burrows
- *R. Cuneata*

Depth (cm)

Clay Silt Sand
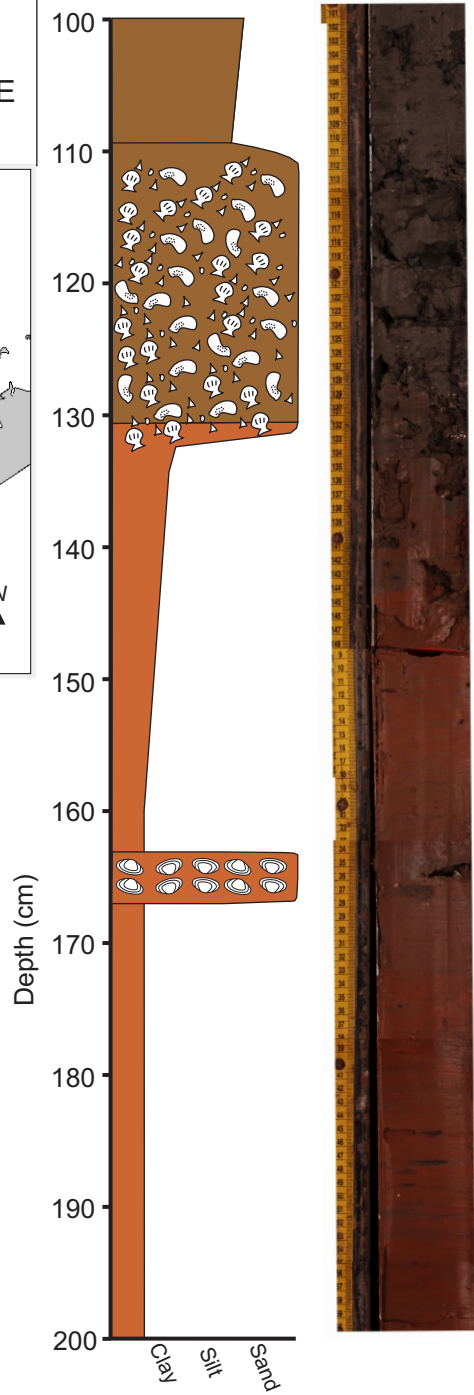
Project: West Bay
Core ID: SLP 8
Section: 200-298 cm
Location (Zone 15 N): 3225083 N, 297090 E
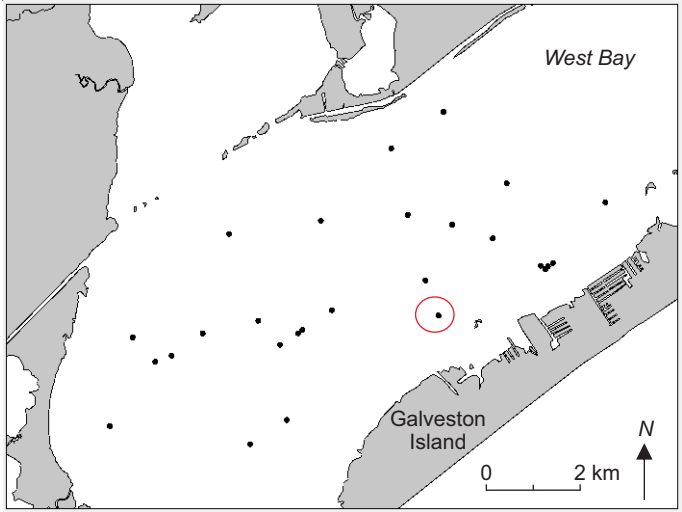
West Bay

Galveston Island

0   2 km

N

Legend

- Lower Estuary
- Middle Estuary
- Paleo-Brazos River Pro-Delta
- Upper Estuary
- Delta Plain
- Mouth Bar
- Beaumont Formation
- Estuarine Shell
- Burrows

Depth (cm)

200
210
220
230
240
250
260
270
280
290
300

Clay   Silt   Sand
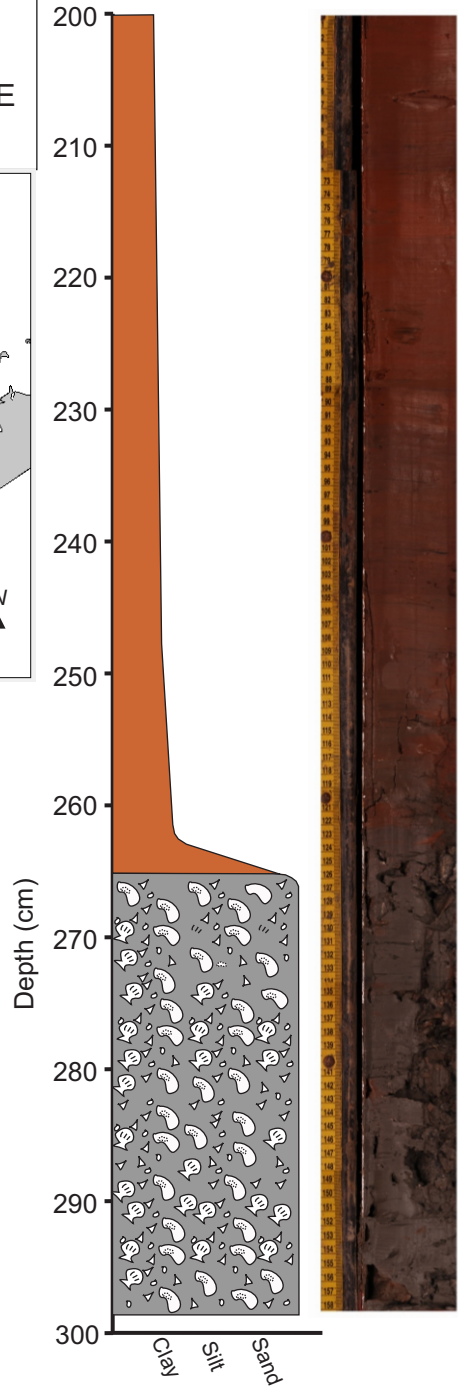
Project: West Bay
Core ID: SLP 12
Section: 0-100 cm
Location (Zone 15 N): 3225185 N, 294974 E
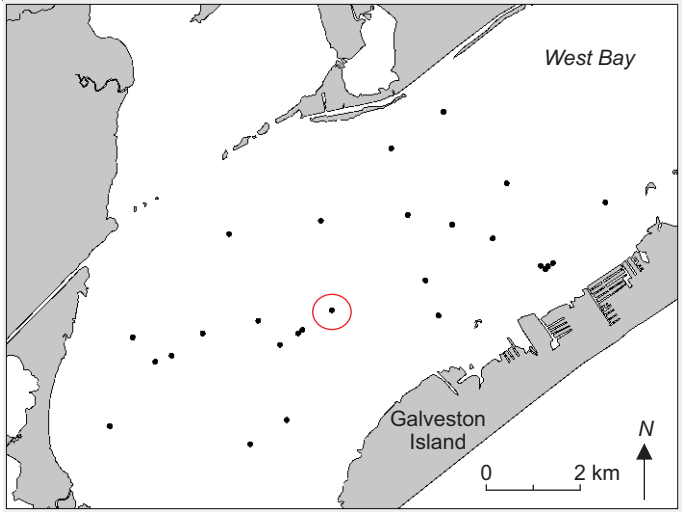
West Bay

Galveston Island

0   2 km   N

Legend

- Lower Estuary
- Middle Estuary
- Paleo-Brazos River Pro-Delta
- Upper Estuary
- Delta Plain
- Mouth Bar
- Beaumont Formation
- Estuarine Shell
- Burrows

Depth (cm)

Clay Silt Sand
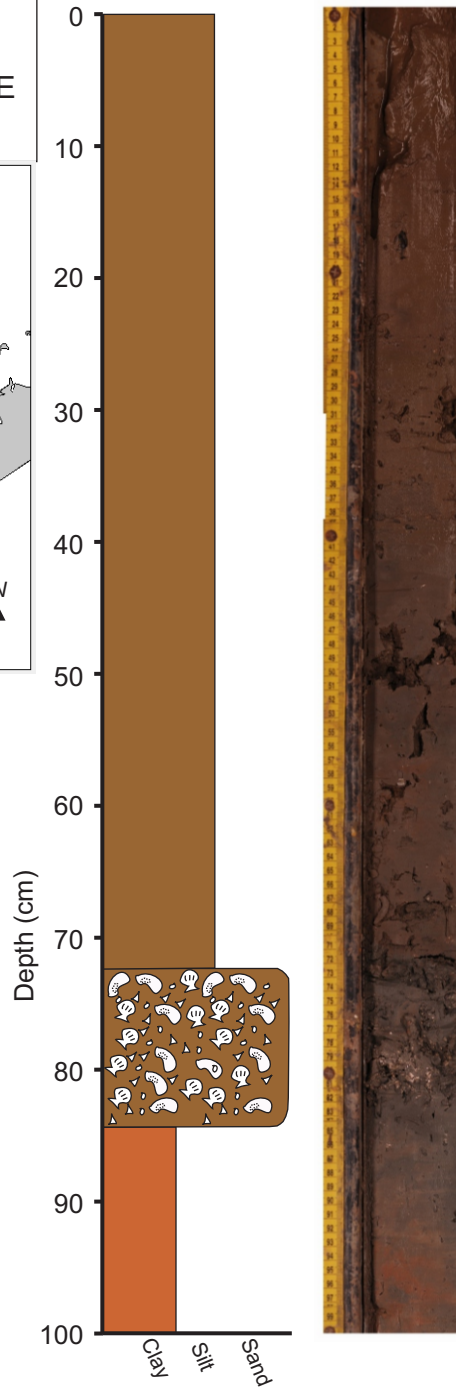
Project: West Bay

Core ID: SLP 12

Section: 100-200 cm
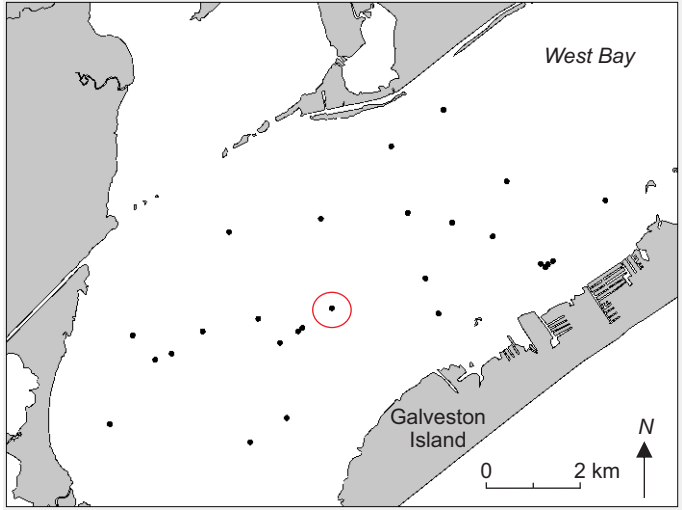
Location (Zone 15 N): 3225185 N, 294974 E

West Bay

Galveston
Island

0   2 km

N

Legend

- Lower Estuary
- Middle Estuary
- Paleo-Brazos River Pro-Delta
- Upper Estuary
- Delta Plain
- Mouth Bar
- Beaumont Formation
- Estuarine Shell
- Burrows
- *R. Cuneata*

Depth (cm)

100
110
120
130
140
150
160
170
180
190
200

Clay   Silt   Sand
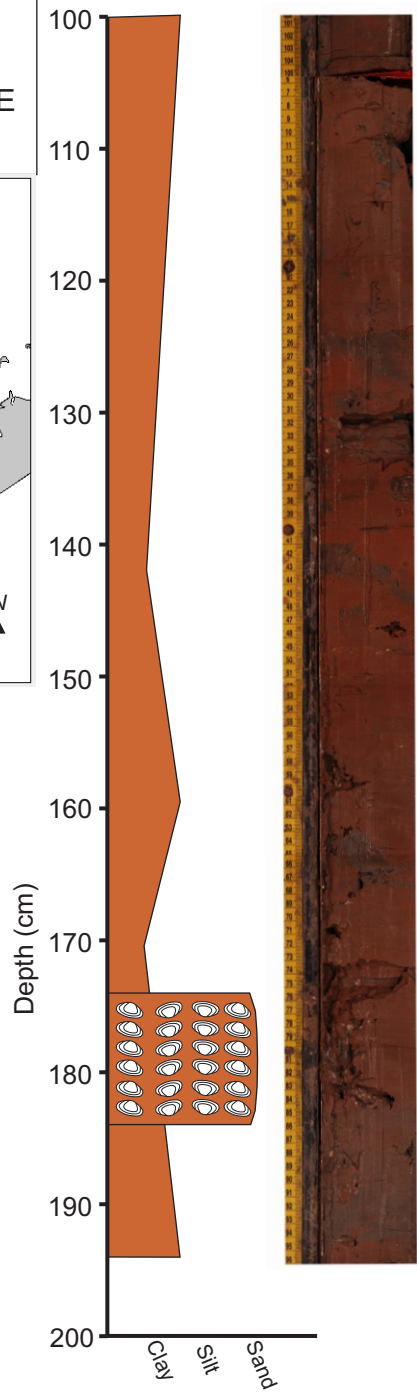
Project: West Bay

Core ID: SLP 13

Section: 0-100 cm

Location (Zone 15 N): 3226611 N, 298166 E
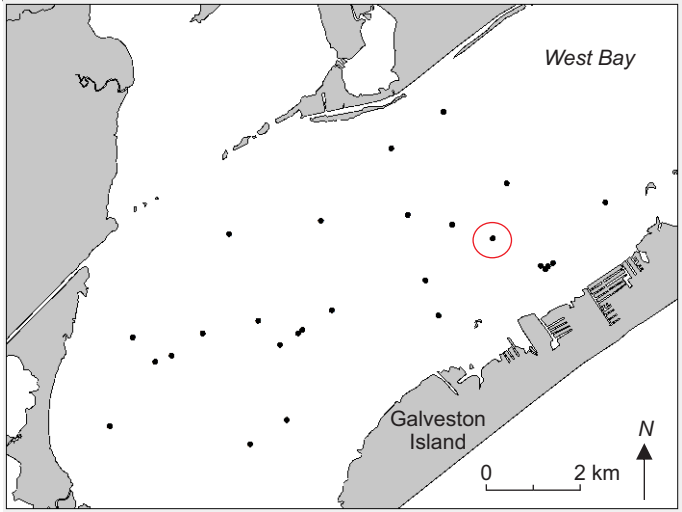
West Bay

Galveston
Island

0   2 km   *N*

Legend

- Lower Estuary
- Middle Estuary
- Paleo-Brazos River Pro-Delta
- Upper Estuary
- Delta Plain
- Mouth Bar
- Beaumont Formation
- Estuarine Shell
- Burrows

Depth (cm)

Clay   Silt   Sand
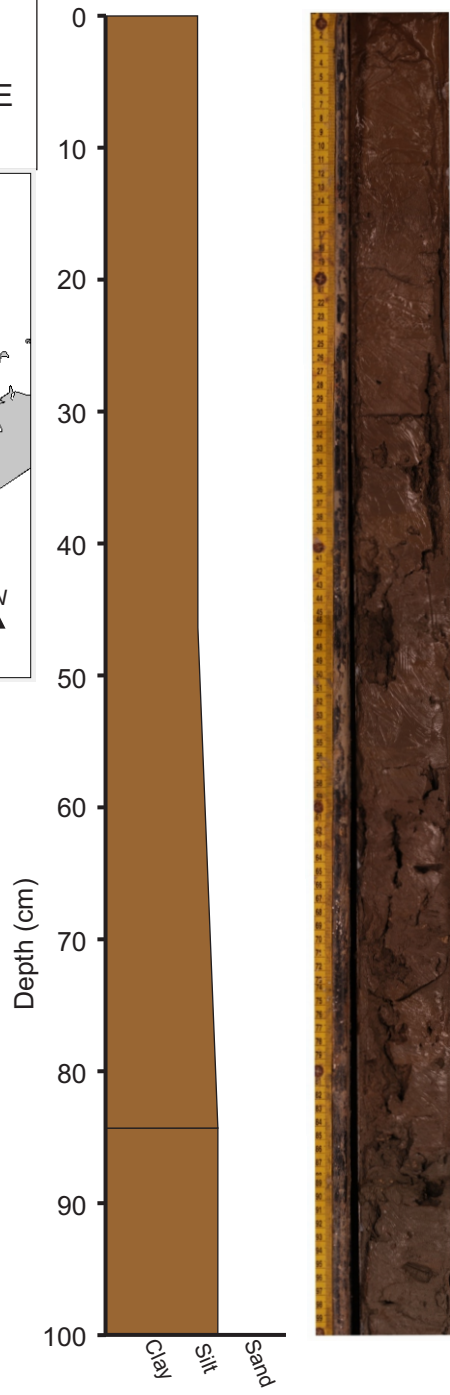
Project: West Bay
Core ID: SLP 13
Section: 100-200 cm
Location (Zone 15 N): 3226611 N, 298166 E
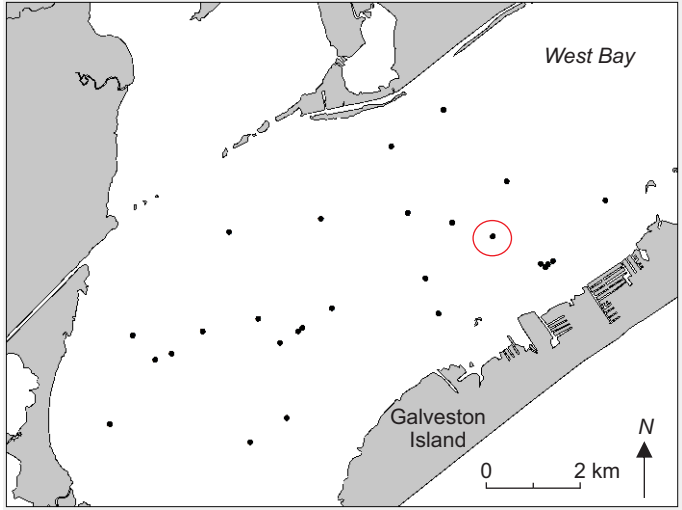
West Bay

Galveston Island

0   2 km

N

Legend

- Lower Estuary
- Middle Estuary
- Paleo-Brazos River Pro-Delta
- Upper Estuary
- Delta Plain
- Mouth Bar
- Beaumont Formation
- Estuarine Shell
- Burrows

Depth (cm)

Clay   Silt   Sand
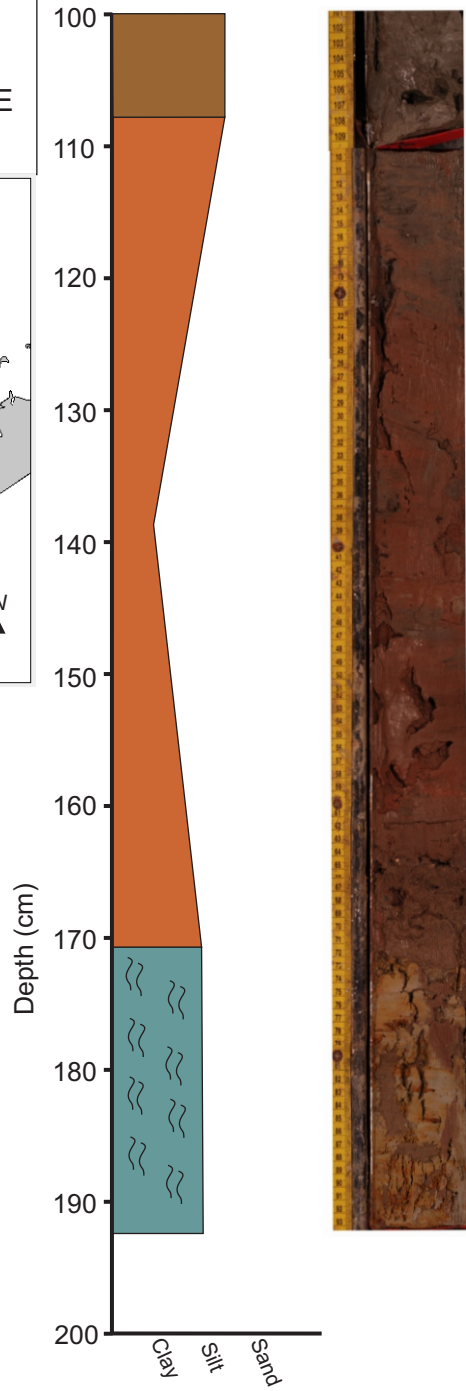
Project: West Bay
Core ID: SLP 14
Section: 0-100 cm
Location (Zone 15 N): 3224799 N, 294389 E
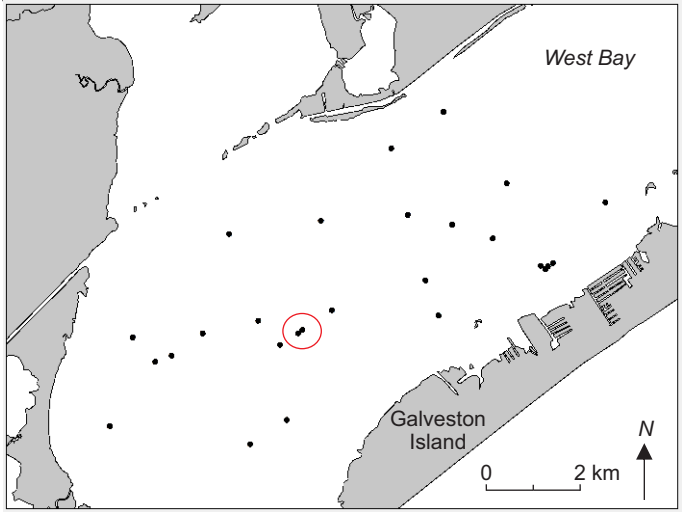
West Bay

Galveston Island

0   2 km

N

Legend

- Lower Estuary
- Middle Estuary
- Paleo-Brazos River Pro-Delta
- Upper Estuary
- Delta Plain
- Mouth Bar
- Beaumont Formation
- Estuarine Shell
- Burrows

Depth (cm)

Clay Silt Sand
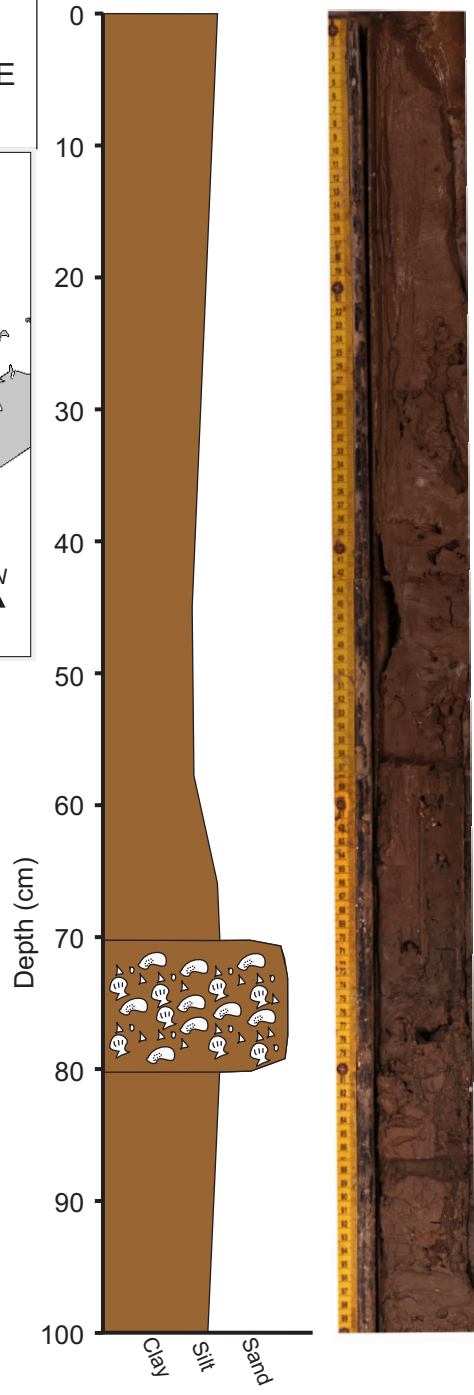
Project: West Bay
Core ID: SLP 14
Section: 100-200 cm
Location (Zone 15 N): 3224799 N, 294389 E
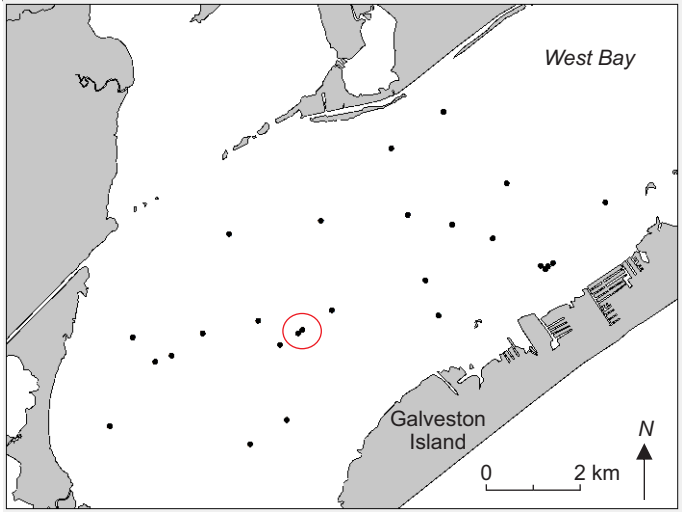
West Bay

Galveston
Island

0   2 km

N

Legend

- Lower Estuary
- Middle Estuary
- Paleo-Brazos River Pro-Delta
- Upper Estuary
- Delta Plain
- Mouth Bar
- Beaumont Formation
- Estuarine Shell
- Burrows
- *R. Cuneata*

Depth (cm)

100
110
120
130
140
150
160
170
180
190
200

Clay   Silt   Sand
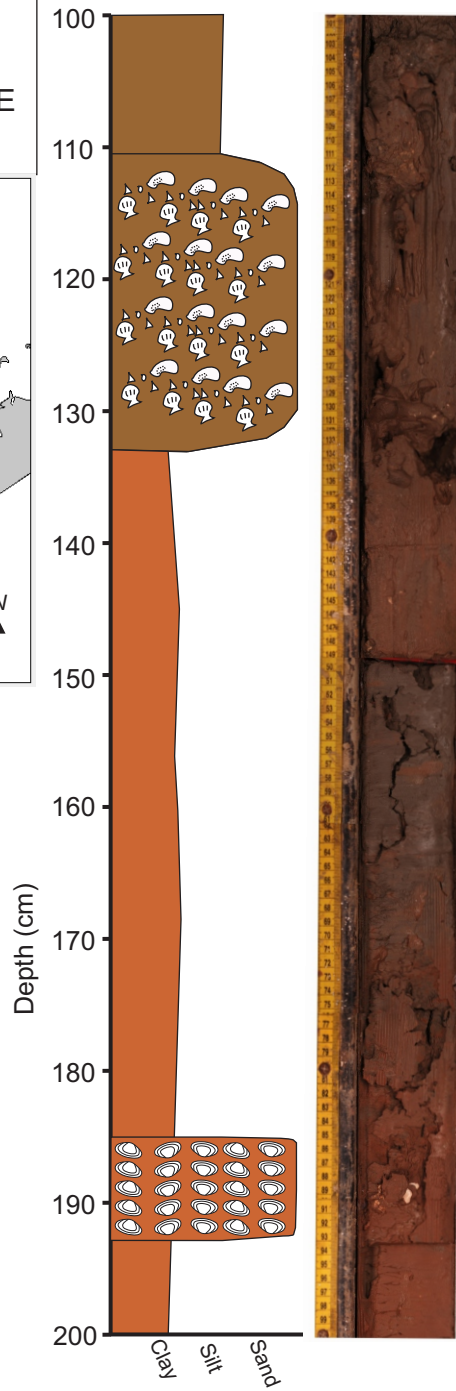
Project: West Bay

Core ID: SLP 14

Section: 200-300 cm
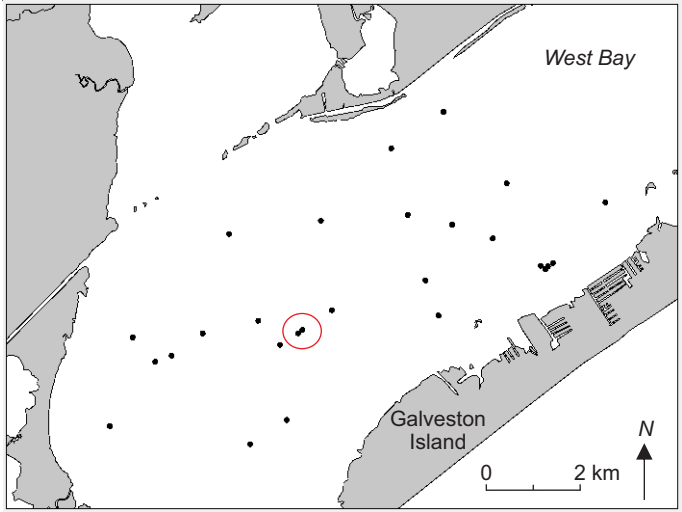
Location (Zone 15 N): 3224799 N, 294389 E

West Bay

Galveston
Island

0   2 km

N

Legend

- Lower Estuary
- Middle Estuary
- Paleo-Brazos River Pro-Delta
- Upper Estuary
- Delta Plain
- Mouth Bar
- Beaumont Formation
- Estuarine Shell
- Burrows

Depth (cm)

200
210
220
230
240
250
260
270
280
290
300

Clay   Silt   Sand
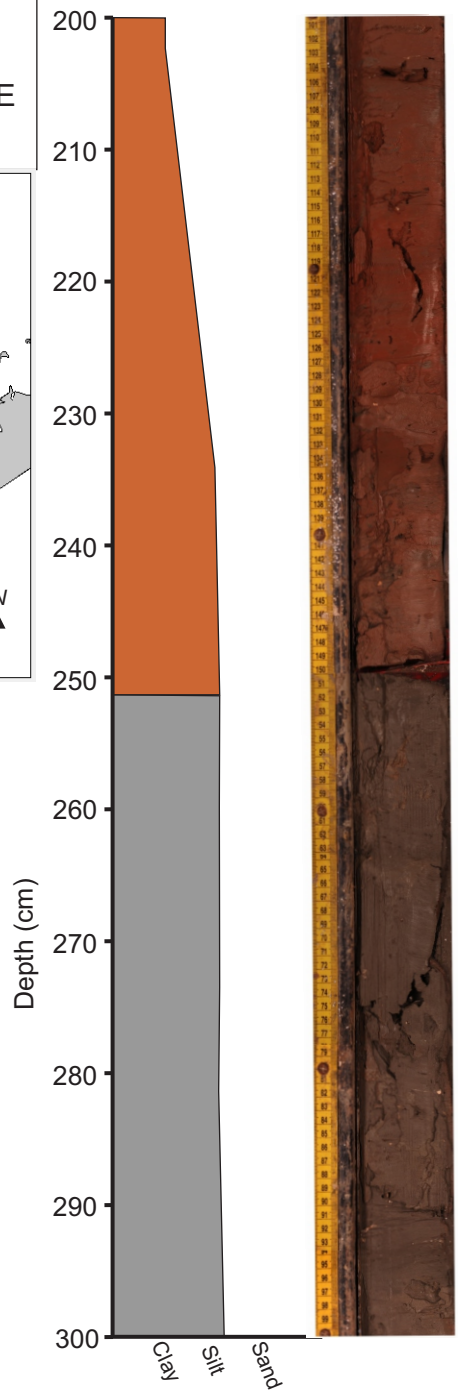
Project: West Bay

Core ID: SLP 14

Section: 300-400 cm
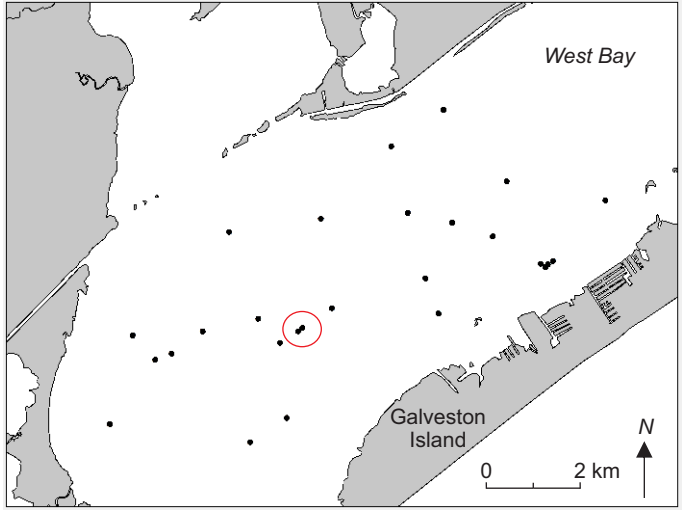
Location (Zone 15 N): 3224799 N, 294389 E

West Bay

Galveston Island

N

0   2 km

Legend

- ■ Lower Estuary
- ■ Middle Estuary
- ■ Paleo-Brazos River Pro-Delta
- ■ Upper Estuary
- ■ Delta Plain
- ☐ Mouth Bar
- ■ Beaumont Formation
- ⚶ Estuarine Shell
- ⟨⟨ Burrows

Depth (cm)

300

310

320

330

340

350

360

370

380

390

400

Clay   Silt   Sand
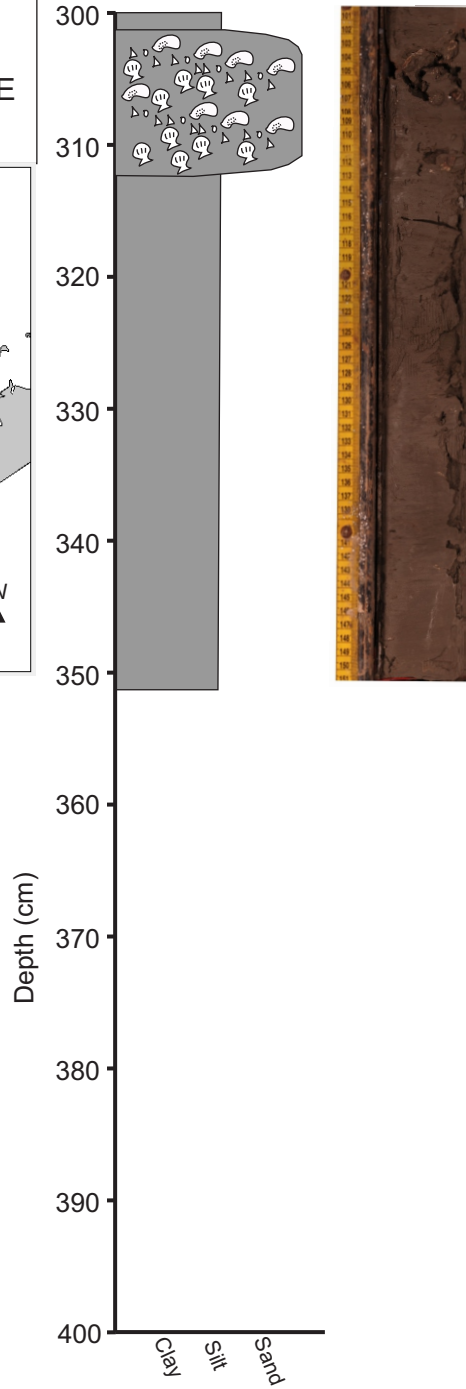
Project: West Bay

Core ID: SLP 15

Section: 0-79 cm

Location (Zone 15 N): 3229116 N, 297188 E
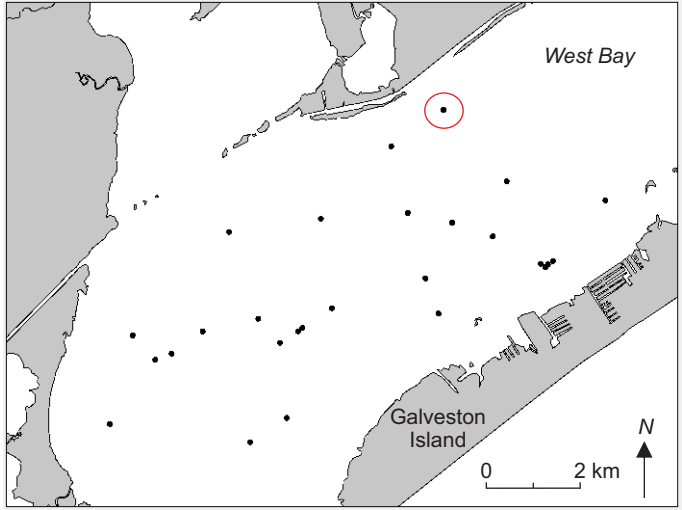
West Bay

Galveston Island

0   2 km

N

Legend

- Lower Estuary
- Middle Estuary
- Paleo-Brazos River Pro-Delta
- Upper Estuary
- Delta Plain
- Mouth Bar
- Beaumont Formation
- Estuarine Shell
- Burrows

Depth (cm)

Clay   Silt   Sand
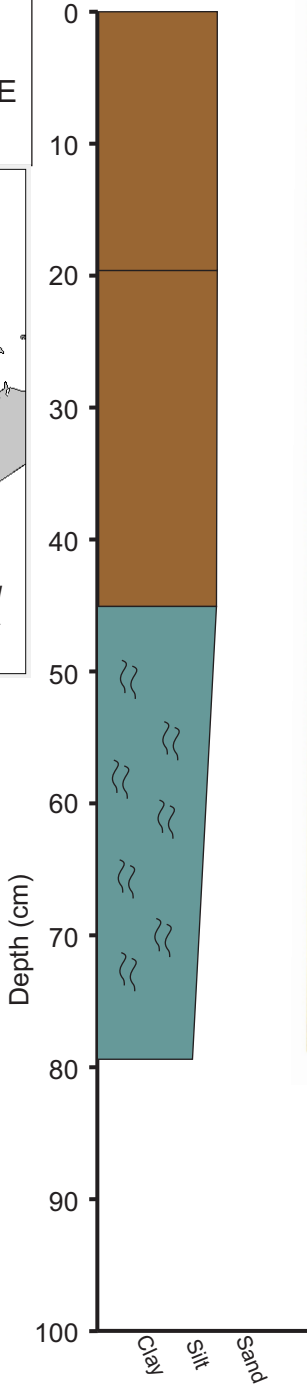
Project: West Bay
Core ID: SLP 16
Section: 0-100 cm
Location (Zone 15 N): 3226067 N, 299118 E
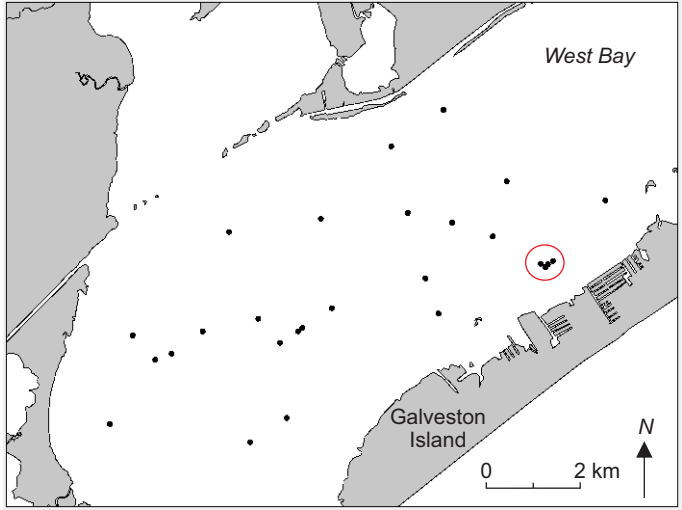
West Bay

Galveston
Island

0   2 km   N

Legend

■ Lower Estuary
■ Middle Estuary
■ Paleo-Brazos River Pro-Delta
■ Upper Estuary
■ Delta Plain
□ Mouth Bar
■ Beaumont Formation
🐚 Estuarine Shell
〰 Burrows

Depth (cm)

0
10
20
30
40
50
60
70
80
90
100

Clay   Silt   Sand
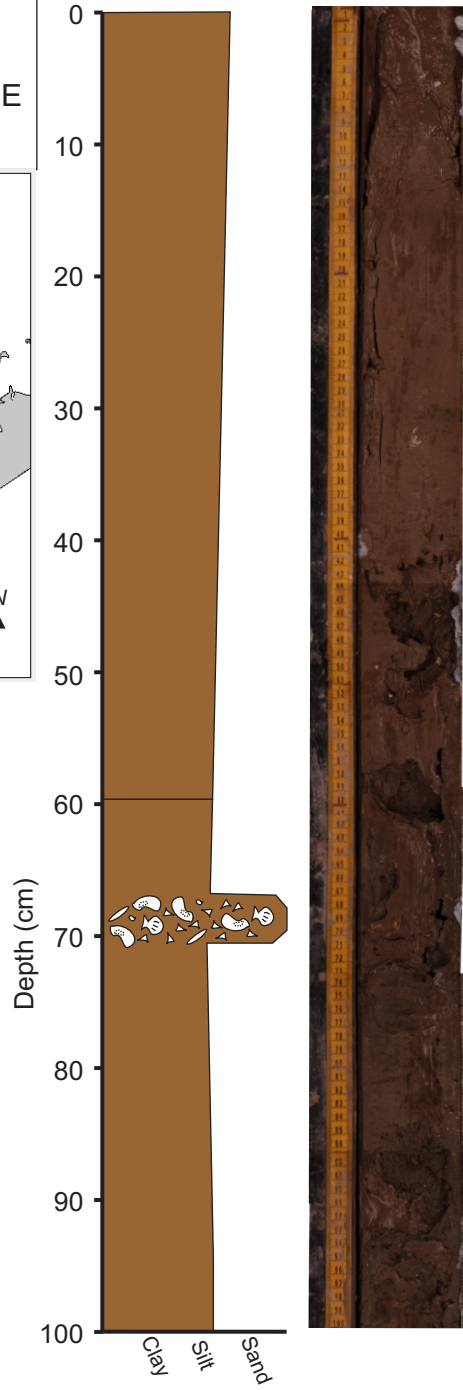
Project: West Bay

Core ID: SLP 16

Section: 100-200 cm
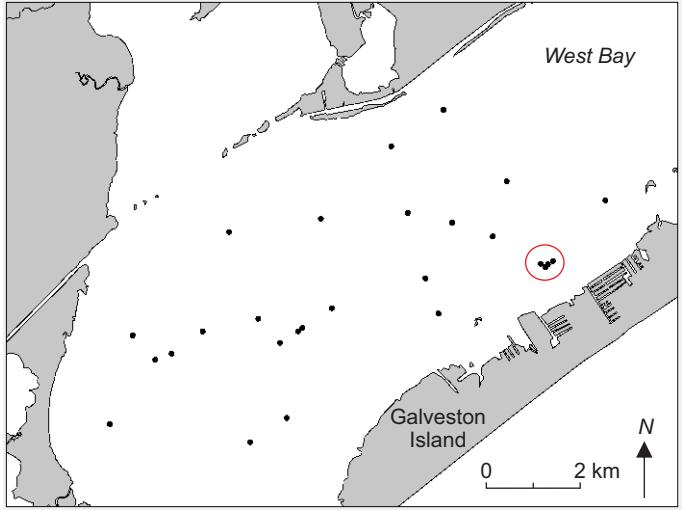
Location (Zone 15 N): 3226067 N, 299118 E

West Bay

Galveston
Island

0   2 km

N

Legend

- Lower Estuary
- Middle Estuary
- Paleo-Brazos River Pro-Delta
- Upper Estuary
- Delta Plain
- Mouth Bar
- Beaumont Formation
- Estuarine Shell
- Burrows

Depth (cm)

100
110
120
130
140
150
160
170
180
190
200

Clay   Silt   Sand
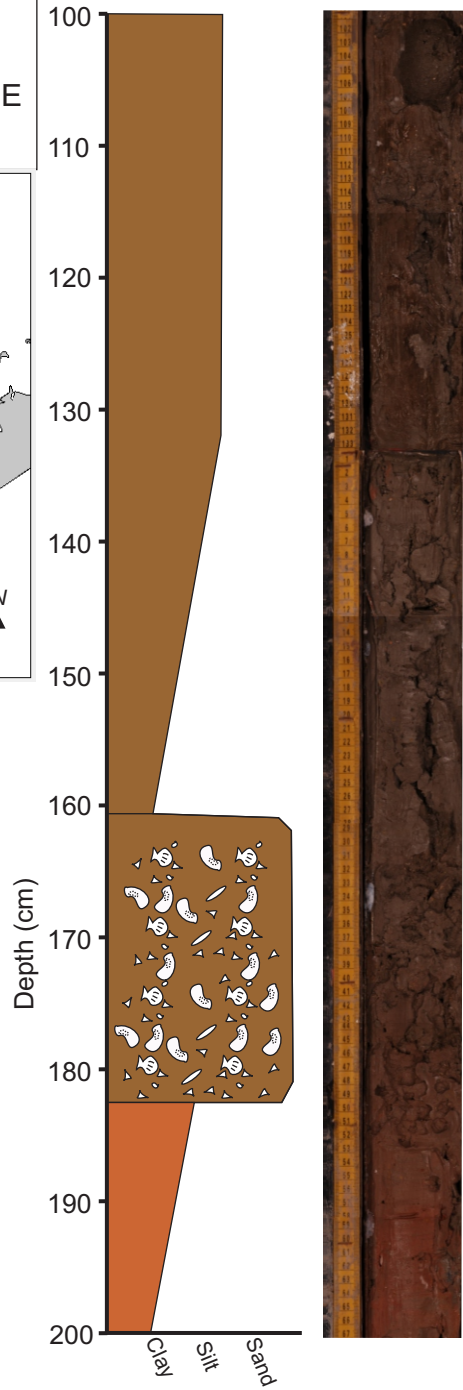
Project: West Bay
Core ID: SLP 16
Section: 200-300 cm
Location (Zone 15 N): 3226067 N, 299118 E
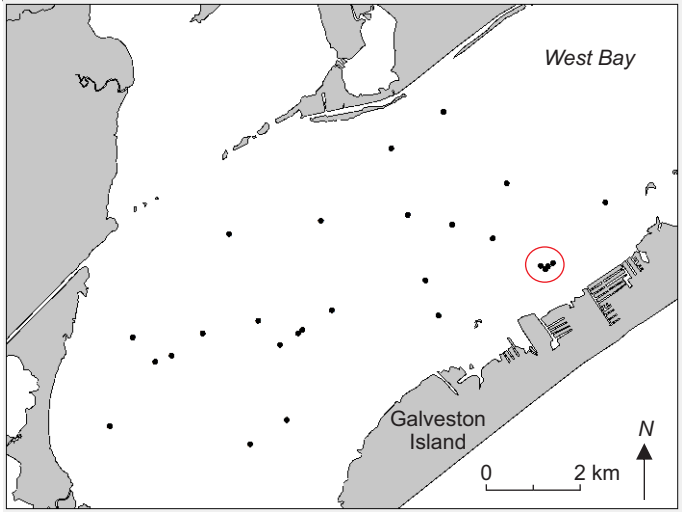
West Bay

Galveston
Island

0   2 km   N

Legend

- Lower Estuary
- Middle Estuary
- Paleo-Brazos River Pro-Delta
- Upper Estuary
- Delta Plain
- Mouth Bar
- Beaumont Formation
- Estuarine Shell
- Burrows

Depth (cm)

Clay   Silt   Sand
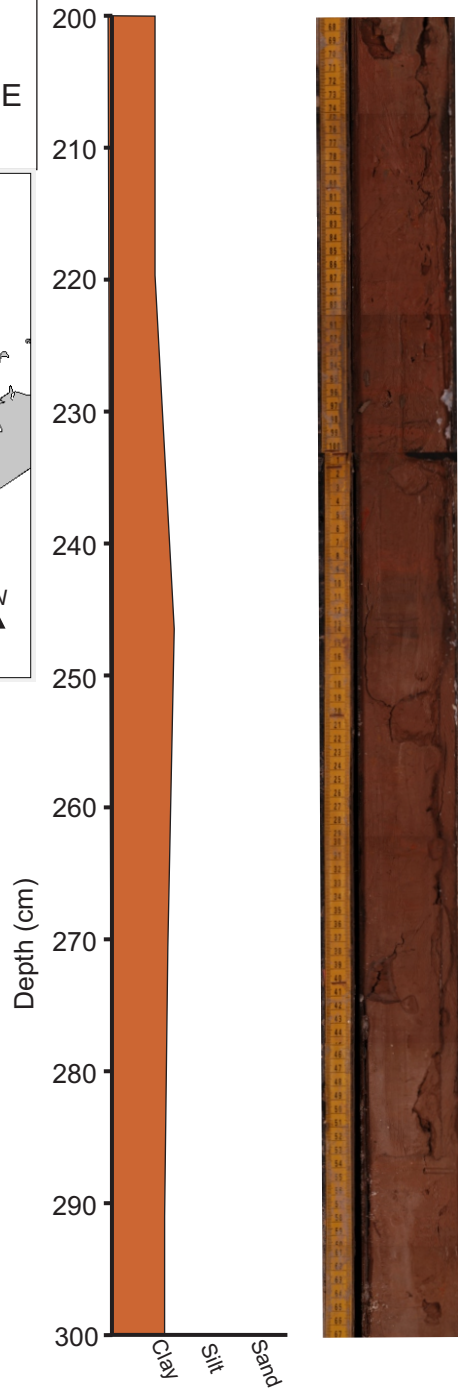
Project: West Bay

Core ID: SLP 16

Section: 300-400 cm
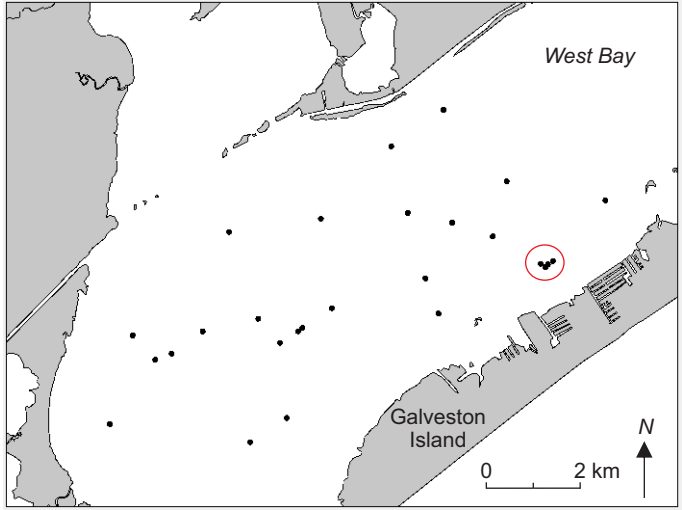
Location (Zone 15 N): 3226067 N, 299118 E

West Bay

Galveston
Island

0   2 km

N

Legend

- Lower Estuary
- Middle Estuary
- Paleo-Brazos River Pro-Delta
- Upper Estuary
- Delta Plain
- Mouth Bar
- Beaumont Formation
- Estuarine Shell
- Burrows

Depth (cm)

300
310
320
330
340
350
360
370
380
390
400

Clay   Silt   Sand
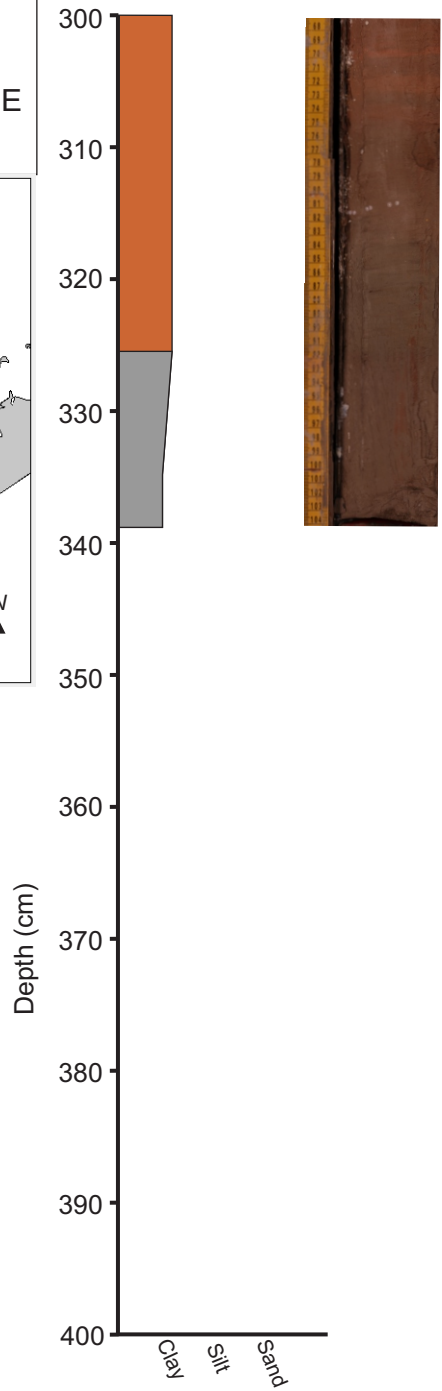
Project: West Bay

Core ID: SLP 17

Section: 0-100 cm

Location (Zone 15 N): 3224288 N, 291792 E
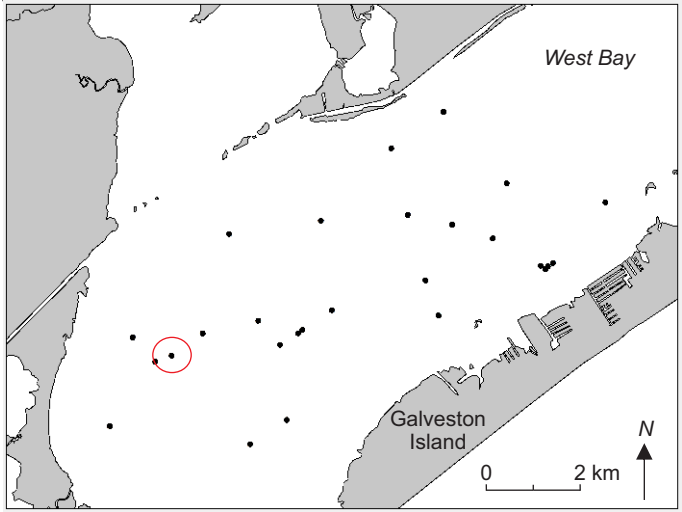
West Bay

Galveston
Island

0   2 km

N

Legend

- Lower Estuary
- Middle Estuary
- Paleo-Brazos River Pro-Delta
- Upper Estuary
- Delta Plain
- Mouth Bar
- Beaumont Formation
- Estuarine Shell
- Burrows

Depth (cm)

Clay   Silt   Sand
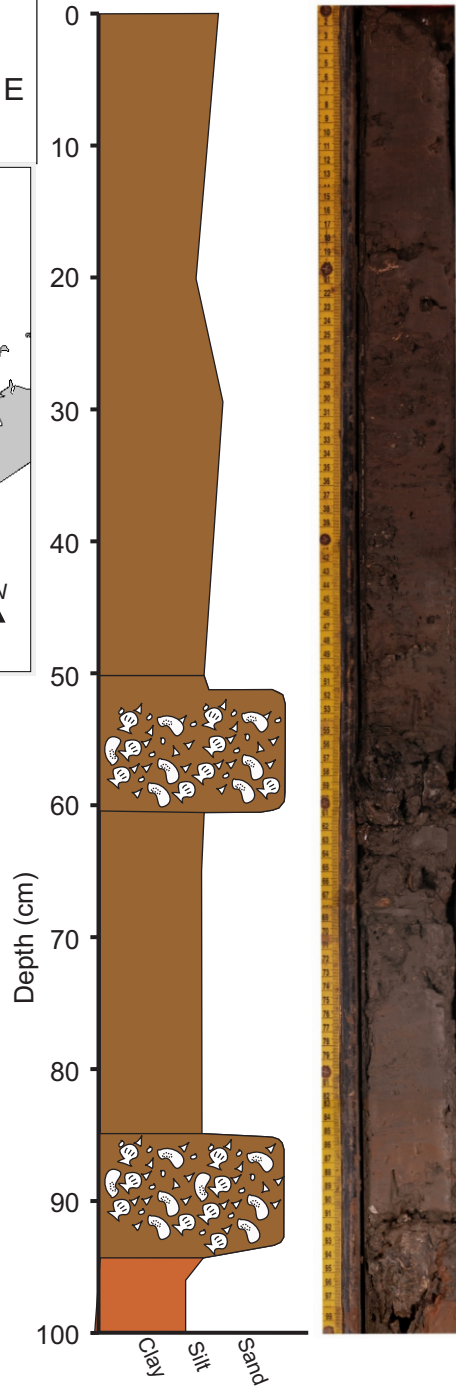
Project: West Bay
Core ID: SLP 17
Section: 100-200 cm
Location (Zone 15 N): 3224288 N, 291792 E
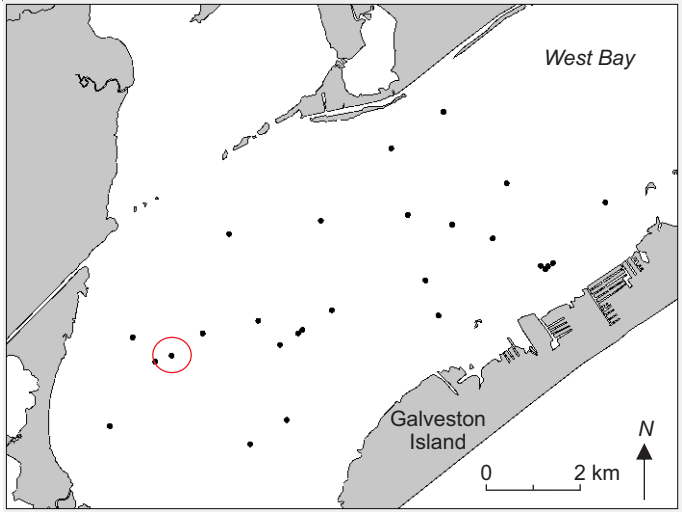
West Bay

Galveston Island

0   2 km

N

Legend

- Lower Estuary
- Middle Estuary
- Paleo-Brazos River Pro-Delta
- Upper Estuary
- Delta Plain
- Mouth Bar
- Beaumont Formation
- Estuarine Shell
- Burrows
- *R. Cuneata*

Depth (cm)

Clay Silt Sand
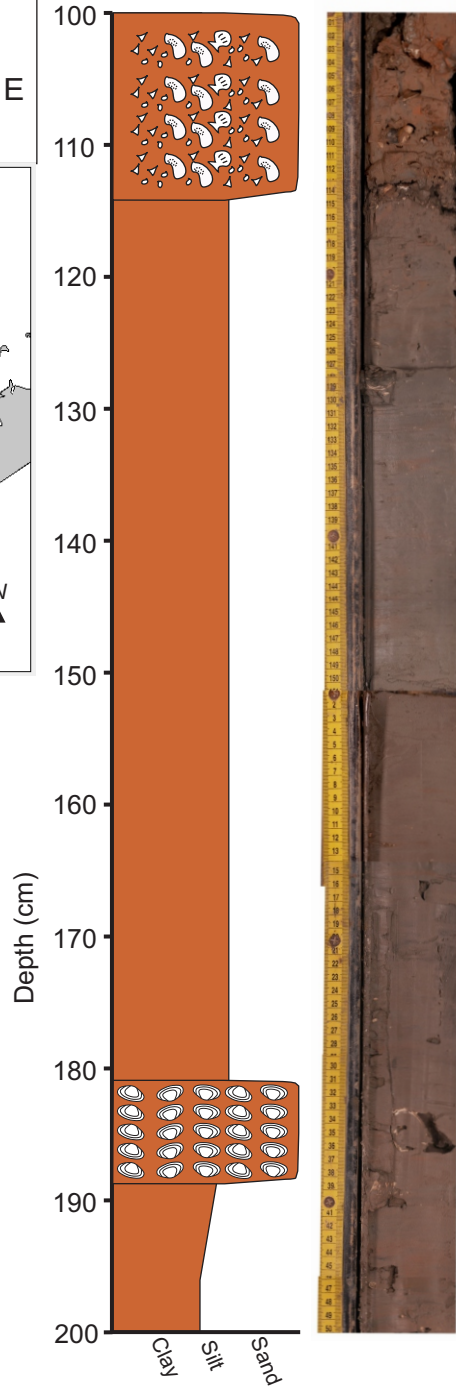
Project: West Bay
Core ID: SLP 17
Section: 200-300 cm
Location (Zone 15 N): 3224288 N, 291792 E
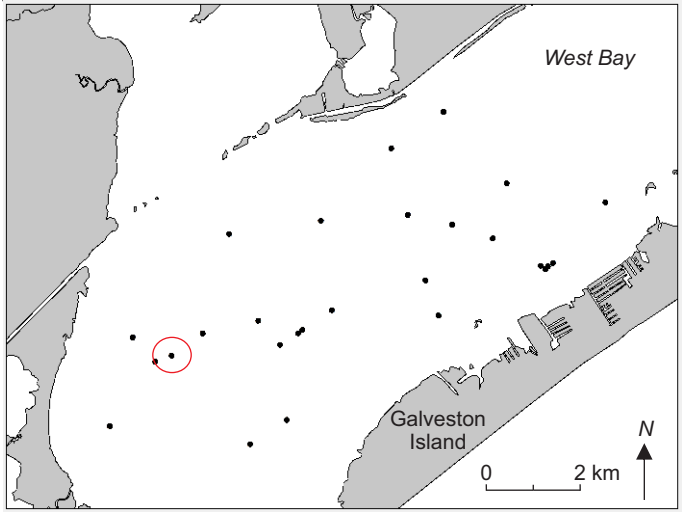
West Bay

Galveston Island

0 __ 2 km

N

Legend

- ☐ Lower Estuary
- ☐ Middle Estuary
- ☐ Paleo-Brazos River Pro-Delta
- ☐ Upper Estuary
- ☐ Delta Plain
- ☐ Mouth Bar
- ☐ Beaumont Formation
- ⬥ Estuarine Shell
- ⬙ Burrows
- � *R. Cuneata*

Depth (cm)

200
210
220
230
240
250
260
270
280
290
300

Clay Silt Sand
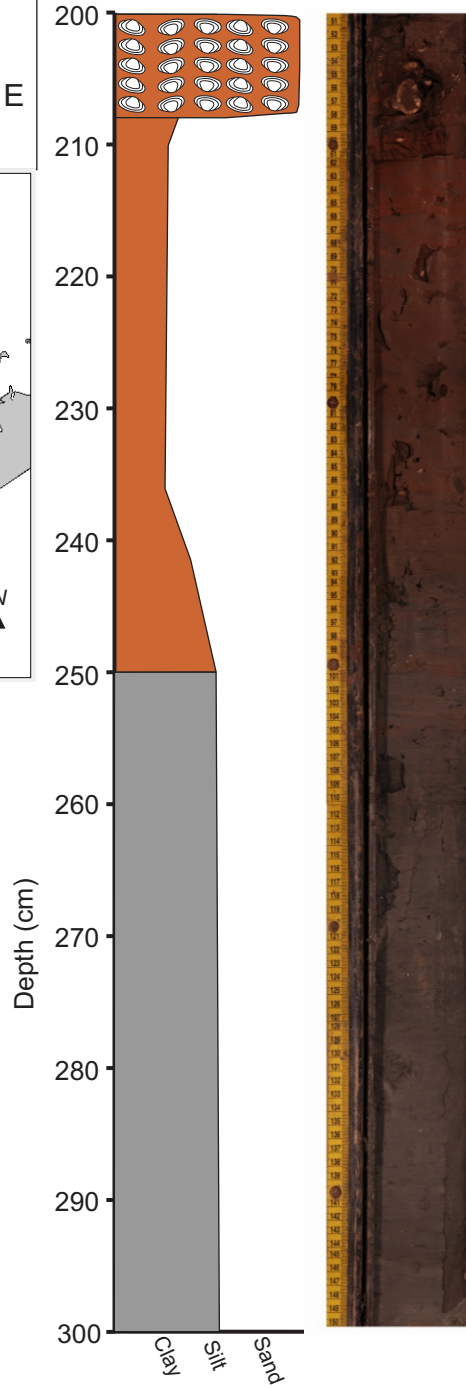
Project: West Bay

Core ID: SLP 18

Section: 0-100 cm

Location (Zone 15 N): 3226883 N, 297359 E
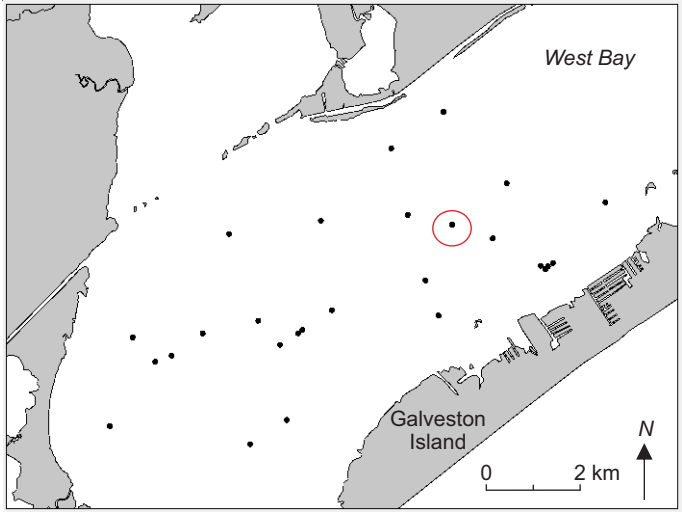
West Bay

Galveston Island

0   2 km

N

Legend

- Lower Estuary
- Middle Estuary
- Paleo-Brazos River Pro-Delta
- Upper Estuary
- Delta Plain
- Mouth Bar
- Beaumont Formation
- Estuarine Shell
- Burrows

Depth (cm)

Clay   Silt   Sand
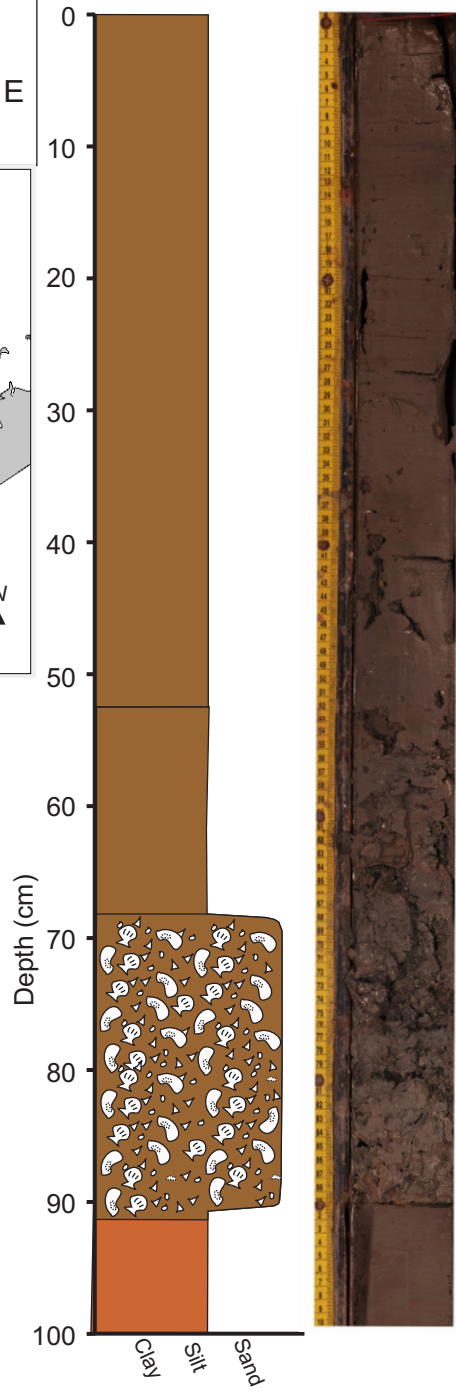
Project: West Bay

Core ID: SLP 18

Section: 100-174 cm

Location (Zone 15 N): 3226883 N, 297359 E
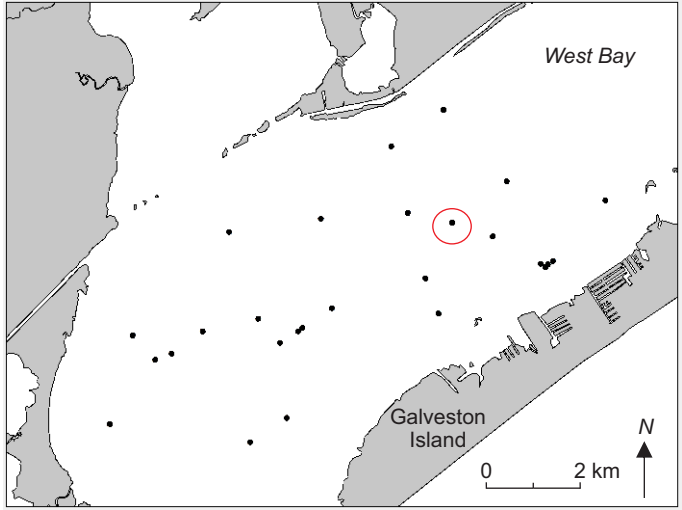
West Bay

Galveston
Island

0   2 km

N

Legend

- ■ Lower Estuary
- ■ Middle Estuary
- ■ Paleo-Brazos River Pro-Delta
- ■ Upper Estuary
- ■ Delta Plain
- ☐ Mouth Bar
- ■ Beaumont Formation
- ⚯ Estuarine Shell
- ⟨⟨ Burrows

Depth (cm)

100
110
120
130
140
150
160
170
180
190
200

Clay   Silt   Sand
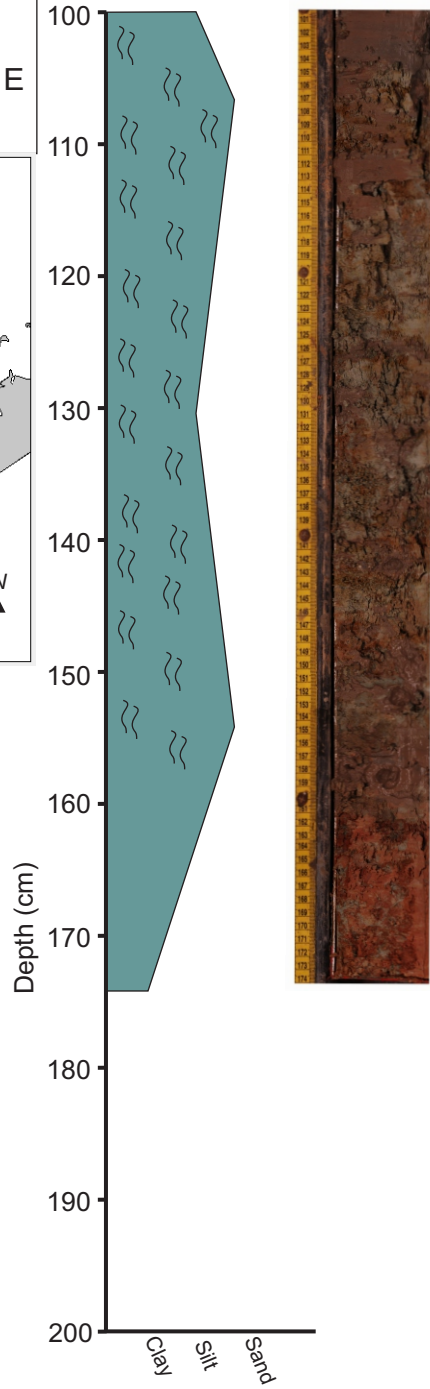
Project: West Bay
Core ID: SLP 19
Section: 0-100 cm
Location (Zone 15 N): 3225778 N, 296829 E
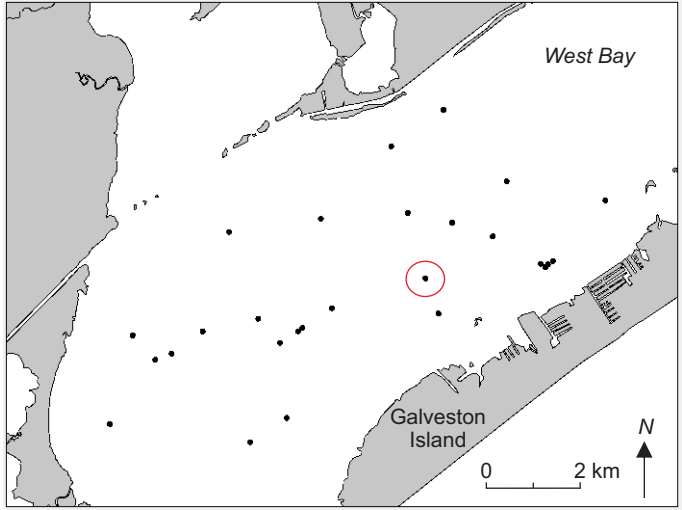
West Bay

Galveston
Island

0   2 km

N

Legend

- Lower Estuary
- Middle Estuary
- Paleo-Brazos River Pro-Delta
- Upper Estuary
- Delta Plain
- Mouth Bar
- Beaumont Formation
- Estuarine Shell
- Burrows

Depth (cm)

Clay   Silt   Sand
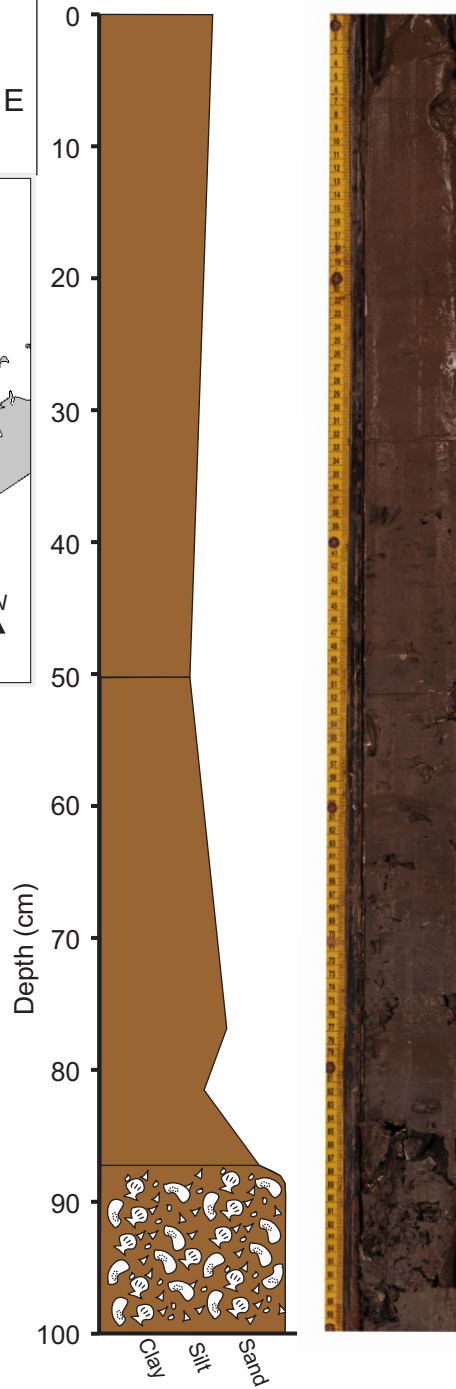
Project: West Bay
Core ID: SLP 19
Section: 100-200 cm
Location (Zone 15 N): 3225778 N, 296829 E
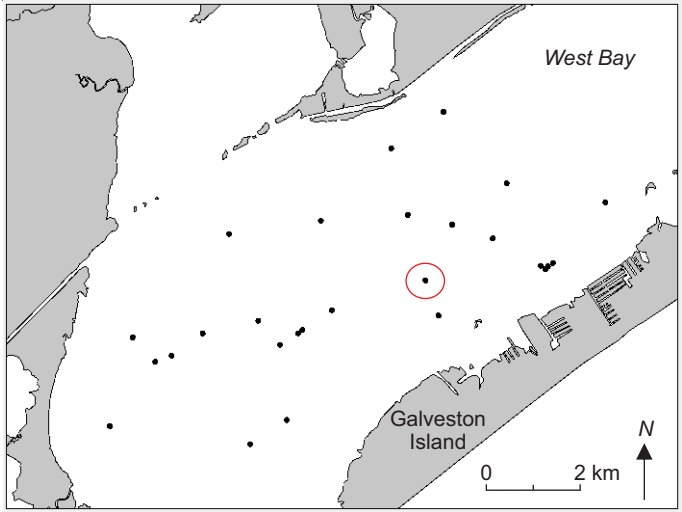
West Bay

Galveston Island

N

0   2 km

Legend

■ Lower Estuary
■ Middle Estuary
■ Paleo-Brazos River Pro-Delta
■ Upper Estuary
■ Delta Plain
□ Mouth Bar
■ Beaumont Formation
𝔞 Estuarine Shell
⟨ Burrows
◖◗ R. Cuneata

Depth (cm)

Clay Silt Sand
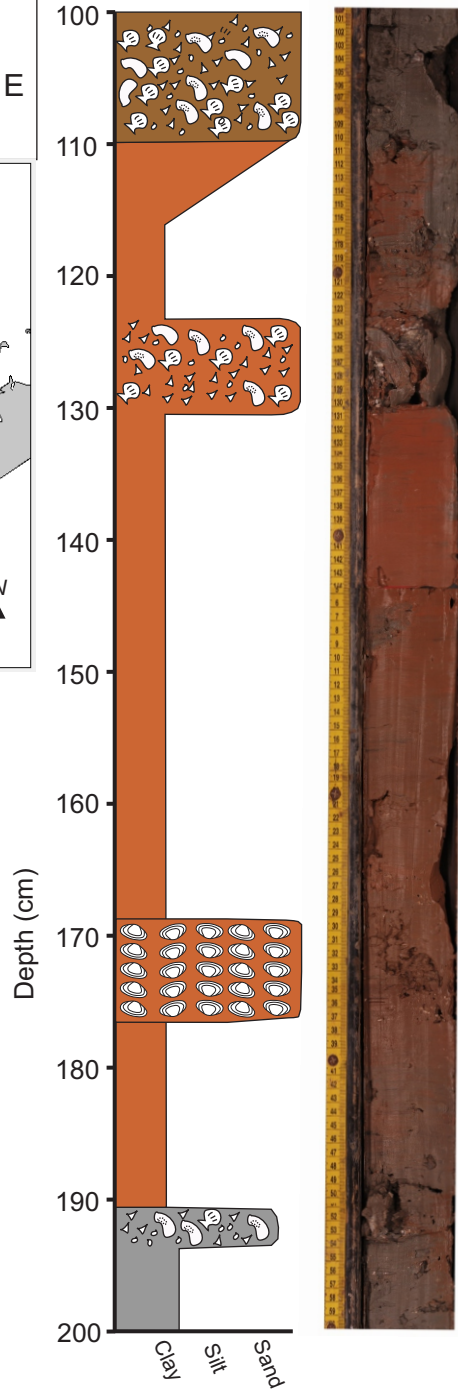
Project: West Bay
Core ID: SLP 19
Section: 200-300 cm
Location (Zone 15 N): 3225778 N, 296829 E
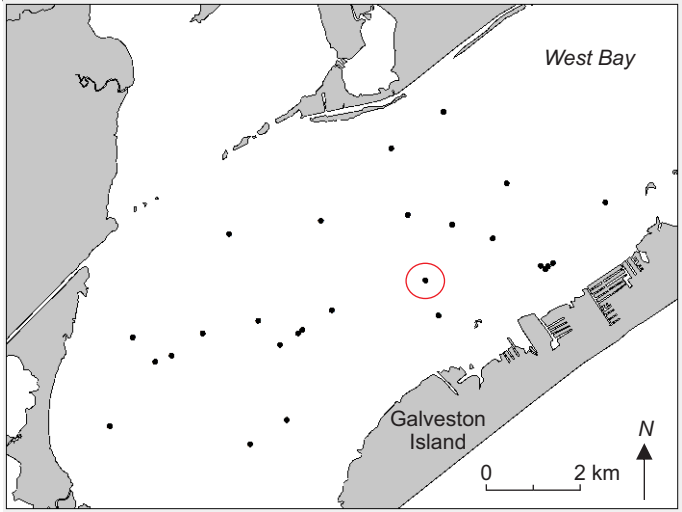
West Bay

Galveston
Island

0   2 km

N

Legend

- ■ Lower Estuary
- ■ Middle Estuary
- ■ Paleo-Brazos River Pro-Delta
- ■ Upper Estuary
- ■ Delta Plain
- ▢ Mouth Bar
- ▢ Beaumont Formation
- ᘛ Estuarine Shell
- ⎇ Burrows

Depth (cm)

200

210

220

230

240

250

260

270

280

290

300

Clay   Silt   Sand
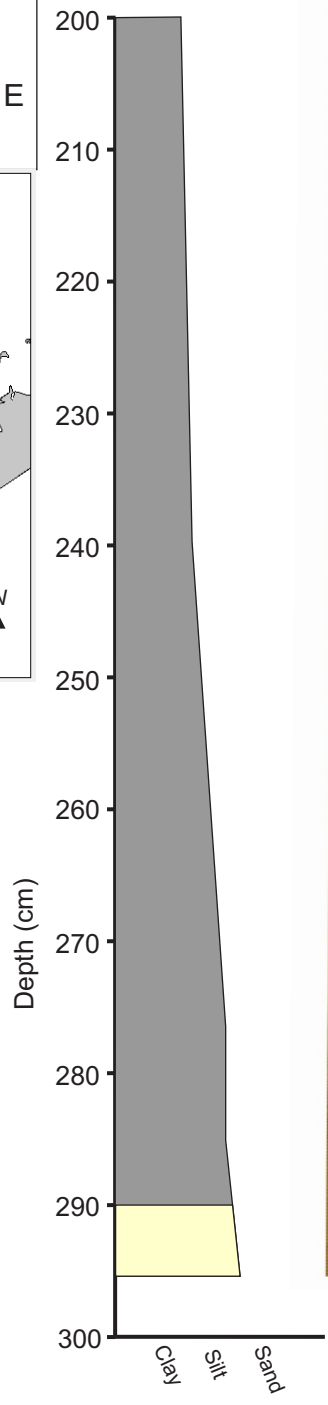
Project: West Bay
Core ID: SLP 22
Section: 0-100 cm
Location (Zone 15 N): 3224502 N, 293944 E
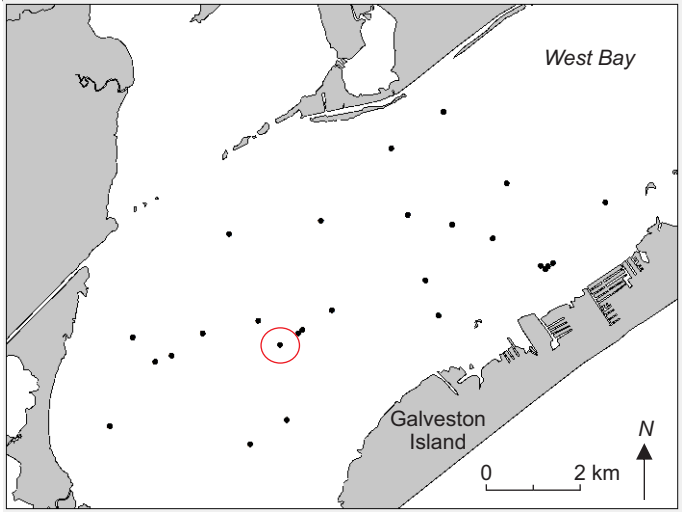
West Bay

Galveston
Island

0   2 km

N

Legend

■ Lower Estuary
■ Middle Estuary
■ Paleo-Brazos River Pro-Delta
■ Upper Estuary
■ Delta Plain
□ Mouth Bar
■ Beaumont Formation
🐚 Estuarine Shell
〰 Burrows

Depth (cm)

Clay   Silt   Sand
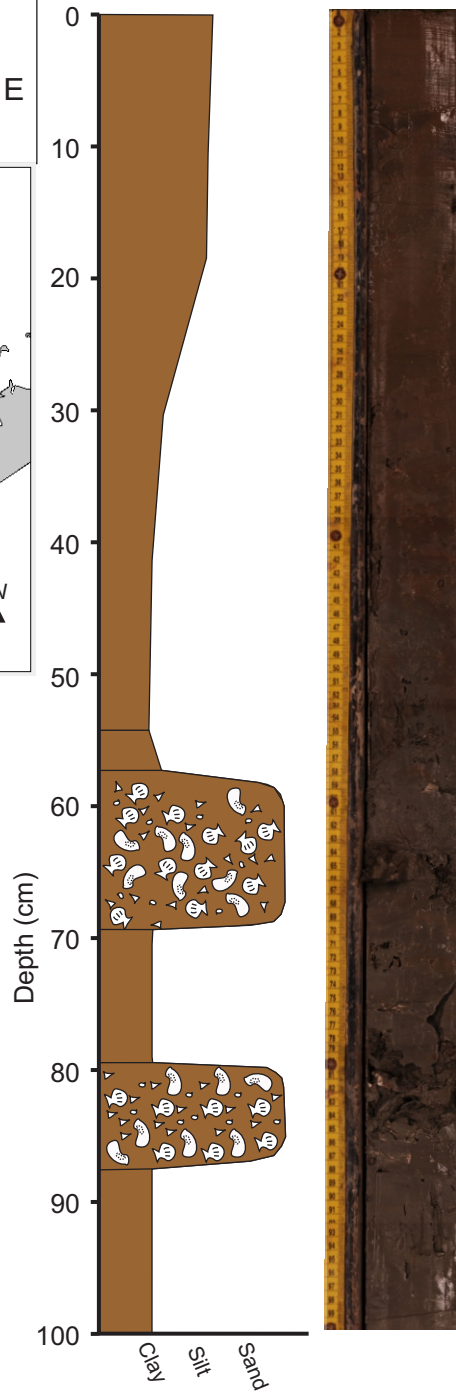
Project: West Bay

Core ID: SLP 22

Section: 100-200 cm
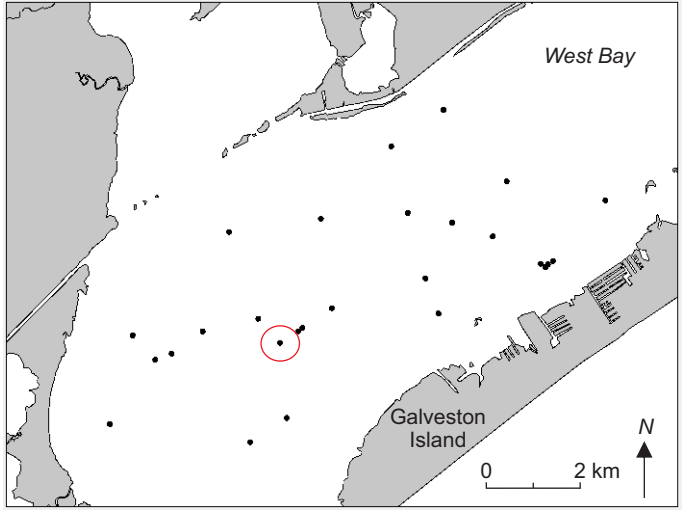
Location (Zone 15 N): 3224502 N, 293944 E

West Bay

Galveston Island

0   2 km

N

Legend

- ■ Lower Estuary
- ■ Middle Estuary
- ■ Paleo-Brazos River Pro-Delta
- ■ Upper Estuary
- ■ Delta Plain
- □ Mouth Bar
- □ Beaumont Formation
- ᶲᶜ Estuarine Shell
- ⟨⟨ Burrows
- ◌◌ *R. Cuneata*

Depth (cm)

Clay   Silt   Sand
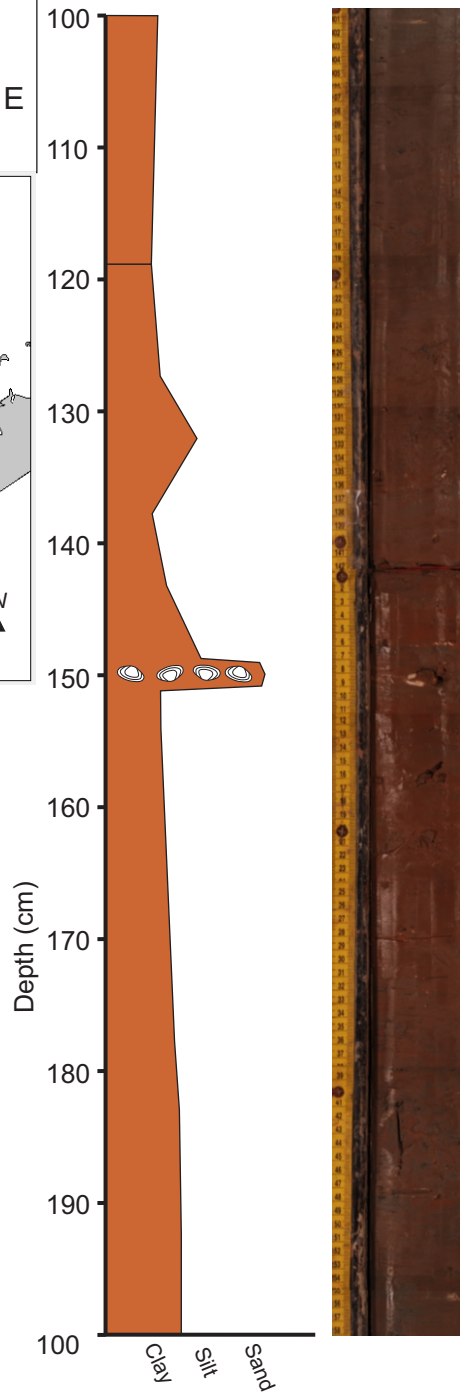
Project: West Bay
Core ID: SLP 22
Section: 200-271 cm
Location (Zone 15 N): 3224502 N, 293944 E
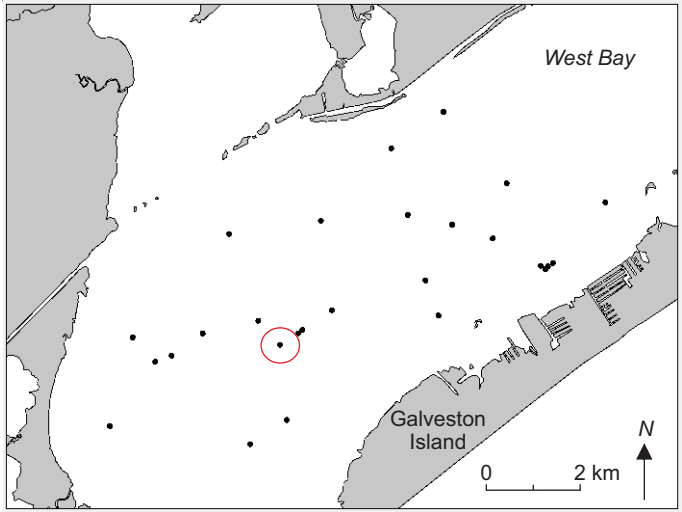
West Bay

Galveston Island

0   2 km

N

Legend

- Lower Estuary
- Middle Estuary
- Paleo-Brazos River Pro-Delta
- Upper Estuary
- Delta Plain
- Mouth Bar
- Beaumont Formation
- Estuarine Shell
- Burrows

Depth (cm)

200
210
220
230
240
250
260
270
280
290
300

Clay Silt Sand
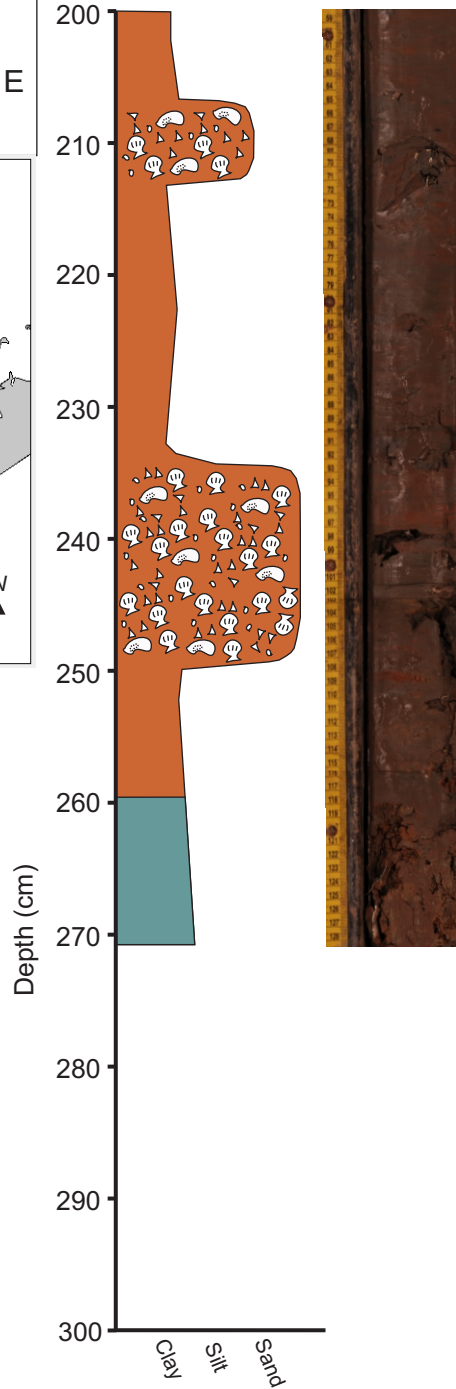
Project: West Bay

Core ID: SLP 23

Section: 0-100 cm

Location (Zone 15 N): 3224727 N, 292408 E
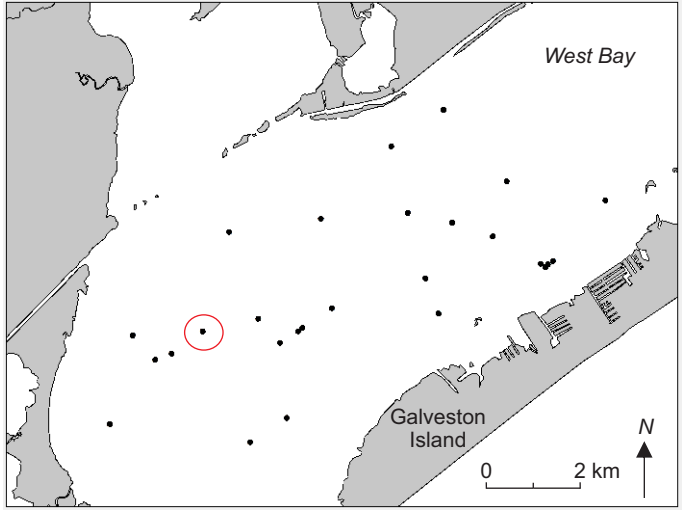
West Bay

Galveston Island

0   2 km

N

Legend

■ Lower Estuary
■ Middle Estuary
■ Paleo-Brazos River Pro-Delta
■ Upper Estuary
■ Delta Plain
□ Mouth Bar
□ Beaumont Formation
🐚 Estuarine Shell
〈 Burrows

Depth (cm)

Clay   Silt   Sand
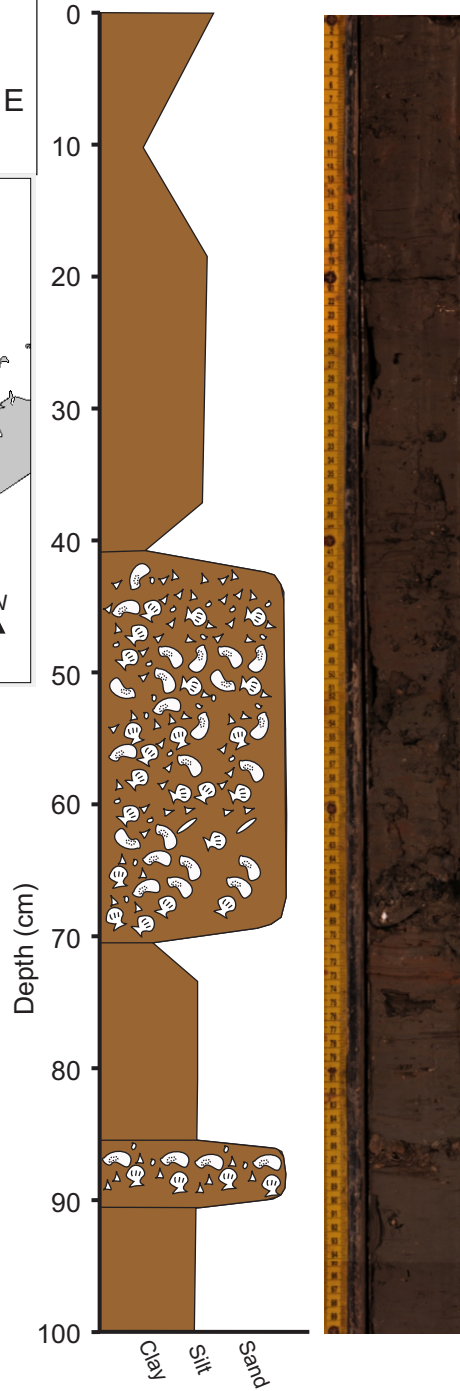
Project: West Bay

Core ID: SLP 23

Section: 100-200 cm
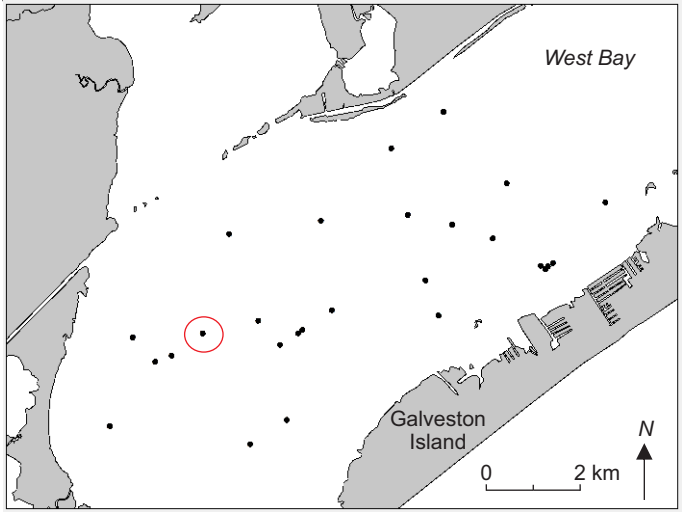
Location (Zone 15 N): 3224727 N, 292408 E

West Bay

Galveston
Island

0   2 km

N

Legend

- Lower Estuary
- Middle Estuary
- Paleo-Brazos River Pro-Delta
- Upper Estuary
- Delta Plain
- Mouth Bar
- Beaumont Formation
- Estuarine Shell
- Burrows
- *R. Cuneata*

Depth (cm)

Clay   Silt   Sand
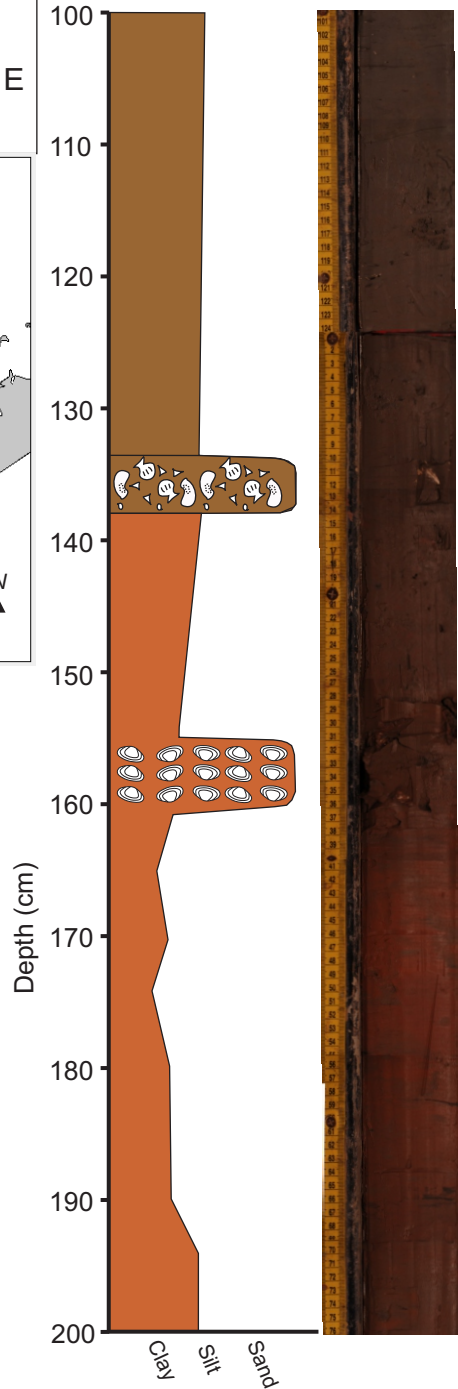
Project: West Bay

Core ID: SLP 23

Section: 400-500 cm
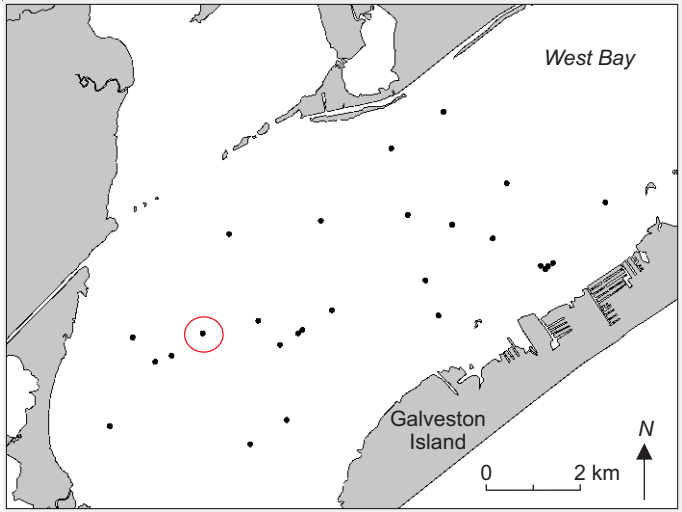
Location (Zone 15 N): 3224727 N, 292408 E

West Bay

Galveston Island

0   2 km

N

Legend

- ■ Lower Estuary
- ■ Middle Estuary
- ■ Paleo-Brazos River Pro-Delta
- ■ Distributary Channel
- ■ Delta Plain
- □ Mouth Bar
- ■ Beaumont Formation
- ⚯ Estuarine Shell
- ⟨⟨ Burrows

Depth (cm)

400

410

420

430

440

450

460

470

480

490

500

Clay   Silt   Sand
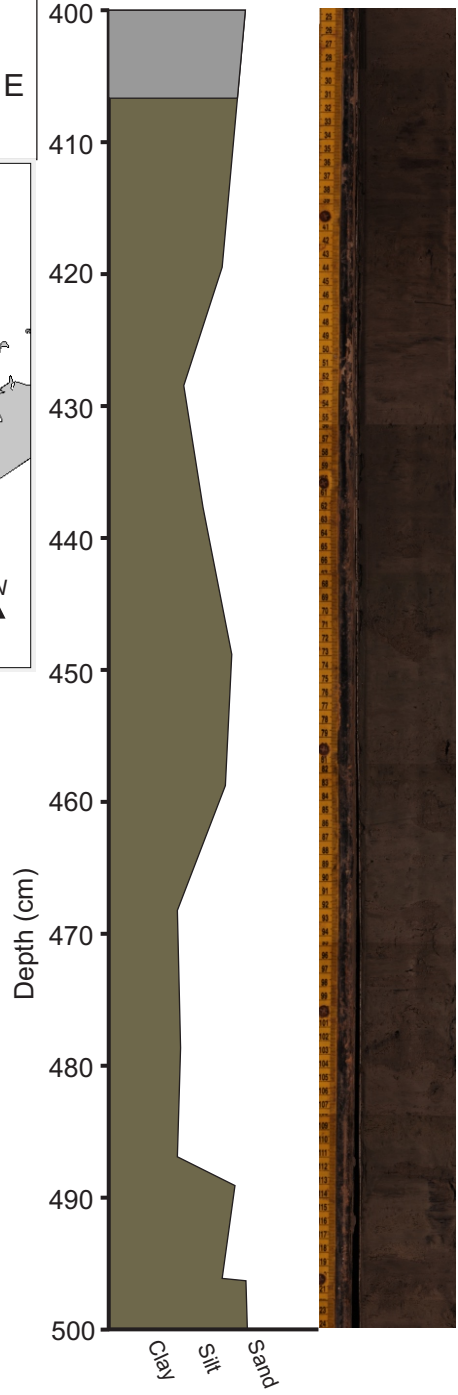
Project: West Bay

Core ID: SLP 23

Section: 500-526 cm

Location (Zone 15 N): 3224727 N, 292408 E
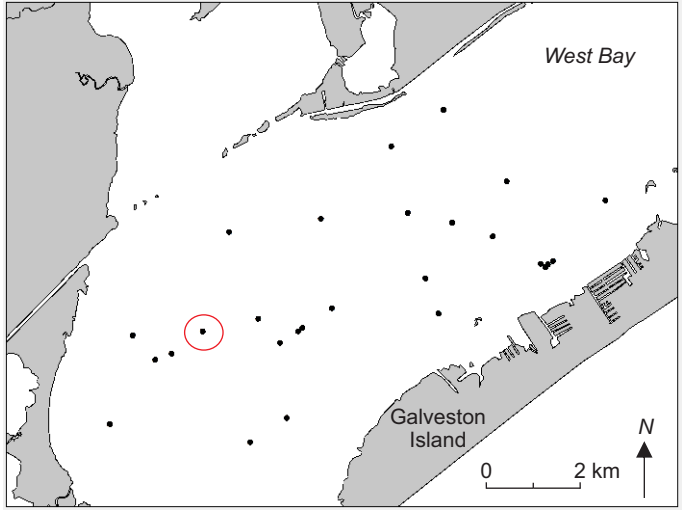
West Bay

Galveston
Island

0   2 km

N

Legend

- ■ Lower Estuary
- ■ Middle Estuary
- ■ Paleo-Brazos River Pro-Delta
- ■ Distributary Channel
- ■ Delta Plain
- □ Mouth Bar
- ■ Beaumont Formation
- ⌇ Estuarine Shell
- ⌇ Burrows

Depth (cm)

Clay Silt Sand
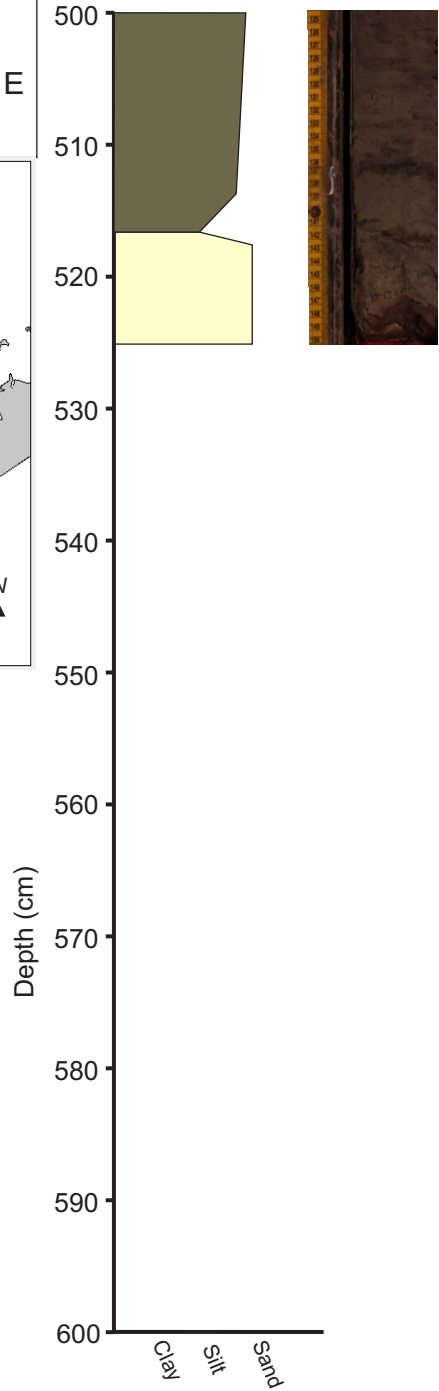
Project: West Bay
Core ID: OC1A
Section: 0-100 cm
Location (Zone 15 N): 3226120 N, 299360 E
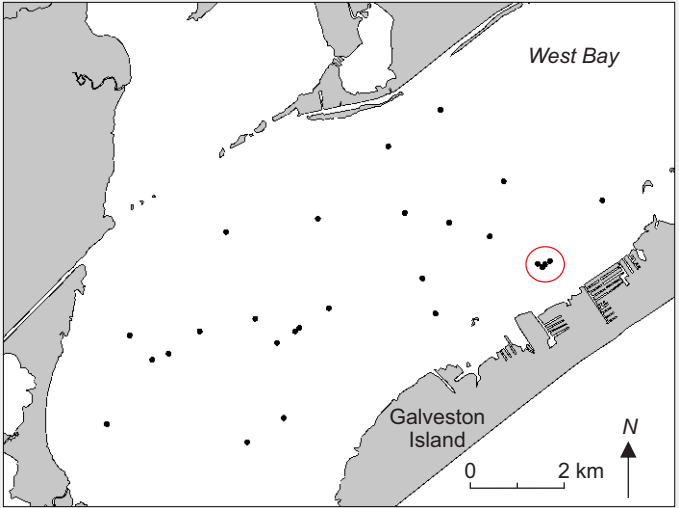
West Bay

Galveston Island

0   2 km

N

Legend

■ Lower Estuary
■ Middle Estuary
■ Paleo-Brazos River Pro-Delta
■ Upper Estuary
■ Delta Plain
□ Mouth Bar
□ Beaumont Formation
❧ Estuarine Shell
〰 Burrows

Depth (cm)

Clay Silt Sand
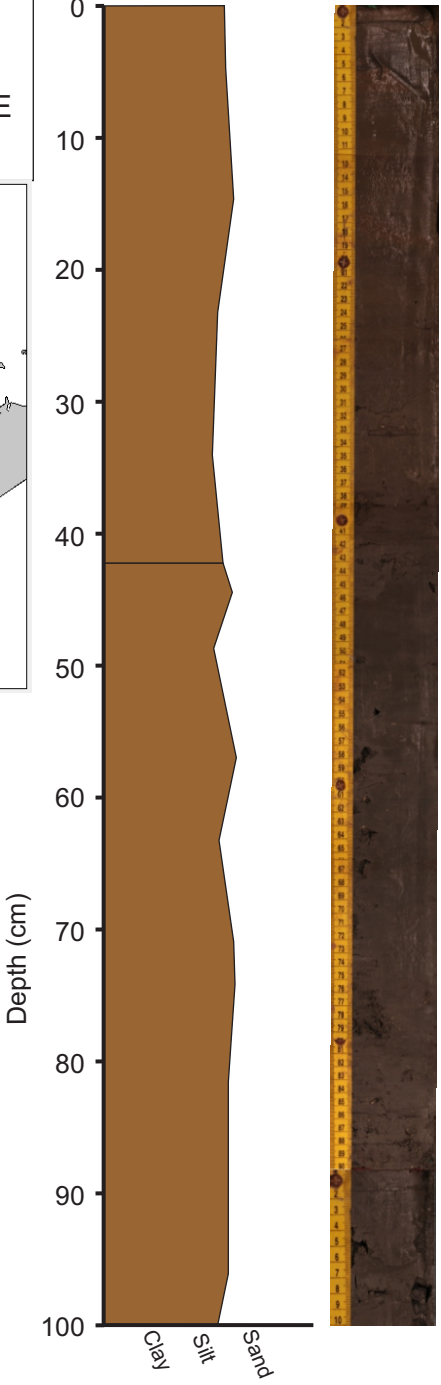
Project: West Bay
Core ID: OC1A
Section: 100-190 cm
Location (Zone 15 N): 3226120 N, 299360 E

West Bay

Galveston Island

0   2 km

N

Legend

■ Lower Estuary
■ Middle Estuary
■ Paleo-Brazos River Pro-Delta
■ Upper Estuary
■ Delta Plain
□ Mouth Bar
■ Beaumont Formation
⌇ Estuarine Shell
⌇ Burrows

Depth (cm)

Clay   Silt   Sand

Project: West Bay
Core ID: OC1AB2
Section: 0-100 cm
Location (Zone 15 N): 3226054 N, 299260 E

West Bay

Galveston
Island

0   2 km

N

Legend

- Lower Estuary
- Middle Estuary
- Paleo-Brazos River Pro-Delta
- Upper Estuary
- Delta Plain
- Mouth Bar
- Beaumont Formation
- Estuarine Shell
- Burrows

Depth (cm)

Clay Silt Sand

Project: West Bay
Core ID: OC1AB2
Section: 100-200 cm
Location (Zone 15 N): 3226054 N, 299260 E
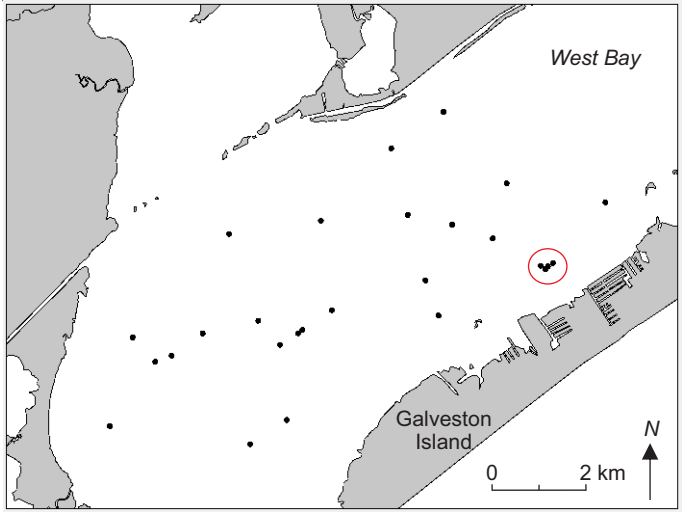
West Bay

Galveston Island

N

0   2 km

Legend

- Lower Estuary
- Middle Estuary
- Paleo-Brazos River Pro-Delta
- Upper Estuary
- Delta Plain
- Mouth Bar
- Beaumont Formation
- Estuarine Shell
- Burrows

Depth (cm)

Clay Silt Sand

Project: West Bay
Core ID: OC1AB2
Section: 200-300 cm
Location (Zone 15 N): 3226054 N, 299260 E

West Bay

Galveston Island

N

0   2 km

Legend

- Lower Estuary
- Middle Estuary
- Paleo-Brazos River Pro-Delta
- Upper Estuary
- Delta Plain
- Mouth Bar
- Beaumont Formation
- Estuarine Shell
- Burrows

Depth (cm)

Clay   Silt   Sand

Project: West Bay
Core ID: OC1AB2
Section: 300-400 cm
Location (Zone 15 N): 3226054 N, 299260 E
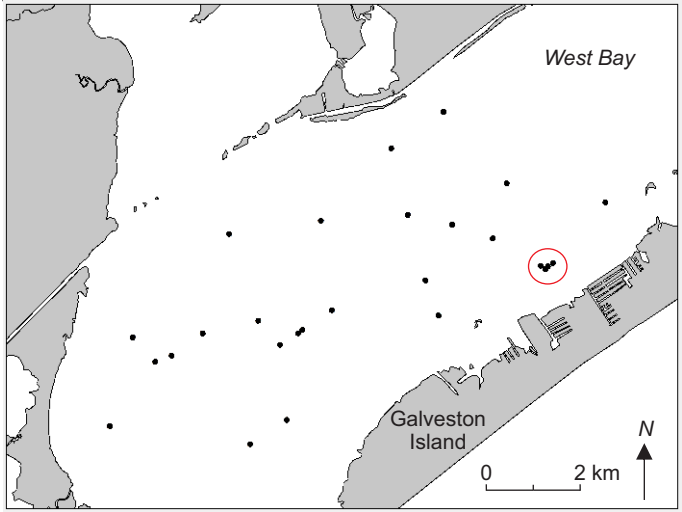
West Bay

Galveston Island

0   2 km   N

Legend

- Lower Estuary
- Middle Estuary
- Paleo-Brazos River Pro-Delta
- Upper Estuary
- Delta Plain
- Mouth Bar
- Oxbow Lake
- Estuarine Shell
- Burrows

Depth (cm)

300
310
320
330
340
350
360
370
380
390
400

Clay   Silt   Sand

Project: West Bay

Core ID: OC1B

Section: 0-100 cm

Location (Zone 15 N): 3226054 N, 299260 E

West Bay

Galveston Island

0   2 km

N

Legend

- Lower Estuary
- Middle Estuary
- Paleo-Brazos River Pro-Delta
- Upper Estuary
- Delta Plain
- Mouth Bar
- Oxbow Lake
- Estuarine Shell
- Burrows

Depth (cm)

Clay   Silt   Sand

Project: West Bay
Core ID: OC1B
Section: 100-200 cm
Location (Zone 15 N): 3226054 N, 299260 E

West Bay

Galveston
Island

0   2 km

N

Legend

- Lower Estuary
- Middle Estuary
- Paleo-Brazos River Pro-Delta
- Upper Estuary
- Delta Plain
- Mouth Bar
- Oxbow Lake
- Estuarine Shell
- Burrows

Depth (cm)

Clay   Silt   Sand

Project: West Bay
Core ID: OC1B
Section: 200-300 cm
Location (Zone 15 N): 3226054 N, 299260 E
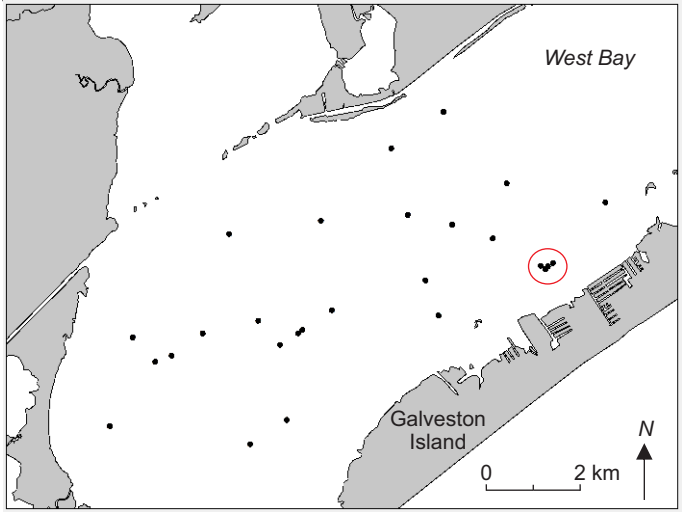
West Bay

Galveston
Island

0   2 km

N

Legend

- Lower Estuary
- Middle Estuary
- Paleo-Brazos River Pro-Delta
- Upper Estuary
- Delta Plain
- Mouth Bar
- Oxbow Lake
- Estuarine Shell
- Burrows

Depth (cm)

200
210
220
230
240
250
260
270
280
290
300

Clay Silt Sand

Project: West Bay

Core ID: OC1B

Section: 300-400 cm
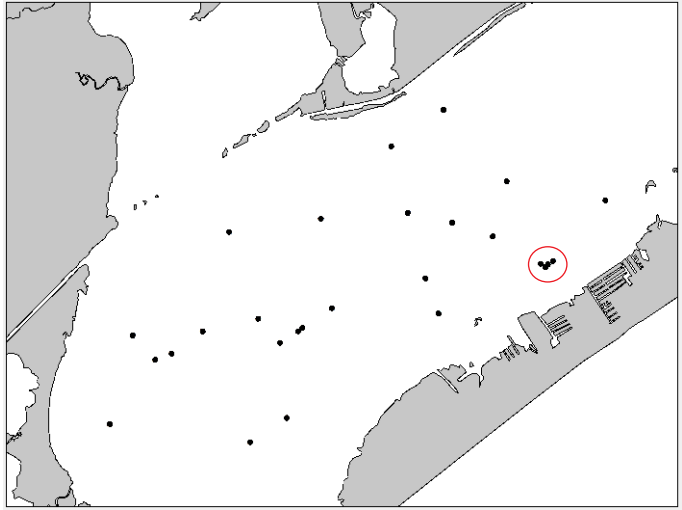
Location (Zone 15 N): 3226054 N, 299260 E

Legend

- Lower Estuary
- Middle Estuary
- Paleo-Brazos River Pro-Delta
- Upper Estuary
- Delta Plain
- Mouth Bar
- Oxbow Lake
- Estuarine Shell
- Burrows

Depth (cm)

Clay   Silt   Sand
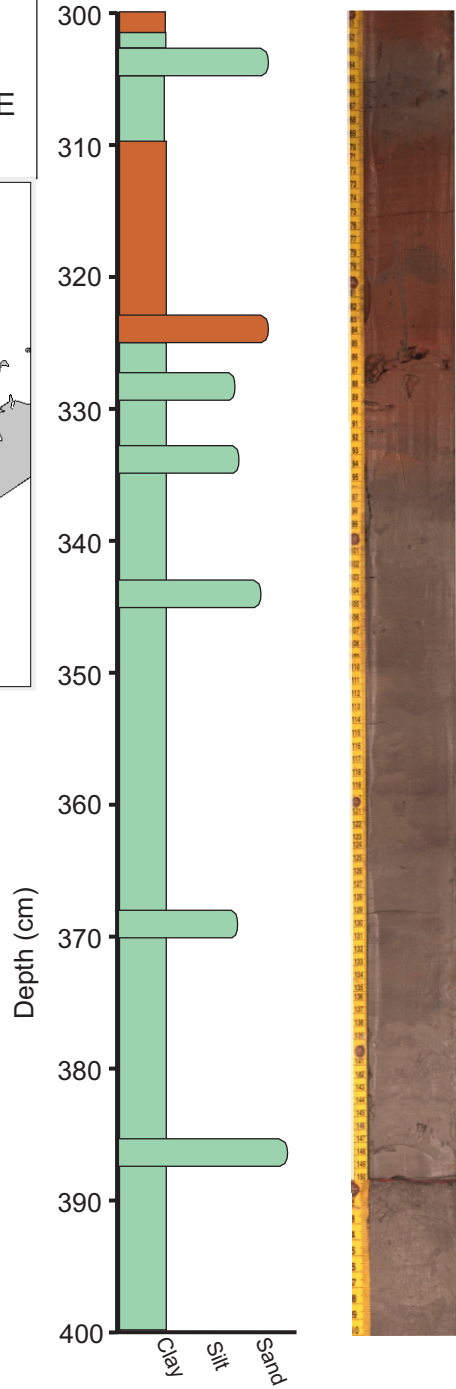
Project: West Bay

Core ID: OC1B

Section: 400-500 cm
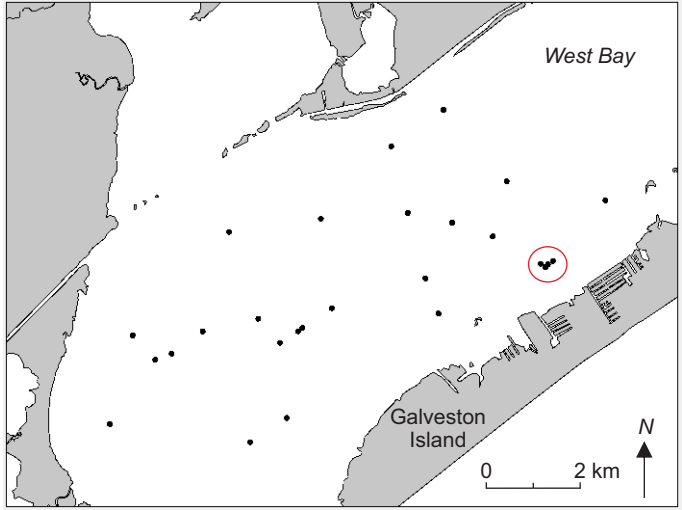
Location (Zone 15 N): 3226054 N, 299260 E

West Bay

Galveston Island

0   2 km

N

Legend

- Lower Estuary
- Middle Estuary
- Paleo-Brazos River Pro-Delta
- Upper Estuary
- Delta Plain
- Mouth Bar
- Oxbow Lake
- Estuarine Shell
- Burrows

Depth (cm)

Clay Silt Sand
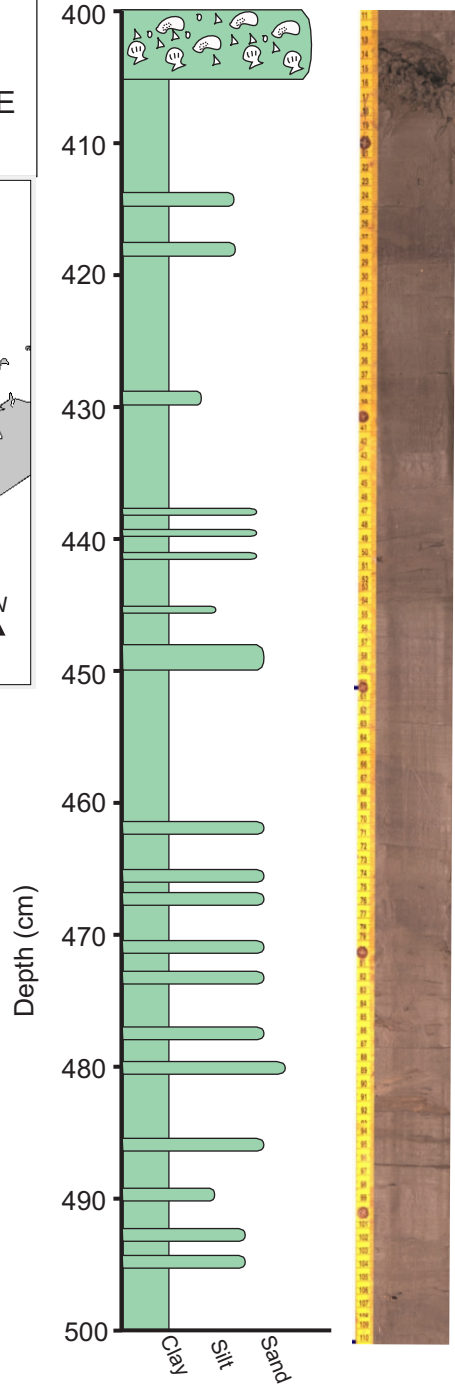
Project: West Bay
Core ID: OC1B
Section: 500-600 cm
Location (Zone 15 N): 3226054 N, 299260 E
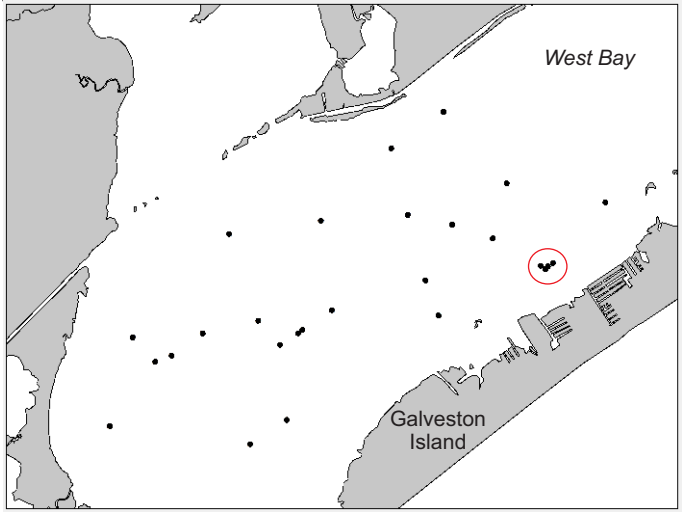
West Bay

Galveston Island

Legend

- Lower Estuary
- Middle Estuary
- Paleo-Brazos River Pro-Delta
- Upper Estuary
- Delta Plain
- Mouth Bar
- Oxbow Lake
- Estuarine Shell
- Burrows

Depth (cm)

Clay Silt Sand

Project: West Bay
Core ID: OC1B
Section: 600-700 cm
Location (Zone 15 N): 3226054 N, 299260 E

West Bay

Galveston Island

N

0   2 km

Legend

- Lower Estuary
- Middle Estuary
- Paleo-Brazos River Pro-Delta
- Upper Estuary
- Delta Plain
- Mouth Bar
- Oxbow Lake
- Estuarine Shell
- Burrows

Depth (cm)

Clay Silt Sand

Project: West Bay
Core ID: OC1B
Section: 700-800 cm
Location (Zone 15 N): 3226054 N, 299260 E
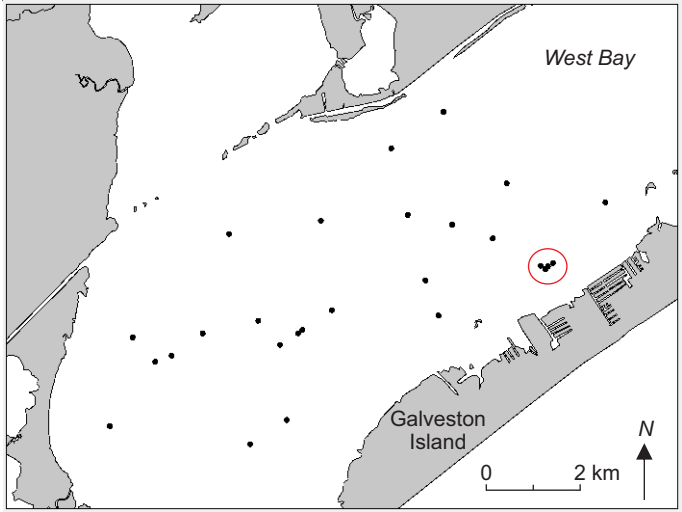
West Bay

Galveston Island

0   2 km

N

Legend

- Lower Estuary
- Middle Estuary
- Paleo-Brazos River Pro-Delta
- Upper Estuary
- Delta Plain
- Mouth Bar
- Oxbow Lake
- Estuarine Shell
- Burrows

Depth (cm)

700
710
720
730
740
750
760
770
780
790
800

Clay   Silt   Sand

Project: West Bay
Core ID: OC1B
Section: 800-900 cm
Location (Zone 15 N): 3226054 N, 299260 E
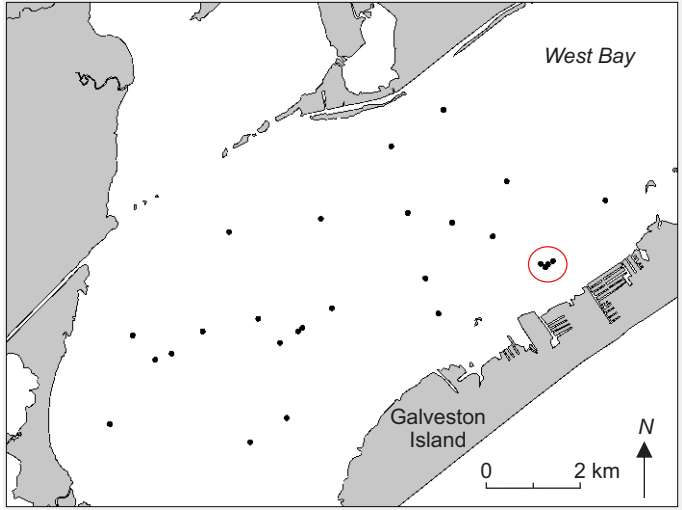
West Bay

Galveston Island

0   2 km

N

Legend

- Lower Estuary
- Middle Estuary
- Paleo-Brazos River Pro-Delta
- Upper Estuary
- Delta Plain
- Mouth Bar
- Oxbow Lake
- Estuarine Shell
- Burrows

Depth (cm)

800

810

820

830

840

850

860

870

880

890

900

Clay   Silt   Sand

Project: West Bay
Core ID: OC1B
Section: 900-1000 cm
Location (Zone 15 N): 3226054 N, 299260 E
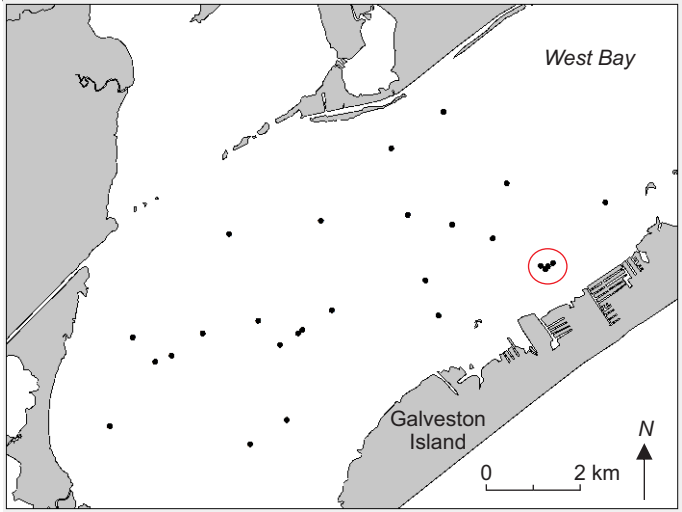
West Bay

Galveston Island

0   2 km

N

Legend

- Lower Estuary
- Middle Estuary
- Paleo-Brazos River Pro-Delta
- Upper Estuary
- Delta Plain
- Mouth Bar
- Oxbow Lake
- Estuarine Shell
- Burrows

Depth (cm)

Clay Silt Sand
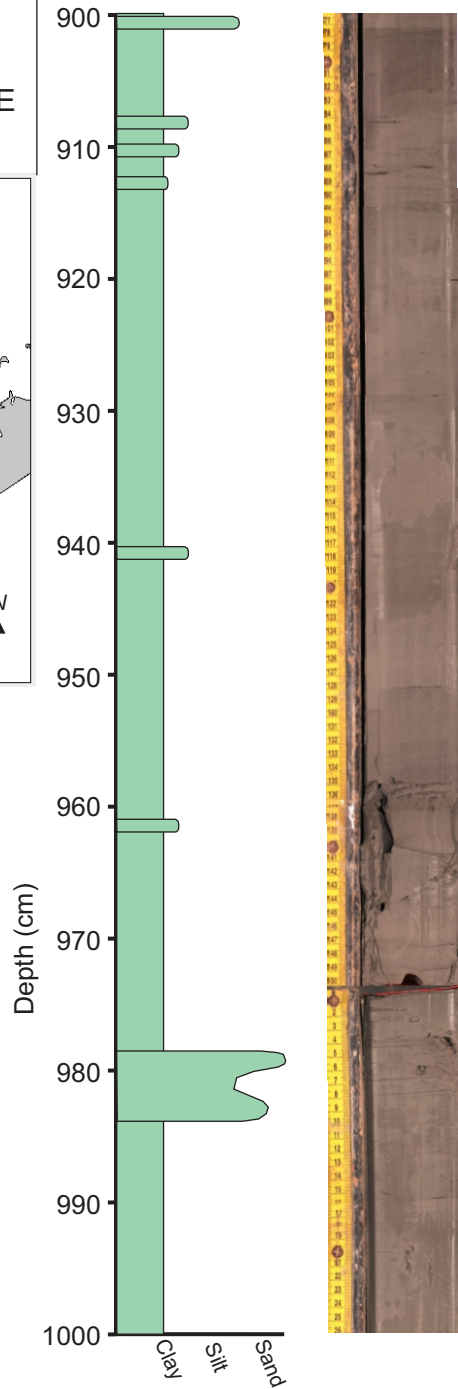
Project: West Bay
Core ID: OC1B
Section: 1000-1100 cm
Location (Zone 15 N): 3226054 N, 299260 E
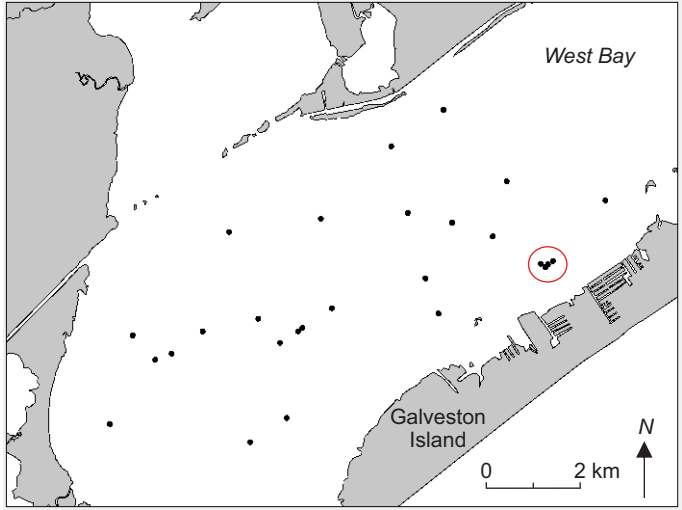
West Bay

Galveston
Island

0   2 km

N

Legend

- Lower Estuary
- Middle Estuary
- Paleo-Brazos River Pro-Delta
- Upper Estuary
- Delta Plain
- Mouth Bar
- Oxbow Lake
- Estuarine Shell
- Burrows

Depth (cm)

Clay Silt Sand
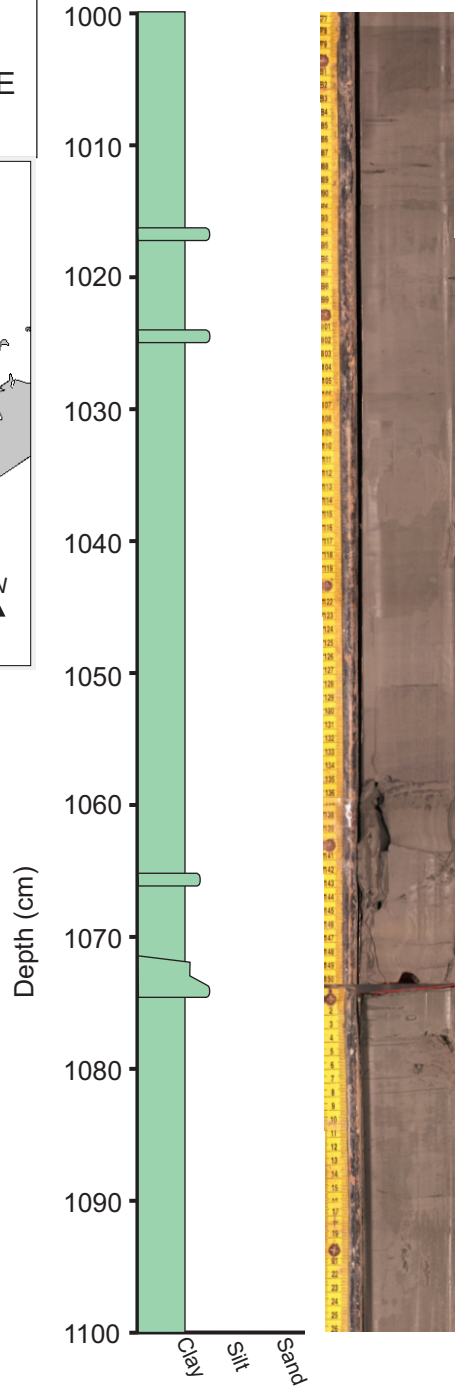
Project: West Bay

Core ID: OC1B

Section: 1100-1114 cm

Location (Zone 15 N): 3226054 N, 299260 E
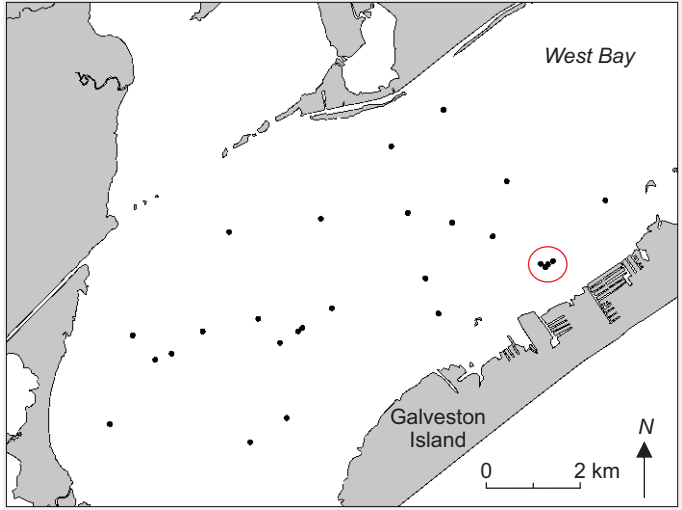
West Bay

Galveston Island

0   2 km

N

Legend

- Lower Estuary
- Middle Estuary
- Paleo-Brazos River Pro-Delta
- Upper Estuary
- Delta Plain
- Mouth Bar
- Oxbow Lake
- Estuarine Shell
- Burrows

Depth (cm)

1100
1110
1020
1130
1140
1150
1160
1170
1180
1190
1200

Clay Silt Sand
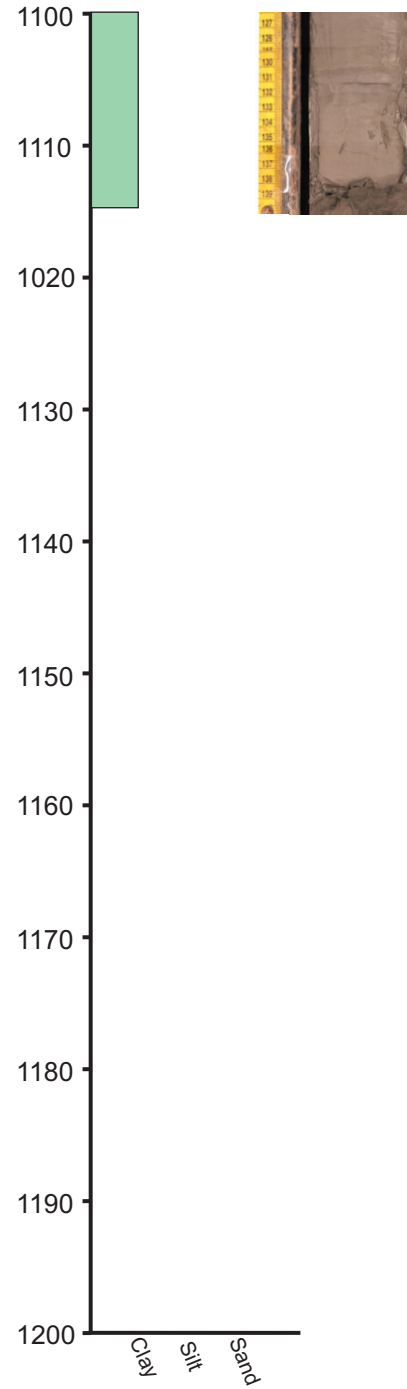
Project: West Bay
Core ID: OC1C
Section: 0-100 cm
Location (Zone 15 N): 3226004 N, 299211 E
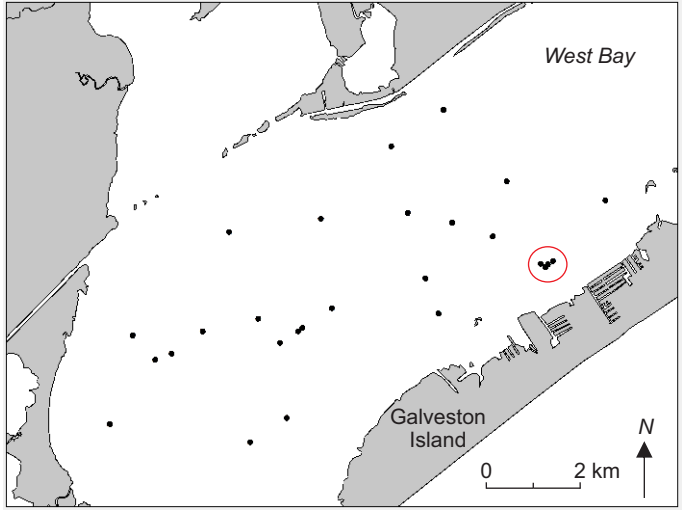
West Bay

Galveston Island

0 _____ 2 km

N

Legend
- Lower Estuary
- Middle Estuary
- Paleo-Brazos River Pro-Delta
- Upper Estuary
- Delta Plain
- Mouth Bar
- Oxbow Lake
- Estuarine Shell
- Burrows

Depth (cm)

Clay Silt Sand

Project: West Bay
Core ID: OC1C
Section: 100-200 cm
Location (Zone 15 N): 3226004 N, 299211 E

West Bay

Galveston
Island

0   2 km

N

Legend

- ■ Lower Estuary
- ■ Middle Estuary
- ■ Paleo-Brazos River Pro-Delta
- ■ Upper Estuary
- ■ Delta Plain
- □ Mouth Bar
- ■ Beaumont Formation
- ⌇ Estuarine Shell
- ⌇ Burrows

Depth (cm)

Clay   Silt   Sand
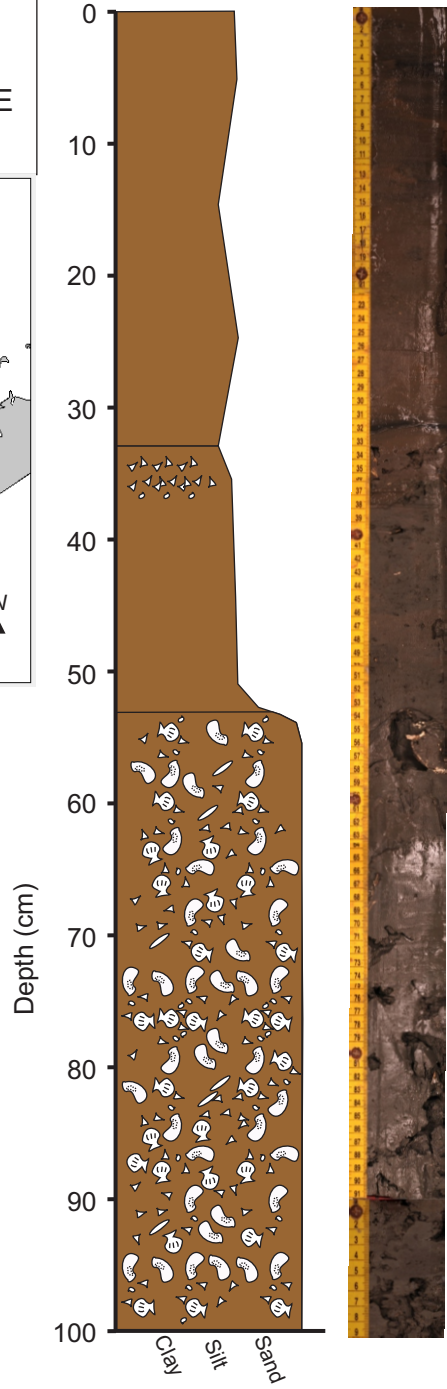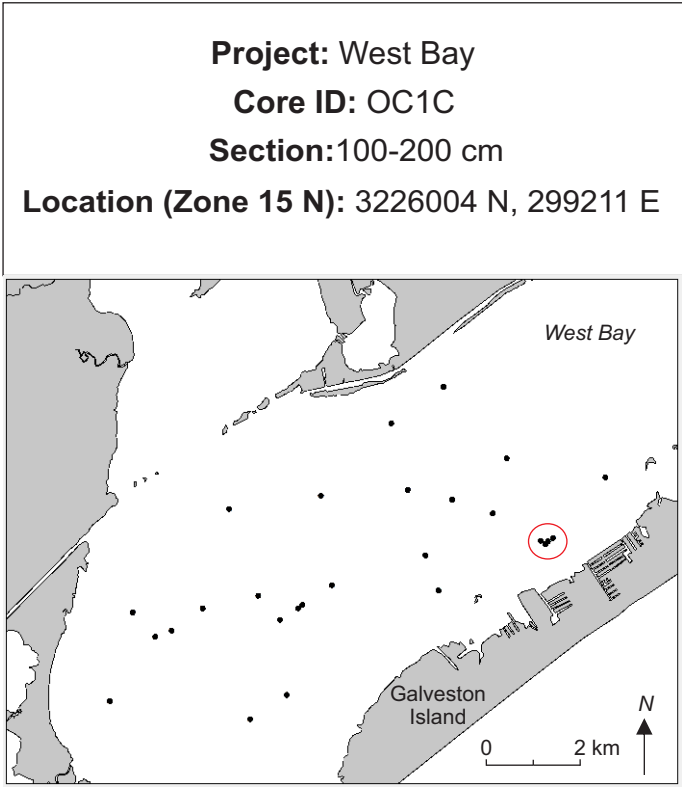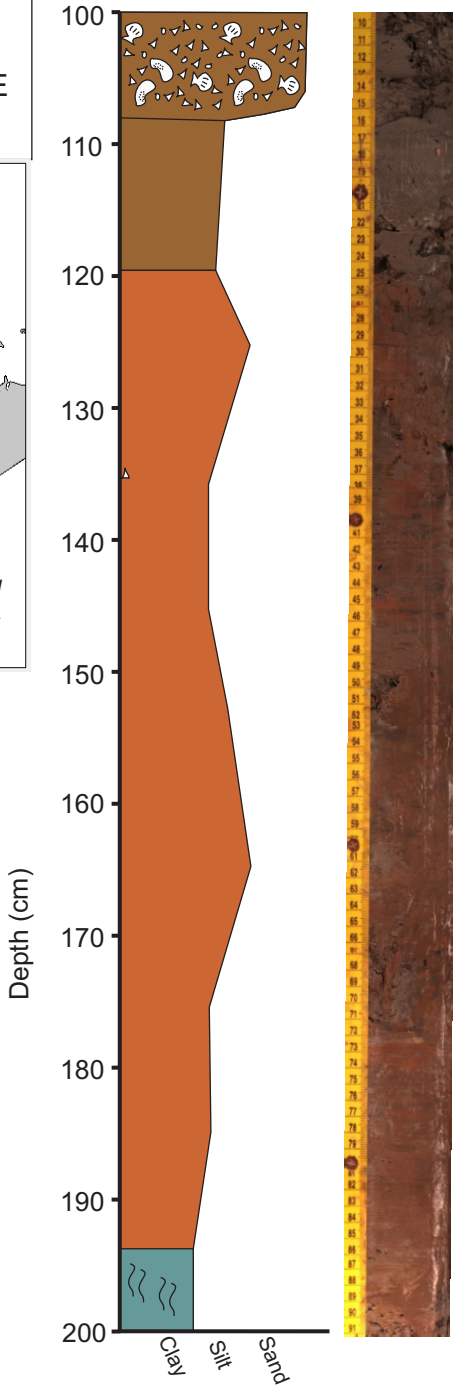
Project: West Bay

Core ID: OC2A

Section:0-100 cm

Location (Zone 15 N): 3226122 N, 299190 E
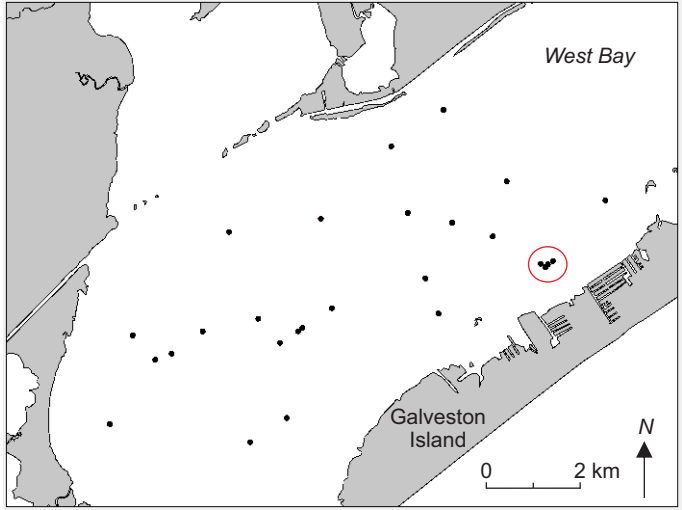
West Bay

Galveston
Island

0   2 km

N

Legend

- Lower Estuary
- Middle Estuary
- Paleo-Brazos River Pro-Delta
- Upper Estuary
- Delta Plain
- Mouth Bar
- Oxbow Lake
- Estuarine Shell
- Burrows

Depth (cm)

Clay Silt Sand
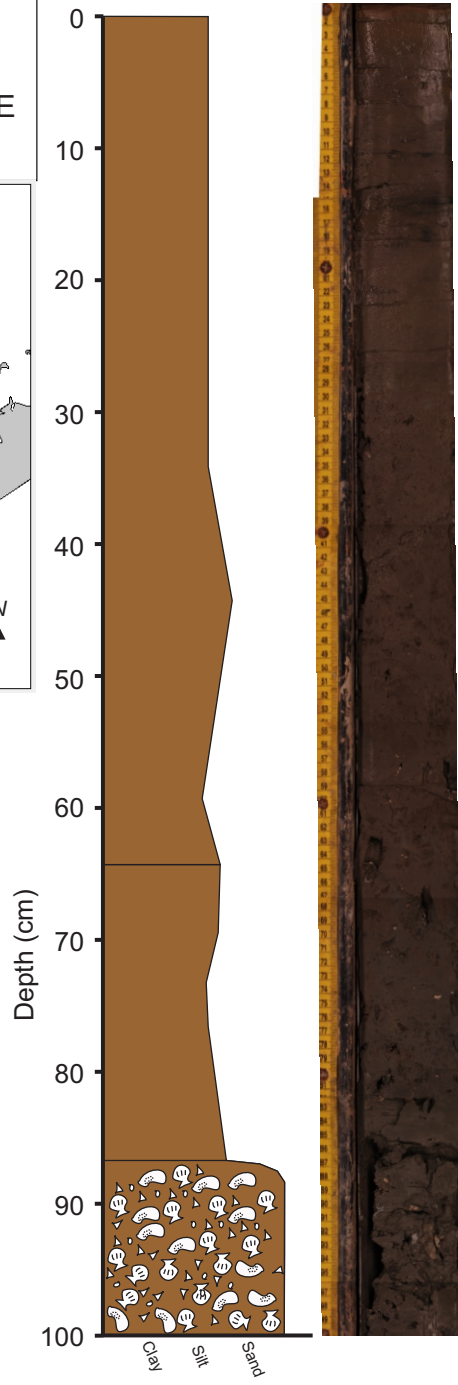
APPENDIX B

SEISMIC SECTIONS

Seismic Section ID: PS21
Ping Section: 5100-6250
Core ID: SLP 1
Core Length: 2.14 m

Legend

Holocene/Pleistocene Boundary

Core Location

Ping Section Location

West Bay

Chocolate Bay

Galveston Island

SLP 1

30 m

5 m
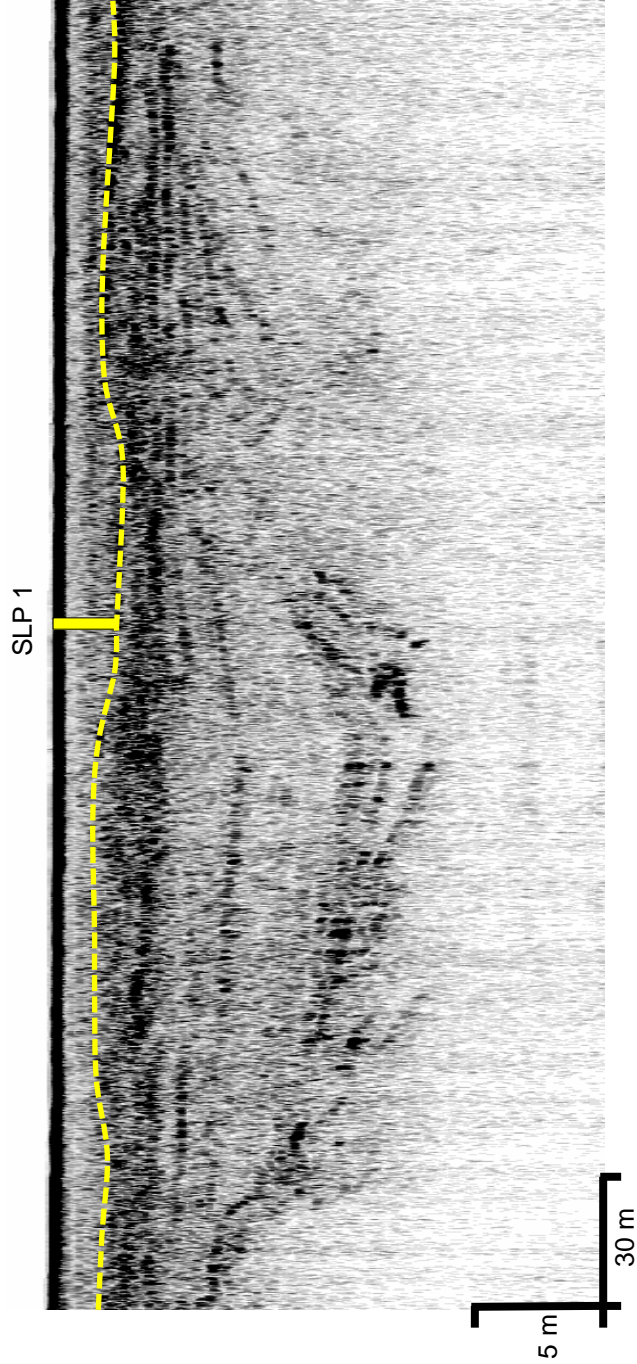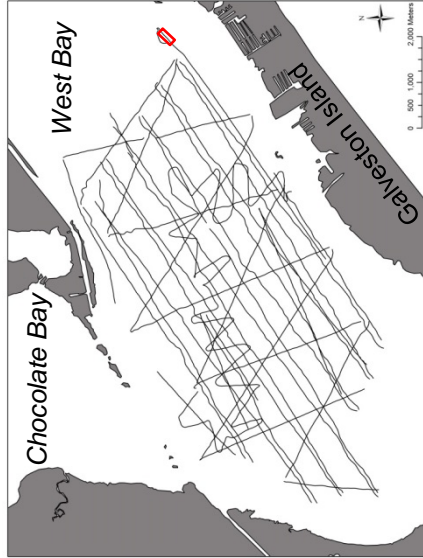
Seismic Section ID: PS11
Ping Section: 146195-147345
Core ID: SLP 2
Core Length: 2.31 m
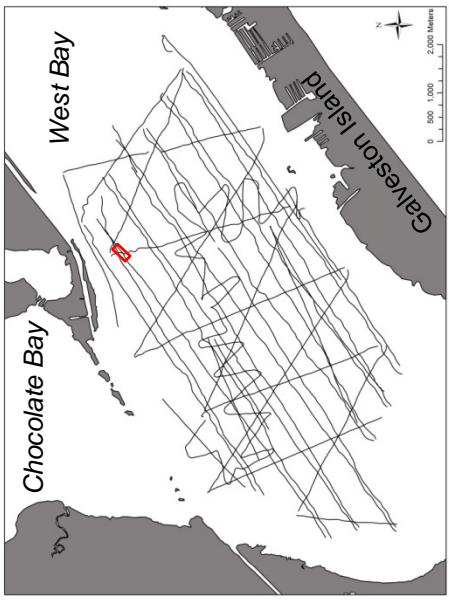
West Bay

Chocolate Bay

Galveston Island

Legend

- - - Holocene/Pleistocene Boundary

▬ Core Location

▭ Ping Section Location

SLP 2

5 m

30 m
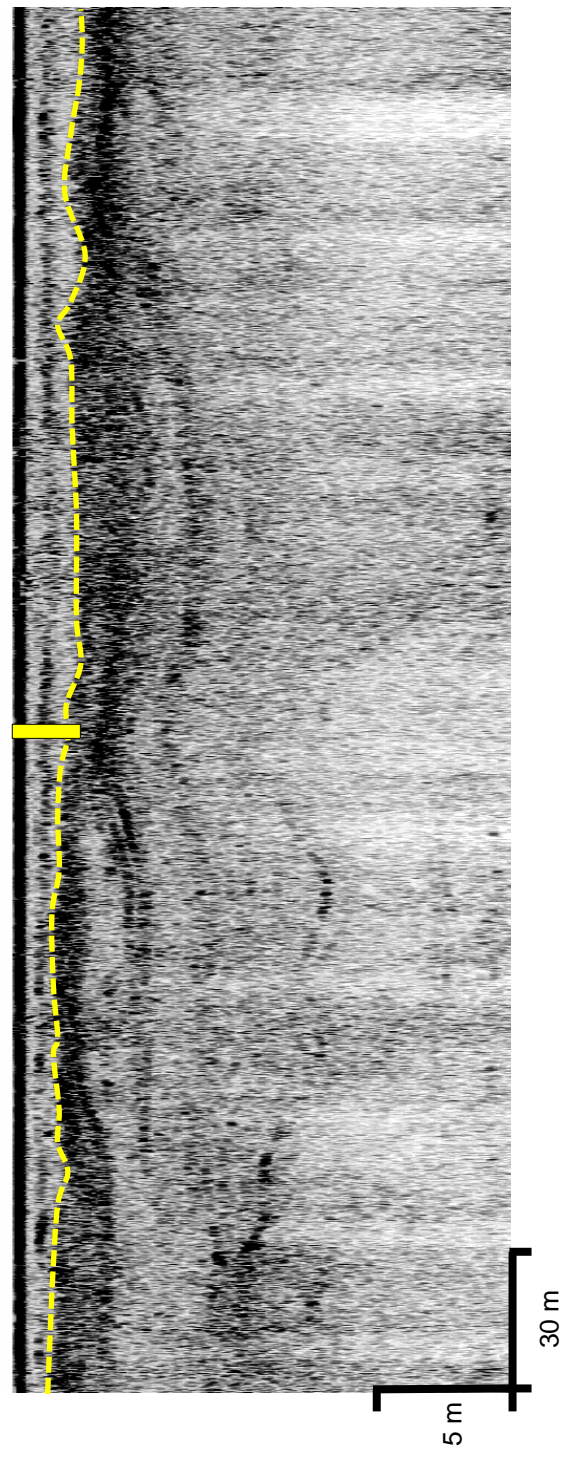
Seismic Section ID: PS19
Ping Section: 43311-44461
Core ID: SLP 3
Core Length: 2.15 m

Legend

- - - Holocene/Pleistocene Boundary

▬ Core Location

▭ Ping Section Location

West Bay

Chocolate Bay

Galveston Island

SLP 3

30 m

5 m

150
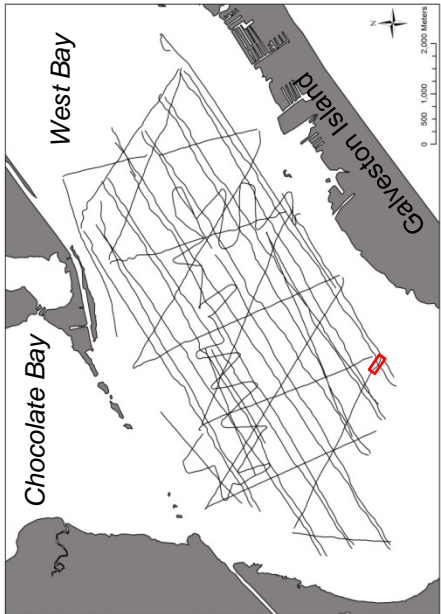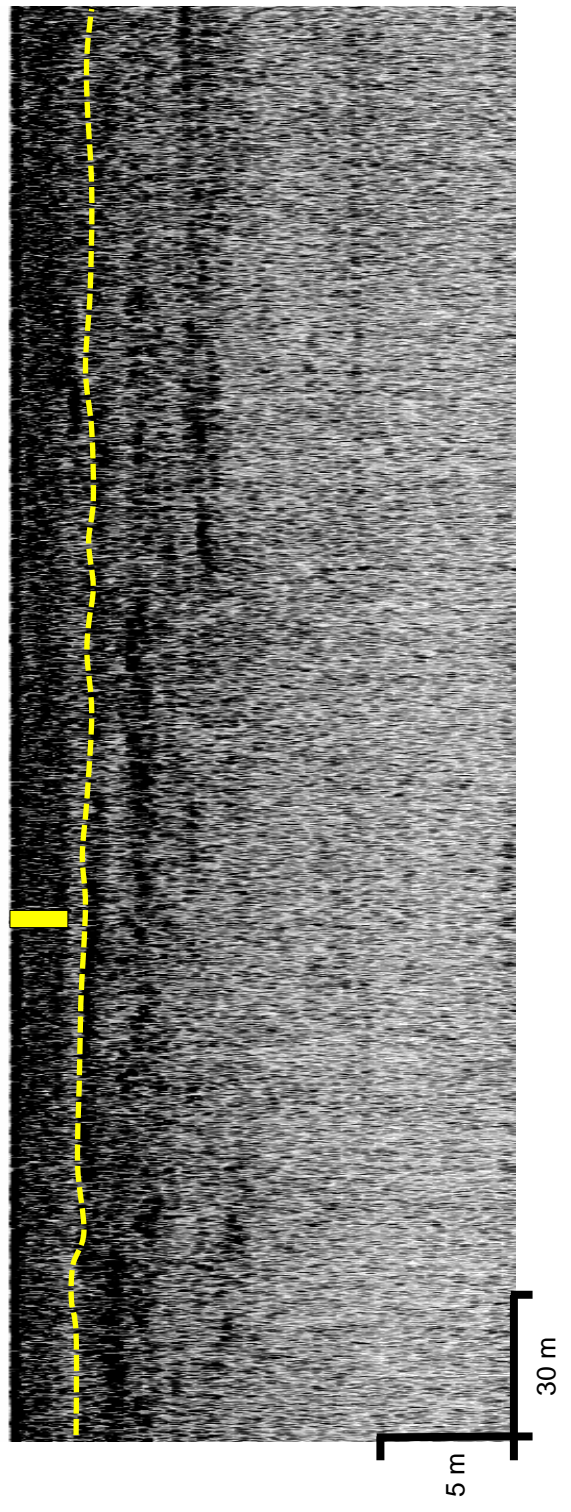
Seismic Section ID: PS19
Ping Section: 59130-60280
Core ID: SLP 4
Core Length: 3.00 m

Legend

- - - - Holocene/Pleistocene Boundary

▬ Core Location

▭ Ping Section Location

West Bay

Chocolate Bay

Galveston Island

SLP 4

5 m

30 m
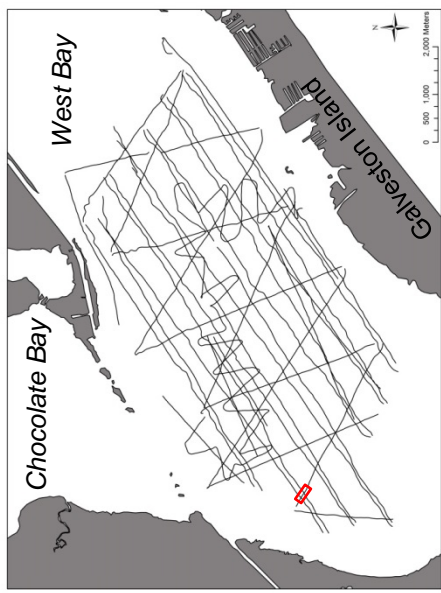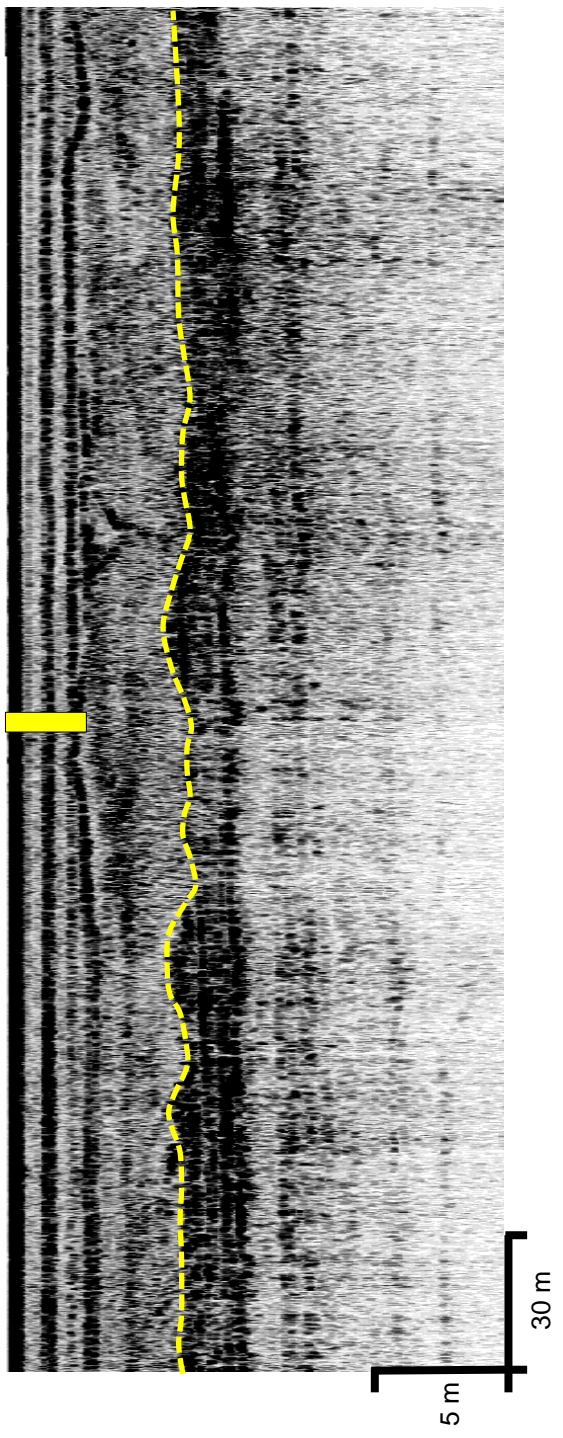
Seismic Section ID: PS19
Ping Section: 69000-70150
Core ID: SLP 5
Core Length: 2.00 m

Legend

— — — Holocene/Pleistocene Boundary

▬ Core Location

☐ Ping Section Location

West Bay

Chocolate Bay

Galveston Island

SLP 5

30 m

5 m

152
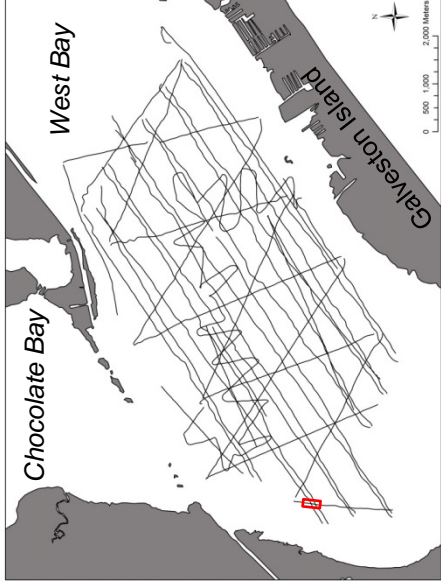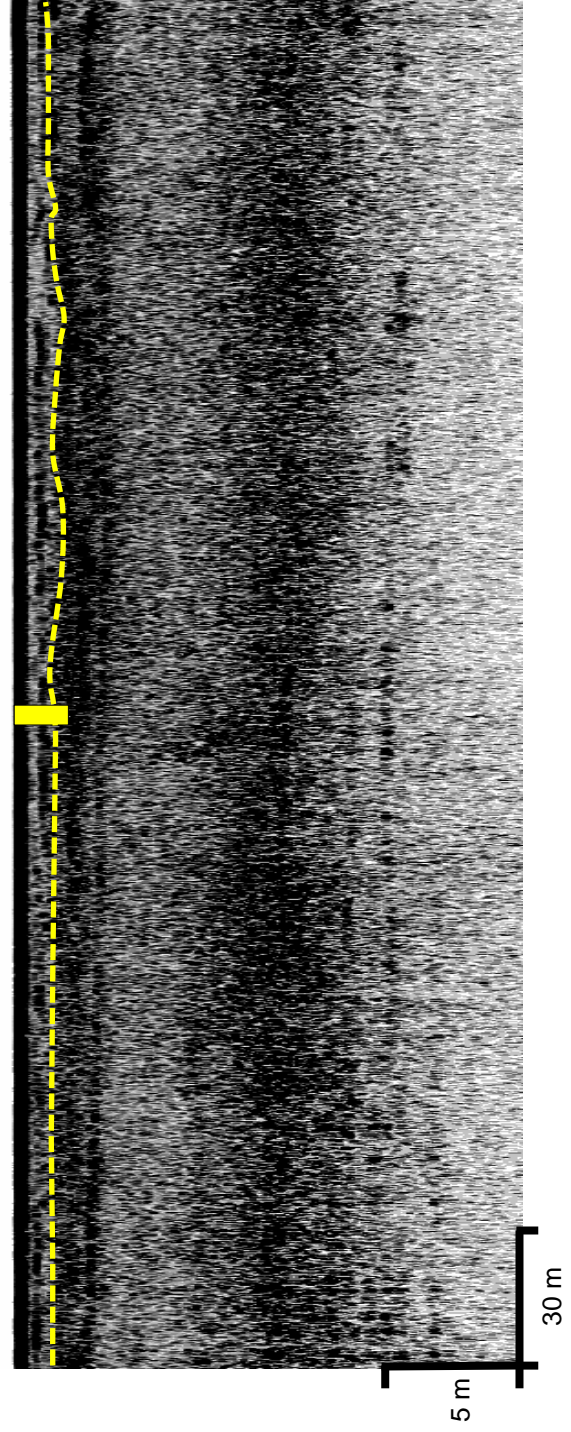
Seismic Section ID: PS7
Ping Section: 44870-46020
Core ID: SLP 6
Core Length: 2.90 m

Legend

— — — Holocene/Pleistocene Boundary

▬ Core Location

▭ Ping Section Location

West Bay

Chocolate Bay

Galveston Island

0 500 1,000 2,000 Meters

SLP 6

30 m

5 m

153
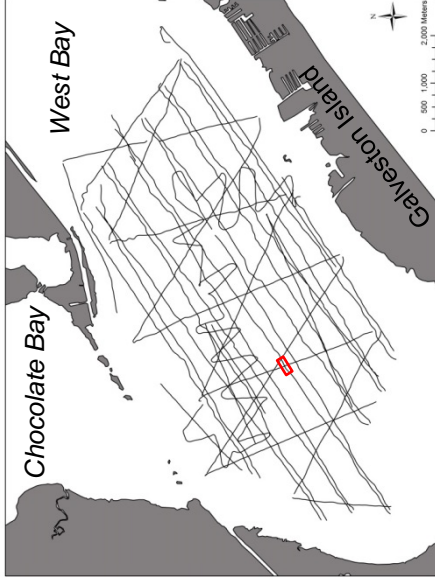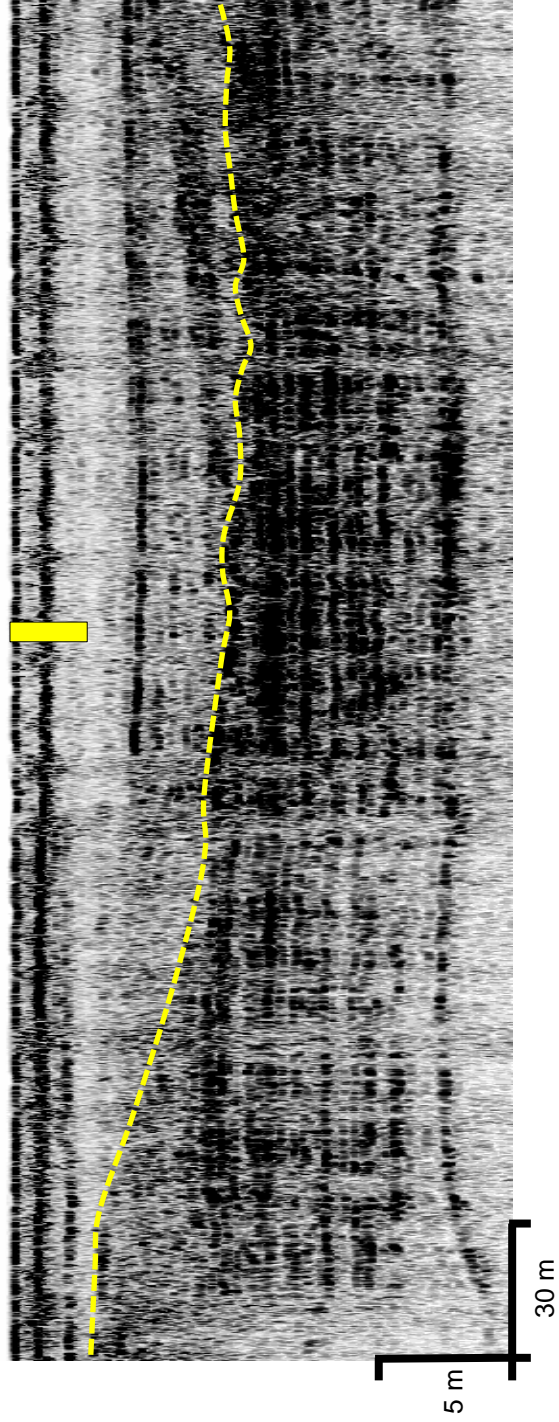
Seismic Section ID: PS17
Ping Section: 21930-23080
Core ID: SLP 7
Core Length: 1.90 m

Legend

- - - Holocene/Pleistocene Boundary

▬ Core Location

▭ Ping Section Location

West Bay

Chocolate Bay

Galveston Island

0 500 1,000 2,000 Meters

SLP 7

30 m

5 m
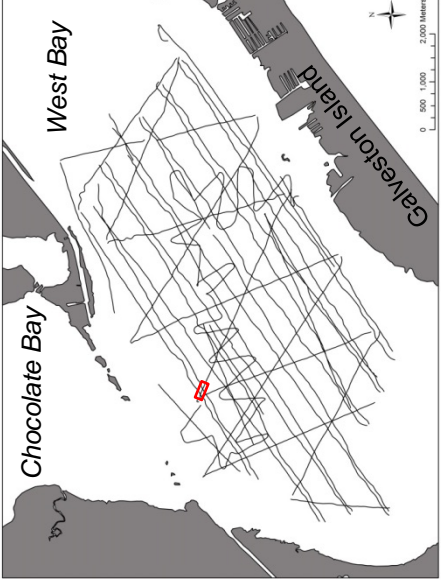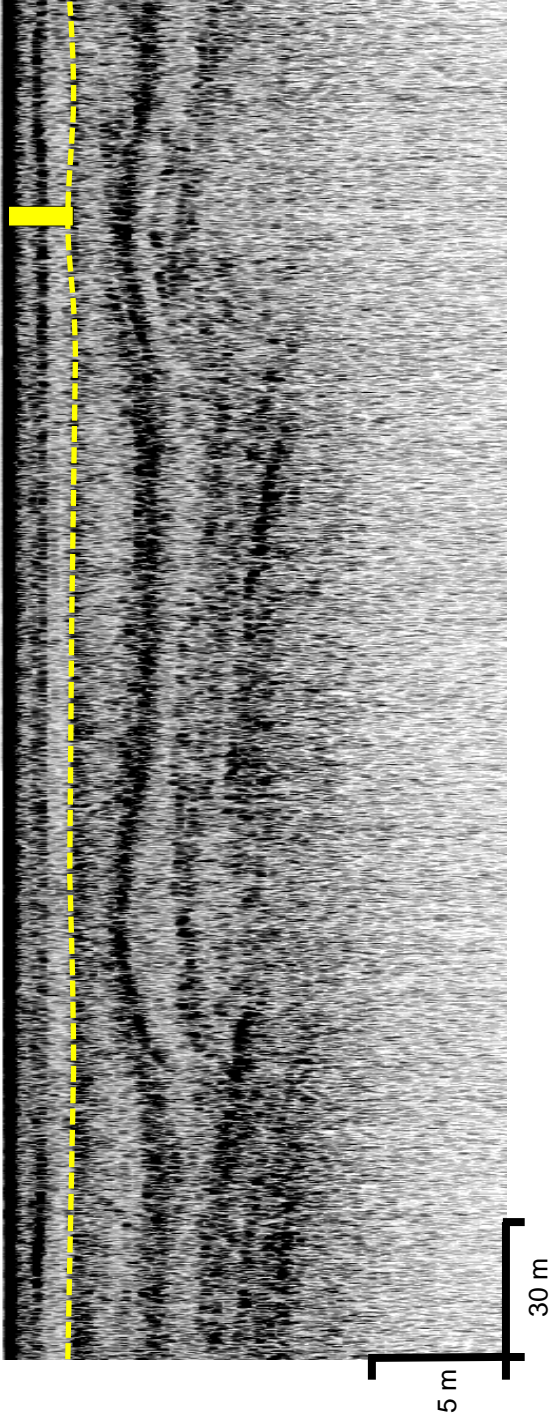
Seismic Section ID: PS16
Ping Section: 106849-107999
Core ID: SLP 8
Core Length: 2.98 m

Legend

- - - Holocene/Pleistocene Boundary

▬ Core Location

▭ Ping Section Location

West Bay

Chocolate Bay

Galveston Island

0 500 1,000 2,000 Meters

SLP 8

30 m

5 m

155
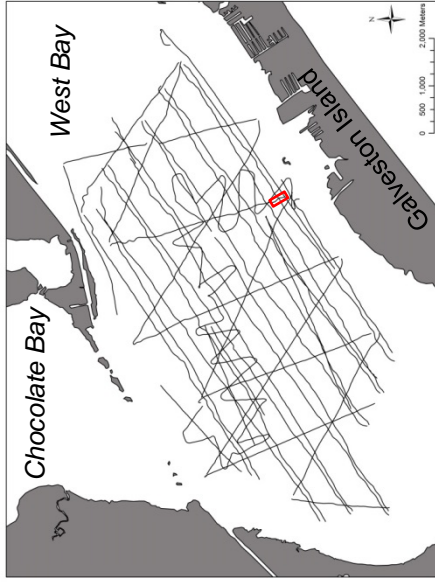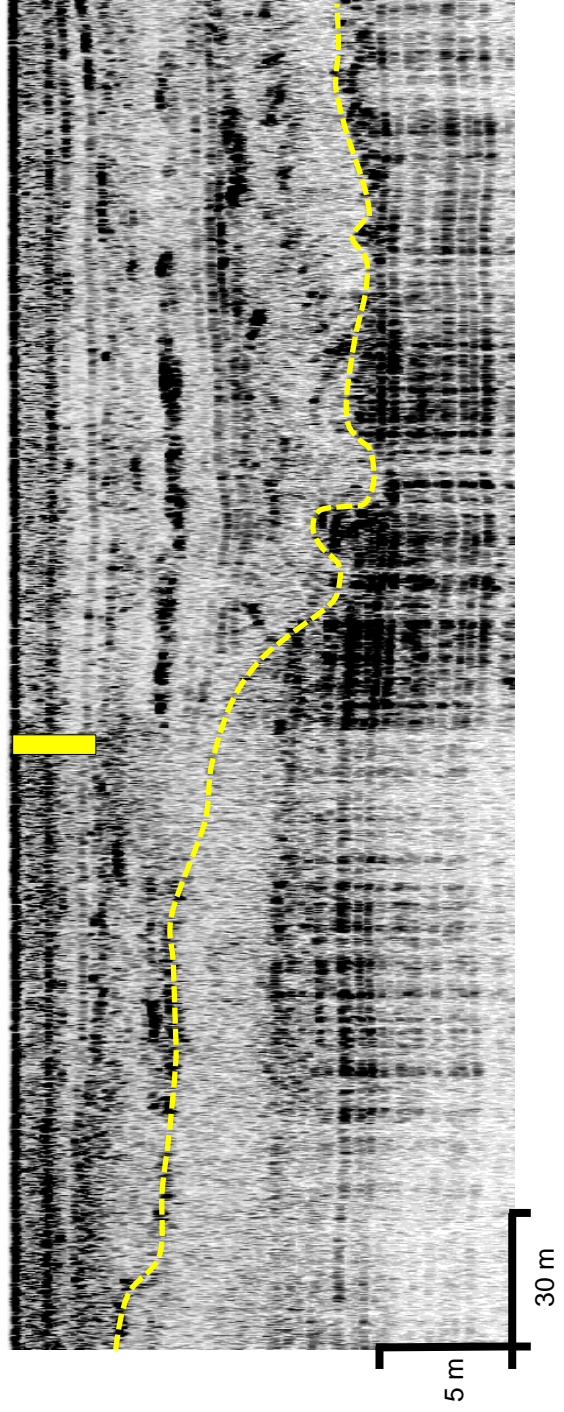
Seismic Section ID: PS16
Ping Section: 97133-98283
Core ID: SLP 9
Core Length: 3.00 m

Legend

— — — Holocene/Pleistocene Boundary

▬ Core Location

▭ Ping Section Location

Chocolate Bay

West Bay

Galveston Island

0 500 1,000 2,000 Meters

SLP 9

5 m

30 m
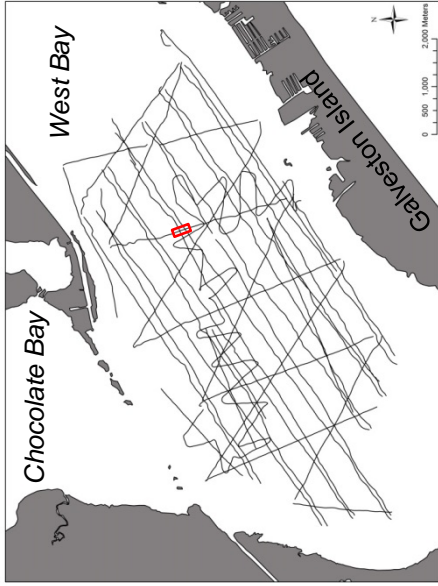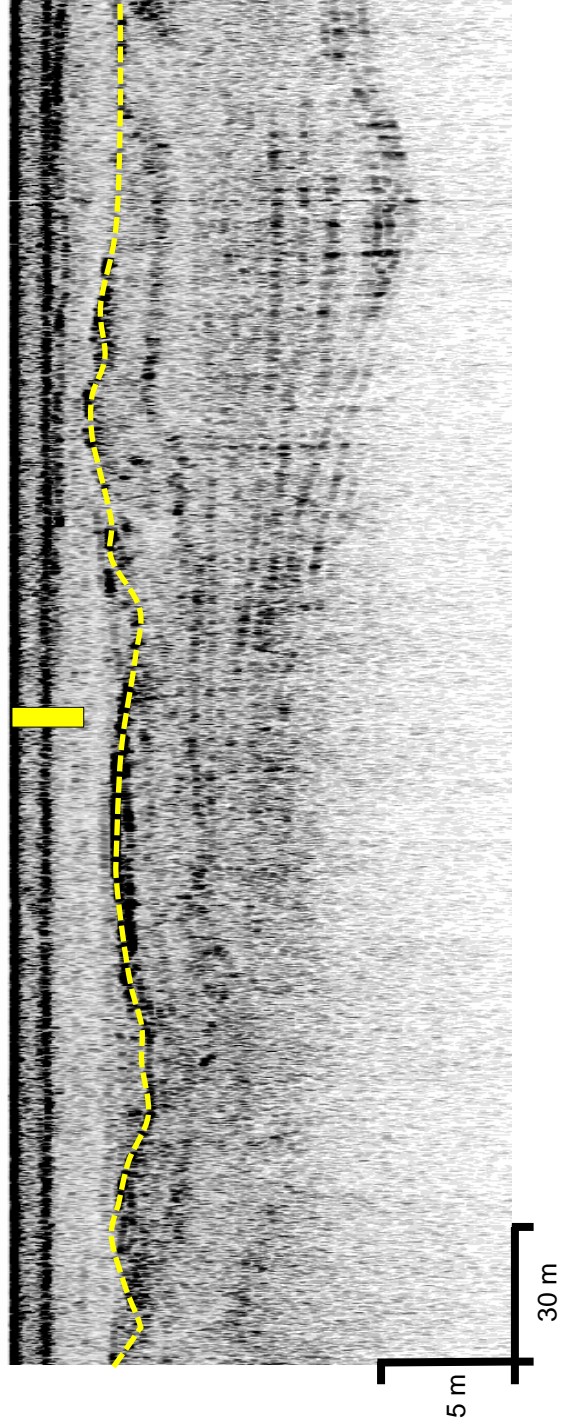
Seismic Section ID: PS10
Ping Section: 96036-97187
Core ID: SLP 10
Core Length: 1.65 m

Legend

- - - Holocene/Pleistocene Boundary

▬ Core Location

▭ Ping Section Location

West Bay

Chocolate Bay

Galveston Island

0 500 1,000 2,000 Meters

SLP 10

5 m

30 m

157
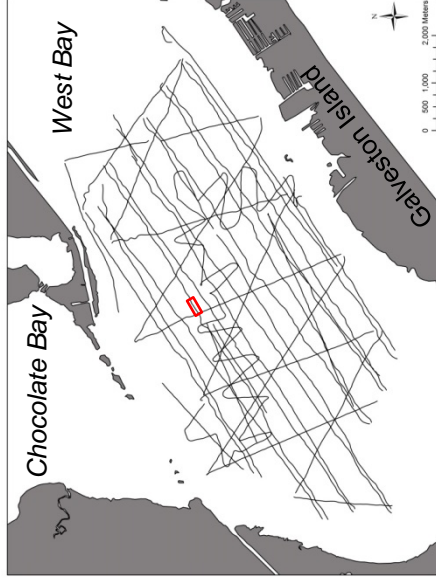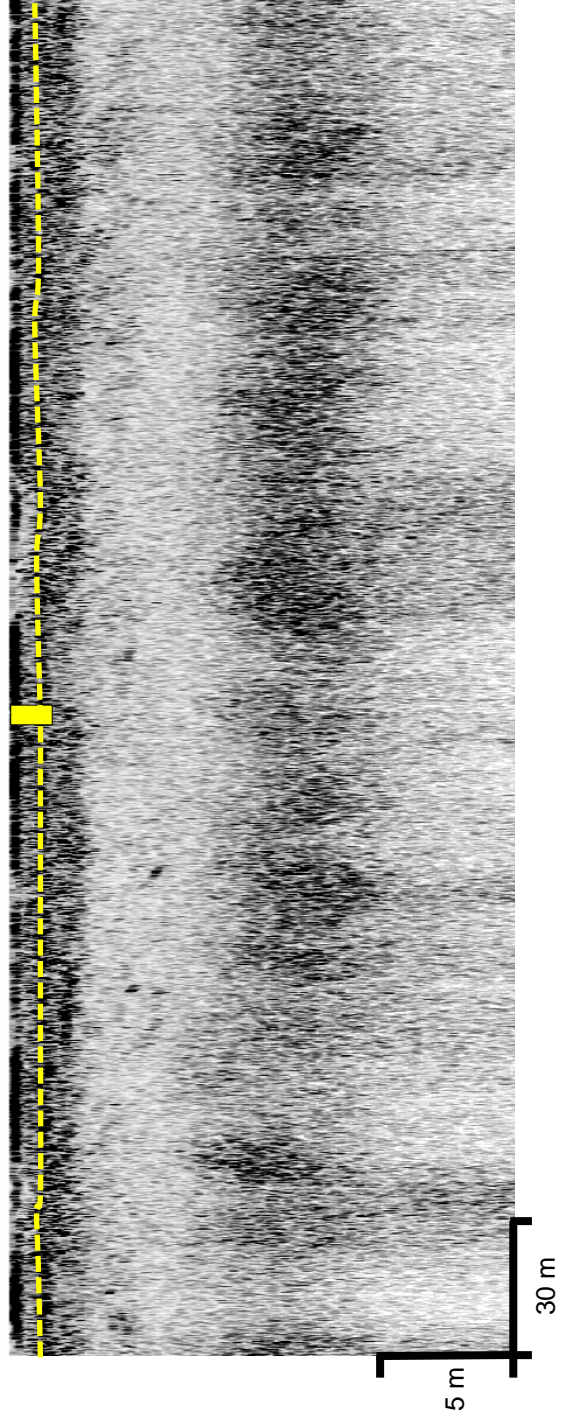
Seismic Section ID: PS5
Ping Section: 78530-79680
Core ID: SLP 12
Core Length: 1.00 m
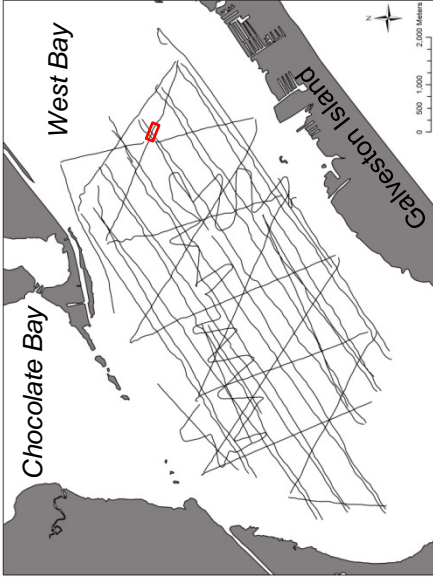
Legend

- - - Holocene/Pleistocene Boundary

� Core Location

▭ Ping Section Location

West Bay

Chocolate Bay

Galveston Island

SLP 11

5 m

30 m

158
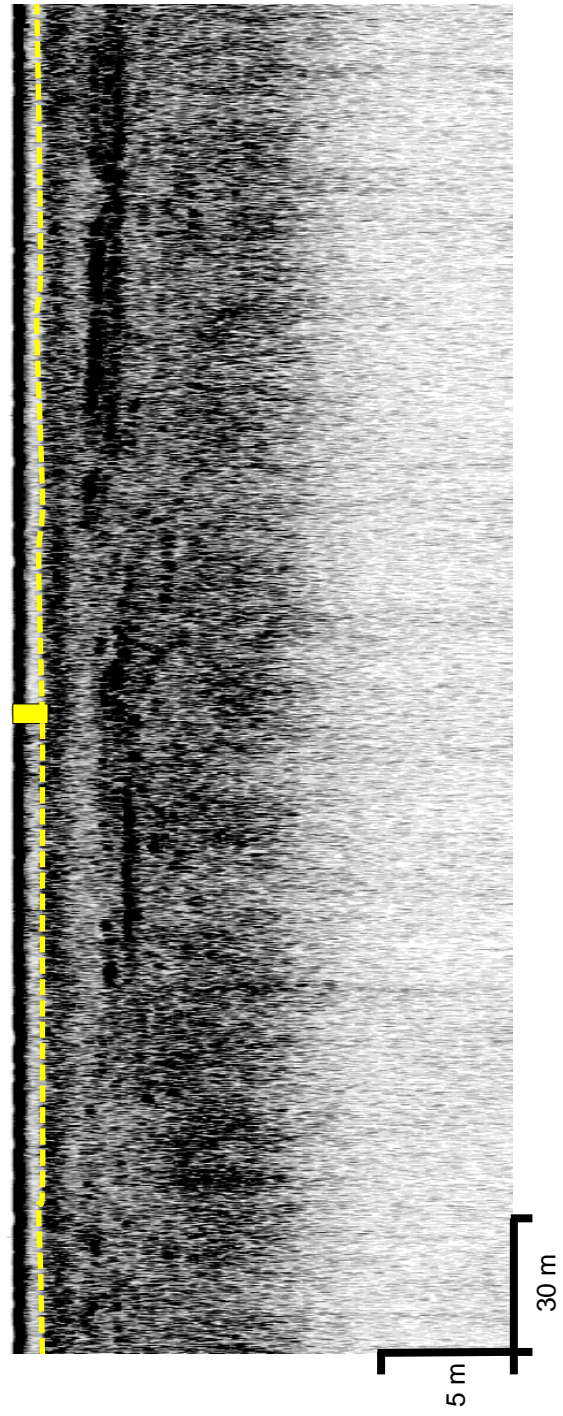
Seismic Section ID: PS5
Ping Section: 158250-159400
Core ID: SLP 12
Core Length: 1.96 m

Legend

Holocene/Pleistocene Boundary

Core Location

Ping Section Location

West Bay

Chocolate Bay

Galveston Island

SLP 12

30 m

5 m

159
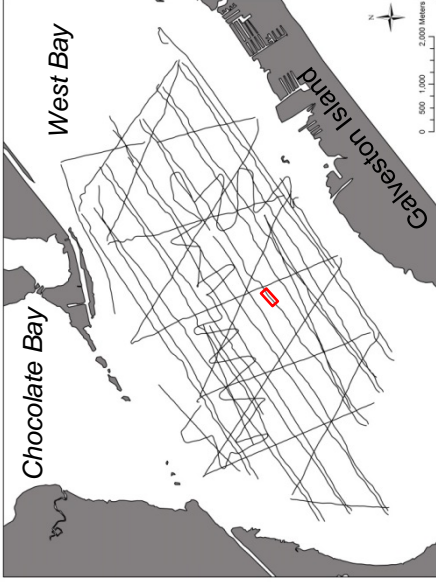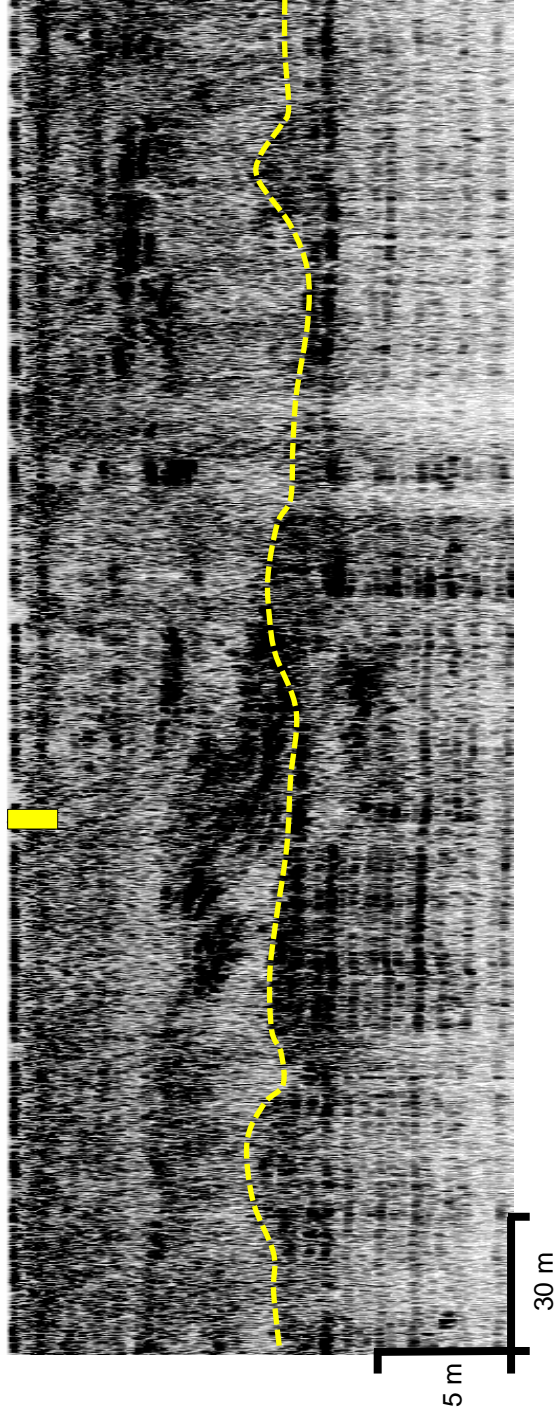
Seismic Section ID: PS3
Ping Section: 113826-114976
Core ID: SLP 13
Core Length: 1.93 m

Legend

Holocene/Pleistocene Boundary

Core Location

Ping Section Location

West Bay

Chocolate Bay

Galveston Island

SLP 13

30 m

5 m

160
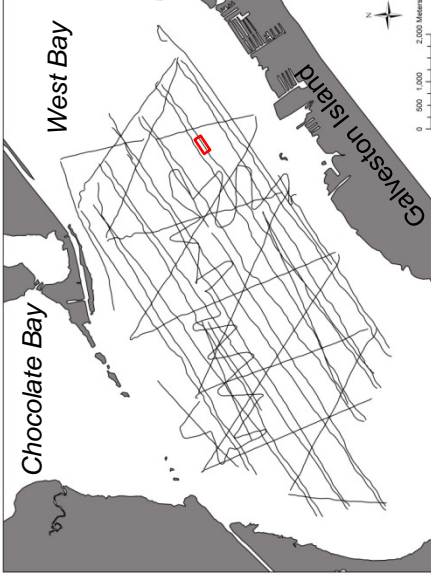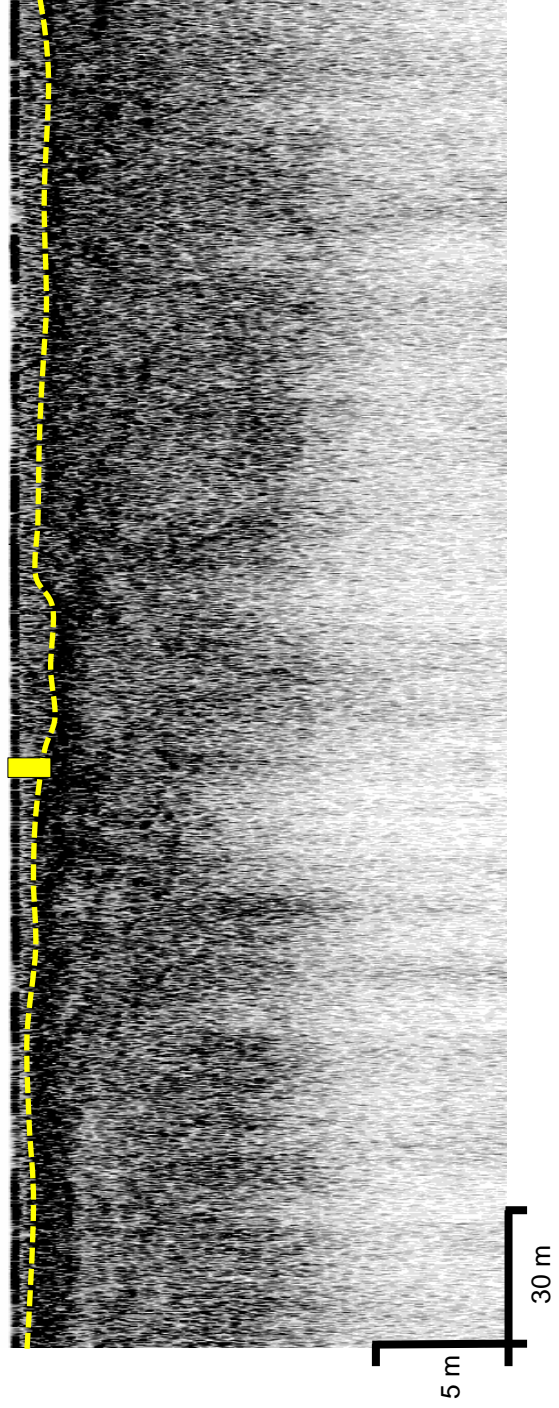
Seismic Section ID: PS5
Ping Section: 156094-157244
Core ID: SLP 14
Core Length: 3.51 m

Legend

- - - - Holocene/Pleistocene Boundary

▬ Core Location

☐ Ping Section Location

West Bay

Chocolate Bay

Galveston Island

SLP 14

5 m

30 m

161
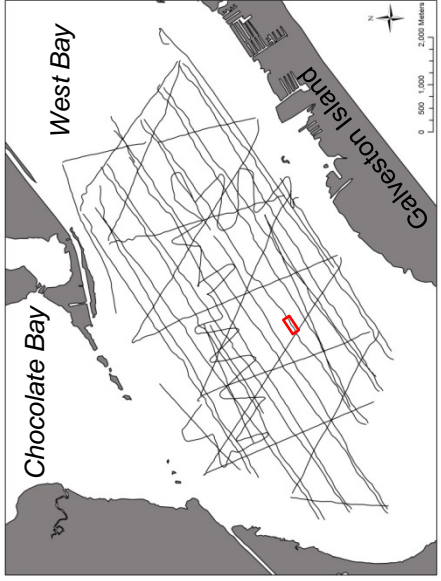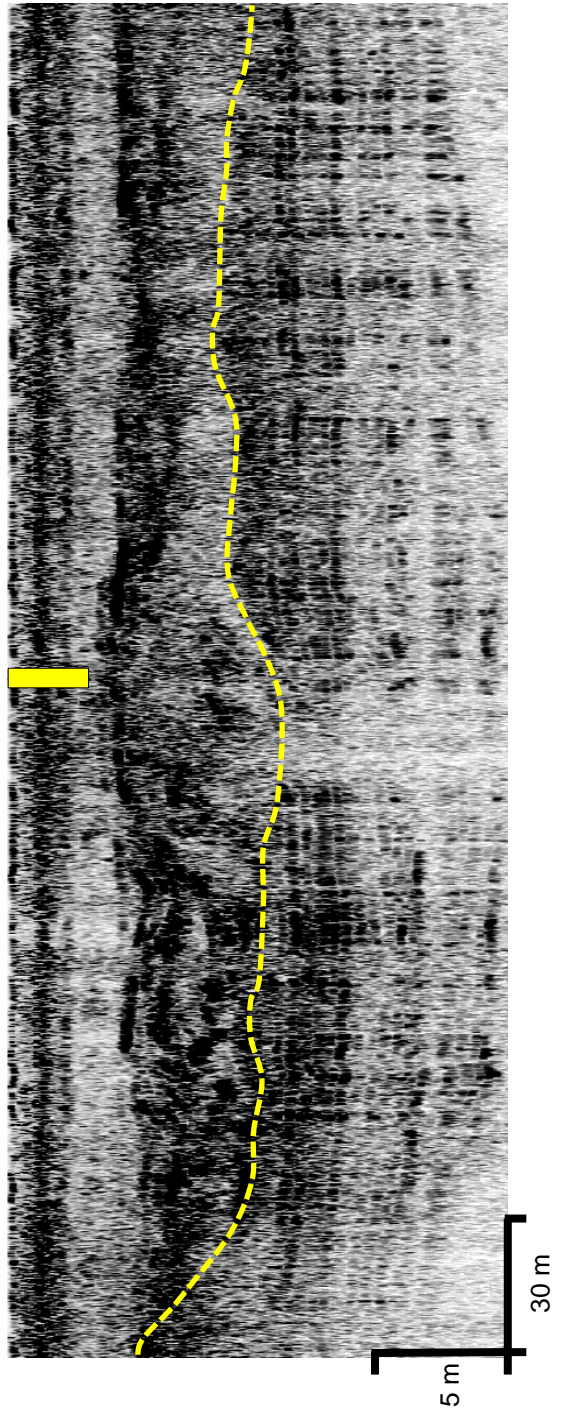
Seismic Section ID: PS14
Ping Section: 56673-57823
Core ID: SLP 15
Core Length: 0.79 m

Legend

— — — Holocene/Pleistocene Boundary

▬ Core Location

▭ Ping Section Location

West Bay

Chocolate Bay

Galveston Island

SLP 15

30 m

5 m

162
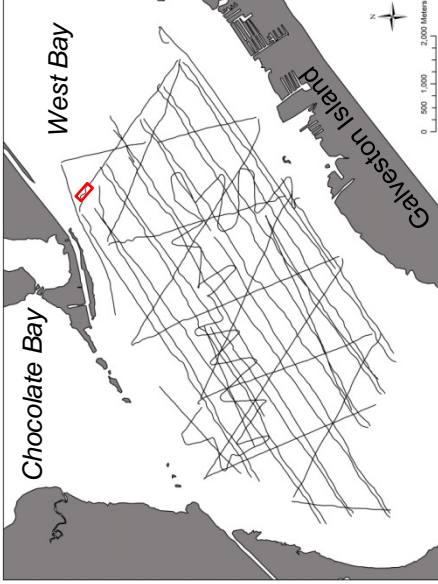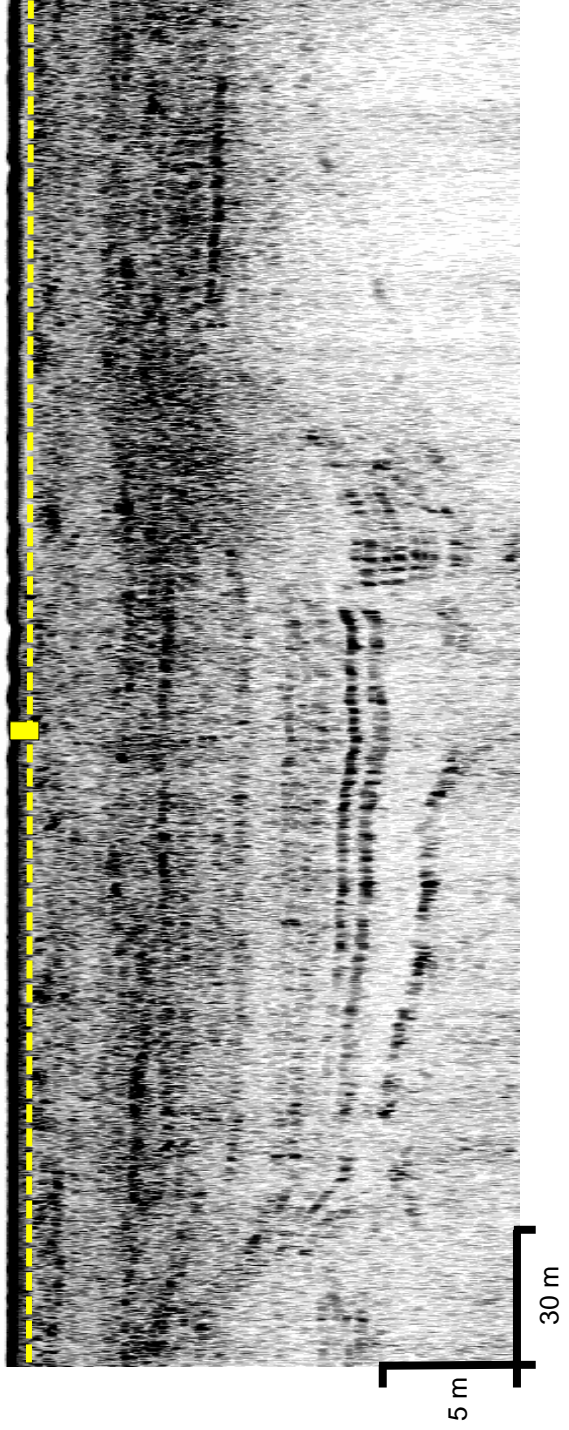
Seismic Section ID: PS19
Ping Section: 55299-56449
Core ID: SLP 17
Core Length: 3.00 m

Legend

- - - Holocene/Pleistocene Boundary

▬ Core Location

▭ Ping Section Location

West Bay

Chocolate Bay

Galveston Island

0 500 1,000 2,000 Meters

SLP 17

30 m

5 m
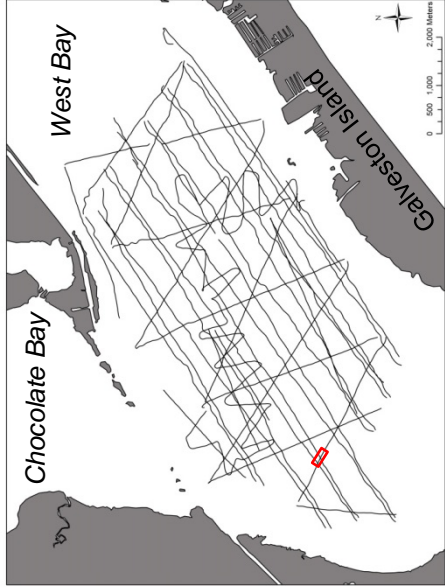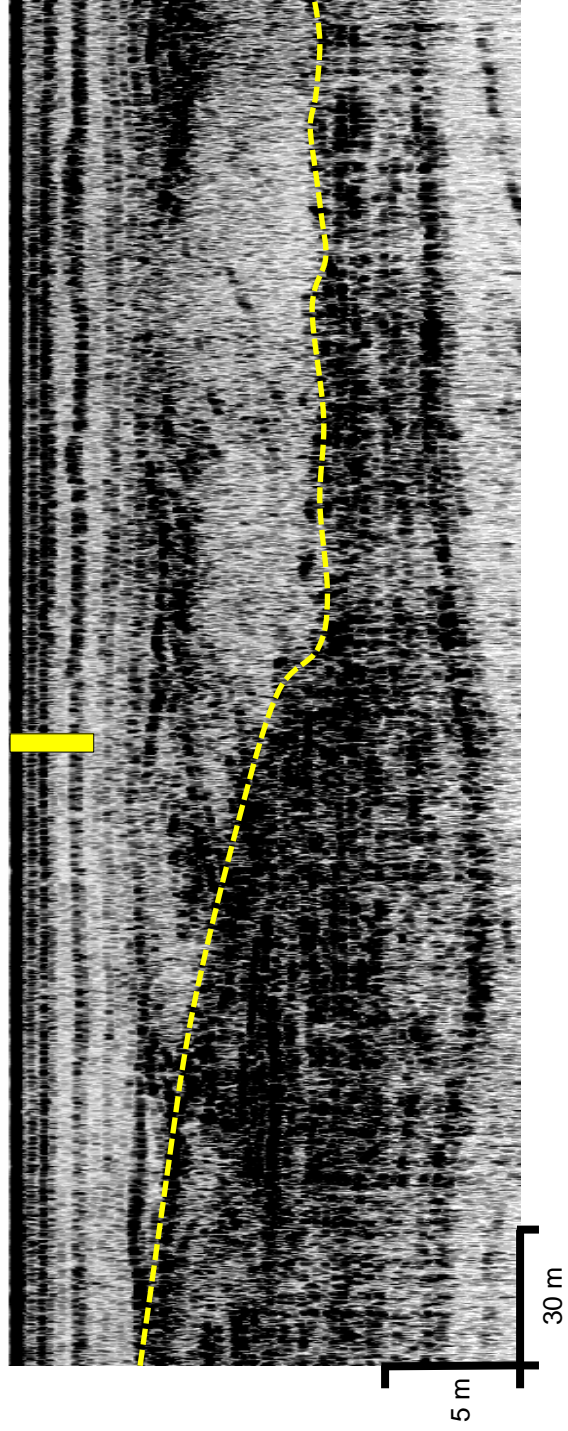
Seismic Section ID: PS5
Ping Section: 167022-168177
Core ID: SLP 18
Core Length: 1.74 m
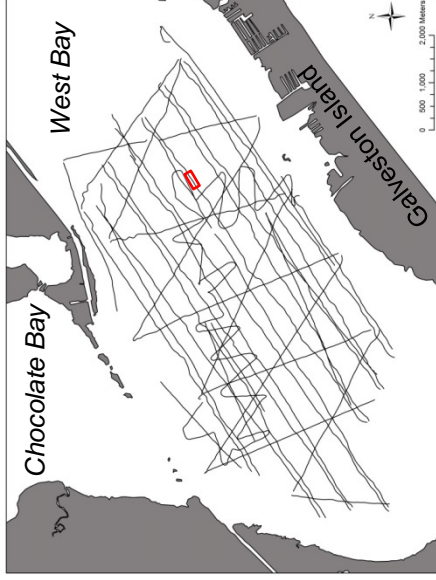
Legend

- - - - Holocene/Pleistocene Boundary

▬ Core Location

▭ Ping Section Location

West Bay

Chocolate Bay

Galveston Island

SLP 18

30 m

5 m

164
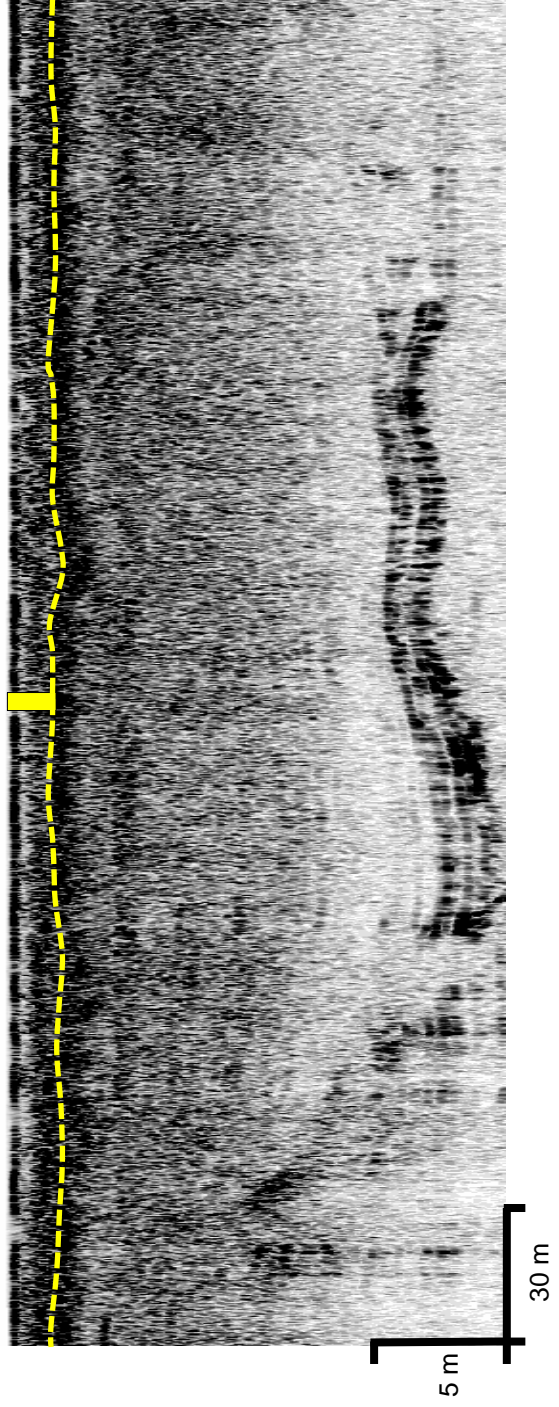
Seismic Section ID: PS16
Ping Section: 103337-104494
Core ID: SLP 19
Core Length: 2.96 m

Legend

— — — Holocene/Pleistocene Boundary

▬ Core Location

▭ Ping Section Location

West Bay

Chocolate Bay

Galveston Island

SLP 19

30 m

5 m

165
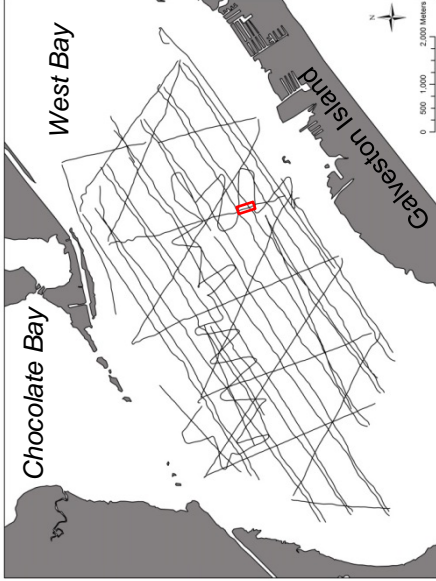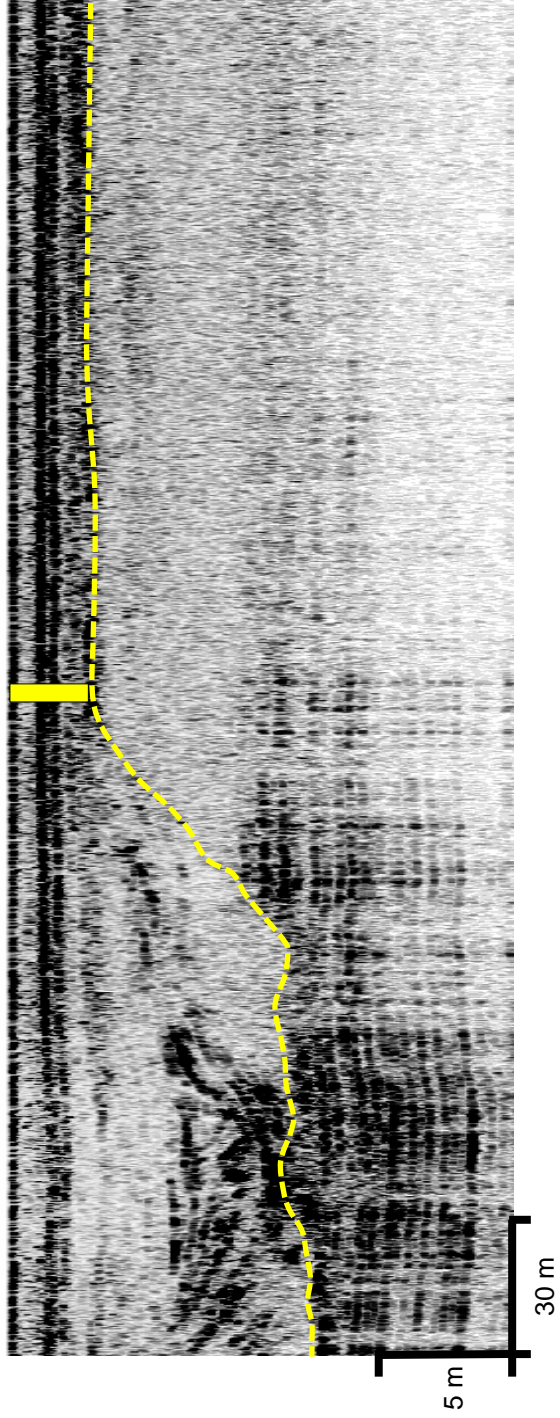
Seismic Section ID: PS5
Ping Section: 155526-156679
Core ID: SLP 21
Core Length: 5.30 m
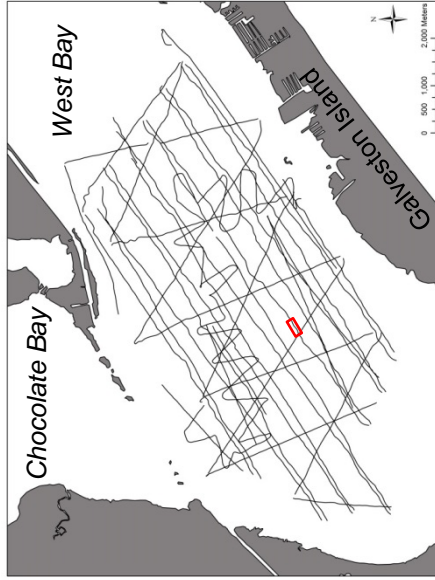
Legend

– – – Holocene/Pleistocene Boundary

▬ Core Location

▭ Ping Section Location

West Bay

Chocolate Bay

Galveston Island

SLP 21

30 m

5 m
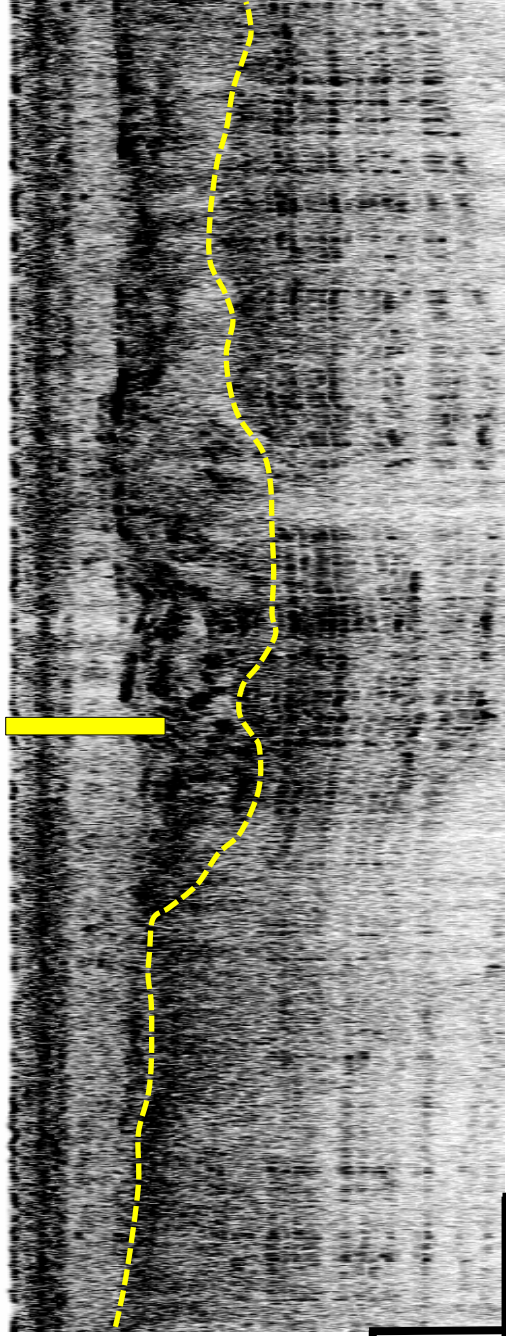
Seismic Section ID: PS5
Ping Section: 155526-157238
Core ID: SLP 22
Core Length: 2.71 m
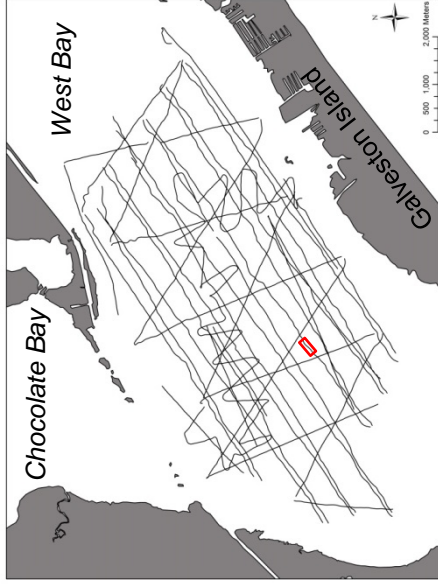
Legend

- - - Holocene/Pleistocene Boundary

▬ Core Location

▭ Ping Section Location

West Bay

Chocolate Bay

Galveston Island

0 500 1,000 2,000 Meters

SLP 22

30 m

5 m

167
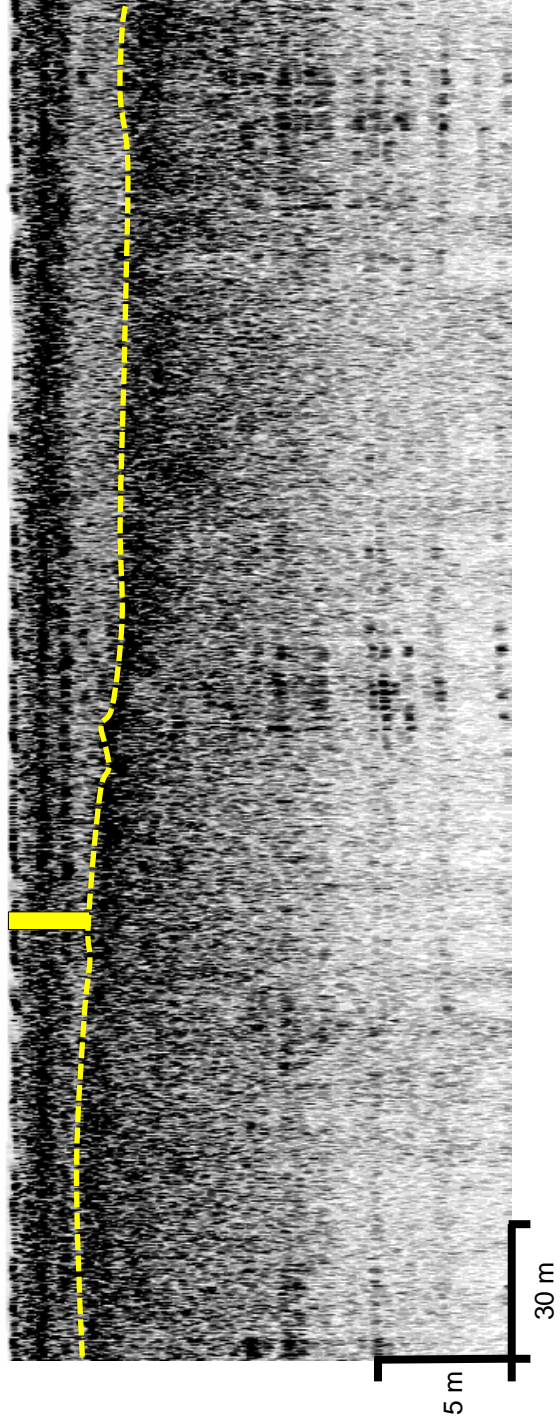
Seismic Section ID: PS8-2
Ping Section: 33932-35050
Core ID: SLP 23
Core Length: 5.26 m

Legend

- - - Holocene/Pleistocene Boundary

▬ Core Location

▭ Ping Section Location

West Bay

Chocolate Bay

Galveston Island

0 500 1,000 2,000 Meters

SLP 23

30 m

5 m

168
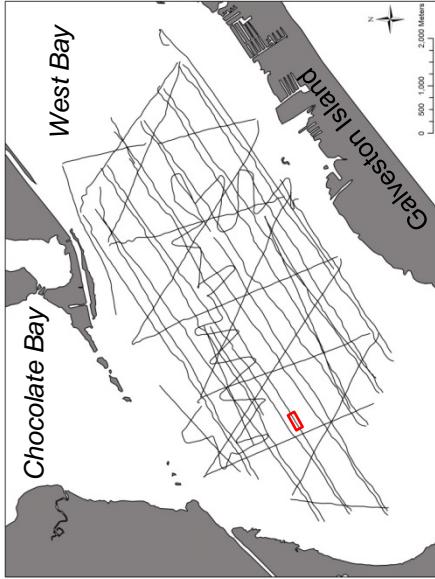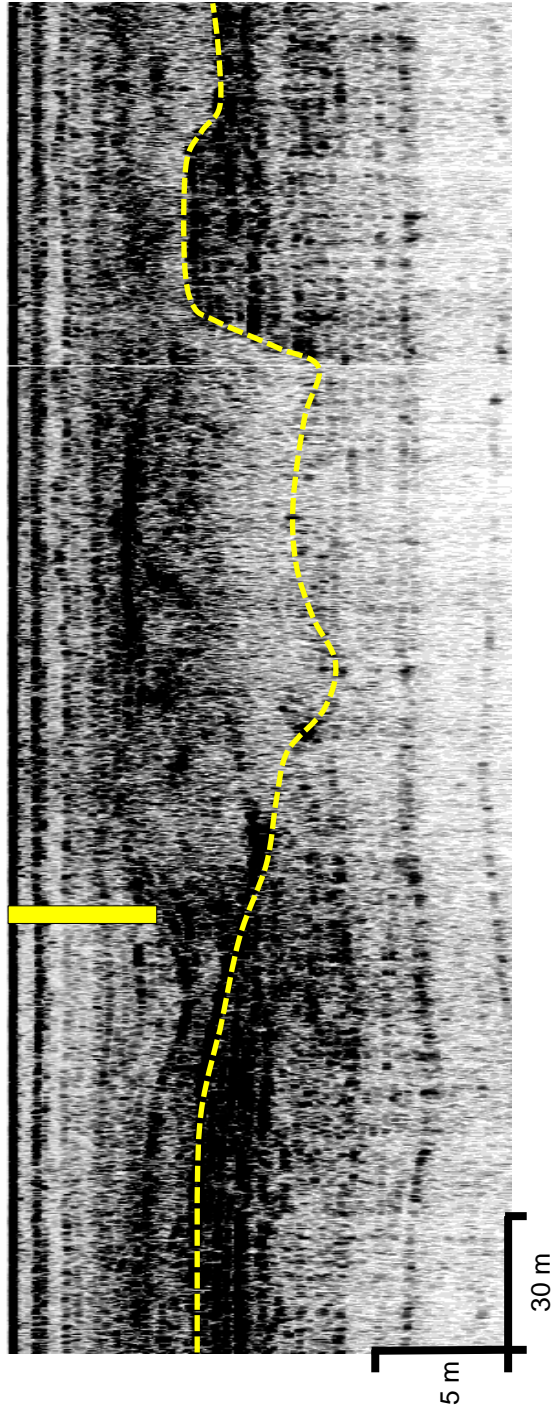
Seismic Section ID: PS8-2
Ping Section: 33932-35050
Core ID: SLP 24
Core Length: 2.77 m

Legend

- - - Holocene/Pleistocene Boundary

▬ Core Location

▭ Ping Section Location

SLP 24

West Bay

Chocolate Bay

Galveston Island

0   500   1,000   2,000 Meters

5 m

30 m

169
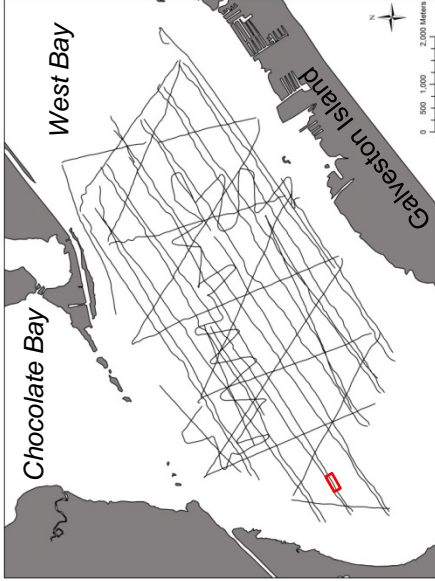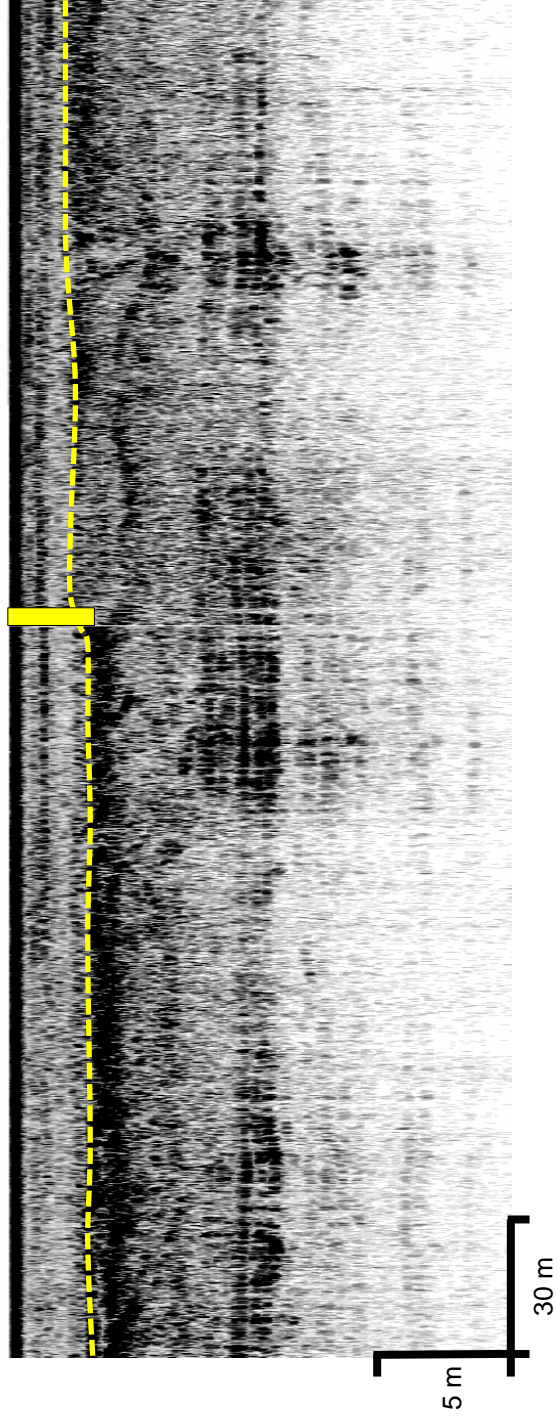
Seismic Section ID: PS21
Ping Section: 24534-25697
Core ID: SLP 27
Core Length: 5.0 m

Legend

- - - Holocene/Pleistocene Boundary

▬ Core Location

▭ Ping Section Location

West Bay

Chocolate Bay

Galveston Island

0 500 1,000 2,000 Meters

SLP 27

30 m

5 m

170
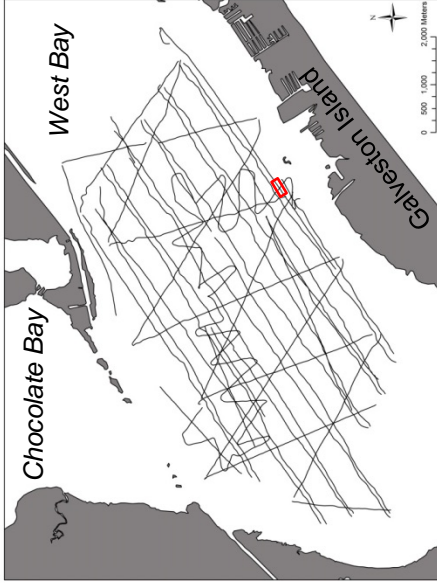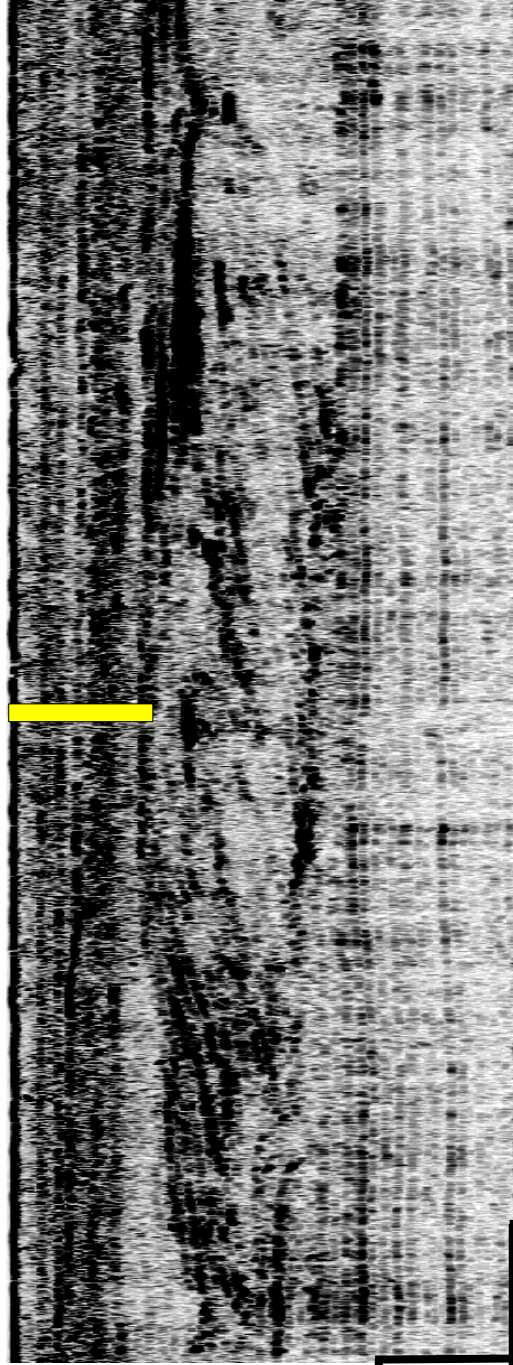
Seismic Section ID: SS4
Ping Section: 15187-16329
Core ID: SLP 16
Core Length: 3.37 m

Legend

- - - Holocene/Pleistocene Boundary

▬ Core Location

▭ Ping Section Location

West Bay

Galveston Island

0 125 250 500 Meters

SLP 16

20 m

4 m
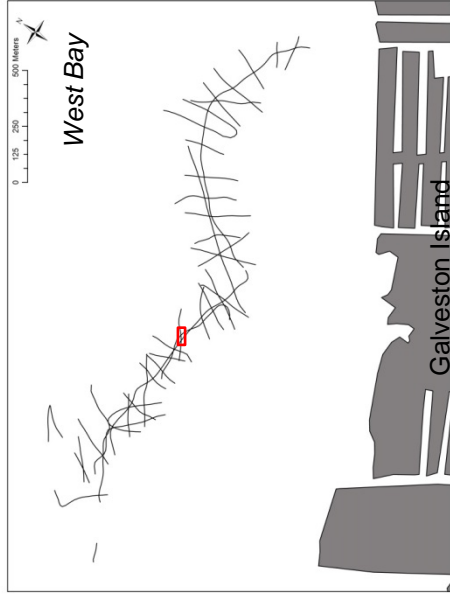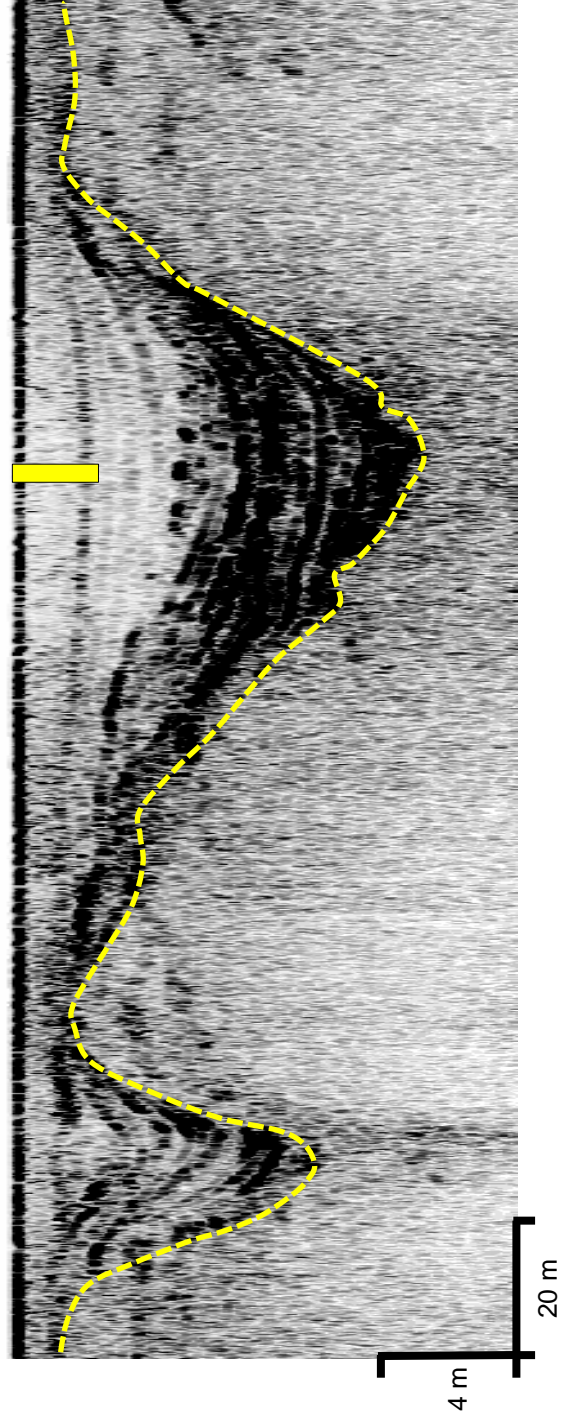
Seismic Section ID: SS4
Ping Section: 15187-16329
Core ID: OC2A
Core Length: 1.00 m

Legend

- - - Holocene/Pleistocene Boundary

▮ Core Location

▭ Ping Section Location

West Bay

Galveston Island

OC2A

20 m

4 m

172
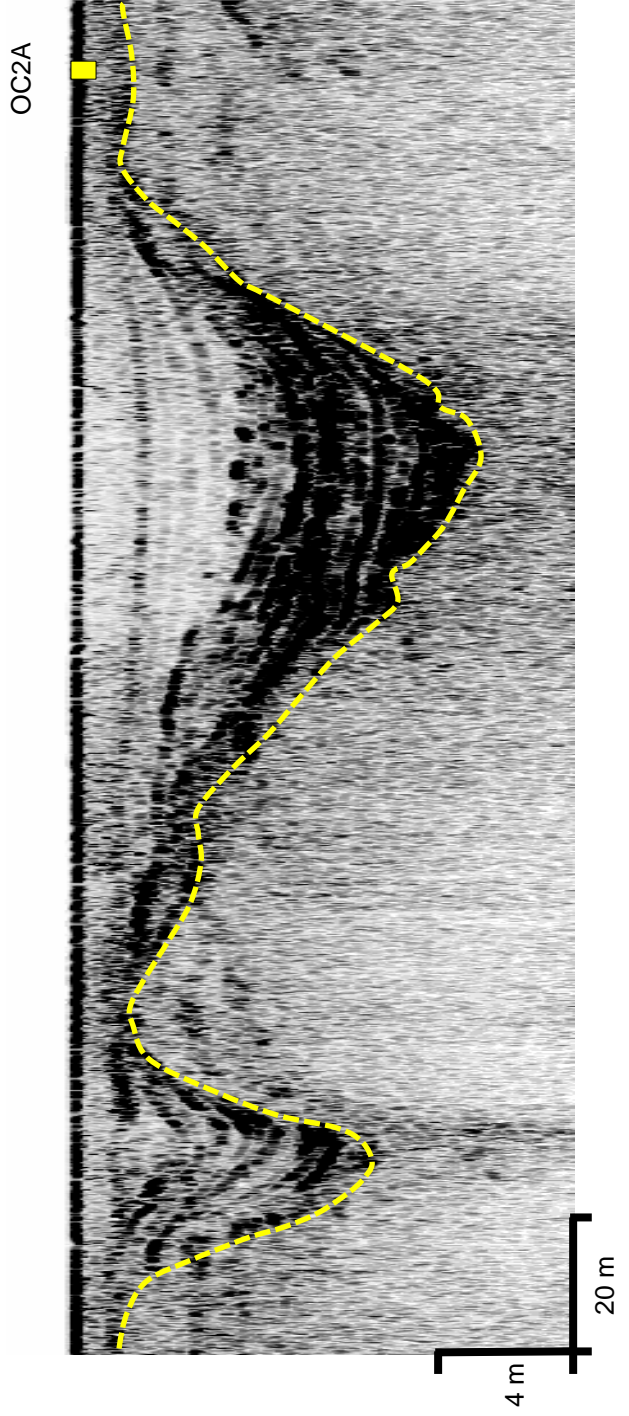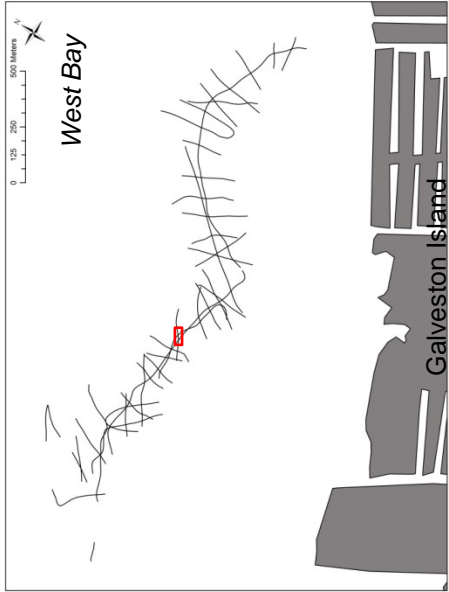
Seismic Section ID: SS2-1
Ping Section: 13942-15228
Core ID: OC1C
Core Length: 2.00 m

Legend

- - - Holocene/Pleistocene Boundary

▭ Core Location

▭ Ping Section Location

West Bay

Galveston Island

0 125 250 500 Meters

OC1C

5 m

15 m

173
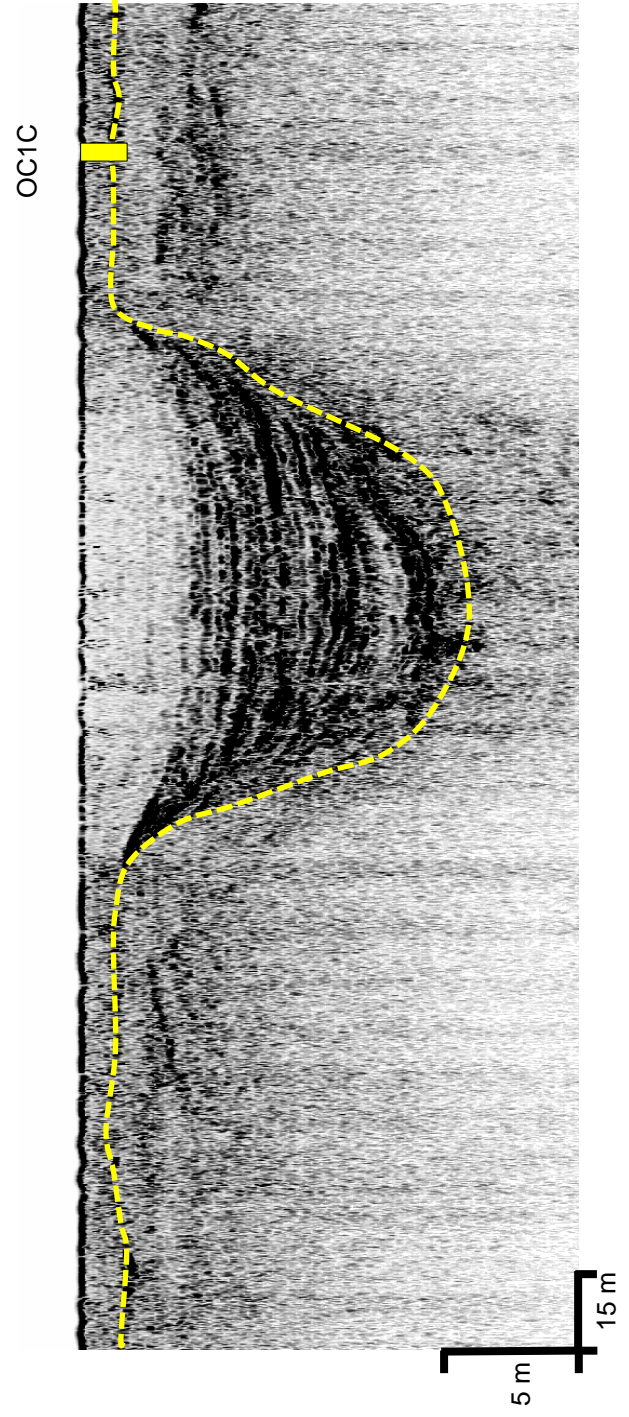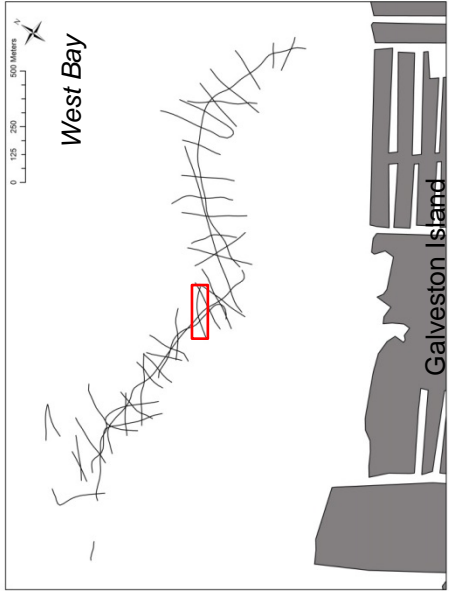
Seismic Section ID: SS2-1
Ping Section: 13942-15228
Core ID: OC1B
Core Length: 5.35 m
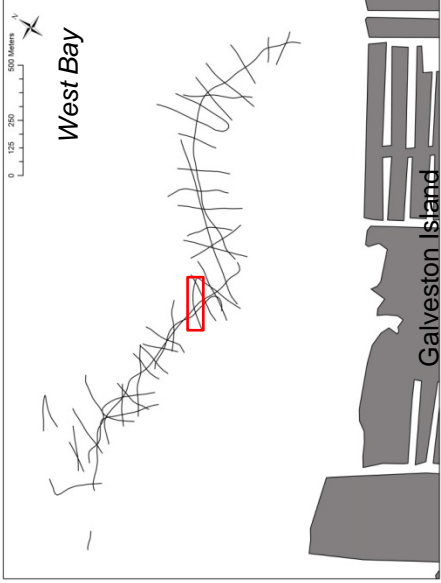
Legend

- - - - Holocene/Pleistocene Boundary

▬ Core Location

▭ Ping Section Location

West Bay

Galveston Island

OC1B

5 m

15 m
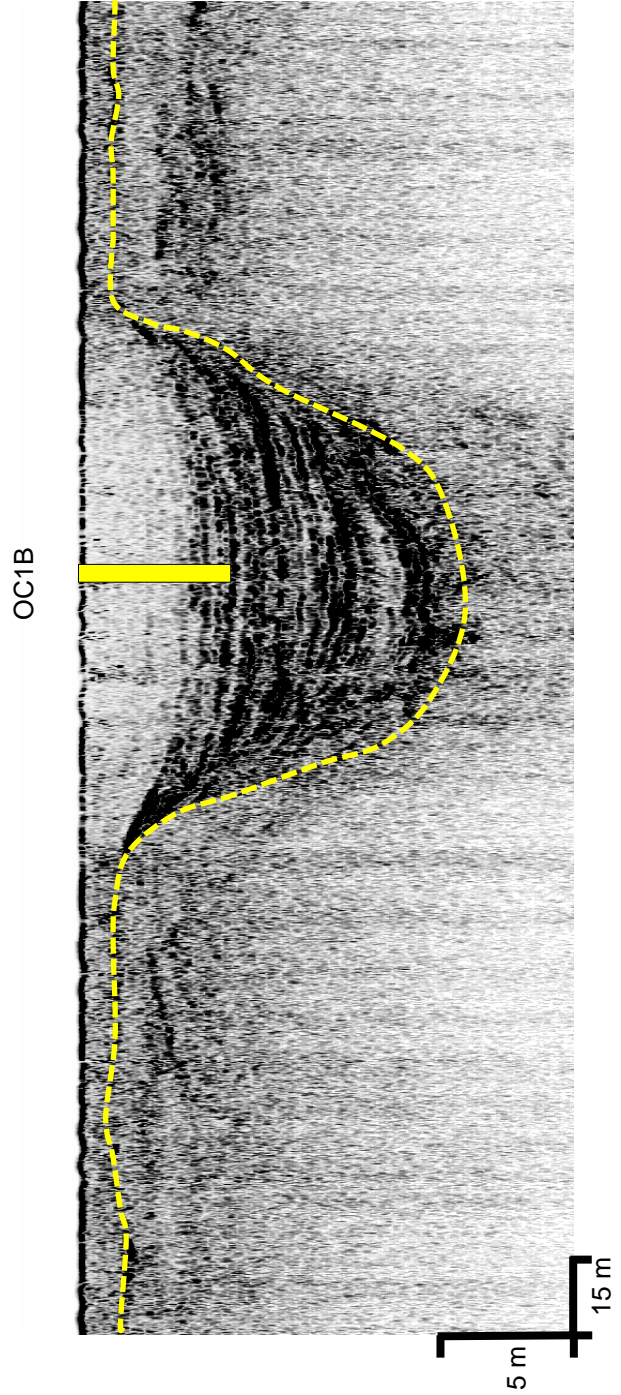
Seismic Section ID: SS2-1
Ping Section: 13942-15228
Core ID: OC1AB2
Core Length: 5.00 m

Legend

- - - Holocene/Pleistocene Boundary
▬ Core Location
▭ Ping Section Location

West Bay

Galveston Island

0 125 250 500 Meters

OC1AB2

5 m

15 m

175
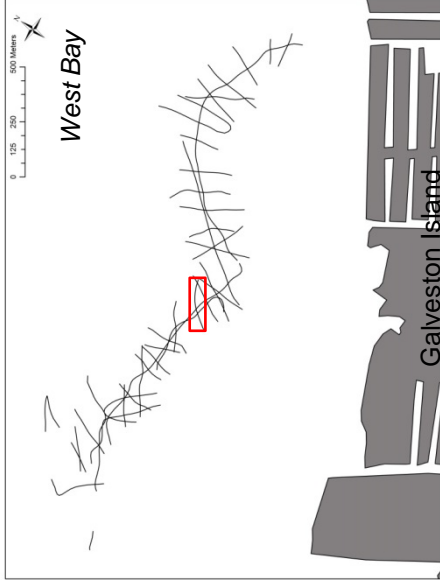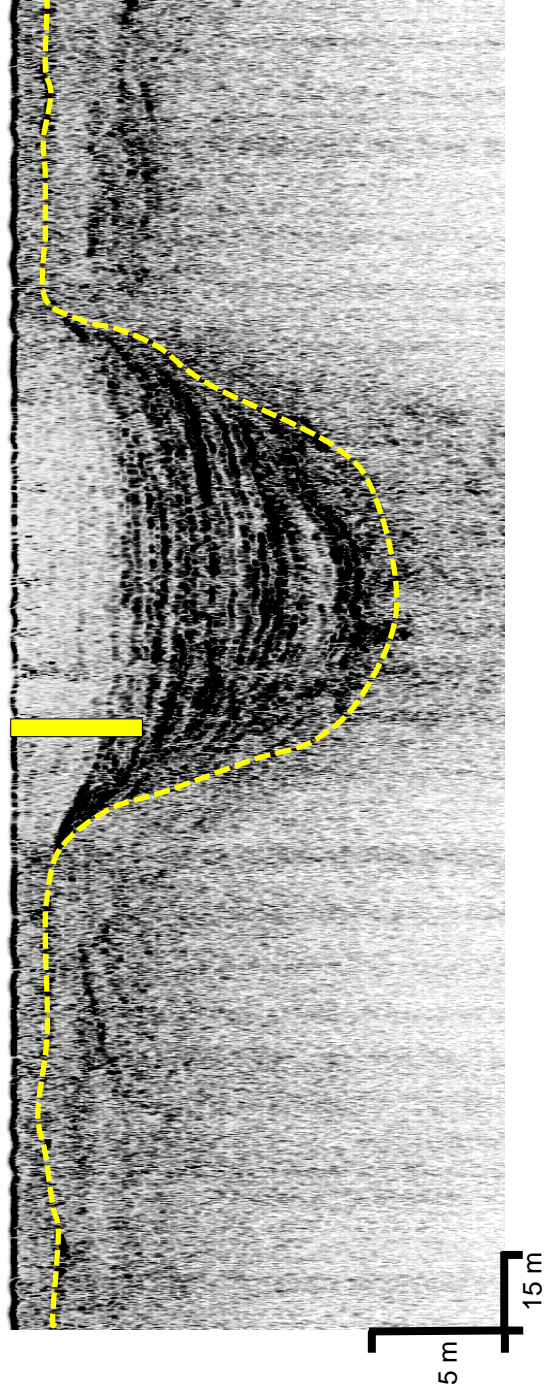
Seismic Section ID: SS2-1
Ping Section: 13942-15228
Core ID: OC1A
Core Length: 1.90 m

Legend

- - - Holocene/Pleistocene Boundary

▬ Core Location

▭ Ping Section Location

West Bay

0 125 250 500 Meters

Galveston Island

OC1A

5 m

15 m

176